EXPRESSION AND FUNCTIONAL ANALYSIS OF CHONDROITIN SULFOTRANSFERASE 3 IN BREAST CANCER

SEN YIN PING
(B.Sc. (Hons), NUS)

A THESIS SUBMITTED
FOR THE DEGREE OF DOCTOR OF PHILOSOPHY
DEPARTMENT OF ANATOMY
YONG LOO LIN SCHOOL OF MEDICINE
NATIONAL UNIVERSITY OF SINGAPORE
2013

DECLARATION

I hereby declare that this thesis is my original work and it has been written by me in its entirety. I have duly acknowledged all the sources of information which have been used in the thesis.

This thesis has also not been submitted for any degree in any university previously.

Sen Yin Ping

23 August 2013

ACKNOWLEDGEMENTS

I would like to express my utmost gratitude to the following people:

- Associate Professor George Yip, my supervisor, for his invaluable guidance and patience throughout my PhD study;

- Professor Bay Boon Huat, Head of Department of Anatomy, NUS, who has allowed me to pursue my graduate studies in the department;

- Associate Professor Tan Puay Hoon, Head of Department of Pathology, Singapore General Hospital (SGH) for providing the tissue microarray slides;

- Dr Aye Aye Thike, Department of Pathology, SGH, for her great help in the immuno-scoring portion of my project;

- Mrs Yong Eng Siang, Mr Poon Zhung Wei, and Mrs Ng Geok Lan for their excellent technical assistance in the labs and for making the labs safe and clean for research work;

- Dr Guo Chun Hua, Dr Koo Chuay Yeng, Dr Yvonne Teng, Dr Omid Iravani, Dr Grace Leong, Dr Zhang Ting, Ms Sim Wey Cheng, Ms Victoria King, Ms Chua Pei Jou, Mr Low Jin Yih, Mr Lo Soo Ling, Ms Sharen Lim See Wee, and Mr Chia Peng Heng for their friendship and great help in the lab;

- My family and Mr Samuel Ooi for their great support and understanding throughout my PhD study.

TABLE OF CONTENTS

DECLARATION 2

ACKNOWLEDGEMENTS 3

TABLE OF CONTENTS 4

ABSTRACT 7

LIST OF FIGURES 9

LIST OF TABLES 11

LIST OF ABBREVIATIONS 12

LIST OF PUBLICATIONS 14

1 INTRODUCTION 17
1.1 The Breast and Breast Cancer 17
1.1.1 Introduction to Breast Carcinoma 17
1.1.2 The Development and Anatomy of the Breast 17
1.1.3 Epidemiology of Breast Cancer 20
1.1.4 Risk Factors of Breast Cancer 21
1.1.4.1 Age 21
1.1.4.2 Family history of breast cancer 22
1.1.4.3 Early Menarche and Late Menopause 22
1.1.4.4 Late or Low Parity 22
1.1.4.5 Use of Hormonal Pills 23
1.1.4.6 High Fat Diet and Sedentary Lifestyle 23
1.1.5 Symptoms of Breast Cancer 24
1.1.6 Classification of Breast Cancer 24
1.1.7 Invasive Ductal Carcinoma 26
1.1.8 Detection of Breast Cancer 27
1.1.8.1 Breast Self-Examination 28
1.1.8.2 Mammography 28
1.1.8.3 Ultrasound 29
1.1.8.4 Magnetic Resonance Imaging 29
1.1.9 Definitive Diagnosis of Breast Cancer 29
1.1.9.1 Tumor Biopsies 29
1.1.9.2 Prognostic Markers for Breast Cancer 30
1.1.10 Treatment for Breast Cancer 34
1.1.10.1 Surgery 34
1.1.10.2 Radiation Therapy 35
1.1.10.3 Chemotherapy 35
1.1.10.4 Hormonal/Biological Therapy 35
1.1.11 Current Challenges in Breast Cancer 36
1.2 Glycosaminoglycans and Proteoglycans 37
1.2.1 Structure of Glycosaminoglycans and Proteoglycans 37
1.2.2 Chondroitin Sulfate and Chondroitin Sulfate Proteoglycans 38
1.2.3 Biosynthesis of Chondroitin Sulfate and Chondroitin Sulfate Proteoglycan 40
1.2.4 Functions of Chondroitin Sulfate and Chondroitin Sulfate Proteoglycans 41
1.2.5 Chondroitin Sulfate and Chondroitin Sulfate Proteoglycans in Cancer 42
1.2.6 Chondroitin Sulfotransferase 3 in Cancer 44
1.3 Scope of Study 45
2 MATERIALS AND METHODS 47

2.1 Cell Culture of Breast Cancer Cells ... *47*
2.1.1 Subculture of Cells ... 47
2.1.2 Cryopreservation of Cells ... 48
2.1.3 Thawing of Cells ... 48
2.2 siRNA Transfection ... *48*
2.3 CHST3 Over-expression ... *50*
2.3.1 CHST3 Over-expression Plasmid Preparation ... 50
2.3.2 CHST3 Over-expression Plasmid Transfection ... 51
2.4 RNA Extraction ... *52*
2.5 cDNA Synthesis ... *53*
2.6 Primers ... *53*
2.7 Quantitative Real-Time Polymerase Chain Reaction ... *54*
2.8 Protein Electrophoresis ... *55*
2.8.1 Protein Extraction ... 55
2.8.2 Protein Quantitation ... 55
2.8.3 Preparation of SDS-Polyacrylamide Gel ... 56
2.8.4 Electrophoresis of SDS-Polyacrylamide Gel ... 56
2.8.5 Semi-Dry Electro-Transfer ... 57
2.8.6 Western Blot ... 57
2.9 Immunofluorescence of Breast Cancer Cells ... *58*
2.10 Functional Analysis of CHST3 in Breast Cancer Cells ... *58*
2.10.1 Cell Migration and Invasion Assays ... 58
2.10.2 Cell Proliferation Assay ... 59
2.10.3 Cell Adhesion Assay ... 59
2.10.4 Cell Cycle Assay ... 60
2.10.5 Cell Apoptosis Assay ... 60
2.10.6 Statistical Analyses ... 61
2.11 Immunohistochemistry of Human Breast Tissues ... *61*
2.11.1 Tissue Specimens ... 61
2.11.2 Immunohistochemistry ... 61
2.11.3 Evaluation of Staining Intensities ... 62
2.11.4 Selection of Cut-Off Score ... 62
2.11.5 IHC Statistical Analysis ... 63
2.12 Genome-wide Expression Profiling using Microarray Gene Chip ... *63*
2.12.1 Microarray Processing using Affymetrix Human Gene U133 Plus 2.0 Array ... 63
2.12.2 Microarray Gene Expression Analysis ... 64
2.12.3 Filtering Criteria for Gene Selection ... 64
2.12.4 Gene Pathway Analysis ... 65
3 RESULTS ... 67
3.1 Expression Analysis of CHST3 in Human Breast Cells ... *67*
3.2 Functional Analysis of CHST3 in Human Breast Cancer Cells ... *69*
3.2.1 Silencing and Over-expression Efficiencies of *CHST3* ... 70
3.2.1.1 CHST7 Expression after Silencing CHST3 ... 75
3.2.1.2 CHST3 affects Cellular Behaviors in Breast Cancer Cells ... 76
3.3 Signaling Pathways Affected through Silencing of CHST3 ... *86*
3.3.1 *CHST3* affects Proteins involved in Epithelial –Mesenchymal Transition ... 86
3.3.2 *CHST3* affects Proteins involved in JAK/STAT Pathway ... 90
3.3.3 *CHST3* affects Protein involved in Cell Apoptosis Pathway ... 92
3.4 Genome –Wide Expression Profiling of CHST3-Silenced T47D Cells ... *94*
3.4.1 RNA Yield, Quality, and Integrity ... 94
3.4.2 Target Preparation ... 95
3.4.3 Gene Microarray Data Analysis ... 96
3.4.4 Functional Categorization of Genes Affected from Silencing *CHST3* ... 96
3.5 Downstream Molecules of CHST3 Silencing ... *100*
3.5.1 CHST3 modulates GPNMB ... 102
3.5.1.1 Silencing Efficiency of CHST3 and GPNMB ... 102
3.5.1.2 Regulation of Cellular Behaviors by CHST3 and GPNMB ... 105
3.5.2 *FLRT3* in Breast Cancer Cells ... 111
3.5.2.1 Silencing Efficiency of FLRT3 ... 111
3.5.2.2 FLRT3 affects Cell Migration in Breast Cancer Cells ... 114

3.5.2.3 FLRT3 affects Cell Invasion in Breast Cancer Cells 115
3.5.2.4 FLRT3 affects Cell Adhesion in Breast Cancer Cells 116
3.5.2.5 FLRT3 affects Cell Proliferation in Breast Cancer Cells 117
3.5.3 CHST3 modulates FLRT3 117
3.5.3.1 Silencing Efficiency of CHST3 and GPNMB 117
3.5.3.2 Regulation of Cellular Behaviors by CHST3 and FLRT3 120
3.5.4 Relationship of *GPNMB* and *FLRT3* 126
3.6 Expression Analysis of CHST3 in Invasive Ductal Carcinoma Tissues 127
3.6.1 Clinicopathological Parameters of IDC Patient Cases 127
3.6.2 CHST3 Expression Pattern in Breast Tissues 129
3.6.3 CHST3 Selected Cut-off Point 130
3.6.4 CHST3 Expression in Normal and Malignant Breast Tissues 131
3.6.5 CHST3 Correlations with Clinicopathological Parameters 132
3.6.6 Survival Analysis of CHST3 Expression 135
3.6.6.1 Survival Analysis using Kaplan Meier 135
3.6.6.2 Survival Analysis using Cox Regression Univariate 136
3.6.6.3 Survival Analysis using Cox Regression Multivariate 139
3.7 Expression Analysis of FLRT3 in Invasive Ductal Carcinoma Tissues 143
3.7.1 FLRT3 Expression Pattern in Breast Tissues 144
3.7.2 FLRT3 Selected Cut-off Point 145
3.7.3 FLRT3 Expression in Normal and Malignant Breast Tissues 146
3.7.4 FLRT3 Correlations with Clinicopathological Parameters 147
3.7.5 Survival Analysis of FLRT3 Expression 149
3.7.5.1 Survival Analysis using Kaplan Meier 149
3.7.5.2 Survival Analysis using Cox Regression Univariate 150
3.7.5.3 Survival Analysis using Cox Regression Multivariate 153
3.8 Correlation of CHST3 and FLRT3 Expression in Invasive Ductal Carcinoma 157
3.9 Summary of Results 158
3.9.1 *CHST3* Regulates Cell Migration 159
3.9.2 *CHST3* Regulates Cell Invasion 159
3.9.3 *CHST3* Regulates Cell Adhesion 159
3.9.4 *CHST3* Regulates Cell Proliferation 160
3.9.5 *CHST3* Regulates Cell Apoptosis 160
3.9.6 *CHST3* Effects on Downstream Molecules 160
3.9.7 CHST3 and FLRT3 in Breast Tissues 161
4 DISCUSSION 163
4.1 Potential Role of CHST3 in Breast Cancer 163
4.1.1 Potential Role of CHST3 through Chondroitin Sulfate 164
4.1.2 CHST3 affects Downstream Molecules GPNMB and FLRT3 169
4.1.3 Potential Regulatory Role of CHST3 through Other Pathways 173
4.1.4 Potential Role of CHST3 through Non-Enzymatic Activity Role 175
4.2 Regulation of CHST3 Expression 176
4.2.1 Regulation by Ligands 176
4.2.2 Regulation at Gene Expression Level 178
4.3 Proposed CHST3 Pathway 182
4.4 Limitations in Study 183
4.4.1 Evaluation of CHST3 and CHST7 Functional Activities 183
4.4.2 Evaluation with Clinical Samples and Animal Models 183
4.4.3 Evaluation using Different Assays 183
5 CONCLUSION AND FUTURE WORK 187
6 REFERENCES 189

ABSTRACT

Chondroitin sulfotransferase 3 (CHST3) is involved in the biosynthesis of chondroitin sulfate (CS), which has been implicated to be involved in tumor progression. CHST3 specifically catalyzes carbon 6 sulfation of the CS molecule, and has not been studied of its effects in breast cancer. In this study, the expression and functional roles of CHST3 are evaluated in breast cancer.

CHST3 expression is found to be significantly lower in malignant breast cells in comparison to that of the normal breast cells. Following that, in the *in vitro* studies, *CHST3*-silenced cells showed significant increases in cell migration and invasion whereas *CHST3*-over-expressed cells showed the opposite trends that are decreases in cell migration and invasion. Changes in cell adhesion, proliferation, and apoptosis are much lesser in comparison to cell migration and invasion. It is observed that *CHST3* enhances cell adhesion and cell apoptosis, as well as suppresses cell proliferation. Therefore, the results show that there is a negative association between *CHST3* expression and the metastatic, proliferative capabilities of breast cancer cells.

Subsequently molecular pathway studies were carried out. *GPNMB* and *FLRT3* are shown to be up-regulated after down-regulation of *CHST3*. A double knockdown of either *CHST3* and *GPNMB* or *CHST3* and *FLRT3* abolished the cell migration, invasion, proliferation, and adhesion changes initially observed in the *CHST3* single silencing experiments. Hence, *CHST3*/*GPNMB* and *CHST3* /*FLRT3* pairings work together in modulating the cancer cells' behaviors and both *GPNMB* and *FLRT3* are downstream targets of *CHST3*. Additionally, epithelial-mesenchymal transition (EMT) markers (E-cadherin and β-catenin) decreased in expression after silencing of *CHST3*. Also, there is a decrease in pBAD/BAD level indicating that the changes observed in cell proliferation and apoptosis seen in the *CHST3* phenotypic experiments could be due to the BAD survival pathway.

Evaluation of CHST3 and FLRT3 expressions through immunohistochemistry in invasive ductal carcinoma tissues revealed enhanced CHST3 and reduced FLRT3 expression in normal tissues in comparison to malignant tissues. The decrease in CHST3 level is also correlated with higher tumor stage and larger tumor size. As for FLRT3, its high expression was associated with patients with older age as well as enhanced staging of lymphovascular invasion. No trend is observed between CHST3 and FLRT3 expression levels. This initial study of CHST3 and FLRT3 hence suggest that both molecules may participate in breast cancer as a tumor suppressor and tumor promoter respectively.

LIST OF FIGURES

Figure 1.1: Anatomy of the breast. 19
Figure 1.2: Histopathology of ductal carcinoma. 27
Figure 1.3: Various forms of CS molecules. 39
Figure 1.4: Structure of CPSG. 39
Figure 2.1: Plasmid maps for CHST3 over-expression study. 51
Figure 3.1: CHST3 expression in breast cells 68
Figure 3.2: Silencing efficiencies of CHST3 in T47D cells 71
Figure 3.3: Silencing efficiencies of CHST3 in MDA-MB-231 cells 72
Figure 3.4: Over-expression efficiencies of CHST3 in MCF7 cells 73
Figure 3.5: Over-expression efficiencies of CHST3 in MDA-MB-231 cells 74
Figure 3.6: CHST7 expression in CHST3-silenced T47D and MDA-MB-231 cells 75
Figure 3.7: Cell migration level after silencing CHST3 77
Figure 3.8: Cell migration level after over-expression of CHST3 78
Figure 3.9: Cell invasion level after silencing CHST3 79
Figure 3.10: Cell invasion level after over-expression of CHST3 80
Figure 3.11: Cell adhesion level after silencing CHST3 81
Figure 3.12: Cell adhesion level after over-expression of CHST3 82
Figure 3.13: Cell proliferation level after silencing CHST3 84
Figure 3.14: Cell proliferation level after over-expression of CHST3 85
Figure 3.15: Cell apoptosis level after silencing CHST3 85
Figure 3.16: E-cadherin expression after silencing CHST3 88
Figure 3.17: β-catenin expression after silencing CHST3 89
Figure 3.18: pJAK2/JAK2 expression after silencing CHST3 91
Figure 3.19: pSTAT3/STAT3 expression after silencing CHST3 92
Figure 3.20: pBAD/BAD expressions after silencing CHST3 93
Figure 3.21: Quality and integrity of RNA samples for microarray 95
Figure 3.22: Functional categorization of affected genes after CHST3 silencing 97
Figure 3.23: GPNMB expression in CHST3 single-silenced T47D cells 103
Figure 3.24: CHST3 and GPNMB levels after different silencing treatments in T47D cells 104
Figure 3.25: Effects of CHST3 and GPNMB double silencing on cell migration 106
Figure 3.26: Effects of CHST3 and GPNMB double silencing on cell invasion 108
Figure 3.27: Effects of CHST3 and GPNMB double silencing on cell adhesion 109
Figure 3.28: Effects of CHST3 and GPNMB double silencing on cell proliferation 110
Figure 3.29: Silencing efficiencies of FLRT3 in T47D cells 112
Figure 3.30: Silencing efficiencies of FLRT3 in MDA-MB-231 cells 113
Figure 3.31: Cell migration level after silencing FLRT3 114
Figure 3.32: Cell invasion level after silencing FLRT3 115
Figure 3.33: Cell adhesion level after silencing FLRT3 116
Figure 3.34: Cell proliferation level after silencing FLRT3 117
Figure 3.35: FLRT3 expression in CHST3 single-silenced T47D cells 118
Figure 3.36: CHST3 and FLRT3 levels after different silencing treatments in T47D cells 119
Figure 3.37: Effects of CHST3 and FLRT3 double silencing on cell migration 121
Figure 3.38: Effects of CHST3 and FLRT3 double silencing on cell invasion 123
Figure 3.39: Effects of CHST3 and FLRT3 double silencing on cell adhesion 124
Figure 3.40: Effects of CHST3 and FLRT3 double silencing on cell proliferation 125
Figure 3.41: GPNMB and FLRT3 correlation in T47D cells 126
Figure 3.42: Staining pattern of CHST3 in breast tissues 129
Figure 3.43: Frequency distribution and ROC curve of CHST3 expression among normal and malignant tissues 130
Figure 3.44: CHST3 immunostaining in normal and malignant breast tissues 131

Figure 3.45: Paired analysis of CHST3 expression in 33 paired normal and malignant breast tissue samples..... 132
Figure 3.46: CHST3 immunostaining in breast tissues of different tumor stage 133
Figure 3.47: Kaplan Meier curves using CHST3 135
Figure 3.48: Staining pattern of FLRT3 in breast tissues. 144
Figure 3.49: Frequency distribution and ROC curve of FLRT3 expression among normal and malignant tissues 145
Figure 3.50: FLRT3 immunostaining in normal and malignant breast tissues..... 146
Figure 3.51: Paired analysis of FLRT3 expression in 26 paired normal and malignant breast tissue samples..... 147
Figure 3.52: Kaplan Meier curves using FLRT3 149
Figure 4.1: Proposed CHST3 pathway in breast cancer. 182

LIST OF TABLES

Figure 1.1: Anatomy of the breast. 19
Table 1.1 Various TNM staging 25
Table 1.2 Classification of tumor by Bloom-Richardson score 26
Table 2.1: siRNA sequences 49
Table 2.2: Volume and concentration of reagents used for siRNA transfection 49
Table 2.3: cDNA synthesis reaction conditions 53
Table 2.4: Primer sequences targeting genes of interest 54
Table 2.5: RT-PCR conditions 55
Table 3.1: Spectrophotometer reading of purified cRNA 96
Table 3.2: Functional categorization of differentially expressed genes (≥ 2 folds change) 97
Table 3.3 Clinicopathological features of 218 cases of invasive ductal carcinoma 128
Table 3.4 Clinicopathological features of 41 cases of normal ductal cases 129
Table 3.5: Analysis of CHST3 expression between normal and malignant breast tissues 132
Table 3.6: Correlations between CHST3 expression and clinicopathological features of IDC 134
Table 3.7: Univariate Cox regression analysis of CHST3 and clinicopathological parameters using DFS time period 136
Table 3.8: Univariate Cox regression analysis of CHST3 and clinicopathological parameters using OS time period 137
Table 3.9: Univariate Cox regression analysis of CHST3 and clinicopathological parameters using SAR time period 138
Table 3.10: Multivariate Cox regression analysis of CHST3 expression using DFS. 140
Table 3.11: Multivariate Cox regression analysis of CHST3 expression using OS. 141
Table 3.12: Multivariate Cox regression analysis of CHST3 expression using SAR. 142
Table 3.13: Analysis of FLRT3 expression between normal and malignant breast tissues 147
Table 3.15: Univariate Cox regression analysis of FLRT3 and clinicopathological parameters using DFS time period 150
Table 3.16: Univariate Cox regression analysis of FLRT3 and clinicopathological parameters using OS time period 151
Table 3.17: Univariate Cox regression analysis of FLRT3 and clinicopathological parameters using SAR time period 152
Table 3.18: Multivariate Cox regression analysis of FLRT3 expression using DFS. 154
Table 3.19: Multivariate Cox regression analysis of FLRT3 expression using OS. 155
Table 3.20: Multivariate Cox regression analysis of FLRT3 expression using SAR. 156
Table 3.21: Correlation of CHST3 with FLRT3 expression in IDC tissues 157
Table 4.1 Potential transcription factors regulating CHST3 180

LIST OF ABBREVIATIONS

APS	Ammonium persulfate
ATCC	American type culture collection
BCL2	B-cell lymphoma 2
BSA	Bovine serum albumin
C6ST1	Chondroitin-6-sulfotransferase 1
cDNA	complementary DNA
CHPF	Chondroitin polymerizing factor
CHST3	Chondroitin sulfotransferase 3
CHST7	Chondroitin sulfotransferase 7
CHSY1	Chondroitin synthase 1
CHSY3	Chondroitin synthase 3
CMF	Cyclophosphamide, methotrexate, and fluorouracil
CS	Chondroitin sulfate
CSGALNACT-1	Chondroitin sulfate N-acetylgalactosaminyltransferase 1
CSGALNACT-2	Chondroitin sulfate N-acetylgalactosaminyltransferase 2
CSGLCAT	Chondroitin sulfate glucuronyltransferase
CSPG	Chondroitin sulfate proteoglycan
DCIS	Ductal carcinoma in situ
DFS	Disease free survival
DMSO	Dimethyl sulphoxide
DS	Dermatan sulfate
DTT	Dithiothretol
ECM	Extracellular matrix
EGFR	Epidermal growth actor receptor
EMT	Epithelial-mesenchymal transition
ER	Estrogen receptor
FLRT3	Fibronectin leucine-rich transmembrane
GAG	Glycosaminoglycan
GalNAc	N-acetyl-galactosamine

GCOS	GeneChip Operating Software
GlcA	Glucuronic acid
GPNMB	Glycoprotein transmembrane nmb
HER2	Human epidermal receptor 2
HS	Heparan sulfate
IDC	Invasive ductal carcinoma
JAK2	Janus kinase 2
LCIS	Lobular carcinoma in situ
OS	Overall survival
PAI-1	Plasminogen activator inhibitor
PAPS	3’-phosphoadenosine-5’-phosphosulfate
PR	Progesterone receptor
PG	Proteoglycan
PI3K	Phosphoinositol-3-kinase
PVDF	Polyvinyl difluoride
SAR	Survival after recurrence
SDS	Sodium dodecyl sulfate
SED	Spondyloepiphyseal dysplasia
SEM	Standard error mean
STAT3	Signal transducer and activator of transcription 3
TEMED	N,N,N',N'-tetramethylethylenediamine
TMA	Tissue microarray
TNM	Tumor-node-metastasis
TPS	Tumor percentage score
uPa	Urokinase plasminogen activator
VCAN	Versican
XYL1	Xylotransferase 1
XYL2	Xylotransferase 2

LIST OF PUBLICATIONS

Journals

1. Shin EM, Hay HS, Lee MH, Goh JN, Tan TZ, Sen YP, Lim SW, Yousef EM, Ong HT, Thike AA, Kong XJ, Wu ZS, Mendoz E, Sun W, Salto-Tellez M, Lim CT, Lobie PE, Lim YP, Yap CT, Zeng Q, Sethi G, Lee MB, Tan P, Goh BC, Miller LD, Thiery JP, Zhu T, Gaboury L, Tan PH, Hui KM, Yip GWC, Miyamoto S, Kumar AP, Tergaonkar V (2014) DEAD-box helicase DP103 defines metastatic potential of human breast cancers. *The Journal of Clinical Investigation* 124 (9): 3807-3824.

2. Kumar AV, Salem GE, Spillmann D, Stock C, Sen YP, Zhang T, Van KTH, Hulsewig C, Koszlowski E, Pavao MS, Ibrahim SA, Poeter M, Rescher U, Kiesel L, Koduru S, Yip GW, Gotte M (2014) HS3ST2 Modulates Breast Cancer Cell Invasiveness via MAP Kinase- and Tcf4 (Tcf712)-Dependent Regulation of Protease and Cadherin Expression. *International Journal of Cancer* 135: 2579-2592.

3. Sen YP, Ker BT, Bay BH, Yip GW (2013) Chondroitin sulfate proteoglycans as drug targets in breast cancer treatment. Recent Patents on Anti-Cancer Drug Discovery. (Ahead of publication)

4. Sen YP, Yip GW (2012) Chondroitin sulfate in breast cancer. Breast Cancer. (Ahead of publication)

5. Koo CY, Sen YP, Bay BH, Yip GW (2012) Heparan sulfate proteoglycans: novel targets for breast cancer treatment. Topics in Anti-Cancer Research 1: 90-112.

6. Sen YP, Yip GW (2009) CD44 (CD44 molecule (Indian blood group)). Atlas Genet Cytogenet Oncol Haematol. URL: http://AtlasGeneticsOncology.org/Genes/CD44ID980CH11p13.html

7. Koo CY, Sen YP, Bay BH, Yip GW (2008) Targeting heparan sulfate proteoglycans in breast cancer treatment. Recent Patents on Anti-Cancer Drug Discovery 3(3).

Abstracts

1. Sen YP, Thike AA, Tan PH, Bay BH, Yip GW (2013) Chondroitin sulfotransferase 3: a potential biomarker for breast cancer. 13th St Gallen International Breast Cancer Conference, St Gallen, Switzerland.

2. Sen YP, Thike AA, Tan PH, Bay BH, Yip GW (2012) Expression of decorin in Singaporean breast cancer patients. Proceedings of the Microscopy Society Singapore Annual General and Scientific Meeting, Singapore.

3. Sen YP, Thike AA, Tan PH, Bay BH, Yip GW (2011) CHSY1: a potential biomarker in breast cancer. Proceedings of the Microscopy Society Singapore Annual General and Scientific Meeting, Singapore.

4. Sen YP, Thike AA, Tan PH, Bay BH, Yip GW (2010) Chondroitin synthase 1 mediates aggressive and metastatic phenotypic behaviors of breast cancer cells. International Anatomical Sciences and Cell Biology Conference, Singapore.

5. Sen YP, Bay BH, Yip GW (2009) Dermatan sulfate modulates chemosensitivity of breast cancer cells to cisplatin. NHG Annual Scientific Congress, Singapore.

CHAPTER 1
INTRODUCTION

1 INTRODUCTION

1.1 The Breast and Breast Cancer

1.1.1 Introduction to Breast Carcinoma

Breast cancer is the most commonly diagnosed carcinoma as well as one of the top-ranked causes of cancer death, among females worldwide. The cancer of the breast may develop from different parts of the mammary gland and can be classified into different groups, as will be further discussed in this chapter. Breast tumors have also been long known to be a heterogeneous disease, as shown from molecular profiling, with varying clinical outcomes. It is hence essential and critical to gain knowledge on not only the anatomical and morphological characteristics of a normal breast and malignant breast tissues, but also the molecular features involved in breast tumor progression.

1.1.2 The Development and Anatomy of the Breast

Breast development in the embryo usually starts at the 5^{th} week. The mammary ridges will form on the ventral surface, lengthening from the axilla to the medial thigh (Howard and Gusterson, 2000). After which, epithelial cells will focus at the center of each mammary ridge, forming the mammary bud (Watson and Khaled, 2008). In the 15^{th} week of development, mesenchymal cells will accumulate around the mammary bud, triggering its outgrowth and sprouting into the mesenchymal tissue (Howard and Gusterson, 2000, Mikkola and Millar, 2006). This would lead to the formation of lobes and ultimately lobules. The mammary bud will become canalized, forming lactiferous ducts. Approximately 15 to 20 lobes will be present in each breast, with their lactiferous ducts converging at the mammary pit that will later on form the nipple (Cowin and Wysolmerski, 2010).

Post-natal, the mammary glands will be structurally similar in both males and females till puberty. For males, the mammary glands will remain rudimentary (Russo et al., 2001). The female breast changes continuously in structure throughout her lifetime, as caused by major physiological factors like puberty,

menstrual cycle, pregnancy, and menopause. When females hit puberty, hormonal secretion will change causing development and structural modifications within the glands (Naccarato et al., 2000). Estrogen and progesterone secretions from the ovaries as well as prolactin from the anterior pituitary gland will instigate further developments of the lobules and ducts (Howard and Gusterson, 2000) Additional hormones such as glucocorticoids and somatotropin are needed for full development of the ducts (Knight and Sorensen, 2001). Simultaneously, the mammary glands will enlarge due to an increase in connective and adipose tissues within the stroma. The female breast will encounter full development at around 20 years of age, with minor cyclical changes during menstrual period and major changes during pregnancy and lactation period (Russo et al., 2001).

The mature breast (as shown in Figure 1.1) is positioned upon the deep pectoral fascia, which in turn overlies the pectoralis major muscle of the chest wall, extending from the second to the sixth ribs in the vertical axis (Abrahams et al., 2013, Standring, 2008). The breast is held by the suspensor-like ligaments of Cooper to the skin, of which provides support for the breast parenchyma (Hoda, 2012, O'Rahilly and Muller, 2004, Standring, 2008). It consists of 15 to 20 lobules, which are responsible for producing and secreting milk into the lactiferous ducts that converge and lead out to the nipple, which is the greatest prominence of the breast (Kossoff et al., 1973, Ramsay et al., 2005). The nipple is surrounded by a circular pigmented area called the areola. Before getting to the nipple, each of the ducts is dilated, forming a lactiferous sinus used for storage of milk during lactation; after which, the ductal passage narrows before passing through the nipple (Love and Barsky, 2004, Doucet et al., 2009). Histologically, the lactiferous duct in the lobe is lined by a double layer of cells (cuboidal or low columnar epithelial cells) that makes up the interior as well as the outer myoepithelial layers, and enclosed by the basal lamina. The lobules constitute alveolar acini that regulate milk production (Kierszenbaum and Tres, 2011). The lobules and ducts are surrounded by the connective tissue stroma, consisting of adipose and collagenous connective tissues (American Cancer Society, 2012a, O'Rahilly and Muller, 2004,

Hoda, 2012, Nawaz, 2011, Moore and Agur, 2007, Gartner and Hiatt, 2007). The stroma region that surrounds the lobules is dense and fibro-collagenous, while the intralobular stroma region has distinctively more loose texture to allow rapid expansion of the secretory tissue especially during pregnancy (Standring, 2008).

During pregnancy, the terminal ducts and lobules will further differentiate causing extensive glandular expansion. Subsequently, the lobules will enlarge and the amount of both adipose and connective fibrous tissues will reduce. After the age of 40 or so, the ducts, lobules, and connective tissues of the breasts will start to atrophy, giving rise to replacement by fatty adipose tissues. This process will continue throughout menopause (Hoda, 2012, Gartner and Hiatt, 2007).

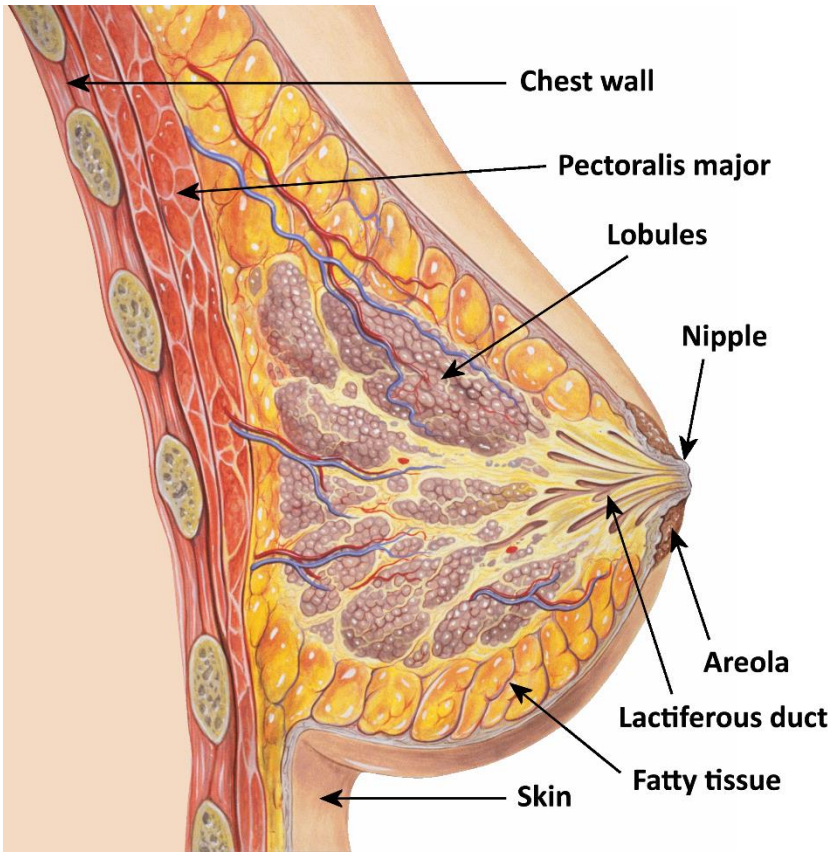

Figure 1.1: Anatomy of the breast.
[This image, illustrated by (Lynch and Jaffe, 2007), is free from copyright and is free to be shared]

1.1.3 Epidemiology of Breast Cancer

Breast cancer is the most frequently diagnosed cancer and a top cancer-related death among females worldwide, accounting for 22.9% and 13.7% of all cancers respectively (American Cancer Society, 2011). The diagnosis and mortality rate in developing countries (20% diagnosis rate and 12.7% mortality rate, of which both are lower than the global means) is lower than that of developed countries (26% diagnosis rate and 15.5% mortality rate, of which both are higher than the global means) (American Cancer Society, 2011). In the United States of America, breast cancer continues to be the top cancer among females constituting 29% or one third of female cancer cases, much higher than the global mean (American Cancer Society, 2012b). In terms of cancer-related death, breast cancer makes up approximately 14% of all cancer deaths in women, second only to lung cancers (26%) (American Cancer Society, 2012a). Nevertheless, the death rate for breast carcinoma has decreased over the past twenty years by ~30%, reflecting the improvements in early breast cancer detection and treatment options. It has been observed that Caucasian females have an overall elevated breast cancer incidence rate in comparison to females of other races, due to later first pregnancies, more frequent use of hormonal therapy, and higher mammography check-ups (Siegel et al., 2013).

In Singapore, breast cancer is also the most frequently diagnosed cancer affecting females, accounting for almost 30% of all cancers in Singaporean women (Teo and Soo, 2013). Furthermore, it is the most common female cancer in the three different main ethnic groups in Singapore that are the Chinese, Malay, and Indian. In addition, from year 1968 to 2002, statistics showed that the Chinese in comparison to Malays and Indians have elevated risk of being diagnosed with cancer of the breast. Similar to global cancer statistics trend, breast carcinoma in Singapore is the top cancer-related death accounting for 18.0% of all female cancer mortalities (National Registry of Diseases Office, 2012). The rise in breast cancer incidence can be attributed to better awareness of breast cancer and wider use of

mammography for the detection of breast carcinoma. Nevertheless, it is also caused by urbanization in Singapore, of which females tend to adopt Western lifestyle and diet, as well as having low and late parity (Verkooijen et al., 2009, Rastogi et al., 2008).

1.1.4 Risk Factors of Breast Cancer

It is hence necessary for females to be aware of the risk factors concerned with breast cancer. The risk factors can be separated into the non-modifiable factors as well as the modifiable factors groups. The non-modifiable risk factors would comprise of patients' age, family history of breast cancer, inherited gene mutations in *BRCA1* and *BRCA2* which are breast cancer susceptibility genes, early menarche and late onset of menopause. On the other hand, modifiable risk factors include late and low parity, use of hormonal therapy, having a high fat diet and sedentary lifestyle.

1.1.4.1 Age

Age in females is a main non-modifiable risk factor of breast carcinoma. The incidence risk in females aged 25 and below is usually very low. However, the risk will double with every 10 years of age (Hamajima et al., 2002) with the risk increasing substantially as females transition though menopause (American Cancer Society, 2011). In the United States of America, females aged 40 years old and older accounted for 95% of all new breast cancer cases, whereas the lowest risk group was in females aged 20 to 24 years old. Additionally, 97% of breast cancer deaths often occur among females of 40 years old and above (American Cancer Society, 2012a). In Singapore, from year 1968 to 2002, almost half of all breast carcinoma cases were diagnosed in females aged 50 years old and above, with women aged 55 to 59 years old having the highest risk (Seow et al., 1996).

1.1.4.2 Family history of breast cancer

Another key risk factor of breast cancer is the genetic predisposition or inheritance of gene mutations in the female. She is more susceptible to breast cancer if she has a positive family history of the disease (Collaborative Group on Hormonal Factors in Breast Cancer, 2001). The degree of the risk involved is also dependent upon her connection with the affected family member or relative, as well as the number of family members or relatives diagnosed with the cancer (Singletary, 2003). An analysis involving 52 epidemiological studies found that 13% of breast carcinoma cases had family history of breast cancer (Hamajima et al., 2002). *BRCA1* and *BRCA2* are the two most established hereditary genes in breast cancer. Females with inherited *BRCA1* mutations are more susceptible of getting breast cancer at around the age of 35 years old, whereas those with inherited *BRCA2* mutations will have a 25% to 45% increased risk of developing breast carcinoma (Ferla et al., 2007, Antoniou et al., 2003).

1.1.4.3 Early Menarche and Late Menopause

Studies have established that most breast cancer risk factors are attributed to elevated exposure to estrogen (Collaborative Group on Hormonal Factors in Breast Cancer, 2012). Females having early onset of menarche and late onset of menopause are at higher risk of developing breast cancer due to prolonged exposure to high levels of estrogen during the menstrual cycle (Singletary, 2003). In fact, females with early menarche at age less than 12 years old have a 10 to 20% elevated risk of breast cancer occurrence. Additionally, females with delayed menopause after the age of 55 years old are more predisposed to getting breast carcinoma (Dumitrescu and Cotarla, 2005, Titus-Ernstoff et al., 1998).

1.1.4.4 Late or Low Parity

Moving on to the modifiable risk factors, a female having her first pregnancy at a younger age and having more children has lower risk of developing breast cancer

(Brinton et al., 1988). On the other hand, null-parity and first pregnancy after the age of 30 years old are two modifiable risk factors that can contribute to increased risk of developing breast cancer (Hulka and Moorman, 2008).

1.1.4.5 Use of Hormonal Pills

Use of oral contraceptives as well as hormone replacement therapy (HRT) is another two modifiable risks that can contribute to higher breast cancer incidence rate (Collaborative Group on Hormonal Factors in Breast Cancer, 1996). A slight increase in risk of developing breast cancer has been reported in females using oral contraceptives especially those with higher amounts of estrogen; nevertheless, the risk is observed to reduce after termination of the oral contraceptive intake (Hulka and Moorman, 2008). The risk of breast cancer development also decreases in females after a 5-year cessation of HRT usage (Boyle, 2005).

1.1.4.6 High Fat Diet and Sedentary Lifestyle

Certain breast cancer risk factors such as physical activity and diet type are modifiable. Alcohol intake has been correlated with enhanced breast cancer risk (Zhang et al., 2007, Terry et al., 2006) due to possible increment in estrogen levels upon intake (Singletary and Gapstur, 2001). Obesity in post-menopausal females is also positively associated with elevated breast cancer risk. The high fat consumption in meals and its accumulation of body fat in these females can have an effect on the incidence of hormonally dependent breast cancer as fats in the plasma can significantly increase the levels of circulating estrogens (McTiernan et al., 2003). Apart from that, there have been controversies on soy intake as certain studies associated soy intake with decreased risk of breast cancer development as soy-based products contain isoflavones (or phyto-estrogen) while some studies showed otherwise (Boyle, 2005). Also, though there is no consistent significant correlation between breast cancer risk and physical activity, it is still suggested that physical activity has an indirect impact on body fats, which can contribute to estrogen levels (Colditz et al., 2003).

Hence, females should reduce the incidence of breast cancer by increasing physical activity, eating low-fat foods, minimizing alcoholic beverage intake, maintaining a healthy body weight, and reducing hormone intake. Breast-feeding by mothers is also encouraged as it decreases estrogen production due to suppression of the ovulatory cycle and increases secretion of prolactin, giving it a protective effect against breast cancer (Vogel, 2012).

1.1.5 Symptoms of Breast Cancer

For early detection of breast cancer, all females should be familiar with both appearance and feel of their breasts in order to promptly report any changes to a doctor. The most frequent physical symptom of a potential breast cancer case is a painless lump in the breast (American Cancer Society, 2012a). At times, the tumor mass can be felt at the axillary lymph nodes (underarm) before the primary breast tumor is sufficiently large to be felt. Other less frequent symptoms consist of breast pain, changes to the breast (swelling, thickening, skin irritation, skin distortion), and abnormalities at the nipple (bleeding discharge, erosion, inversion) (Osteen, 2001, American Cancer Society, 2012a).

1.1.6 Classification of Breast Cancer

Classification of breast carcinoma provides details on the extent of the disease at the point of diagnosis i.e. the size and location of the primary tumor as well as presence and extent of metastasis to other parts of the body. The classification of a breast cancer tumor is vital in determining the therapy choice and estimating the prognosis of the patient. The tumor-node-metastasis (TNM) staging system, proposed by Pierre Denoix, is commonly used in clinical settings and it evaluates tumors in three aspects: (T) assesses size and extent of the primary tumor; (N) investigates the absence or presence of regional lymph node involvement; (M) evaluates the absence or presence of distant metastases (Arnone et al., 2010, Escobar et al., 2007). Upon determination of the TNM characteristics, stages are assigned with stage 0 being in situ while stage IV being invasive carcinoma (Sobin

et al., 2009, American Cancer Society, 2012a). Table 1.1 gives a brief description of the various TNM staging:

Table 1.1 Various TNM staging

Stage	Description
0	The breast tumor is at in situ stage, whereby the cancer cells are still contained within the duct or lobule.
I	The breast tumor is relatively small with a maximum size of 2cm. No lymph node metastasis is involved at this stage.
II	The breast tumor size is between 2 and 5cm, with lymph node metastasis to the ipsilateral axillary nodes. Breast tumors larger than 5cm with negative lymph node involvement are also categorized as Stage II.
IIIA	The breast tumor is of any size or more than 5cm, with lymph node metastasis to the ipsilateral axillary lymph nodes or other surrounding structures.
IIIB	Inflammatory carcinoma usually occurs at this stage. The breast tumor can be of any size with metastasis to the ipsilateral lymph nodes.
IV	The breast tumor is of any size with metastasis beyond the ipsilateral supraclavicular lymph nodes.

Breast tumor originates in the breast tissue, mostly from the epithelia of ducts and lobules. Most lumps or masses are benign, that is they do not have uncontrolled growth or spread and are not life-threatening. Breast cancer of in situ stage is characterized by tumor cells that are still confined within their site of origin: ducts (ductal carcinoma in situ or DCIS, as shown in Figure 1.2) and lobules (lobular carcinoma in situ or LCIS). DCIS accounts for majority of the in situ breast cancer cases, accounting about 83%, while LCIS takes up 11% of in situ cases. The remaining in situ types have features of both DCIS and LCIS or have unspecified site of origin. Most breast cancer cases are of the invasive type, whereby the tumor cells from the ducts or lobules have broken through the basement membrane to invade into the surrounding breast tissues, and if left undiagnosed, metastasis may occur (American Cancer Society, 2012a). Metastatic spread occurs mainly through lymphatic drainage of the breast. The lymph passes from the nipple, ducts and lobules to the subareolar lymphatic plexus; after which, majority (more than 75%) of lymph drains through the axillary lymph nodes (Nawaz, 2011, Moore and Agur, 2007). The remainder of the lymph will drains into the internal mammary nodes. (Hoda, 2012).

Apart from ductal carcinoma and lobular carcinoma, there are other various types of breast cancer including inflammatory breast cancer, triple negative breast cancer, phyllodes tumor, mucinous carcinoma, and medullary carcinoma (van Bogaert, 1981). In this study, I will be focusing on invasive ductal carcinoma (IDC) tumors. Hence, the details of IDC tumors will be discussed in greater detail.

1.1.7 Invasive Ductal Carcinoma

IDC is the most frequently diagnosed breast carcinoma, constituting 60 to 80% of all breast cancer cases (Rosen, 2009). IDC cases make up 79.2% of all breast cancer cases in Singapore (Seow et al., 1996). IDC is marked by its characteristics of having malignant ductal epithelial cells with abnormal growth and their invasion into the surrounding breast stromal tissue (as depict in Figure 1.2). The gross appearance of the breast tumor is often a fibrous and solid lump. At the histology level of IDC, the tumorigenic ductal cells would often invade in an irregular manner and are at times correlated with lymphoplasmacytic infiltrate. It is hence important for histopathologists to utilize a grading system to evaluate the breast tumor.

The grading system of IDC tissues can be performed based on three histological factors, namely mitotic frequency, degree of nuclear pleomorphism, and extent of tubule formation. Each of these three factors is given a score of 1 to 3. After which, the scorings of the three factors will be added up to give the Bloom-Richardson score (Meyer et al., 2005). Table 1.2 shows a description of the score range. Classifying IDC patient tumors into their respective grades will aid physicians in predicting treatment response to chemotherapy as well as patient's prognosis.

Table 1.2 Classification of tumor by Bloom-Richardson score

Tumor Grade	Bloom-Richardson Score	Description
1	3 to 5	Well-differentiated
2	6 to 7	Intermediate
3	8 to 9	Poorly differentiated

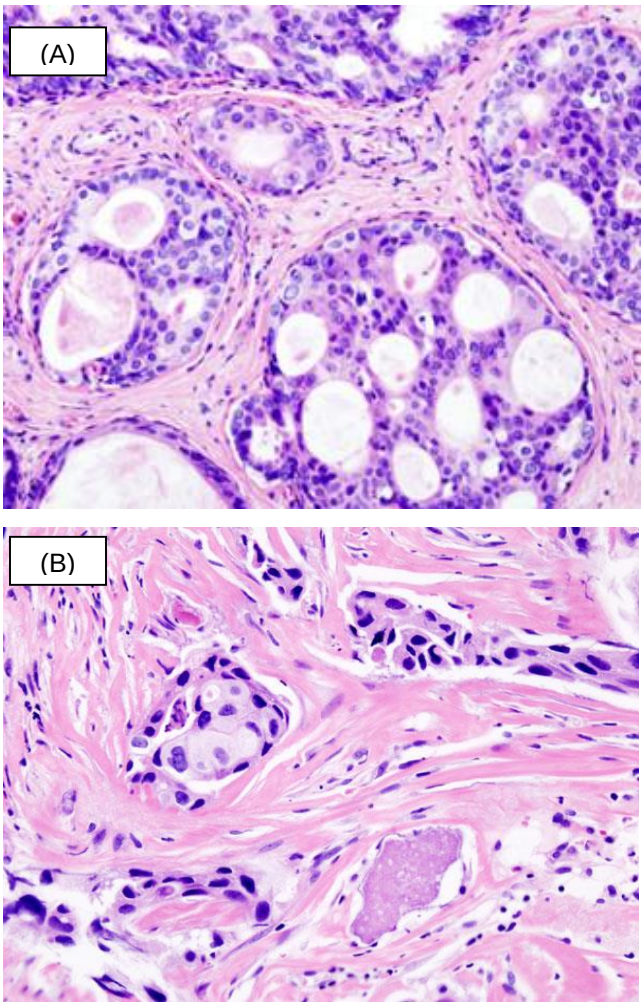

Figure 1.2: Histopathology of ductal carcinoma.
(A) depicts ductal carcinoma in situ, whereby the malignant ductal epithelial cells are still within the basement membrane. (B) illustrates IDC, whereby the malignant ductal epithelial cells have broken passed the basement membrane and invaded into the surrounding breast tissues. [This image is free from copyright and is free to be shared]

1.1.8 Detection of Breast Cancer

Apart from reducing risk factors involved, every female above age 40 years old should consider annual clinical breast examination and standard radiological imaging (such as mammography, ultrasound scan, and magnetic resonance imaging) for early breast cancer detection to increase their survival rate (Saslow et al., 2007). Early breast cancer detection can help reduce breast tumor recurrence as well as breast cancer-related mortality as treatment is more effective in patients at this stage of breast carcinoma (Hakim et al., 2012). Detection of the tumor at later

stages will give rise to poorer patient prognosis. For US females, the overall five-year survival for those with early breast cancer stage is 98% in comparison to those with late breast cancer stage with the tumor cells spread to regional lymph nodes (84%) or distant organs (23%) (American Cancer Society, 2011). Therefore, public health campaigns are constantly carried out to raise awareness of the importance of early detection for breast cancer.

1.1.8.1 Breast Self-Examination

Every female is able to perform their own breast examination, of which is non-invasive and it can be done comfortably on a regular basis to detect any changes in the breast. It is recommended that females be taught the correct techniques by their physicians for breast self-examination. In developing countries, as mammography screening can be costly, the recommended early detection strategies there are to create awareness of breast cancer, its signs and symptoms, and carry out self breast examination (Anderson et al., 2008).

1.1.8.2 Mammography

Mammography screening has been shown of its capability in detecting breast cancer at an earlier stage when more treatment options are available; the treatment(s) would also be more effective and survival rate is higher (American Cancer Society, 2011). Mammography will specifically aid in detecting the presence of potential malignant masses seen as a stellate opacity, accompanied with architectural distortion of the surrounding parenchyma. At times, a DCIS mass may appear as micro-calcification on the mammogram (Standring, 2008). In the United States of America female population, mammography screening done every 1 to 2 years showed a decrease in breast cancer-related mortality especially for females aged 40 years old and beyond (Smith et al., 2004). In Singapore, 64% of breast cancer cases detected were of the early stage (Tan et al., 1999). The Singapore Health Promotion Board has subsequently held nation wide mammography screenings in order to decrease breast cancer-related mortality (Wang, 2003).

1.1.8.3 Ultrasound

Ultrasound is another method used to help detect solid form of cystic masses, as well as differentiate malignant mass from benign lumps through different attenuation features of the ultrasound waves and blood flow patterns (Gabriel and Domchek, 2010). Nowadays, ultrasound is used as an additional important aid to mammography for breast cancer detection. It is usually used on females with potentially higher risk of breast cancer or with high breast tissue density (Irwig et al., 2004).

1.1.8.4 Magnetic Resonance Imaging

Magnetic resonance imaging (MRI) is sometimes used to further define the extent of the cancer (Saslow et al., 2007). MRI has higher sensitivity but lower specificity of tumor detection; hence, it is lesser used compared to mammography and ultrasound scan, and is particularly used in younger females having more dense breasts (Standring, 2008). Nevertheless, it can be used to follow tumor response after a patient undergoes chemotherapy (Hakim et al., 2012).

1.1.9 Definitive Diagnosis of Breast Cancer

After acquiring a plausible detection/diagnosis using radiological imaging, microscopic examination of the breast tissue would be required to give a definitive diagnosis of breast cancer as well as to determine the type of breast cancer, such as whether the cancer is of in situ or invasive type, and if the tumor is of ductal or lobular carcinoma type (American Cancer Society, 2012a).

1.1.9.1 Tumor Biopsies

Fine needle aspiration is able to achieve a cytological diagnosis of the breast lump, providing information on the cellular component of the lump. It can also be used to drain symptomatic breast cysts (Abati and Simsir, 2005). Wide-bore needle biopsy, on the other hand, is performed under local anaesthetic to attain specimen samples

for a histological diagnosis, permitting diagnosis of the tumor subtype through evaluation of various pathological characteristics (Standring, 2008).

1.1.9.2 Prognostic Markers for Breast Cancer

Even though lymph node status and primary tumor size are two powerful prognostic factors, at times, they can give inaccurate predictions of the survival outcome of the patients (Chen et al., 2009a, Gebauer et al., 2002). This may lead physicians to be more cautious in eradicating all possible tumors and hence recommending chemotherapy, of which patients may or may not benefit from.

Tumor biomarkers are increasingly being used in the clinical setting to aid in the estimation of patients' prognosis, determination of treatment choices, prediction of treatment outcome, and for better treatment response monitoring (American Cancer Society, 2012a). Some of the more well-known validated biomarkers for breast carcinoma include estrogen receptor (ER), progesterone receptor (PR), human epidermal receptor 2 (HER2), *BRCA1*, uPa/PAI1, and Ki67.

Breast cancer cells with ER and/or PR are dependent on their respective ligands, estrogen and progesterone, for cell growth. ER, in the form of ERα, is present in 70% of breast cancer cases. Evaluation for ER and PR status in patients' tumor samples can be carried out to determine if the tumor can be successfully treated with hormone therapy, such as tamoxifen. ER+ and PR+ will generally offer better survival outcome as well as better response to hormone therapy (Onitilo et al., 2009). Tamoxifen will block ER and give rise to anti-malignant properties such as reduction in cancer cell growth. Tamoxifen is able to significantly decrease tumor recurrence risk within 5 years by 40% and increase overall survival by 31% (Early Breast Cancer Trialists' Collaborative Group, 2005). Other than that, aromatase inhibitors such as anastrozole work through the inhibition of conversion of precursor molecules to estradiol. Besides that, the presence of ER in a patient's tumor is usually correlated with less beneficial effects from adjuvant chemotherapy.

This would help avoid unnecessary over-treatment and possible adverse side effects in the patient. As for PR, it is strongly dependent upon ER activity. Hence, PR+ breast tumors also have better patient survival outcome in comparison with PR- breast tumors (Anderson et al., 2001). Both ER and PR status in breast cancer tissues can be evaluated through immunohistochemistry by a pathologist.

Human epidermal growth factor receptor 2 (HER2 or ERBB2), a transmembrane receptor with constitutive tyrosine kinase activity, is another well-established biomarker (Weigelt et al., 2005). HER2 has been reported to be involved in cell motility, adhesion, and differentiation. Clinical studies have generally shown that HER2 is over-expressed in breast tumors of higher grade (Slamon et al., 1987, Slamon et al., 2001). In addition, high expression of HER2 has been associated with higher risk of tumor recurrence and worse prognosis (Slamon et al., 1987, Ross and Fletcher, 1998). The finding of HER2 has an important biomarker has led to the development of a humanized monoclonal antibody (trastuzumab), designed against HER2 (Baselga et al., 1998). Trastuzumab is used in combination with chemotherapy in breast cancer patients diagnosed with over-expression of HER2 antigen (Weigelt et al., 2005). Studies including randomized clinical trials have demonstrated reduced risk of tumor recurrence, decreased metastasis and improved survival rate in patients given trastuzumab treatment in comparison to those not receiving trastuzumab therapy (Slamon et al., 2001, Viani et al., 2007).

BRCA1 gene is a well-known hereditary marker in breast cancer (Scully and Puget, 2002). It is involved in the regulation of cell cycle, chromosomal remodeling and DNA repair. Loss of *BRCA1* in breast carcinoma would not only cause decreased expression of *BRCA1*, but also incorrect sub-cellular localization (Rebbeck et al., 1996). This in turn would lead to worse prognosis in breast cancer patients. Additionally, loss of *BRCA1* has been correlated with tumors of higher grade and larger size, advanced lymph node involvement, vascular invasion, as well as ER and PR negative statuses (Heisey et al., 1999).

Urokinase plasminogen activator (uPa) and plasminogen activator inhibitor (PAI-1), involved in the plasminogen activating system, have crucial roles in cell invasion, metastasis and angiogenesis (Stephens et al., 1998). Both uPa and PAI-1 are highly expressed in breast cancer tissues (Duffy, 2002). In addition, both biomarkers have been validated of their prognostic importance in several retrospective studies as well as in a multi-center randomized prospective clinical trial (Janicke et al., 2001, Look et al., 2003). According to the American Society of Clinical Oncology (ASCO), both biomarkers can be utilized to determine patients' prognosis, especially for those diagnosed with node-negative breast carcinoma (Duffy, 2013). In general, patients with high expression of uPa and PAI-1 have been associated with significantly higher risk of tumor recurrence. For these patients, adjuvant chemotherapy, specifically CMF-based which consists of cyclophosphamide, methotrexate, and fluorouracil, would be more beneficial compared to observation alone (Harris et al., 2007).

Ki67 is a prognostic biomarker involved in tumor cell proliferation. Its expression level has been reported to be elevated in malignant breast tissues (Harper-Wynne et al., 2002), its expression increasing progressively from DCIS to IDC breast cancer type (Kontzoglou et al., 2013). Therefore, high expression of Ki67 is associated with better therapeutic response towards chemotherapy as well as being a good biomarker for poor prognosis.

Developing single gold-standard biomarkers is however difficult as tumor cells are known for their genetic instability and plasticity, which help in the tumor cells' change and response towards the host defense system. It would also make it tricky for physicians to determine a patient's relapse risk after treatment. Therefore, having biomarker panels and developing more improved panels that are able to identify high-risk and low-risk groups by providing a "yes" or "no" answer on tumor recurrence in a patient will significantly improve disease management. Hence, it is crucial for the cancer research community to understand a network of

genes significantly involved in breast cancer tumor progression, in order to improve disease management.

Some biomarker panel assays available include the 70-gene MammaPrint® signature assay and the 21-gene Oncotype DX panel, both of which are able to determine the risk of tumor recurrence and prognosis outcome in a patient (Manjili et al., 2012, Espinosa et al., 2012). As an example, the assays can generate gene signatures that will determine that a patient in the high risk group has 30% chance of having tumor recurrence while a patient in the intermediate risk group will have a 14.3% chance of tumor recurrence within 5 to 10 years (Manjili et al., 2012). As for patients in the low risk group, they have a recurrence free survival rate of over 90% without having the need to receive chemotherapy (Espinosa et al., 2012).

The MammaPrint® assay has been cleared for use by the US Food and Drug Administration (FDA) in patients with lymph node negative status (and ER+ or ER- status) and tumors smaller than 5cm to determine the prognosis outcome of the patients (van 't Veer et al., 2002, van de Vijver et al., 2002). The assay can help in refining the prognostic value of traditionally-used biomarkers such as HER2. Recent studies also suggest that the MammaPrint® assay has predictive value, being able to predict the patients' treatment response (Straver et al., 2010). The microarray-based assay utilizes high quality RNA, obtained from patients' tumor tissue samples, which would then be processed to be used to obtain 70 gene expression levels. The 70-gene signature includes genes associated with cell invasion, metastasis, proliferation, and angiogenesis, of which would be used to determine if a patient has low or high risk of tumor recurrence. This is beneficial for patients as it would prevent over-treatment in patients with a low risk cancer and under-treatment of patients with high risk cancer (Gokmen-Polar and Badve, 2012). Generally, patients of high risk, as determined by standard clinicopathological parameters (such as tumor grade and tumor size) and MammaPrint® gene signature would be administered with chemotherapy. On the other hand, patients identified with low risk will receive hormonal therapy. The

MammaPrint assay helps these patients with low risk avoid unnecessary chemotherapy, giving them a maximum 10% risk of tumor recurrence within a minimum of 5 years (Manjili et al., 2012).

The 21-gene Oncotype DX assay is able to evaluate 16 cancer-related and 5 control genes through RT-PCR using RNA isolated from paraffin-embedded breast cancer tissue (Elloumi et al., 2011). The assay is mainly used among patients with lymph node negative and ER+ status, of which cancer-associated genes such as ER, PR, HER2, and Ki-67 are evaluated. A recurrence score will be generated with heavier weightage on ER and proliferation-related genes. Studies have shown that the Oncotype DX assay is better than standard clinicopathological parameters in predicting tumor recurrence (Gokmen-Polar and Badve, 2012). From the retrospective case-control clinical trial (NSABP Trial B-20), results showed that patients with high recurrence risk score benefit significantly from chemotherapy, compared to patients with low recurrence risk score who had minimal benefit (Paik et al., 2006). Moreover, adjuvant chemotherapy improved recurrence-free survival in 30% of patients with high recurrence risk score. While the Oncotype DX test is recommended by expert panels, it is not validated in a large prospective, randomized clinical trial. The TAILORx clinical trial is currently being carried out to address this validation (Manjili et al., 2012).

1.1.10 Treatment for Breast Cancer

Treatment options are dependent upon the stage, size and other clinical characteristics of the tumor, as well as patient preference.

1.1.10.1 Surgery

Surgery methods comprise of lumpectomy (removal of the tumor within the breast) or mastectomy (removal of the whole breast) with removal of some axillary lymph nodes. The surgical method to be used is dependable upon the stage and distribution of the tumor as well as the patient's choice (American Cancer Society, 2012a). At

present times, lumpectomy is more often carried out compared to mastectomy to extract out only the tumor and surrounding tissues following radiation therapy as part of breast conserving surgery (Anderson et al., 2008, Moore and Agur, 2007).

1.1.10.2 Radiation Therapy

Radiation therapy can be administered prior to and after surgery in order to reduce the patient's tumor size and to eliminate remaining cancer cells respectively (Clarke et al., 2005). Reports showed that tumor recurrence is reduced and patient's survival is improved following radiation therapy that is used after surgery (Ragaz et al., 1997).

1.1.10.3 Chemotherapy

Chemotherapy is administered before or after surgery, and is often given to patients with metastasis, to reduce the risk of tumor recurrence in the patients (Falo et al., 2005). Some more common chemotherapeutic drugs used in treating breast cancer include doxorubicin, methotrexate, and 5-fluorouracil (Falo et al., 2005). Also, a combination of different chemotherapeutic drugs is more effective compared to a single drug for therapy (Hortobagyi, 1998). Some examples of successful drug combinations include doxorubicin and cyclophosphamide as well as methotrexate, 5-fluorouracil and cyclophosphamide [Brennan 2005].

1.1.10.4 Hormonal/Biological Therapy

Hormonal or biological therapy is administered, for example, when the patient's breast tumor is positive for ER/PR. The basis of this therapy is to introduce an agent that will bind to ER, inhibiting the binding of estrogen ligand with ER, and hence decreasing estrogen levels to the cancer cells. Tamoxifen is a common hormonal therapeutic drug given to both pre- and post-menopausal females (Fabian, 2007). HER2 biomarker is another well-known example involved in hormonal/biological therapy. As HER2 is over-expressed in 20 to 25% of breast cancer cases,

trastuzumab, a humanized monoclonal antibody, has been developed to directly target HER2 (Slamon et al., 1987). The binding of the antibody to the receptor will inhibit tumor cell proliferation in breast cancer cells over-expressing HER2. Another approach in hormonal therapy is to inhibit the formation of estrogen by introducing aromatase inhibitors; the inhibitors will inhibit cytochrome P450 activity, of which will subsequently prevent androgens from converting to estrogens (Chumsri et al., 2011). This approach however can only be used in post-menopausal females, as pre-menopausal females still have functional ovaries which are still able to generate estrogen (Milla-Santos et al., 2003, Mouridsen et al., 2003).

1.1.11 Current Challenges in Breast Cancer

Conventionally, physicians use well-established breast cancer clinical parameters such as tumor size, tumor grade, lymph node stage, and well-studied biomarkers – hormonal markers (ER, PR, and HER2) (Hatsell et al., 2005), hereditary molecules (*BRCA1* and *BRCA2*) (Parsons, 2005) – to diagnose, determine suitable treatment options for patients and estimate the survival outcome of the patients. In the current medical world, although these characteristics are useful, basing diagnosis, therapy, and prognosis solely on them alone is not enough. Breast cancer is a heterogeneous disease with, at times, unpredictable survival outcome. There are still groups of breast cancer patients that do nor respond well to current available treatments or encounter tumor recurrence at a shorter period of time. It is therefore critical to achieve more reliable characterization of the tumor to enable more accurate diagnosis of the breast cancer subtype and hence improved treatment options and prediction of treatment response and survival outcome. Breast tumors cannot be oversimplified of its classification by just separating tumor cases by carcinoma in situ and invasive carcinoma, or ER+ and ER- tumor types. More specific biomarkers for screening in conjunction with current clinicopathological parameters are hence needed to identify the patient's breast tumor subtype more accurately (Masood and Dabbs, 2012).

1.2 Glycosaminoglycans and Proteoglycans

The ongoing need to discover additional distinctiveness of breast cancer is critical to further understand breast cancer and to help patients cope with the cancer more effectively through a more personalized treatment option, thus improving their quality of life. Biomarkers has been gaining potentiality to help in diagnosis, prognosis, and treatment of the patients. Knowing the expression of the marker can aid in determining the stage of the cancer, estimate the survival rate and tumor progression of the patient, and provide targeted therapy options to effectively reduce the tumor size and increase the patient's survival rate. Glycosaminoglycan molecules have recently been of great interest to researchers studying their associations to breast cancer. Initial findings have related changes in glycosaminoglycan expression levels to breast tumorigenesis.

1.2.1 Structure of Glycosaminoglycans and Proteoglycans

Glycosaminoglycans (GAG) are heteropolysaccharides, composed of alternating uronic acid units and hexoamine amino sugars, found in various tissues (Yip et al., 2006, Feldner et al., 2006). There are four major classes of GAGs constituting of chondroitin/dermatan sulfate, heparan sulfate, keratan sulfate, and hyaluronan (Yip et al., 2006). GAGs, except hyaluronan, are expressed in tissues as proteoglycans, of which are covalently bounded sulfated GAGs on core proteins (Yip et al., 2006, Berto et al., 2003). The GAG chains would be attached to a serine residue on the core protein via a tetrasaccharide linkage region as shown in Figure 1.4 (Yip et al., 2006).

Proteoglycans (PG) are principal structures found on cell surfaces and in the extracellular matrix (Berto et al., 2003). PGs play vital roles in the regulation of multiple signaling pathways and in the interactions between cells and their environment (Wade et al., 2013). They have major roles in cell proliferation, migration, adhesion, and angiogenesis (Raman et al., 2005, Cecchi et al., 2012).

GAGs and PGs have garnered much interest as their expression can potentially indicate diagnostic and prognostic values in cancer, and pave the way for novel targeted therapeutics (Yip et al., 2006). For example, studies have indicated that alterations in CS/CSPG expression and structure are seen in a wide variety of cancers such as breast cancer, prostate cancer, gastric cancer, pancreatic cancer, and melanoma (Suwiwat et al., 2004, Yang et al., 2004, Pirinen et al., 2005, Pukkila et al., 2007). In this study, chondroitin sulfate is my GAG of interest; hence, its characteristics will be elaborated.

1.2.2 Chondroitin Sulfate and Chondroitin Sulfate Proteoglycans

Chondroitin sulfate (CS) is located mainly on the cell surface and in the extracellular matrix (ECM) (Huang, 1974). CS consists of repeating disaccharide units of alternating N-acetyl-galactosamine (GalNAc) and glucuronic acid (GlcA) (Sugahara et al., 2003, Silbert and Sugumaran, 2002). There are various forms of CS molecules, including CS-A, CS-C, CS-D, and CS-E (CS-B is reclassified as dermatan sulfate (DS)). Each of these CS molecules is distinctive of one another by its sulfation patterns (Sugahara et al., 2003, Kusche-Gullberg and Kjellen, 2003). The various CS molecule forms of different sulfation configurations are formed through sulfation modification. Figure 1.3 illustrates the differences in sulfation patterns between the various CS molecules. CS-A and CS-E are sulfated at carbon 4 of the GalNAc unit, whereas CS-C and CS-D have a sulfated site at carbon 6 of the GalNAc unit (Grande-Allen et al., 2007). Additionally, CS-D and CS-E have an extra sulfation site in their disaccharide units; the additional sulfate site for CS-D is located at the carbon 2 of GlcA while CS-E is also sulfated at carbon 6 of GalNAc (Sugahara et al., 2003, Kusche-Gullberg and Kjellen, 2003). Hence, at times, CS-A, CS-C, CS-D, and CS-E are sometimes known as C4S, C6S, C-2,6-S, and C-4,6-S respectively. The distinctive sulfation patterns would not only give rise to structural diversity of the CS molecules, but also cause a variety of ligand-binding capacities, diverse signaling effects, and hence varied modulations of cellular behaviors (Kusche-Gullberg and Kjellen, 2003).

The CS molecules are usually attached to a core protein, therefore forming CS proteoglycan (CSPG) (Souza-Fernandes et al., 2006). The attachment is possible via a protein scaffold (as depicted in Figure 1.4) (Parcell, 2002, Bali et al., 2001). The CSPG family also has a variety of family members, ranging from CSPG1 to CSPG8, some of which have been implicated to have major functional roles in breast cancer.

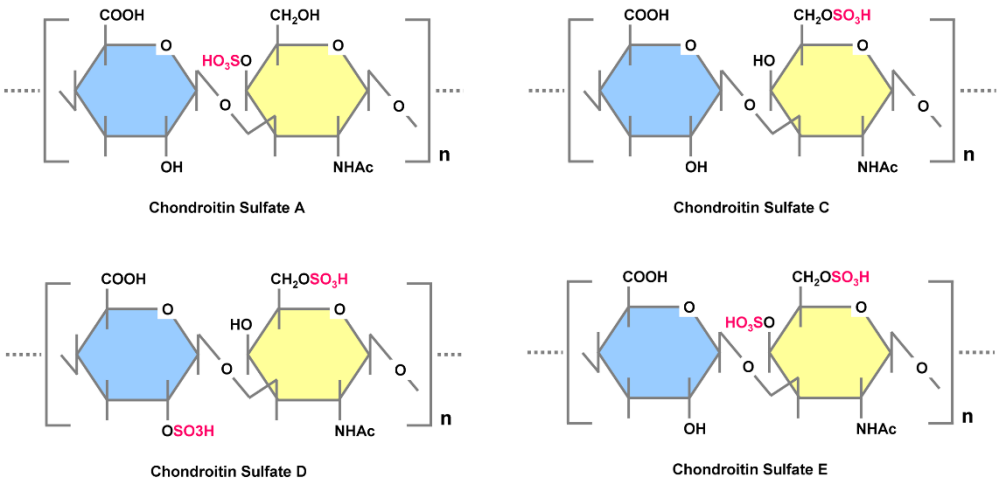

Figure 1.3: Various forms of CS molecules.

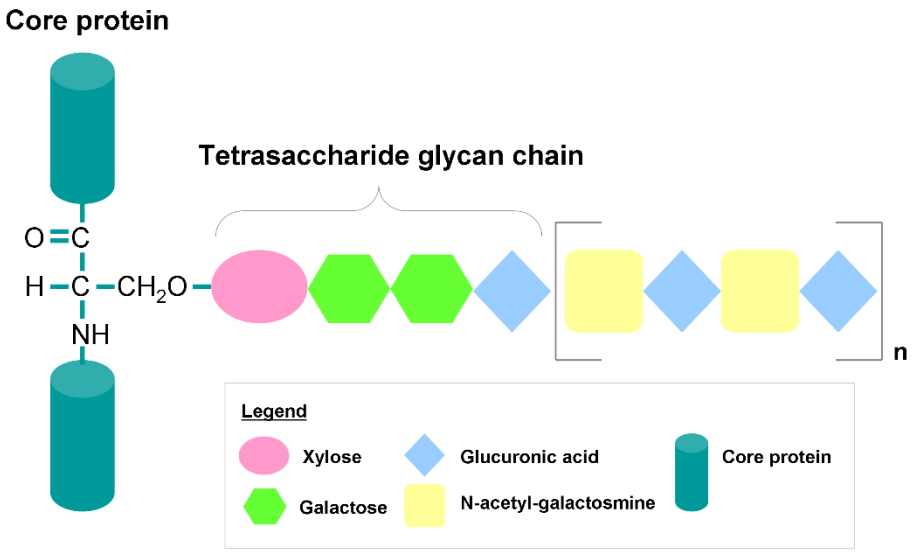

Figure 1.4: Structure of CPSG. The CS molecules are attached to the core protein via a short tetrasaccharide glycan chain, consisting of one xylose, two galactose units, and one

GlcA, at the serine residue of the core protein. After which, polymerization of the CS disaccharide units (GalNAc and GlcA) would follow on. The CS molecules then undergo modification through sulfation to form variable CS forms (Sugahara et al., 2003, Silbert and Sugumaran, 2002).

1.2.3 Biosynthesis of Chondroitin Sulfate and Chondroitin Sulfate Proteoglycan

CS and CSPG expression is regulated by a wide range of enzymes in a complex biosynthesis pathway, leading to their variability in structure and function. Briefly, the tetrasaccharide glycan linkage is firstly synthesized by Xylotransferase 1 (XYL1) and Xylotransferase 2 (XYL2) through the addition of xylose to the serine residue of the core protein (Gotting et al., 2000). The addition of two galactose units to xylose is next catalyzed by two galactosyltransferases, coded by B3GALT6 and B4GALT7 (Bai et al., 2001). The last unit of the glycan linkage, glucuronic acid, is added by glucuronyltransferase I, which is coded by B3GAT3 (Potapenko et al., 2010, Kitagawa et al., 1998).

The synthesis of the CS chain is next initiated by chondroitin sulfate N-acetylgalactosaminyltransferase 1 (CSGALNACT-1), which adds a galactosamine to the linkage region (Sato et al., 2003, Uyama et al., 2002). Subsequent chain polymerization of CS (i.e. the elongation of CS chain through addition of the disaccharide units of glucuronic acid and galactosamine) is catalyzed by chondroitin sulfate N-acetylgalactosaminyltransferase 2 (CSGALNACT-2), chondroitin sulfate glucuronyltransferase (CSGLCAT), chondroitin synthase 1 (CHSY1), chondroitin synthase 3 (CHSY3), and chondroitin polymerizing factor (CHPF) (Potapenko et al., 2010).

Sulfation modifications subsequently take place to generate the various types of CS chains. The modifications are catalyzed by chondroitin sulfotransferases (CHSTs) (Potapenko et al., 2010). Some examples of CHSTs include CHST3 and CHST7 as well as CHST11 and CHST13, which aid in the transfer of the sulfate group from 3'-phosphoadenosine-5'-phosphosulfate (PAPS) to the galactosamine unit

specifically at carbon 6 and carbon 4 respectively (Hiraoka et al., 2000, Kitagawa et al., 2000, Cooney et al., 2011).

1.2.4 Functions of Chondroitin Sulfate and Chondroitin Sulfate Proteoglycans

GAGs were once thought to only serve as space-filling function required for the orientation and organization of the exogenous matrix (Meyer and Palmer, 1934). CSPGs via their CS chains would interact with the extracellular matrix substances such as fibronectin, collagen, and laminin, generating stabilization in structure (Bernfield et al., 1999) (Jalkanen., 1992). Advances in glycobiology have shown otherwise.

CS is a major component of cartilages, making it vital in maintaining elasticity and integrity of the cartilage matrix in the joints. In the form of CSPG, CS within the interfibrillar collagen matrix have great affinity for water and capable of generating compressive resilience, giving rise to cartilages with shock-absorbing properties (Chan et al., 2005). Also, CS is important in inhibiting proteases and cytokines responsible for cartilage destruction, of which would cause arthritis (Lesjak and Ghosh, 1984). In the clinical setting, the chondroprotective properties of CS make it possible for clinicians to use them as alternative agents in the treatment of osteoarthritis. Apart from the cartilage, CS is also found naturally in other parts of the human body such as bones and skin (Parcell, 2002).

Additionally, CS/CSPGs have been discovered to be vital regulators of various cellular signaling processes affecting cell proliferation, migration, and adhesion (Yin, 2005). Deregulation of the CS/CSPGs cause significant functional repercussions, including skeletal disorders, viral and bacterial infections, and cancers (Mikami and Kitagawa, 2013).

1.2.5 Chondroitin Sulfate and Chondroitin Sulfate Proteoglycans in Cancer

Studies conducted have shown significant associations of CS expression with regard to breast cancer. The alterations in cell surface CS expression and consequently, ECM-degradative enzymes, such as matrix metalloproteinases, can change the cell's invasiveness and cell-matrix interactions (Yip et al., 2006). From *in vitro* studies, breast cancer cells have been observed to have a general increase in CS expression, of which has been correlated to enhanced cell proliferation and migration (Kieber-Emmons et al., 2011, Alini and Losa, 1991, Olsen et al., 1988). At the tissue level, CS in general are significantly highly elevated in the stromal compartment of breast tumors (Ricciardelli et al., 2002, Suwiwat et al., 2004). Supporting this, MDA-MB-231 breast cancer cells releases high amounts of CSPGs into the culture medium, suggesting the enhanced level of CS in the stromal compartment. Additionally, in general, high CS level in breast cancer cells is linked to shorter overall survival and recurrence-free survival (Svensson et al., 2011). CS expression has been shown to be an independent predictive prognostic factor, with high CS expression levels having a hazard ratio of 1.71 to 2.28 in the cohort of breast cancer patients studied (Svensson et al., 2011). A mouse model study demonstrated that removal of cell surface CS from mouse breast cancer cells led to decreased tumor progression after intravenous injection (Cooney et al., 2011). This highly suggests that cell surface CS may have pivotal role in promoting metastasis and hence, may potentially lead to higher mortality risk. Looking into specific CS molecule type, CS-A chain has been shown to have increased expression level in human breast cancer cells with high metastatic capability (MDA-MB-231 and MDA-MET) compared to less aggressive breast cancer cells, MCF7 (Cooney et al., 2011). CS-E has also been marked as a tumor promoter (Cooney et al., 2011); functional studies *in vitro* showed that the over-expression of CS-E promotes angiogenesis and anti-apoptotic cell behavior (Grose and Dickson, 2005). On the other hand, the opposite trend has been observed for CS-C and CS-D chains; both of these CS molecules are reported to be down-regualted in breast carcinomas

(Potapenko et al., 2010), making them characterized as tumor suppressors instead, unlike their other two CS counterparts.

At the core protein level, studies have also described breast tumor biopsies to have general increases in CSPG expression, particularly CSPG2 and CSPG4, compared against the adjacent normal breast tissues of patients (Vijayagopal et al., 1998). This would hence suggest the possibility of an association between CSPG levels and their role in tumor progression and metastases (Vijayagopal et al., 1998, Delehedde et al., 1997). Two CSPG members have been well-studied in breast cancer, which are versican (CSPG2) and NG2 (CSPG4).

Versican (VCAN or CSPG2) is a large CSPG, which regulates cell adhesion, cell motility, and cell proliferation (Yee et al., 2007, Beck et al., 2008, Bhardwaj et al., 2008). Its role in the regulation of different cellular behaviors is possible through its interactions, via the CS chains (Hirose et al., 2001, Wu et al., 2005, Suwan et al., 2009) with a wide variety of ligands including collagen, fibronectin, chemokines, and epidermal growth factor receptor (EGFR) (Hirose et al., 2001, Zimmermann, 2000). VCAN is up-regulated in malignant breast tissues and is associated with the severity of the cancer (Yee et al., 2007, Brown et al., 1999). Cox regression survival analysis indicated that VCAN expression is a good predictor of relapse-free survival; enhanced expression of VCAN is correlated with higher risk and rate of relapse in patients diagnosed with node-negative breast cancer (Ricciardelli et al., 2002, Suwiwat et al., 2004).

NG2 (or CSPG4) is a cell surface proteoglycan, with enhanced expression levels in malignant breast tissues compared against normal breast tissues. From an *in vitro* study, CSPG4 is up-regulated in triple negative breast cancer cells (MDA-MB-231, MDA-MB-435, HS578T, and SUM149) in comparison to luminal breast cancer cells (MCF7, T47D, and SK-BR-3), which are less aggressive. Further evaluation on primary breast lesions showed that majority (>70%) of triple negative breast cancer tissues displayed higher expression levels of CSPG4 against ER+/HER2+

breast cancer tissues (of which 30% has immunoreactivity to CSPG4 antibody). Moreover, CSPG4 protein was enhanced in breast cancer cells extracted from pleural effusion of patients diagnosed with metastatic breast cancer (Wang et al., 2010b, Wang et al., 2010a). With CSPG4 emerging as a potential diagnostic and prognostic marker, scientists have looked into the development of a CSPG4 antibody-based immunotherapy. *In vitro* evaluation showed that CSPG4-specific antibody regressed cancer cell growth and cell migration. More importantly, in *in vivo*, CSPG-4 specific antibody inhibited tumor growth and metastasis (Wang et al., 2010a). As such, CSPG4 is one promising target for monoclonal antibody-based treatment especially for patients with high CSPG4 expression in their tumor.

1.2.6 Chondroitin Sulfotransferase 3 in Cancer

Chondroitin sulfotransferase 3 (CHST3 or sometimes known as chondroitin-6-sulfotransferase 1 (C6ST1)) gene is located at chromosome 10, with an mRNA and protein size of 1440 base pairs and 55 kDa. CHST3 is one of the many enzymes involved in the sulfation modification of CS molecules, specifically forming CS-C (C6S) and CS-D (C-2,6-S). Its principal role is in catalyzing the transfer of sulfate from 3'-phosphoadenosine-5'-phosphosulfate (PAPS) to the carbon 6 of galactosamine unit (Silbert and Sugumaran, 2002). CHST3 has been reported to be involved in extracellular matrix remodeling (Deeken et al., 2010), hence it is suggested that CHST3 has roles in cell adhesion as well as cell invasion and metastasis.

The role of CHST3 has not been widely studied in cancer. In laryngeal carcinoma, *CHST3* expression level was reduced in malignant tissues compared to normal tissues. Also, lower level of C-6 sulfation was observed to be correlated with higher tumor stage, suggesting CHST3 to have a potential tumor suppressor role in laryngeal cancer (Kalathas et al., 2010). In prostate cancer, single nucleotide polymorphisms in *CHST3* were seen to be associated with toxicity of chemotherapeutic drugs, thalidomide or docetaxel, used on prostate cancer patients.

In pancreatic cancer, *CHST3* expression is postulated to be involved in TGFβ-induced epithelial-mesenchymal transition (EMT) model, indicating *CHST3* potential role in metastasis (Maupin et al., 2010). To date, there is a lack of understanding of CHST3 in breast cancer.

1.3 Scope of Study

Therefore, in this study, CHST3 expression and functional roles are investigated in breast cancer. The outcomes from this study may provide a novel pathway map for the downstream gene(s) involved in cell migration, invasion, adhesion, and proliferation of the breast cancer cells after alteration of *CHST3* expression. Additionally, immunohistochemical expression of CHST3 was examined on clinical tissue samples of IDC. This would allow a possible novel diagnostic and prognostic biomarker for breast cancer and potentially other cancers. Specific objectives of this study are as follows:

- To examine the expression of *CHST3* in various normal and malignant breast cells
- To study the functional role of *CHST3* in breast cancer cells through silencing and over-expression of *CHST3*
- To explore the downstream molecular pathways involving *CHST3* that regulate the phenotypic behavior changes
- To determine the correlations between CHST3 expression and various clinicopathological parameters of patients with IDC
- To evaluate if CHST3 expression could be a potential diagnostic or prognostic biomarker in IDC cases

CHAPTER 2
MATERIALS AND METHODS

2 MATERIALS AND METHODS

2.1 Cell Culture of Breast Cancer Cells

Non-malignant MCF12A as well as malignant T47D, MCF7 and MDA-MB-231 breast epithelial cell lines were obtained from the American Type Culture Collection (ATCC, Manassas, VA, USA) for this study. MCF12A is an immortalized, non-malignant cell lines, established after a long-term cultivation of MCF12M mortal cells, that were harvested at reduction mammoplasty from fibrocystic breast tissue with focal areas of intraductal hyperplasia (Paine et al., 1992). The MCF12A cells were maintained in DMEM-F12 medium supplemented with 5% fetal bovine serum (FBS), 20ng/ml human epidermal growth factor, 100ng/ml cholera toxin, 0.01 mg/ml bovine insulin, and 500ng/ml hydrocortisone. T47D, a Grade 1 IDC cell line, was obtained from the pleural effusion of a 54-year-old female diagnosed with IDC (Keydar et al., 1979). MCF7, another Grade 1 IDC cell line, was derived from the pleural effusion of a 69-year-old female who had metastasis even after having two mastectomies in a span of 5 years (Dickson et al., 1986). Compared to T47D and MCF7 cell lines that are poorly invasive, MDA-MB-231 cell line is a highly invasive human breast adenocarcinoma cell line and is representative of Grade 3 IDC. MDA-MB-231 cells were harvested from a pleural effusion of a 51-year old female (Cailleau et al., 1978). T47D and MDA-MB-231 cells were cultured in RPMI medium while MCF7 cells were given DMEM medium. Both medium were supplemented with 10% FBS. All cell lines were grown at 37^{o}C in a 5% CO_2 atmosphere.

2.1.1 Subculture of Cells

Subculture was performed when cells reach 80 to 90% confluency. Firstly, the culture medium from the flask was aspirated out. This is followed by washing with PBS, to remove residual culture supernatant. The cells were then incubated with trypsin/EDTA for 5 to 10 min at 37^{o}C, for cell detachment. Following incubation, the trypsin activity was neutralized using culture medium. The cell suspension was transferred into a 15ml tube for centrifugation at 1000rpm for 5 minutes. Fresh

culture medium was used to re-suspend the cell pellet and an appropriate volume of cell suspension was transferred into a T25 or T75 flask. Cells above passage number of 30 were discarded.

2.1.2 Cryopreservation of Cells

Cell detachment through trypsinization from culture flasks was firstly carried out. After the centrifugation step and removal of the culture medium, the cell pellet was re-suspended with culture medium containing 20% FBS and 10% dimethyl sulphoxide (DMSO). The cell suspension was transferred into cryovials, which were then placed in a freezing container, Mr Frosty (Nalgene, Rochester, NY, USA). The freezing container will enable uniform cooling of the cryovials at a rate of 1^{o}C per minute in a -80^{o}C freezer. After an overnight storage in the -80^{o}C freezer, the cryovials were placed in a liquid nitrogen storage tank for long term storage.

2.1.3 Thawing of Cells

Frozen vials of cells, taken out from liquid nitrogen storage tank, were thawed immediately. The thawed cell suspension was transferred into a 15 ml tube and re-suspended with 5ml of culture medium. The cell suspension was next centrifuged at 1000rpm for 5 minutes to remove the cytotoxic, cryoprotective DMSO component. After disposing the culture medium supernatant, the cell pellet was re-suspended with 5ml culture medium and transferred into a 25cm^2 culture flask (T25 flask). The cell culture was incubated at 37^{o}C in a 5% CO_2 environment.

2.2 siRNA Transfection

Silencing experiments were carried out using T47D and MDA-MB-231 cell lines. One day prior to siRNA transfection, T47D and MDA-MB-231 cells were seeded in 6-well plates at cell densities of 3.0 x 10^5 cells/well and 2.0 x 10^5 cells/well respectively. The cells were transfected with siRNA targeting the gene of interest (Ambion, CA, USA) or scrambled siRNA (Ambion, CA, USA) as negative control

using Oligofectamine transfection reagent (Invitrogen, Carlsbad, USA) following the manufacturer's protocol. Cells were exposed to the siRNAs in OPTIMEM for 8 hours, after which the medium was replaced with RPMI containing 10% FBS. The transfected cells were then incubated for 48 hours before subsequent assays. Table 2.1 and Table 2.2 show the sequences of the siRNAs specifically targeting the genes of interest used as well as the final siRNA concentrations used respectively.

Table 2.1: siRNA sequences

siRNA (Silencer Select)			**Sequence**
CHST3 (Ambion)	Negative		Scrambled
	siRNA sequence 1	Forward	5'–GAC UGG AUC CAA AAG AAC ATT–3'
		Reverse	5'–UGU UCU UUU GGA UCC AGU CTT–3'
	siRNA sequence 2	Forward	5'–CAU GUA CAC CAU ACA UAG ATT–3'
		Reverse	5'–UCU AUG UAU GGU GUA CAU GTA–3'
GPNMB (Ambion)	Negative		Scrambled
	siRNA	Forward	5'–GGA AUA CAA CCC AAU AGA ATT–3'
		Reverse	5'–UUC UAU UGG GUU GUA UUC CTT–3'
FLRT3 (Ambion)	Negative		Scrambled
	siRNA	Forward	5'–CAA CCA CCC UCA AUC GAG ATT–3'
		Reverse	5'–UCU CGA UUG AGG GUG GUU GTA–3'

Table 2.2: Volume and concentration of reagents used for siRNA transfection

	Reagent	Volume per well (µl)
CHST3 (Final concentration 10nM)	siRNA (1µM)	10
	OPTIMEM	100
	Total	110
GPNMB (Final concentration 5nM)	siRNA (1µM)	5
	OPTIMEM	105
	Total	110
FLRT3 (Final concentration 5nM)	siRNA (1µM)	5
	OPTIMEM	105
	Total	110
Master mix	Oligofectamine	10
	OPTIMEM	100
	Total	110

2.3 CHST3 Over-expression

2.3.1 CHST3 Over-expression Plasmid Preparation

CHST3 over-expression plasmid (OriGene, Rockville, MD, USA) and the corresponding pCMV6-AC-GFP empty vector (OriGene, Rockville, MD, USA) used as negative control were purchased. The maps of the plasmids are shown in Figure 2.1. 1ul of the plasmids (100ng/ul) were used for bacteria transformation into 50ul of DH5α competent Escherichia coli cells. The transformed DH5α bacteria were spread on to LB plates containing 100g/ml ampicillin. The LB plates were then incubated overnight at 37^{o}C. Subsequently, colony PCR was carried out using *CHST3* qPCR primer for the colonies containing *CHST3* over-expression plasmid. As for colonies transformed with the empty vector, VP1.5 and XL39 primers provided by OriGene were used for the colony PCR procedure. Upon confirmation of the plasmid transformation by colony PCR, the same colonies were picked and expanded in 5ml of LB medium containing 100ug/ml ampicillin. The LB/Amp culture was incubated on a shaker (200rpm) overnight at 37^{o}C. The following day, bacterial stocks were preserved in glycerol and stored at -80^{o}C. The

remaining bacterial culture was used for plasmid extraction using QIAprep Spin Miniprep kit (Qiagen, Hilden, Germany). After which, the concentrations of both plasmids were determined using nanodrop spectrophotometry (Thermo Scientific, Asheville, NC, USA).

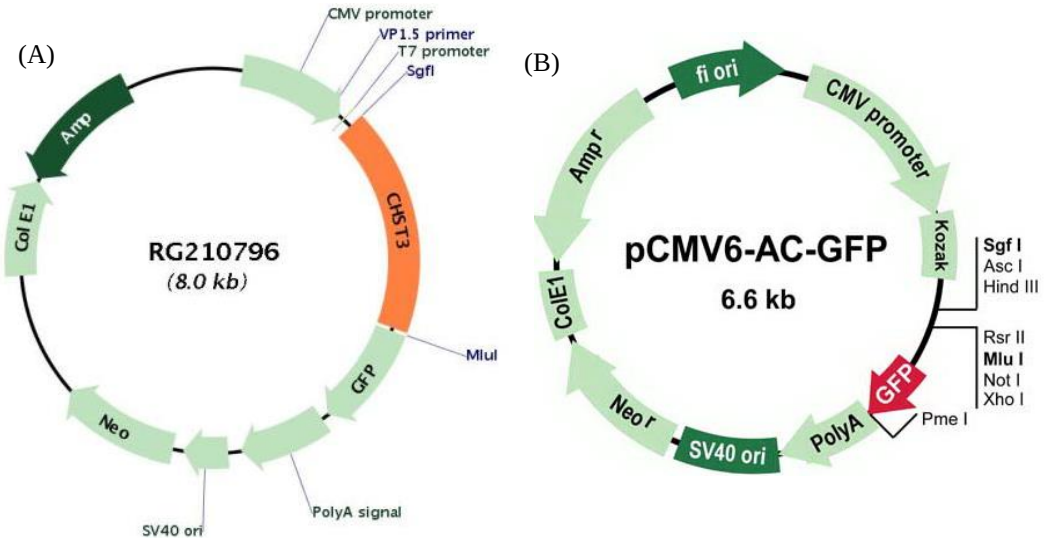

Figure 2.1: Plasmid maps for *CHST3* over-expression study.
(A) shows the plasmid map of the *CHST3*-over-expression plasmid, of which *CHST3* gene is within the empty vector plasmid, pCMV-AC-GFP depicted in (B).

2.3.2 CHST3 Over-expression Plasmid Transfection

Plasmid transfection into two breast cancer cell lines, MCF7 and MDA-MB-231, were carried out using Lipofectamine 2000. Cells were first seeded onto a 6-well plate at cell density of 2 x 10^5 cells per well. Upon 80 to 90% cell confluency at the time of transfection, 1ug of the plasmid topped up with OPTIMEM to 100ul and 3ul of Lipofectamine 2000 in 97ul OPTIMEM were incubated separately at room temperature for 5min. The two mixtures were then combined and incubated for 20min at room temperature to allow formation of plasmid-Lipofectamine complexes. A total of 200ul plasmid-Lipofectamine complexes were added drop-by-drop into 800ul OPTIMEM in each well of the 6-well plate. The transfected culture was then incubated at 37^{o}C, 5% CO_2 for 5 hours before the medium was changed to medium consisting of 10% FBS and 450ug/ml geneticin. The following

day, the cells were re-seeded into a 24-well plate. The medium was changed every 2-3 days for two weeks to allow selection of cells with the over-expression plasmid or empty vector. After two weeks of selection, a single colony of cells was picked from each well and grown in a 96-well plate. Fresh medium supplemented with 10% FBS and 450ug/ml geneticin was replaced in the well every 2-3 days. Upon 80-90% cell confluency, the cells were subcultured into a 24-well plate and subsequently, 6-well plate. The over-expression efficiencies were then measured through qPCR. The cells were subcultured for further experiment use and for generation of frozen stock.

2.4 RNA Extraction

Total RNA was isolated from breast cancer cells using the RNeasy Mini Kit (Qiagen, Hilden, Germany) according to the manufacturer's protocol. Cells grown in 6-well plates were washed with PBS before adding RNA lysis buffer, consisting a 1:100 ratio of 1% β-mercaptoethanol:Buffer RLT, at a volume of 350ul per well. After one minute incubation at room temperature, a disposable cell scraper was used to detach the cells from the 6-well plate. The cell contents were transferred into microcentrifuge tubes. Homogenization was performed using needles and syringes. The homogenized cell lysate was then mixed with 1 volume (350ul) of 70% ethanol. The mixture was next transferred into RNeasy MiniElute spin column. Centrifugation was carried out at 13,000rpm for 30 seconds. After the flow through was discarded, 350ul of Buffer RW1 was used to wash the membrane in the spin column. Centrifugation was carried out at 13,000rpm for 30 seconds. The RNA was subsequently treated with 10ul DNase I diluted in 70ul Buffer RDD for 15 minutes at room temperature, to remove any traces of DNA contamination. Prior to centrifugation, 350ul Buffer RW1 was added to wash the spin column membrane. Further washing of the column was performed using 500ul of Buffer RPE. Centrifugation was repeated twice to ensure no carryover of the Buffer residuals. For the elution step, the total RNA was eluted out in 32ul RNase-free water through centrifugation. The RNA concentration and purity was determined using nanodrop

ND-100 spectrophotometer (Thermo Scientific, Asheville, NC, USA). 2ul of the eluted total RNA was loaded onto the pedestal containing fibre optic cable, that is able to generate a spectral measurement. The RNA integrity and purity can be obtained from the absorbance value at A260/280 ratio. An A260/280 ratio between 1.8 and 2.0 indicates relatively pure RNA. The total RNA was stored at -80^{o}C for future use.

2.5 cDNA Synthesis

The synthesis of first strand cDNA was achieved through reverse transcription of 1000ng RNA diluted in RNase-free water. The mastermix reaction consists of 50ng random primers, 10nM dNTP mix, 5x First Strand buffer, 0.1M DTT, 40U RNaseOUT^{TM} and 1U SuperScript^{TM} III Reverse Transcriptase, bringing the final reaction volume to 20ul. SuperScript^{TM} III First Strand Synthesis System (Invitrogen, Carlsbad, CA, USA) was performed according to the manufacturer's protocol and used according to the reaction conditions in Table 2.3.

Table 2.3: cDNA synthesis reaction conditions

Temperature	**Time**
65°C	5 min
0°C	3 min
25°C	10 min
50°C	60 min
70°C	15 min

2.6 Primers

PCR grade oligonucleotides specific to genes of interest were purchased from 1st Base (Singapore). The primers were designed using Primer 3 v.0.4.0 to span across introns for detection of genomic contamination. They also have optimal amplicon size between 100 to 200 base pairs, target all transcript variants at their coding

regions, and have optimal BLAST values. Table 2.4 shows the primer sequences used to amplify and evaluate the gene expression of interest.

Table 2.4: Primer sequences targeting genes of interest

Gene of Interest		Sequence	Product Size (bp)
CHST3	Forward	5' – ACGCCCTTTTCTTGGTTTTT – 3'	107
	Reverse	5' – AGAGCTTGGGGAATCTGCTT – 3'	
GAPDH	Forward	5' – GAAGGTGAAGGTCGGAGTCAACG – 3'	158
	Reverse	5' – TGCCATGGGTGGAATCATATTGG – 3'	
GPNMB	Forward	5' – TGTGAACACAGCCAATGTGA – 3'	196
	Reverse	5' – GGGGAGATCTTTGAGGAAGG – 3'	
FLRT3	Forward	5' – GCTCATCTGCTCCTGCTTCT – 3'	127
	Reverse	5' – AGGGGACTTGAGGATGACCT – 3'	

2.7 Quantitative Real-Time Polymerase Chain Reaction

Quantitative real-time PCR was performed using SYBR Green Master Mix (Qiagen, Hilden, Germany). The final reaction of 10ul consists of SYBR Green, 10ng of cDNA template, and 0.5µM of specific primers. Amplification was performed on the LightCycler 1.5 (Roche Diagnostics, Indianapolis, USA) following the protocol in Table 2.5. Normalization was calculated using *GAPDH* values and the relative expression levels were calculated through the $2^{-\Delta\Delta CT}$ formula (Livak and Schmittgen, 2001) as shown below.

$\Delta CT^{\text{Target gene}} = CT^{\text{Target gene in treatment group}} - CT^{\text{Target gene in control group}}$

$\Delta CT^{\text{Housekeeping gene}} = CT^{\text{Housekeeping gene in treatment group}} - CT^{\text{Housekeeping gene in control group}}$

$\Delta\Delta CT = \Delta CT^{\text{Target gene}} - \Delta\, CT^{\text{Housekeeping gene}}$

Fold change $= 2^{-\Delta\Delta CT}$

Table 2.5: RT-PCR conditions

	Temperature	**Time**	**Cycles**
Initial denaturation	95°C	15 min	-
Denaturation	94°C	15sec	45
Annealing	60°C	25sec	
Extension	72°C	15sec	
Hold	4°C	Forever	

2.8 Protein Electrophoresis

2.8.1 Protein Extraction

Cells were washed in ice-cold PBS before adding a mix of Mammalian Protein Extraction Reagent (Thermos Scientific, Asheville, NC, USA), HALT^{TM} Protease Inhibitor (Pierce, Illinois, USA), and EDTA (Pierce, Illinois, USA). After a minute incubation on ice, a disposable cell scraper was used to detach the cells. The cell lysates was collected into microcentrifuge tubes. Subsequently, centrifugation was performed at 13,000rpm for 10 minutes at 4^{o}C to pellet the cell debris. Collected supernatants containing cell proteins were stored in -80^{o}C for future use.

2.8.2 Protein Quantitation

Protein concentration was determined using the bicinchoninic acid (BCA) protein assay kit (Pierce, Illinois, USA), which also adopts colorimetric method. The basis behind this kit is the reduction occurrence of Cu^{2+} to Cu^{+} by protein available. Hence, the protein concentration would be proportional the amount of reduction (generation of purple coloration). Extracted protein samples were diluted and added to BCA^{TM} Reagent A and B (Pierce, Illinois, USA), which were mixed at a ratio of 50:1 respectively. Millipore water was used as a blank. The mixture in a 96-well plate was incubated in the dark on an orbital shaker (180rpm, 30 min, 37^{o}C). The absorbance values for the protein samples were obtained using a microplate reader (Tecan, Switzerland). Protein standard (bovine serum albumin) of different

dilutions were also measured of their concentrations to obtain a protein standard curve, which would be used to determine the protein concentrations of each sample.

2.8.3 Preparation of SDS-Polyacrylamide Gel

The Western blot gel was firstly cast using gel casting frames, glass plates, and spacers. A 10% resolving gel, that makes up the bottom three quarter of the entire gel, was prepared through the mixture of deionized water, 30% acrylamide mix, 1.5M Tris at pH8.8, 10% sodium dodecyl sulfate (SDS), 10% ammonium persulfate (APS), and N,N,N',N'-tetramethylethylenediamine (TEMED). Isopropanol was used to even out the surface of the resolving gel. The gel was then left to polymerize for approximately 30 minutes.

Following that, the gel casting stand was inverted to drain out the isopropanol. A 5% stacking gel, which makes up the top one quarter of the entire gel, was next prepared using a mixture of deionized water, 30% acrylamide mix, 1.0M Tris at pH6.8, 10% SDS, 10% APS, and TEMED. After overlaying the stacking gel mixture on the resolving gel, a well comb was gently inserted into the stacking gel. The gel was then left to polymerize for another 30 minutes.

2.8.4 Electrophoresis of SDS-Polyacrylamide Gel

Protein samples at 30µg each were used; the samples were diluted in 5x SDS gel-loading buffer, consisting of 250mM Tris-Cl (pH 6.8), 10 % SDS, 30% glycerol, 5% dithiothretol (DTT) and 0.02% bromophenol blue. The diluted samples were heated at 95^{o}C for 3 minutes. After polymerization of the SDS-polyacrylamide gel, the well comb was removed. Subsequently, the electrophoresis module was assembled. Tris-glycine buffer was used in the electrophoresis run. The protein samples as well as the protein ladder (Precision Plus Protein dual color marker (Biorad, Hercules, CA, USA)) were loaded into the wells. The gel electrophoresis was then allowed to run at 100V for protein separation.

2.8.5 Semi-Dry Electro-Transfer

The separated proteins on the gel were next electro-transferred onto a polyvinyl difluoride (PVDF) membrane. The membrane was firstly activated through soaking in methanol for 10 seconds. It was next soaked in deionized water for one minute before soaking in transfer buffer. Additionally, two thick filter pads were pre-soaked in the transfer buffer. After the completion of the gel electrophoresis run, the gel was removed from the electrophoresis module. A gel-sandwich was assembled using the sequence of the first filter pad at the bottom, followed by the PVDF membrane, gel and lastly, the second filter pad. Trapped air bubbles were released by rolling over the filter pad surface. The electro-transfer was carried out using the TransBlot Semi-Dry Transfer Cell (Biorad, Hercules, CA, USA) at 15V for 45 minutes.

2.8.6 Western Blot

Following electro-transfer, the membranes were blocked overnight at 4^{o}C using 5% fat-free milk in Tris-buffered saline containing 0.05% Tween-20 (TBS-T). The next day, the membrane was incubated with the primary antibody of interest at 1:500 dilution factor for 1 hour at room temperature. Primary antibodies used were anti-CHST3 (Proteintech, Catalog No. 18242-1-AP), anti-GPNMB (R&D Systems, Catalog No. AF2550), anti-FLRT3 (Abcam, Catalog No. ab97267), anti-E-cadherin (Santa Cruz, Catalog No. sc-8426), anti-β-catenin (Santa Cruz, Catalog No. sc-7963), anti-BAD (Cell Signaling, Catalog No. #9268), anti-phospho-BAD (Cell Signaling, Catalog No. #5284), anti-JAK2 (Cell Signaling, Catalog No. #3230), anti-phospho-JAK2 (Cell Signaling, Catalog No. #3771), anti-STAT3 (Cell Signaling, Catalog No. #4904), anti-phospho-STAT3 (Cell Signaling, Catalog No. #9145), anti-β-actin (Sigma, Catalog No. A2228). After which, the membranes were incubated with their respective horseradish peroxidase conjugated secondary antibodies for 1 hour at room temperature: anti-mouse (GE Healthcare; 1:5000 dilution) and anti-rabbit (Dako; 1:3000 dilution). The blots were developed using chemiluminescence substrate solution (Pierce) and visualized with an image

analyzer. The intensities of the protein bands were obtained through ImageJ software. Each protein sample was normalized against house-keeping protein β-actin.

2.9 Immunofluorescence of Breast Cancer Cells

Cells were seeded onto cover slips placed in 6-well plates. After a 72-hour transfection period, the attached cells on the cover slips were fixed with ice-cold methanol or 4% paraformaldehyde for 15 minutes. The fixed cells were then blocked with 5% BSA in PBS. Subsequently, the primary antibody of interest was added and incubation was carried out for 2 hours at room temperature: anti-CHST3 (1:100 dilution), anti-E-cadherin (1:100 dilution), and anti-β-catenin (1:100 dilution). Specific secondary antibody incubation was next carried out for 1 hour at room temperature at 1:400 dilution. The cover slips with the stained cells were mounted onto glass slides using DAPI-containing mounting medium (DAKO). Fluorescence microscopy was used to view the fluorescent cells.

Image J software (National Institutes of Health, USA) was used to quantify the immunofluorescence level. The fluorescence intensity of the targeted protein was quantified for each cell. Background intensity was subtracted off the initial intensity score. The intensity was averaged out against total number of cells quantified.

2.10 Functional Analysis of *CHST3* in Breast Cancer Cells

2.10.1 Cell Migration and Invasion Assays

Cell migration and invasion were assessed using 24-well transwell system (8um pore size) with Transwell migration chambers (BD Biosciences, CA, USA) and Matrigel chambers (BD Biosciences, CA, USA) respectively. The chambers were firstly hydrated with culture medium for 1 hour at 37^{o}C. The culture medium was aspirated out prior to cell seeding. Cells were seeded into the chambers at a cell density of 5 x 10^4 cells/well for migration chambers and 1 x 10^5 cells/well for

Matrigel chambers, using 0.2ml of serum-free medium. A total of 0.6ml medium containing 20% FBS was added below the chamber to allow cell migration/invasion via chemotaxis. After a 24-hour incubation at 37^{o}C in 5% CO_2 atmosphere, cells on the transwells were fixed with methanol for 15 minutes and stained with 0.5% crystal violet for 30 minutes. Non-migrated cells inside the chamber were removed using a cotton swab. Cells that had migrated/invaded to the underside of the membrane were counted in five different fields under light microscope.

2.10.2 Cell Proliferation Assay

To evaluate cell proliferation, cultured cells was first serum-starved (using culture medium without FBS) for 24 hours to induce G1 cell cycle phase arrest in all cells. After which, the serum-free medium was replaced with culture medium supplemented with 10% FBS to allow the cell growth. Subsequently, after 48 hours, cell proliferation was evaluated using CellTiter 96® AQueous One Solution Cell Proliferation Assay kit (Promega, Madison, WI, USA), which is a colorimetric method used to analyze the amount of viable cells in proliferation. The kit utilizes a tetrazolium compound or more commonly known as MTS. Mitochondrial dehydrogenase from viable cells will bioreduce the yellow-colored MTS compound into purple-caolored formazan. Hence, the amount of formazan formed would be proportional to the amount of living cells. Following the manufacturer's protocol, cells were incubated with MTS solution and culture medium at a ratio of 1:5 for 3 hours at 37^{o}C before the absorbance level was measured at 490nm using a plate reader (Tecan, Switzerland).

2.10.3 Cell Adhesion Assay

Collagen and fibronectin were used to coat the wells of 96-well plates at final concentration of 20µg/ml. Cells were seeded into the coated plates at cell density of 5 x 10^4 cells/well and incubated for 30 min. After which, cells were washed twice with PBS to remove non-adherent cells. The amount of remaining cells was measured using CellTiter 96® AQueous One Solution Cell Proliferation Assay kit,

as mentioned in Section 2.10.2. Absorbance level was assessed at 490nm using a plate reader (Tecan, Switzerland).

2.10.4 Cell Cycle Assay

Cell cycle analysis (Cunningham, 1994) was carried out using a flow cytometer (Becton Dickinson, NJ, USA). Post 48-hour siRNA transfection, the culture medium was first collected into 15ml tubes (to collect the dead cells). The culture cells were next detached from the well through trypsinization. The cells were transferred into the corresponding 15ml tubes. The collected dead and live cells were centrifuged at 1000rpm for 5min. After the supernatant was discarded, the cells were washed with PBS and centrifuged. This washing step was repeated to allow removal of the culture medium. After which, the pelleted cells were resuspended in 500ul of PBS. The cell suspension was added drop-by-drop into a new 15ml tube containing 4.5ml of ice cold ethanol. The cells were then left overnight at 4^{o}C for fixation process.

The following day, the tubes were centrifuged. The pelleted cells were then washed with PBS and centrifuged twice to remove the ethanol. The cells in each tube were subsequently resuspended in a 1ml cocktail containing propidium iodide (1mg/ml), PBS, Triton X-100 (0.1%), and RNase A. The propidium iodide-stained DNA of the fixed cells were measured using the Dako Cytomation Cyan LX (Dako, CA, USA) flow cytometer with laser excitation at 488nm wavelength. Analysis was performed comparing the DNA content of the silenced and control groups at different cell cycle phases.

2.10.5 Cell Apoptosis Assay

Caspase 3/7 assay kit (Promega, Madison, WI, USA) was used to evaluate cell apoptosis. Cells were seeded into a black 96-well plate at 8 x 10^3 cells/well and incubated for 48 hours at 37^{o}C. The assay solution was then added to the cell culture and absorbance was measured using a plate reader (Tecan, Switzerland).

2.10.6 Statistical Analyses

Results were performed with at least triplicates from one experiment set or two independent experiment sets and data obtained were expressed as mean ± standard error mean (SEM). The student's t-test (using GraphPad Prism 5.0) was used to perform statistical analysis on experiments with two different treatment groups. For experiments with more than two treatment groups, 1-way ANOVA was utilized. P-values of less than 0.05 were deemed as statistically significant, with p-values < 0.05, < 0.01, and < 0.001 represented as *, **, and *** respectively. All error bars shown on graphs represent SEM.

2.11 Immunohistochemistry of Human Breast Tissues

2.11.1 Tissue Specimens

Tissue microarray (TMA) slides consisting of 255 IDC cases and 77 normal ductal tissue cases were obtained from the Department of Pathology, Singapore General Hospital. Clinicopathological parameters of the cases were acquired for statistical analyses, inclusive of patients' age, tumor size, histological grade of the tumor, lymphovascular invasion, stage of lymph node metastasis, ER status, PR status, and HER2 status. The age of the patients ranged from 23 to 89 years old, with a mean of 56.1 years and a median of 55.5 years. As for patient follow-up, the follow-up period ranged from 0 to 175.5 months. Ethics approval for the project was obtained from the Institutional Review Board, Singapore General Hospital.

2.11.2 Immunohistochemistry

Briefly, the TMA slides were de-paraffinized in clearene and re-hydrated through a graded series of ethanol. Endogenous peroxidase activity was quenched with 3% hydrogen peroxide for 30 minutes. The TMA slides were then blocked with goat serum (DAKO) for 1 hour prior to overnight incubation at $4^{o}C$ with the primary antibodies (CHST3 antibody from Proteintech, FLRT3 antibody from Abcam) using 1:100 dilution factor. The following day, the secondary antibody (DAKO

Polymer Kit) was added and incubated for 1 hour at room temperature. The tissue sections on the TMA were visualized using diaminobenzidine as the substrate and counterstained with Shandon's haematoxylin. The stained TMA sections were assessed by two independent blinded observers.

2.11.3 Evaluation of Staining Intensities

The staining intensities of the epithelial components in the IDC tissues were noted as: 0 (no staining), 1+ (weak), 2+ (moderate), and 3+ (strong). The percentage of cells that were stained was also recorded. The figures were converted into weighted average score (WAI) using the following equation, of which the total of different staining intensities multiplied with the percentage of each intensity are divided against percentage of positively stained area (Lo et al., 2011). WAI score was utilized in this study as it considers the staining intensities of the protein expression of interest in the breast tissues studied.

$$WAI = \frac{\left[\begin{matrix}(\%\ of\ no\ staining\ x\ 0) + (\%\ of\ weak\ intensity\ x\ 1) \\ +(\%\ of\ moderate\ intensity\ x\ 2) + (\%\ of\ strong\ intensity\ x\ 3)\end{matrix}\right]}{\%\ of\ positively\ stained\ area}$$

2.11.4 Selection of Cut-Off Score

The cut-off score was determined based on the median intensity and receiver operating characteristic (ROC) curve analysis. Selecting the cut-off score from median or mean would allow a better selection of a representative score for the cohort of patients studied. As the staining intensity values follow a skewed distribution, the median intensity was selected as the cut-off score to represent the average expression level in the patients' breast tissues.

ROC curve analysis (staining intensity against tissue type – normal and malignant) was also performed to consider both sensitivity and specificity of the median intensity. Maximum sensitivity and specificity are signified from the score being

closer to the curve following the left hand border and then the top border of the ROC curve space. The area under the ROC curve will depict the discriminatory power of the biomarker with values of 0.5 indicating lower power and value nearer to 1.0 indicating higher power (Greiner et al., 2000, Zweig and Campbell, 1993).

2.11.5 IHC Statistical Analysis

Statistical analyses were carried out using SPSS Statistics 17 software (SPSS). Associations between the immunostaining in the IDC tissues and various clinicopathological parameters were analyzed using Fisher's Exact and Kendall Tau's tests. In addition, Kaplan Meier and Cox regression analyses were performed to evaluate possible correlations between the immunostaining in the IDC tissues with patients' survival outcome. Disease-free survival (DFS), overall survival (OS), and survival after recurrence (SAR) durations were used for the survival analyses. DFS and OS define the duration from date of diagnosis to the date of first tumor recurrence and death respectively. SAR describes the duration from the date of first tumor recurrence to date of death. In addition, patient cases that did not reach the defined end-points of interest (first tumor recurrence and death) were censored at the last follow-up date. Statistical significance was defined when p-value was less than 0.05.

2.12 Genome-wide Expression Profiling using Microarray Gene Chip

2.12.1 Microarray Processing using Affymetrix Human Gene U133 Plus 2.0 Array

Total RNA were extracted from cultured cells using RNeasy Mini Kit. The RNA concentration and purity (260/280 OD) were measured by nanodrop. The silencing or over-expression efficiency was checked through qPCR before the RNA samples were sent to Origen (Origen, Singapore) for microarray processing. Briefly, the quality of the RNAs was further evaluated using an Agilent Bioanalyzer. The RNA samples were then processed based on Affymetrix recommended protocol for

whole transcript analysis. 300ng of total RNA was reverse transcribed to cDNA, which was used as a template to produce cRNA. The cRNA was then converted to single stranded DNA, which was biotin-labeled, fragmented, and hybridized to the Affymetric Human Gene U133 Plus 2.0 Array for 16 hours at 45^{o}C with rotation at 60rpm. Subsequently, the array was washed and stained using FS450_0007 fluidics protocol and visualized using Affymetrix 30007G scanner. Hybridization efficiency was inspected through the scanned images. CEL files generated from GeneChip Operating Software (GCOS) were imported into Expression Console software for array quality control. RMA normalization was carried out on the samples to create a quality control metrics.

2.12.2 Microarray Gene Expression Analysis

Genespring 7.0 (Silicon Genetics, CA, USA) and Expression Console 1.1.1 (Affymetrix, CA, USA) softwares were used to analyze the microarray gene expression. Genespring 7.0 was used to normalize the CEL files generated from the Human Gene U133 Plus 2.0 Array to the median intensity of the same array. Following that, the median value of genes in the control samples was used to normalize the intensity of corresponding genes in the treatment group. Algorithmic model (RMA) was performed in Genespring to process the CEL files.

Expression Console 1.1.1 summarized the probe set and checked the initial data quality. Algorithmic model (RMA) was also used for probe summarization and gene expression analysis. Upon completion of the data processing, CHP files are generated and intensities of all probe sets (genes) were reported after normalization.

2.12.3 Filtering Criteria for Gene Selection

After obtaining the intensities of the probe sets, filtering was carried out to select genes for further study.

Filter 1: Fold change of at least 2 for relative gene expression was considered

Filter 2: p-value below 0.05 from unpaired t-test was considered after comparing the intensities of control and treated groups.
Filter 3: Overlapped genes obtained from softwares used with different algorithmic models were selected.

2.12.4 Gene Pathway Analysis

Extensive literature review was carried out to find relevant gene(s) to justify the phenotypic changes observed upon silencing or over-expression of *CHST3*. The functional linkage between *CHST3* and potential downstream genes was validated through experiments.

CHAPTER 3
RESULTS

3 RESULTS

3.1 Expression Analysis of CHST3 in Human Breast Cells

As CHST3 has not been studied in breast cancer, the expression level of CHST3 in various breast cell lines (MCF-12A, MCF7, T47D, and MDA-MB-231) was firstly evaluated through immunofluorescence and western blot using a CHST3-specific antibody. As shown in Figure 3.1, it was observed that normal breast cells, MCF-12A, have a higher expression level of CHST3 as compared to that of the breast cancer cell lines (MCF7, T47D and MDA-MB-231). Hence, it is notable that the differences in CHST3 expression may be associated with breast tumor progression and that CHST3 may be involved in alleviating metastatic and aggressive characteristics.

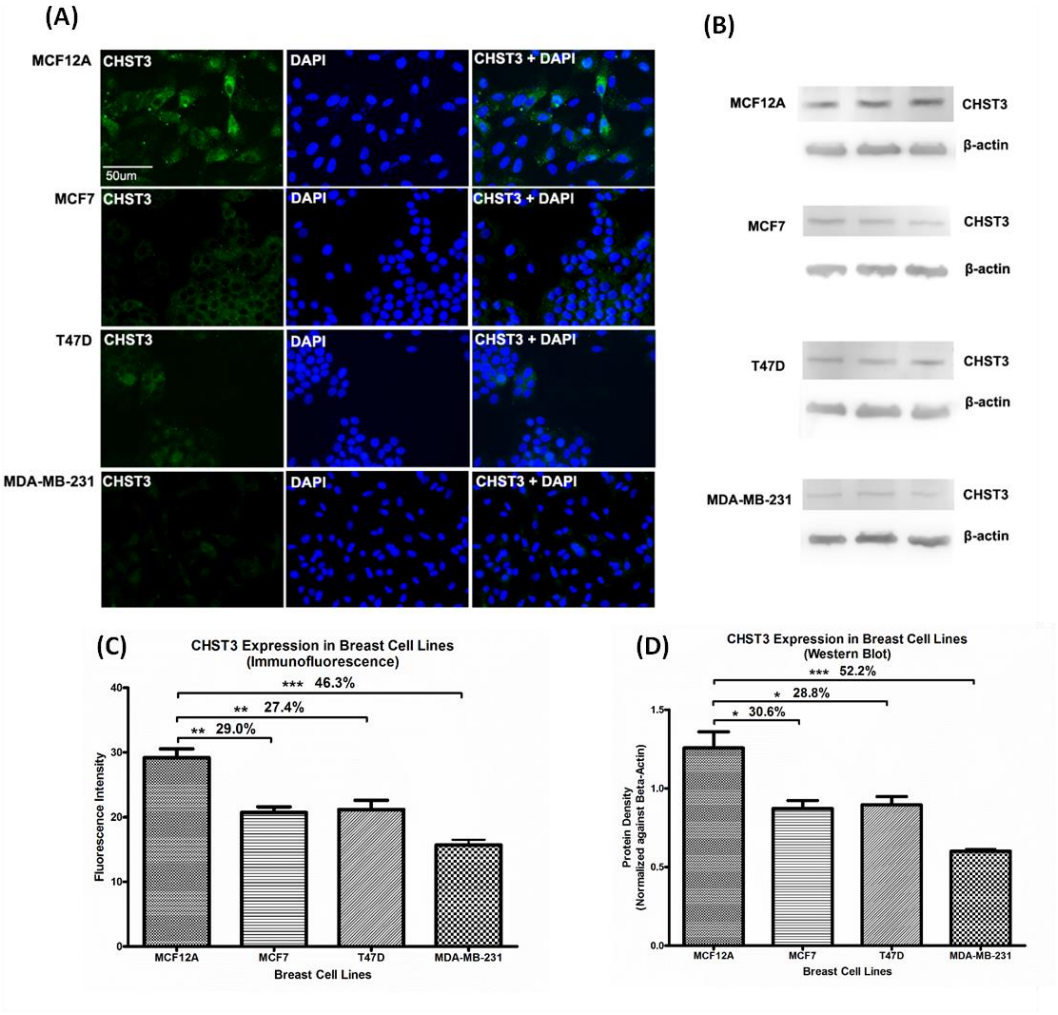

Figure 3.1: CHST3 expression in breast cells

Increased CHST3 expression was observed in normal breast cells, followed by Grade 1 breast cancer cells, and lastly Grade 3 breast cancer cells. (A) Immunofluorescence staining and (B) Western Blot analysis depict the protein expression level of CHST3 in the different breast cell lines. For the immunofluorescence staining, CHST3 expression is expressed in green fluorescence as an anti-CHST3 primary antibody and a secondary antibody conjugated with FITC are used, while the nuclei staining are shown in blue DAPI. In the Western Blot analysis, CHST3 expression levels were normalized against housekeeping protein, β-actin. From the graphs comparing (C) immunofluorescence staining and (D) Western Blot analysis, MCF-12A normal breast cells have increased CHST3 expression against MCF7, T47D and MDA-MB-231 breast cancer cell lines. Data shown was from one independent experiment performed with three biological replicates for each cell line. * $P < 0.05$; ** $P < 0.01$; *** $P < 0.001$ compared with MCF12A cell line.

3.2 Functional Analysis of *CHST3* in Human Breast Cancer Cells

With reference to the CHST3 expression study in breast cells, of which higher CHST3 expression level was observed in normal breast cells, followed by Grade 1 breast cancer cells and lastly Grade 3 breast cancer cells, it is hypothesized that the cells will be more metastatic and proliferative after down-regulation of *CHST3* and vice versa, that is the cells will be less metastatic and proliferative after over-expression of *CHST3*. To investigate the functional roles of *CHST3* in breast cancer cells, silencing and over-expression studies of *CHST3* were carried out. The execution of both silencing and over-expression experiments would validate the observations obtained from both experiment sets.

In the silencing experiments, *CHST3* was silenced in two different breast cancer cell lines, namely T47D (Grade 1 breast cancer cells) and MDA-MB-231 (Grade 3 breast cancer cells), to evaluate if the silencing of *CHST3* in different grades of breast cancer cells will lead to similar or different functional behavior changes. Also, *CHST3* was silenced in the breast cancer cells using two different siRNA sequences that specifically target the gene itself. Each sequence is essential to validate the phenotypic outcomes observed upon silencing of *CHST3* using the other sequence.

For the over-expression studies, two breast cancer cell lines namely MCF7 (Grade 1 breast cancer cells) and MDA-MB-231 (Grade 3 breast cancer cells) were used. A different breast cancer cell line, MCF7, was chosen to evaluate if *CHST3* has similar or different functional roles in different breast cancer cell lines. Additionally, two over-expression clones for each cell line were generated to confirm results that were observed.

3.2.1 Silencing and Over-expression Efficiencies of *CHST3*

Prior to carrying out the various phenotypic assays, the silencing and over-expression efficiencies of CHST3 at both the mRNA and protein levels were firstly determined. In the silencing experiments, *CHST3* was silenced through transient transfection in T47D and MDA-MB-231 cells using Silencer Select siRNA accompanied by delivery reagent, Oligofectamine. From the qPCR results, *CHST3* mRNA was at least 93.7% and 85.6% silenced compared to the scrambled siRNA groups in T47D cells (Figure 3.2A) and MDA-MB-231 cells (Figure 3.3A) respectively. From the immunocytochemistry and western blot results, CHST3 protein was at least 46.4% and 37.3% silenced in comparison to the scrambled siRNA groups in T47D cells (Figure 3.2B-E) and MDA-MB-231 cells (Figure 3.3B-E) respectively.

For the over-expression experiments, stable over-expression of *CHST3* was carried out in MCF7 and MDA-MB-231 cells using over-expression plasmids accompanied by delivery reagent, Lipofectamine, and antibiotic for selection, Geneticin. The qPCR analysis showed *CHST3* mRNA was over-expressed by at least 17.8 folds and 1.7 folds compared to the empty vector groups in MCF7 cells (Figure 3.4B) and MDA-MB-231 cells (Figure 3.5B) respectively. Over-expression of CHST3 protein levels were measured from immunofluorescence experiments. CHST3 protein was over-expressed by at least 2.3 folds and 2.7 folds against the empty vector groups in MCF7 cells (Figure 3.4A and C) and MDA-MB-231 cells (Figure 3.5 A and C) respectively.

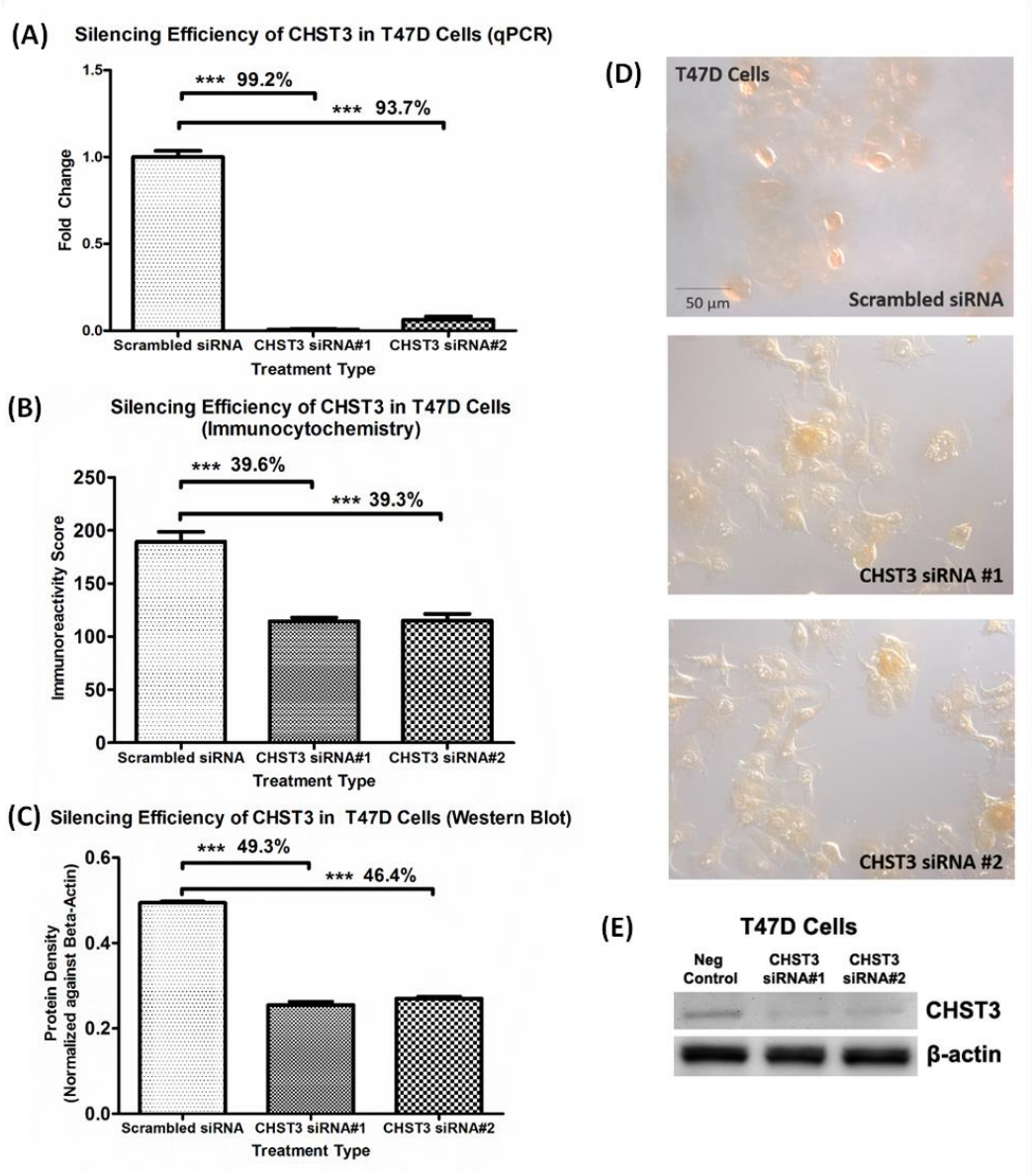

Figure 3.2: Silencing efficiencies of CHST3 in T47D cells
Silencing efficiencies of CHST3 mRNA and protein levels were obtained for both siRNA sequences specifically targeting *CHST3*. In the qPCR analysis (A), the mRNA expression levels of *GAPDH* house-keeping genes were used for normalization. (D) Immunocytochemistry staining and (E) Western Blot analysis depict the silencing efficiencies of CHST3 protein expression level in T47D cells. Cells in the immunocytochemistry experiment was captured using differential interference contrast (DIC) to quantify both staining intensity and nuclei. CHST3 expression is observed in both nuclei and cytoplasm of the cells. In the Western blot analysis, the protein expression of CHST3 was normalized against house-keeping protein, β-actin. Graphs (B) and (C) show the silencing efficiencies of CHST3 protein observed in immunocytochemistry and Western blot respectively. Data shown were each from one independent experiment set performed with three biological replicates. * $P < 0.05$; ** $P < 0.01$; *** $P < 0.001$ compared with scrambled siRNA group.

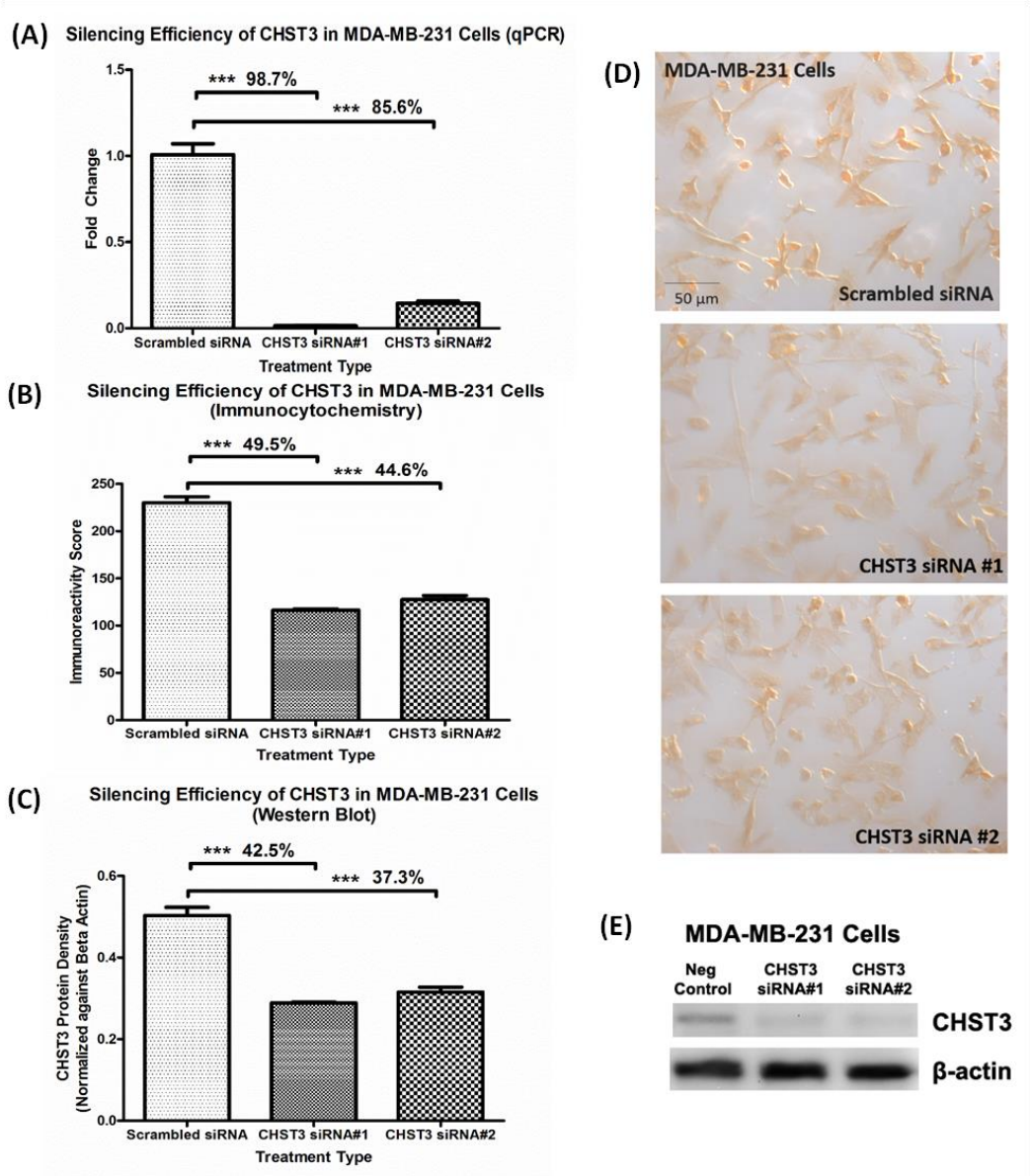

Figure 3.3: Silencing efficiencies of CHST3 in MDA-MB-231 cells

Silencing efficiencies of CHST3 mRNA and protein levels were obtained for both siRNA sequences specifically targeting *CHST3*. In the qPCR analysis (A), the mRNA expression levels of *GAPDH* house-keeping genes were used for normalization. (D) Immunocytochemistry staining and (E) Western Blot analysis depict the silencing efficiencies of CHST3 protein expression level in MDA-MB-231 cells. Cells in the immunocytochemistry experiment was captured using differential interference contrast (DIC) to quantify both staining intensity and nuclei. CHST3 expression is observed in both nuclei and cytoplasm of the cells. In the Western blot analysis, the protein expression of CHST3 was normalized against house-keeping protein, β-actin. Graphs (B) and (C) show the silencing efficiencies of CHST3 protein observed in immunocytochemistry and Western blot respectively. Data shown were each from one independent experiment set performed with three biological replicates. * $P < 0.05$; ** $P < 0.01$; *** $P < 0.001$ compared with scrambled siRNA group.

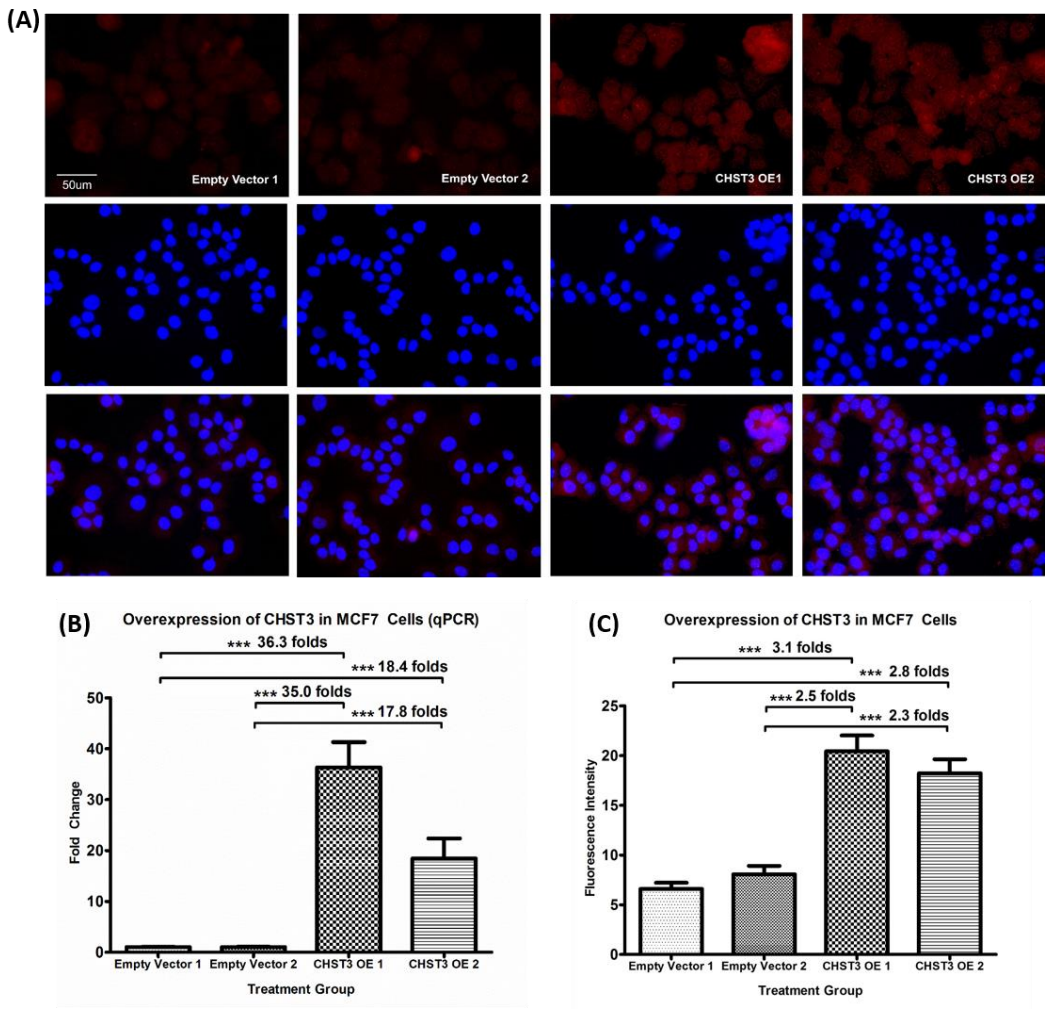

Figure 3.4: Over-expression efficiencies of CHST3 in MCF7 cells
Over-expression efficiencies of CHST3 mRNA and protein levels were obtained for both over-expression clones against the empty vector clones. In the qPCR analysis (B), the mRNA expression levels of *GAPDH* house-keeping genes were used for normalization. (A) Immunofluorescence staining depict the over-expression efficiencies of CHST3 protein expression level in MCF7 cells. The immunostaining was observed in both nucleus and cytoplasm of the cells. Graph (C) shows the over-expression analysis of CHST3 protein observed in the immunofluorescence experiment. Data shown in (B) were each from one independent experiment performed with three biological replicates. Data shown in (C) were from two independent experiments performed with three biological replicates for each experiment set. * $P < 0.05$; ** $P < 0.01$; *** $P < 0.001$ compared with empty vector group.

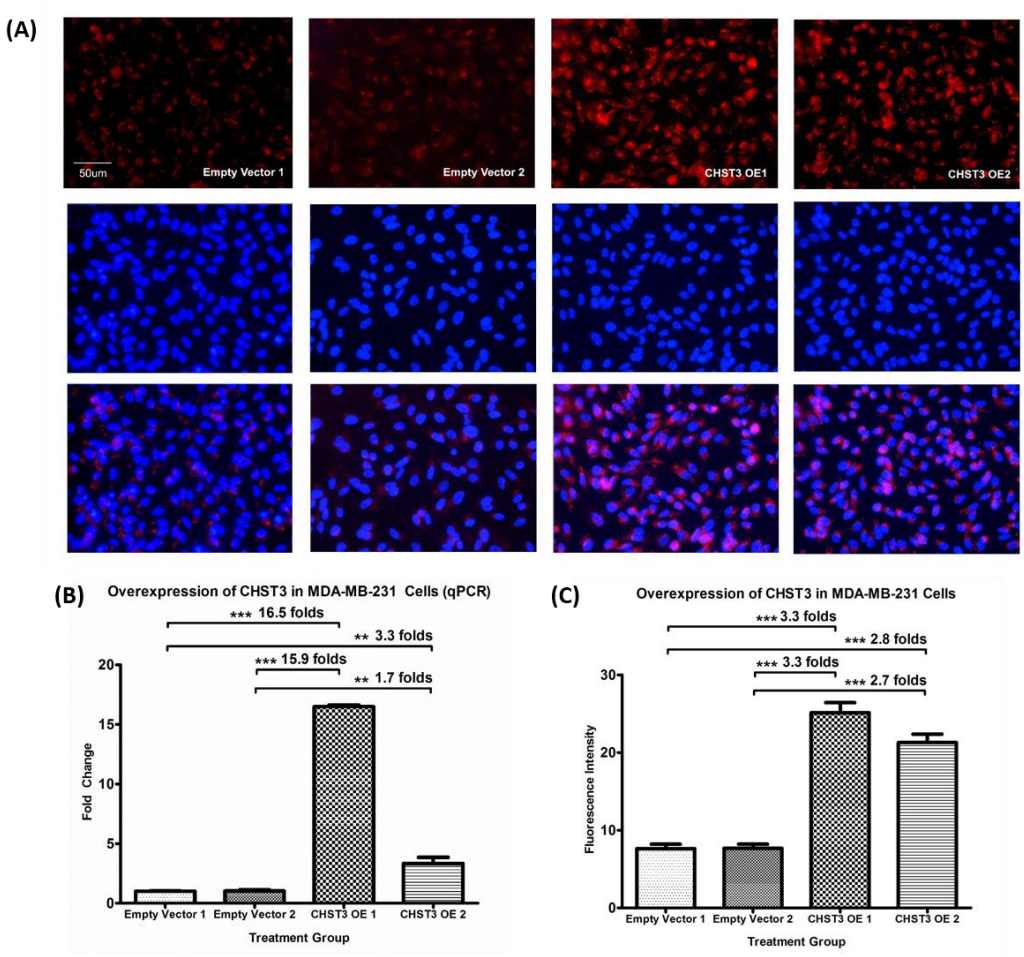

Figure 3.5: Over-expression efficiencies of CHST3 in MDA-MB-231 cells
Over-expression efficiencies of CHST3 mRNA and protein levels were obtained for both over-expression clones against the empty vector clones. In the qPCR analysis (B), the mRNA expression levels of *GAPDH* house-keeping genes were used for normalization. (A) Immunofluorescence staining depict the over-expression efficiencies of CHST3 protein expression level in MDA-MB-231 cells. The immunostaining was observed in both nucleus and cytoplasm of the cells. Graph (C) shows the over-expression analysis of CHST3 protein observed in the immunofluorescence experiment. Data shown in (B) were each from one independent experiment performed with three biological replicates. Data shown in (C) were from two independent experiments performed with three biological replicates for each experiment set. * $P < 0.05$; ** $P < 0.01$; *** $P < 0.001$ compared with empty vector group.

3.2.1.1 CHST7 Expression after Silencing CHST3

Apart from CHST3, CHST7 is also known to transfer the sulfate group from PAPS to the 6th carbon of the galactosamine unit. Hence, before proceeding to the phenotypic assays, *CHST7* was examined through qPCR to observe if its expression level was affected after silencing *CHST3*. From the qPCR results shown in Figure 3.6, *CHST7* expression was similar in both scrambled siRNA and *CHST3*-silenced groups, indicating that *CHST7* was not affected when *CHST3* was silenced in the breast cancer cells.

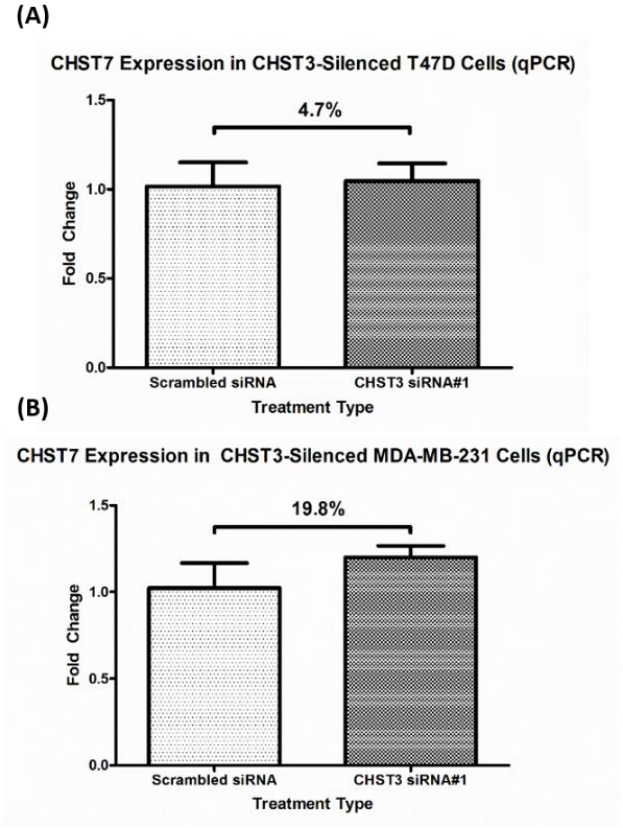

Figure 3.6: *CHST7* expression in *CHST3*-silenced T47D and MDA-MB-231 cells
The mRNA expression level of *CHST7* was obtained after silencing of *CHST3* in (A) T47D and (B) MDA-MB-231 cells. *GAPDH* mRNA expression level was used as the house-keeping gene for normalization. *CHST7* level was not affected by the down-regulation of *CHST3* in both cell lines. Data shown were each from one independent experiment performed with three biological replicates. * $P < 0.05$; ** $P < 0.01$; *** $P < 0.001$ compared with scrambled siRNA group.

3.2.1.2 CHST3 affects Cellular Behaviors in Breast Cancer Cells

Upon obtaining the silencing and over-expression efficiencies at the mRNA and protein levels, phenotypic assays – migration, invasion, adhesion, proliferation, cell cycle, and apoptosis assays – were performed to evaluate the functional roles that CHST3 may have in breast cancer cells. In the silencing experiments, the phenotypic assays were carried out post 48-hour transfection to investigate the effects of silencing *CHST3*. On the other hand, for the over-expression experiments, the phenotypic assays were performed after stable over-expression of *CHST3* in the cells.

3.2.1.2.1 CHST3 affects Cell Migration in Breast Cancer Cells

Acquisition and enhancement of cell migration through the basement membrane is one of the main characteristics of malignant cells. To investigate if a change in *CHST3* expression level in breast cancer cells would result in a change in tumor progression, cell migratory ability was evaluated after silencing and over-expression of *CHST3* using transwell migration chambers. After silencing of *CHST3* in T47D (Figure 3.7A and C) and MDA-MB-231 (Figure 3.7B and D) cells, cell migration level was observed to be increased compared to the scrambled siRNA group. On the other hand, after over-expression of *CHST3* in MCF7 (Figure 3.8A and C) and MDA-MB-231 (Figure 3.8B and D) cells, decreased in cell migration levels for both cell lines was observed in comparison to the empty vector groups.

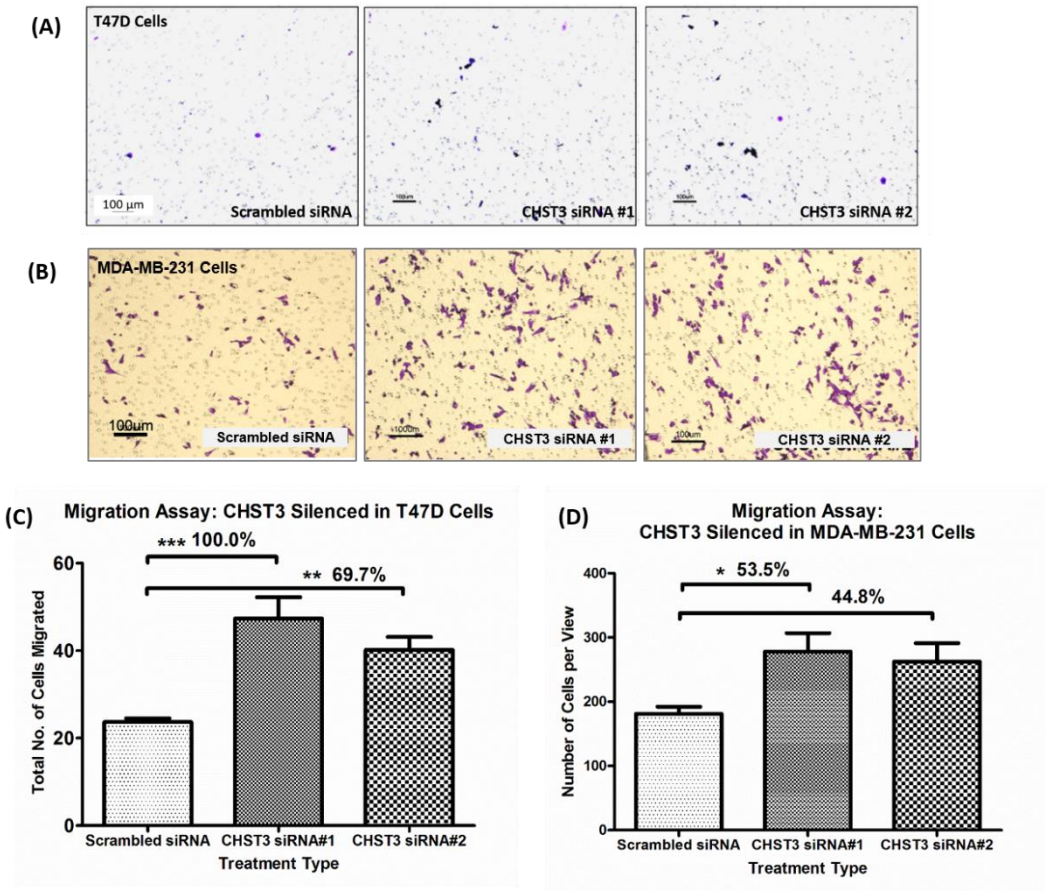

Figure 3.7: Cell migration level after silencing CHST3

Increase in cell migration was observed in the *CHST3*-silenced groups compared to the scrambled siRNA group after down-regulation of *CHST3* in (A and C) T47D and (B and D) MDA-MB-231 cells. Data shown were each from two independent experiment sets performed with three biological replicates for each experiment set. * $P < 0.05$; ** $P < 0.01$; *** $P < 0.001$ compared with scrambled siRNA group.

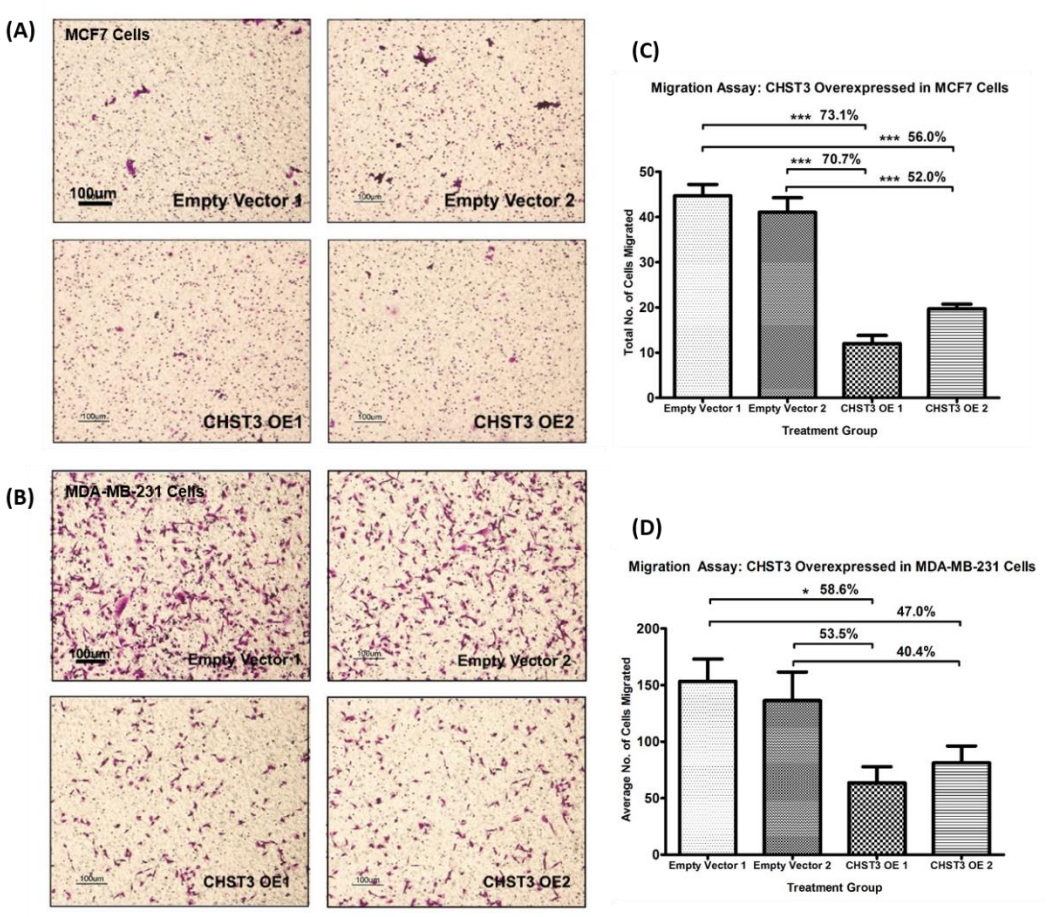

Figure 3.8: Cell migration level after over-expression of *CHST3*
Decrease in cell migration was observed in the *CHST3*-over-expressed groups compared to the empty vector groups after up-regulation of *CHST3* in (A and C) MCF7 and (B and D) MDA-MB-231 cells. Data shown in (C) were each from one independent experiment performed with three biological replicates. Data shown were each from two independent experiment sets performed with three biological replicates for each experiment set. * $P < 0.05$; ** $P < 0.01$; *** $P < 0.001$ compared with empty vector group.

3.2.1.2.2 CHST3 affects Cell Invasion in Breast Cancer Cells

Acquisition of cell invasion into the basement membrane and extracellular matrix is another main phenotypic behavior of malignant cells. Cell invasion ability was evaluated after silencing and over-expression of *CHST3* in breast cancer cells, using matrigel-coated transwell chamber. After silencing of *CHST3* in T47D (Figure 3.9A and C) and MDA-MB-231 (Figure 3.10B and D) cells, cell invasion level was observed to be increased compared to the scrambled siRNA group. On the other hand, after over-expression of *CHST3* in MCF7 (Figure 3.10A and C) and MDA-MB-231 (Figure 3.10B and D) cells, decreased in cell invasion levels for both cell lines was observed in comparison to the empty vector groups.

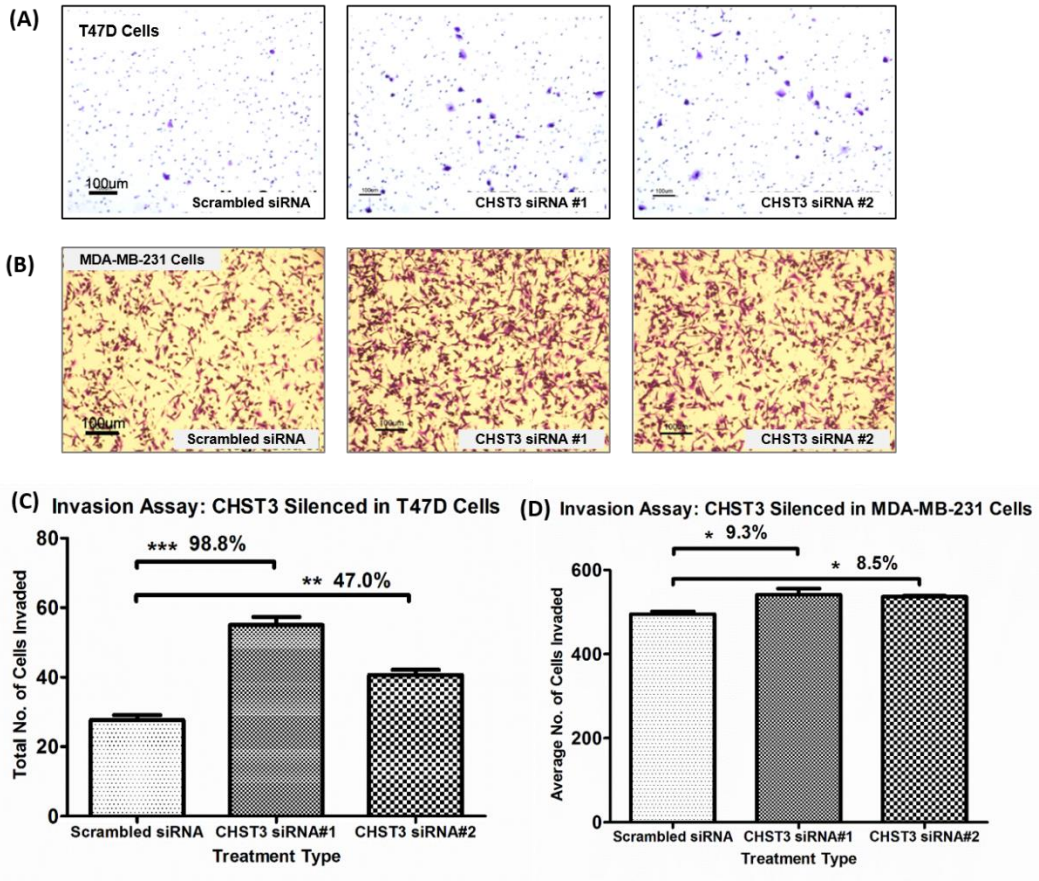

Figure 3.9: Cell invasion level after silencing *CHST3*
Increase in cell invasion was observed in the *CHST3*-silenced groups compared to the scrambled siRNA group after down-regulation of *CHST3* in (A and C) T47D and (B and D) MDA-MB-231 cells. Data shown were from one independent experiment set performed with three biological replicates. * $P < 0.05$; ** $P < 0.01$; *** $P < 0.001$ compared with scrambled siRNA group.

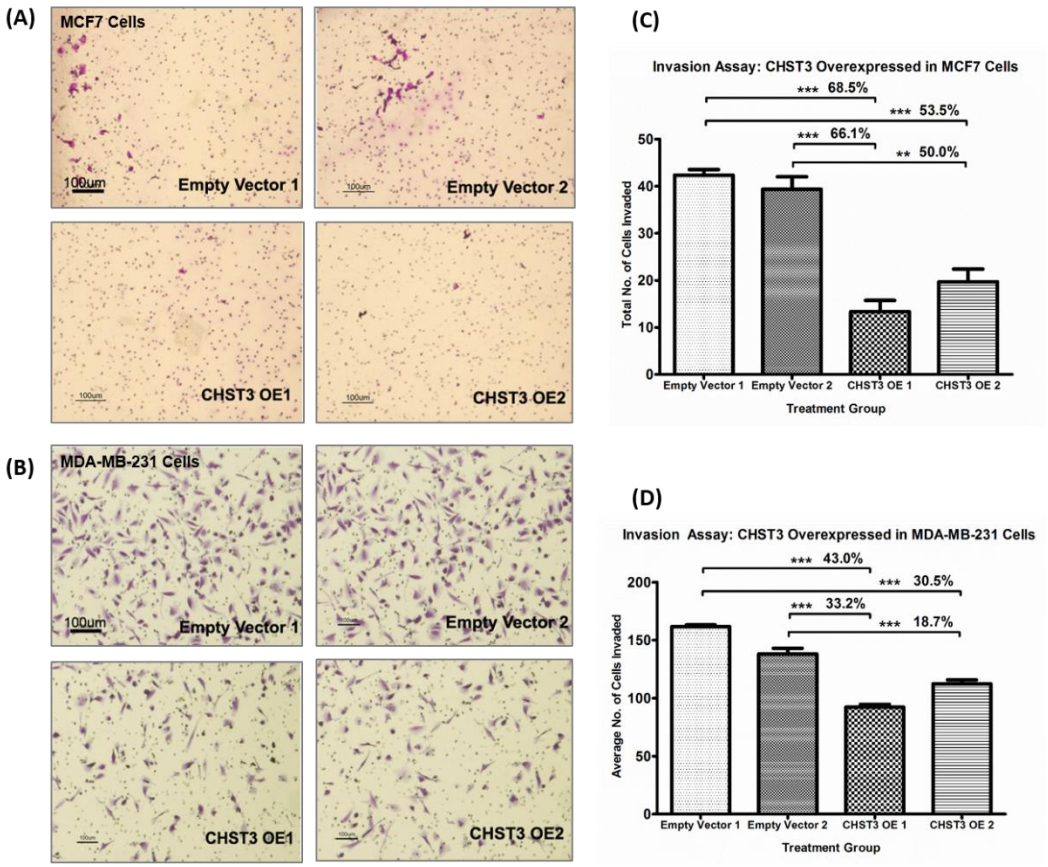

Figure 3.10: Cell invasion level after over-expression of *CHST3*
Decrease in cell invasion was observed in the *CHST3*-over-expressed groups compared to the empty vector groups after up-regulation of *CHST3* in (A and C) MCF7 and (B and D) MDA-MB-231 cells. Data shown were each from one independent experiment set performed with three biological replicates. * $P < 0.05$; ** $P < 0.01$; *** $P < 0.001$ compared with empty vector group.

3.2.1.2.3 CHST3 affects Cell Adhesion in Breast Cancer Cells

Cell adhesion to the basement membrane and extracellular matrix is an important component for malignant cells' capability to migrate and invade into the surrounding tissues as well as to other organs in the body. The effects of *CHST3* down-regulation and up-regulation on breast cancer cells' adhesion ability were evaluated. From the silencing experiment, it was observed that cell adhesion, using fibronectin- and collegen-coated plates, decreased compared to the scrambled siRNA group in both T47D (Figure 3.11A and C) and MDA-MB-231 (Figure 3.11B and D) cells. On the other hand, in the over-expression experiment, cell adhesion increased in comparison to the empty vectors groups in both MCF7 (Figure 3.12A and C) and MDA-MB-231 (Figure 3.12B and D).

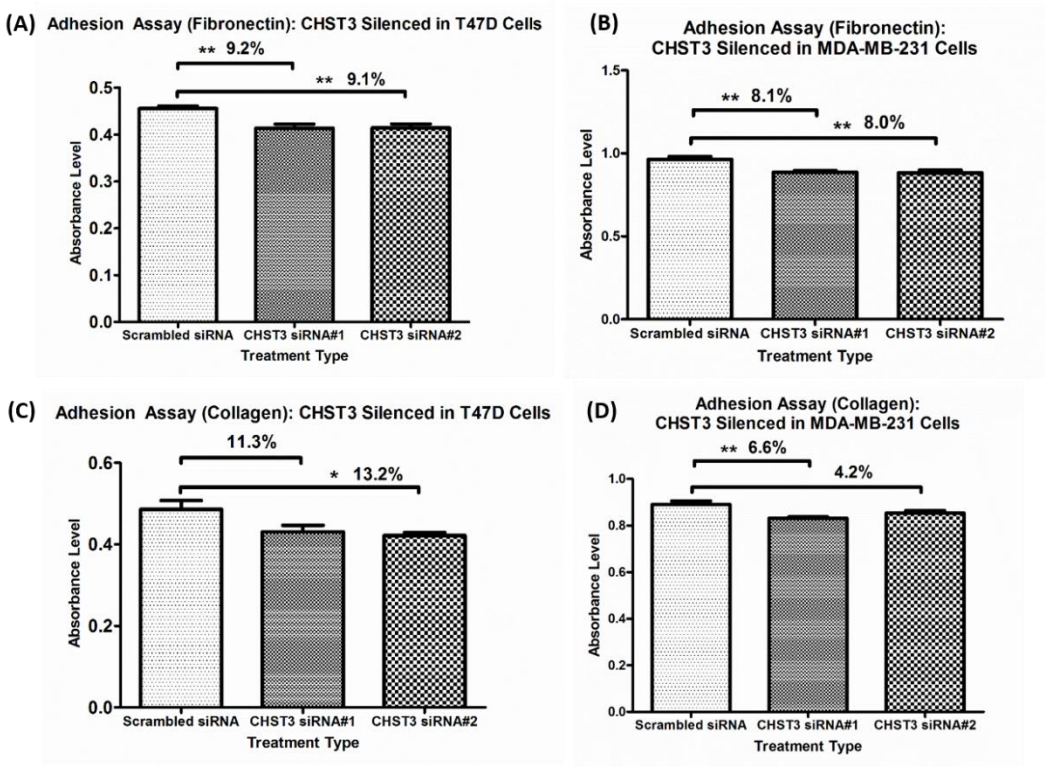

Figure 3.11: Cell adhesion level after silencing *CHST3*
Decreases in cell adhesion was observed in the *CHST3*-silenced groups compared to the scrambled siRNA group after down-regulation of *CHST3* in (A and C) T47D and (B and D) MDA-MB-231 cells, using fibronectin- and collagen-coated plates. Data shown were each from two independent experiment sets performed with three biological replicates for each experiment set. * $P < 0.05$; ** $P < 0.01$; *** $P < 0.001$ compared with scrambled siRNA group.

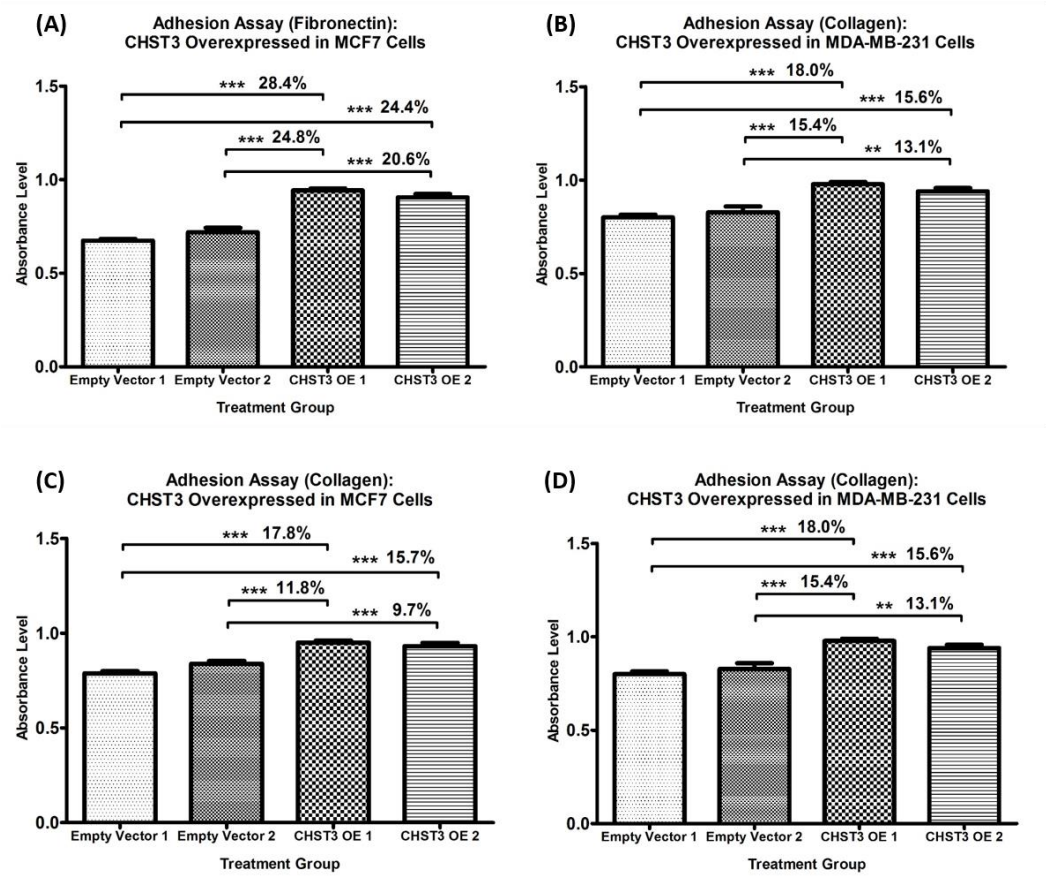

Figure 3.12: Cell adhesion level after over-expression of *CHST3*
Increase in cell adhesion was observed in the *CHST3*-over-expressed groups compared to the empty vector groups after up-regulation of *CHST3* in (A and C) MCF7 and (B and D) MDA-MB-231 cells, using fibronectin- and collagen-coated plates. Data shown were each from two independent experiments performed with three biological replicates for each experiment set. * $P < 0.05$; ** $P < 0.01$; *** $P < 0.001$ compared with empty vector group.

3.2.1.2.4 CHST3 affects Cell Proliferation in Breast Cancer Cells

Increase in cell proliferation and aggressiveness is another hallmark of tumor cells. Proteoglycans have been reported to play a role in cell proliferation through their binding to growth factors, initiating cell growth and multiplication. The effects of *CHST3* silencing and over-expression in breast cancer cells was investigated, using a tetrazolium reagent. After down-regulation of *CHST3*, cell proliferation was observed to be slightly increased in T47D (Figure 3.13A) and MDA-MB-231 (Figure 3.13C) cells. Contrary to this, over-expression of *CHST3* gave decreases in cell proliferation in MCF7 (Figure 3.14A and Figure 3.14B). As small changes were observed in cell proliferation assay using MTS solution, cell cycle analysis was performed through flow cytometry using detergent-based method and propidium iodide. After down-regulation of *CHST3*, changes was observed at the sub-G1 phase, indicating possible cell death occurrence as shown for T47D (Figure 3.13B) and MDA-MB-231 (Figure3.13D) cells. However, only T47D cells showed changes at the S phase that is small reductions in DNA replication phase was observed in both *CHST3*-silenced groups compared to the scrambled siRNA group.

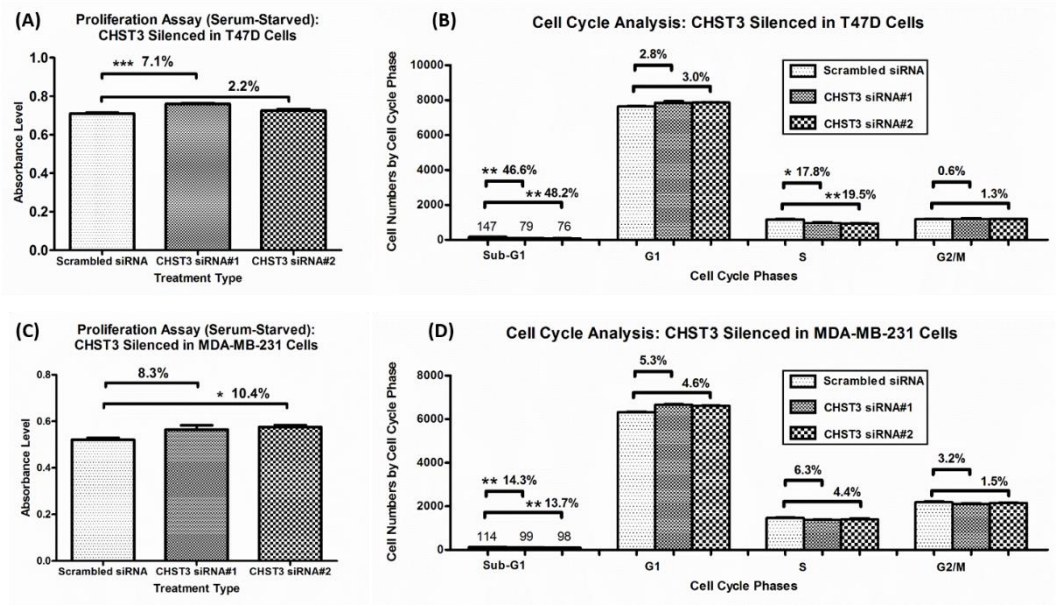

Figure 3.13: Cell proliferation level after silencing *CHST3*

Slight increases in cell proliferation were observed in the *CHST3*-silenced groups compared to the scrambled siRNA group after down-regulation of *CHST3* in (A) T47D and (C) MDA-MB-231 cells. Decreases in cell death were observed in the *CHST3*-silenced groups compared to the scrambled siRNA groups after silencing of *CHST3* in (B) T47D and (D) MDA-MB-231 cells. Only T47D cells showed decreases in cell number in S phase of the cell cycle. For cell proliferation performed using MTS solution, data shown were each from two independent experiments performed with three biological replicates for each experiment set. For flow cytometry, data shown were from one independent experiment performed with three biological replicates. * $P < 0.05$; ** $P < 0.01$; *** $P < 0.001$ compared with scrambled siRNA group.

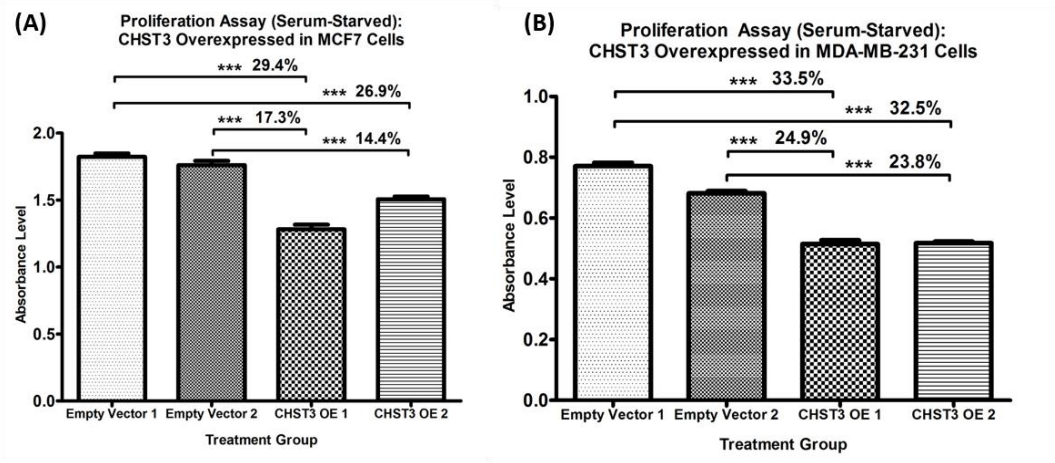

Figure 3.14: Cell proliferation level after over-expression of *CHST3*
Decreases in cell proliferation were observed in the *CHST3*-over-expressed groups compared to the empty vector groups after up-regulation of *CHST3* in (A) MCF7 and (B) MDA-MB-231 cells. Data shown were from two independent experiments sets performed with three biological replicates for each experiment set. * $P < 0.05$; ** $P < 0.01$; *** $P < 0.001$ compared with empty vector group.

3.2.1.2.5 CHST3 affects Cell Apoptosis in Breast Cancer Cells

As changes in cell proliferation were observed after regulating *CHST3* expression, cell apoptosis assay was carried out, specifically looking at Caspase3/7 levels. After silencing *CHST3*, cell apoptosis was observed to be decreased in T47D (Figure 3.15A) and MDA-MB-231 (Figure3.15B) cells.

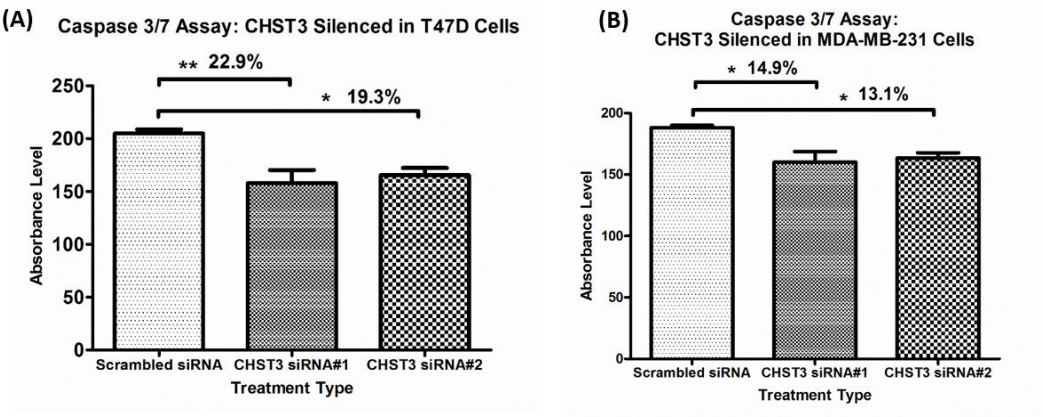

Figure 3.15: Cell apoptosis level after silencing *CHST3*
Decreases in cell apoptosis were observed in the *CHST3*-silenced groups compared to the scrambled siRNA group after down-regulation of *CHST3* in (A) T47D and (B) MDA-MB-231 cells. Data shown were each from one independent experiment performed with three biological replicates. * $P < 0.05$; ** $P < 0.01$; *** $P < 0.001$ compared with scrambled siRNA group.

3.3 Signaling Pathways Affected through Silencing of *CHST3*

From the functional analyses performed, results suggest that *CHST3* has a tumor suppressing role in breast cancer cells. To understand the pathways involved for *CHST3* that could have potentially regulated the phenotypic behavioral changes, several proteins from different signaling pathways associated with tumorigenesis were chosen for evaluation of their expression level after silencing of *CHST3*. The proteins investigated are involved in epithelial-mesenchymal transition, JAK-STAT pathway, and apoptosis pathway.

3.3.1 *CHST3* affects Proteins involved in Epithelial –Mesenchymal Transition

The metastatic capability of breast cancer cells was observed to be enhanced by down-regulation of *CHST3* and suppressed by up-regulation of *CHST3*, suggesting the possibility of *CHST3* pathway in the epithelial-mesenchymal transition (EMT) process that occurs in cancer cells for the initiation of metastasis. In general, cancer cells will lose cell-cell adhesion as well as gain invasive and migratory characteristics. A wide range of well-established EMT molecules are involved in the EMT process including E-cadherin and ZO-1 (for the breakdown of cell-cell adhesion), β-catenin and Snail (for the regulation and localization of transcription factors and repressors), as well as cytokeratin and vimentin (for the changes in the cytoskeleton organization) (Quaggin and Kapus, 2011). The expression levels of two epithelial markers - E-cadherin and β-catenin – were examined in this study.

E-cadherin belongs to the cadherin transmembrane glycoprotein family, which regulate cell-cell adhesion, making cells cohesive and stably immotile (Guarino et al., 2007, Kemler, 1993, Takeichi, 1991, Shiozaki et al., 1996). It interacts with catenins including β-catenin, forming cadherin/catenin complexes that anchor to actin filaments of the cytoskeleton (Aberle et al., 1996, Lu et al., 2012). The formation of the complexes is crucial for optimal epithelial cell function and tissue integrity (Zappulli et al., 2012). The decreased expression of E-cadherin is possibly

the most crucial event of EMT that leads to changed phenotypic behavior of the tumor cells (Schmalhofer et al., 2009, Dubois-Marshall et al., 2011). Both E-cadherin and β-catenin expression is dys-regulated by genetic and epigenetic events in various cancers (including breast, prostate, lung, liver, and kidney cancers). This hence leads to loss of epithelial phenotype, metastases and poor survival outcome (Zappulli et al., 2012, Simic et al., 2013). E-cadherin plays significant role as a predictor of primary tumor disease-free survival and distant disease-free survival. It is also an independent prognostic marker in predicting reduced survival duration for breast cancer patients with lymph node positive status (Park et al., 2007). In IDC, loss of E-cadherin and β-catenin expression is reported. It has hence been postulated that down-regulation of E-cadherin promotes the release of membrane-bound β-catenin into the cytosol, enhancing the tumor progression promoting Wnt signaling (Prasad et al., 2009). Canonical Wnt signaling is one of the key signaling pathways involved in the promotion of metastatic behavior in breast cancer (Prasad et al., 2007).

Upon silencing of *CHST3* in T47D cells, the expression levels of E-cadherin and β-catenin were observed to be significantly reduced as shown in Figures 3.16 and 3.17 respectively.

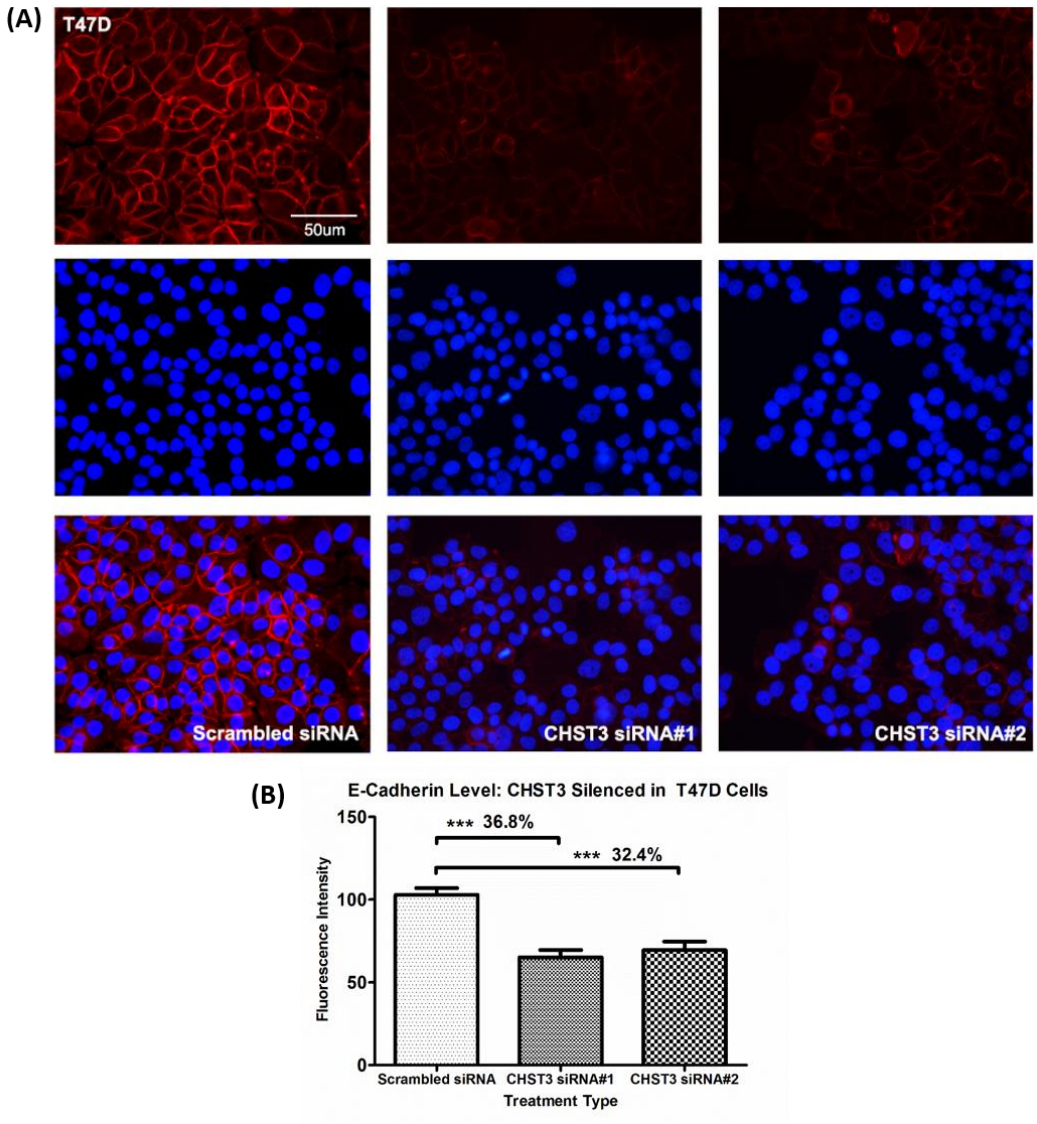

Figure 3.16: E-cadherin expression after silencing *CHST3*
Reductions in E-cadherin expression level were observed in the *CHST3*-silenced groups compared to the scrambled siRNA group after down-regulation of *CHST3* as shown in the (A) immunofluorescence pictures and (B) graph comparing the fluorescence intensities of each group. Data shown were from one independent experiment performed with three biological replicates. * $P < 0.05$; ** $P < 0.01$; *** $P < 0.001$ compared with scrambled siRNA group.

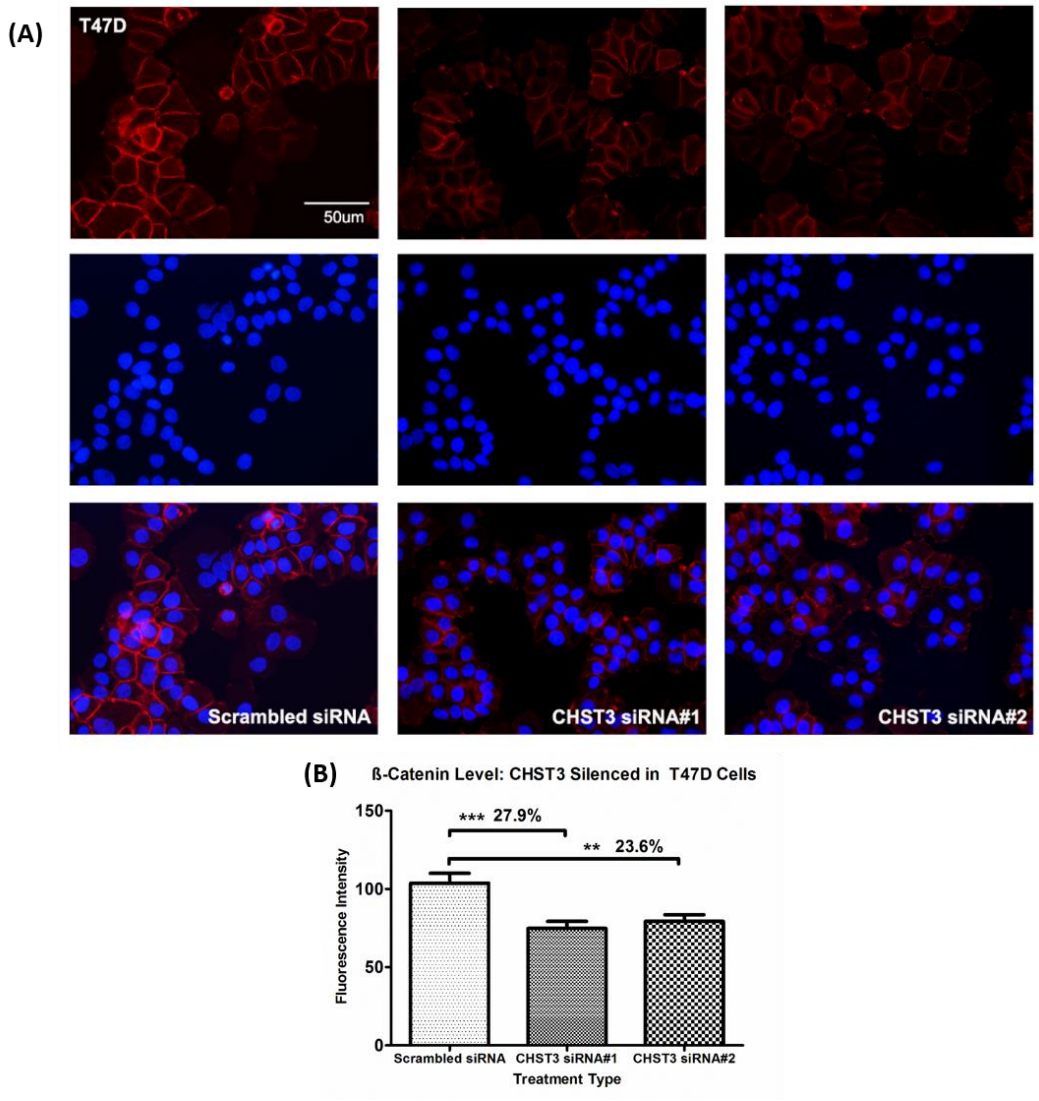

Figure 3.17: β-catenin expression after silencing *CHST3*
Reductions in β-catenin expression level were observed in the *CHST3*-silenced groups compared to the scrambled siRNA group after down-regulation of *CHST3* as shown in the (A) immunofluorescence pictures and (B) graph comparing the fluorescence intensities of each group. Data shown were from one independent experiment performed with three biological replicates. * $P < 0.05$; ** $P < 0.01$; *** $P < 0.001$ compared with scrambled siRNA group.

3.3.2 *CHST3* affects Proteins involved in JAK/STAT Pathway

EMT also acts through the activation of the JAK/STAT pathway, affecting cancer cell proliferation, migration and invasion. The well-established JAK/STAT signaling pathway is an evolutionarily conserved cascade that regulates cellular processes including cell migration and survival (Ekas et al., 2010, Arbouzova and Zeidler, 2006). It has been well-documented to be mis-regulated in various cancers including ovarian cancer, pancreatic cancer, and breast cancer (Spangenburg and Booth, 2002, Burke et al., 2001, Toyonaga et al., 2003), It is one of the key drivers for breast tumor aggressive progression and metastasis (Ling et al., 2013).

In this study, JAK2/STAT3 proteins from the JAK/STAT pathway are observed through Western Blot analyses after silencing of *CHST3* in T47D breast cancer cells. Janus kinase 2 (JAK2) is a cystolic non-receptor tyrosine kinase, that is widely expressed and localized at the intracellular domains of cytokine receptors (Sayyah et al., 2011, Wagner and Schmidt, 2011, Gilbert et al., 2005). When phosphorylated, JAK2 is activated and undergoes dimerization (Sayyah et al., 2011). Despite having numerous phosphorylation sites, auto-phosphorylation of Tyr1007 is essential for JAK2 activation, function, and regulation (Nam et al., 2012). JAK2 plays vital roles in mammary gland development and breast cancer tumor progression (Burke et al., 2001). A known downstream component of JAK2 is signal transducer and activator of transcription 3 (STAT3), a transcription factor that is also commonly expressed in cells and tissues (Gilbert et al., 2005, Yang et al., 2012). STAT3 is activated via phosphorylation by JAK2 at its primary site Tyr705, leading to the dimerization of STAT3 through the SH2 domain interaction (Gilbert et al., 2005, Wagner and Schmidt, 2011, Behera et al., 2010, Wakahara et al., 2012). From the cytoplasm, active STAT3 dimers will translocate into the nucleus and promote the transcription of specific genes, affecting cellular behaviors including cell proliferation and metastasis (Ekas et al., 2010, Arbouzova and Zeidler, 2006, Sansone and Bromberg, 2012). Reported as an oncogenic transformation regulator, STAT3 is involved in approximately 60% of breast tumors (Behera 2009). Constitutive activation of

STAT3 via phosphorylation can promote cell migration, survival and angiogenesis in high grade breast carcinoma (Walker et al., 2009, So et al., 2013, Balanis et al., 2013). Tumor formation and growth as well as metastasis are inhibited upon STAT3 knockdown (through STAT3 shRNA silencing or STAT3 phosphorylation inhibitors) in *in vivo* tumor transplant model (So et al., 2013, Ling et al., 2013)

The phosphorylated forms or active molecular forms that are pJAK2 and pSTAT3, as well as the total JAK2 and total STAT3 protein levels were analyzed. Through Western Blot analyses, observations suggest that activated JAK2 over total JAK2 (Figure 3.18), and activated STAT3 over total STAT3 (Figure 3.19) protein expressions did not show significant differences.

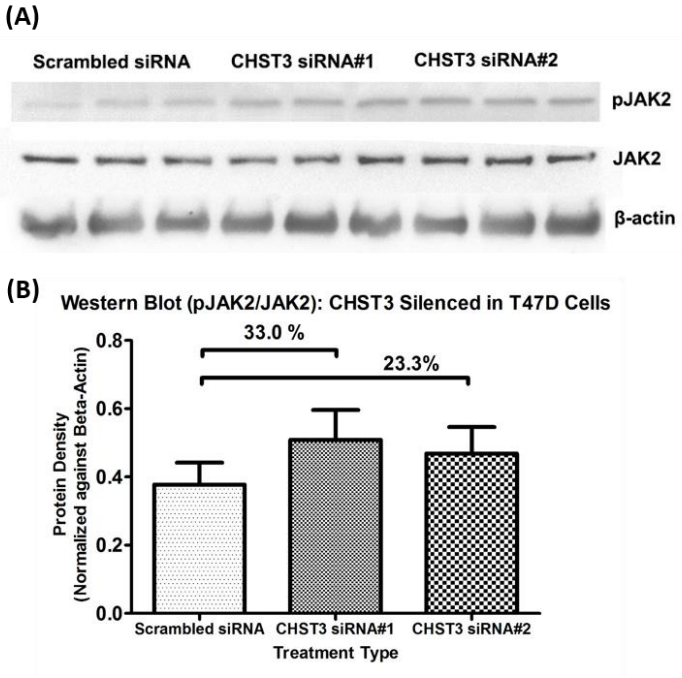

Figure 3.18: pJAK2/JAK2 expression after silencing *CHST3*
Non-significant changes in (B) pJAK2/JAK2 expression levels were observed in the *CHST3*-silenced groups compared to the scrambled siRNA group after down-regulation of *CHST3* as shown in the (A) Western Blot. Protein expressions were normalized against house-keeping protein, β-actin. Data shown were from two independent experiments sets performed with three biological replicates for each experiment set. * $P < 0.05$; ** $P < 0.01$; *** $P < 0.001$ compared with scrambled siRNA group.

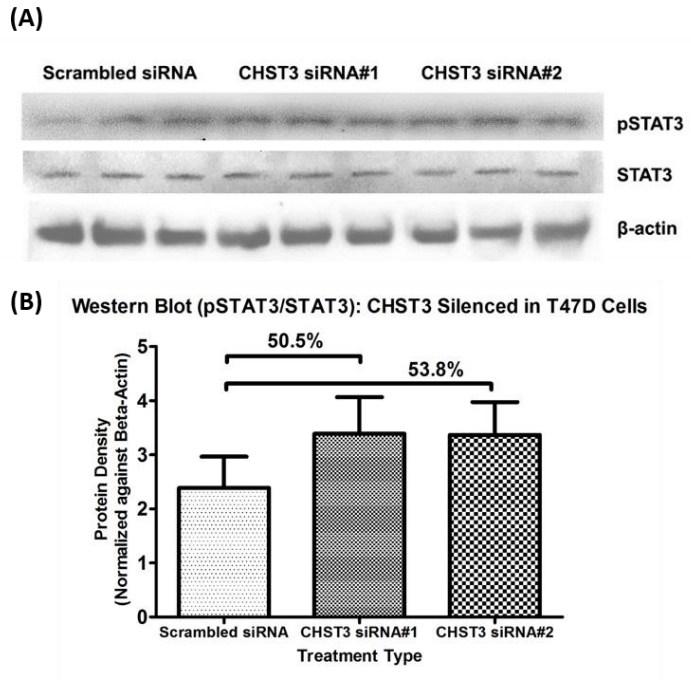

Figure 3.19: pSTAT3/STAT3 expression after silencing *CHST3*
Non-significant changes in (B) pSTAT3/STAT3 expression levels were observed in the *CHST3*-silenced groups compared to the scrambled siRNA group after down-regulation of *CHST3* as shown in the (A) Western Blot. Protein expressions were normalized against house-keeping protein, β-actin. Data shown were from two independent experiments sets performed with three biological replicates for each experiment set. * $P < 0.05$; ** $P < 0.01$; *** $P < 0.001$ compared with scrambled siRNA group.

3.3.3 *CHST3* affects Protein involved in Cell Apoptosis Pathway

As small changes were observed in cell proliferation and cell apoptosis levels upon regulation of *CHST3* in breast cancer cells, the expression level of one protein from the apoptosis pathway, BAD, was examined to validate the observations. Pro-apoptotic BAD is part of the B-cell lymphoma 2 (BCL2) family. BAD is activated via dephosphorylation and forms an inhibitory heterodimer with Bcl-2 or Bcl-xL to catalyze the oligomerization of BAK and BAX (Howells et al., 2010, Berndtsson et al., 2005). After which, mitochondrial outer membrane permeabilization occurs causing cytosolic release of DIABLO and cytochrome c, eliciting cell death (Howells et al., 2010, Cannings et al., 2007). Three main phosphorylation sites are situated at position Ser112, Ser136, and Ser155. Both Ser112 and Ser136 phosphorylation facilitates 14-3-3 binding and kinase access to Ser155, while Ser155 phosphorylation hinders Bcl-xL binding (Datta et al., 2000). Although

phosphorylation at Ser136 is necessary to regulate pro-apoptotic function of BAD, phosphorylation at Ser112 protects the dephosphorylation of Ser136, indicating that BAD function is dependent on the dephosphorylation of Ser112 (Chiang et al., 2003). The phosphorylation of BAD protein has been associated with cell survival and proliferation of some cancers (Howells et al., 2010). *In vitro* and *in vivo* studies in non-small lung cancer revealed that the over-expression of BAD inhibits cell growth and promotes cell apoptosis (Huang et al., 2012). BAD in BRAF mutant melanoma cells is also implicated in cell proliferation (Polzien et al., 2011). Additionally, patients with high Bad expression in their tumors had improved survival outcome compared against patients with low Bad expression (Cannings et al., 2007). Through Western Blot analyses (Figure 3.20), observations suggest that inactivated BAD over BAD protein expressions were enhanced upon down-regulation of *CHST3* in T47D cells.

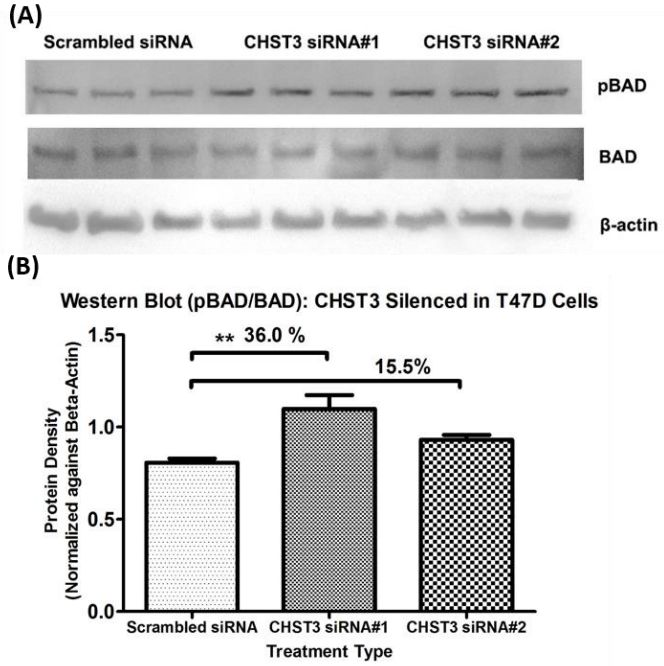

Figure 3.20: pBAD/BAD expressions after silencing *CHST3*
Increases in (B) pBAD/BAD expression levels were observed in the *CHST3*-silenced groups compared to the scrambled siRNA group after down-regulation of *CHST3* as shown in the (A) Western Blot. Protein expressions were normalized against house-keeping protein, β-actin. Data shown were from two independent experiment sets performed with three biological replicates for each experiment set. * $P < 0.05$; ** $P < 0.01$; *** $P < 0.001$ compared with scrambled siRNA group.

3.4 Genome –Wide Expression Profiling of *CHST3*-Silenced T47D Cells

CHST3, from observations obtained, has thus far been found to be more expressed in normal breast cells as well as less aggressive breast cancer cells compared to more aggressive and metastatic breast cancer cells. Additionally, *CHST3* is found to have tumor suppressor roles in breast carcinoma according to the phenotypic behavior studies performed. Protein expression studies have also suggested associations of several proteins in different cellular behavioral pathways to the effects observed in the phenotypic behavioral changes after regulation of *CHST3* expression level. Following this, *CHST3* was silenced in T47D cells and genome-wide microarray was carried out to identify significant gene expression changes in *CHST3*-related genes, in order to further explore potential pathways in which *CHST3* is possibly involved in the malignant process of tumorigenesis.

3.4.1 RNA Yield, Quality, and Integrity

The quality and integrity of the RNA samples sent for microarray processing were important factors to be taken into account to ensure success of gene microarray hybridization. The quality of RNA samples were defined by A260/A280 absorbance ratio as well as the RNA integrity number (RIN) value, as summarized in Figure 3.21A. RIN value is ranged from 1 (degraded RNA) to 10 (intact RNA) and is calculated based on the ratio of 28S/18S ribosomal RNA using Agilent 2100 Bioanalyzer. All samples showed RIN values above 9 indicating that the RNA samples were of good quality.

The gel image in Figure 3.21B showed two specific distinct bands (representing 18S and 28S ribosomal subunits). Additionally, electropherograms as illustrated in Figure 3.21C depicting two sharp peaks at 18S and 28S indicate good integrity of the RNA samples. After strict quality control evaluation, the RNA samples were qualified to be used for subsequent steps in the microarray sample processing.

(A)

Criteria	Scrambled siRNA	*CHST3*-Silenced
RIN	9.87 ± 0.09	9.93 ± 0.07
Conc (ng/ul)	37.44 ± 1.17	39.06 ± 1.13
A260/A280	1.93 ± 0.12	1.92 ± 0.03

(B)

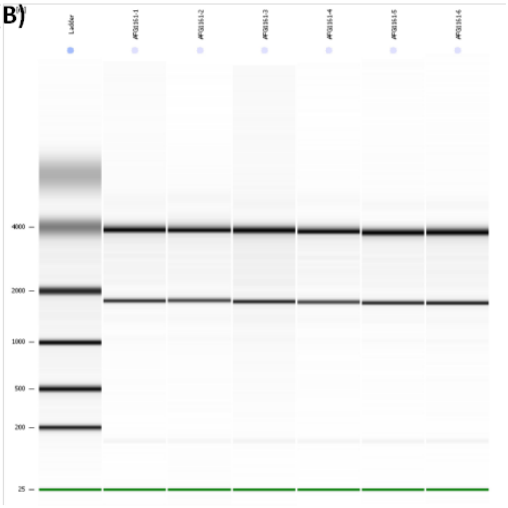

(C)

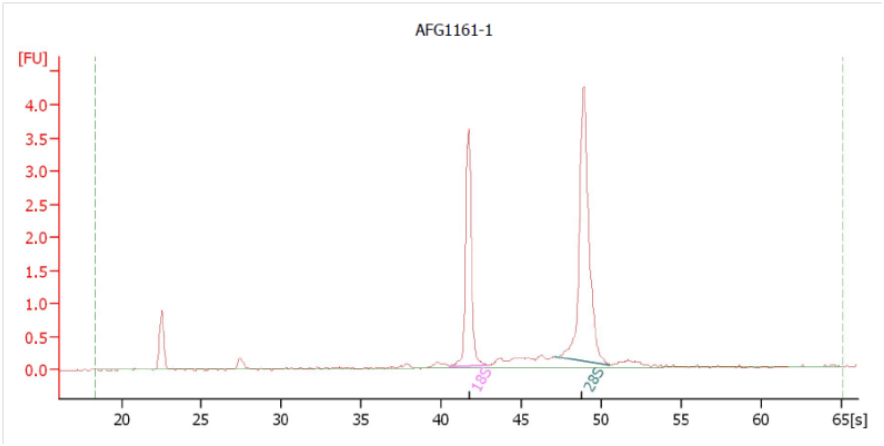

Figure 3.21: Quality and integrity of RNA samples for microarray
The RNA quality and integrity of the samples were shown through their (A) RIN number, concentration, and A260/280, (B) gel image consisting 18S (lower band) and 28S (upper band) in every lane, and (C) electropherogram image showing sharp peaks at 18S and 28S indicating highly intact RNA. Triplicates for each group (scrambled siRNA and *CHST3*-silenced) were used in the processing. Values in (A) are indicated as mean ± standard error.

3.4.2 Target Preparation

For each sample, 100ng of total RNA was used for the assay. Table 3.1 shows the results of the purified cRNA, that was later fragmented and the size distribution of the resulting product was checked by gel electrophoresis.

Table 3.1: Spectrophotometer reading of purified cRNA
Values are indicated as mean ± standard error.

Criteria	Control	Silenced
260/280 Ratio	2.076 ± 0.002	2.084 ± 0.007
Conc (ng/ul)	1470 ± 50.00	1433 ± 46.67
Yield (ug)	73.50 ± 2.500	71.67 ± 2.333

3.4.3 Gene Microarray Data Analysis

Synthesized biotin-labeled cRNA were hybridized on to the Human U133 Plus 2.0 Arrays. Arrays were washed and stained prior to scanning using Affymetrix 3000 7G scanner. The resultant scanned image file and raw signal intensities for all probe sets were obtained. After which, Expression Console and Genespring softwares were utilized to process the microarray data. Based on stringent criteria including p-value below 0.05 and fold change of at least 2 folds, 58 genes obtained showed significant alteration after silencing of *CHST3* in T47D cells. Of the 58 genes, 15 genes were up-regulated and 43 genes were down-regulated after silencing of *CHST3*.

3.4.4 Functional Categorization of Genes Affected from Silencing *CHST3*

The list of 58 differentially expressed genes were categorized in accordance to their gene function(s) using Database for Annotation, Visualization, and Integrated Discovery (DAVID) microarray analysis software. Figure 3.22 depicts the number of genes involved in various cellular processes upon down-regulation of *CHST3*. Table 3.2 shows the various up-regulated and down-regulated genes regulated after silencing of *CHST3* in T47D cells. It is noted that a substantial number of genes are involved in cell migration and invasion as compared to genes involved in other phenotypic behaviors, which suggests consistency with the phenotypic behavioral changes observed.

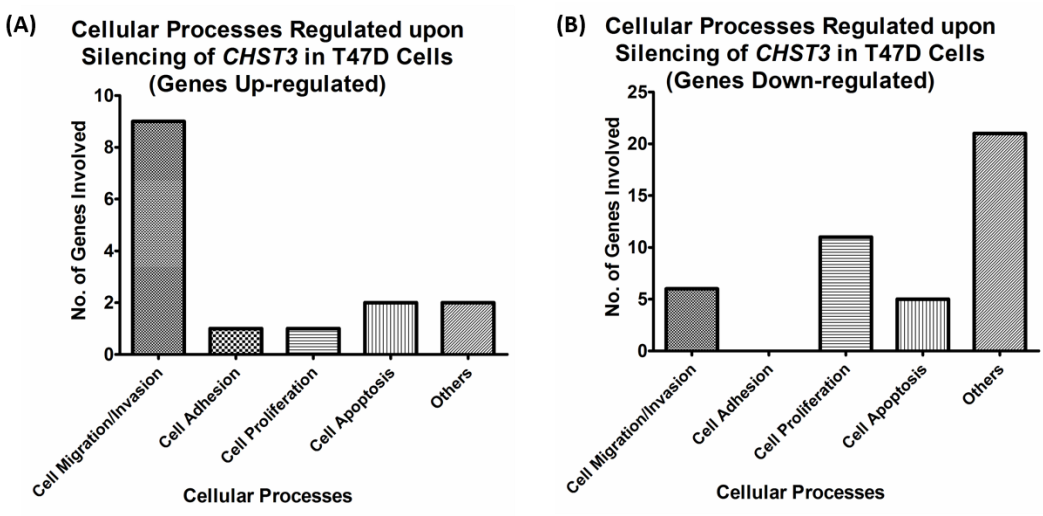

Figure 3.22: Functional categorization of affected genes after *CHST3* silencing
Graphs (A) and (B) depict the functional categorization of up-regulated and down-regulated genes respectively (≥ 2 folds change) after down-regulation of *CHST3* in T47D cells.

Table 3.2: Functional categorization of differentially expressed genes (≥ 2 folds change)

Function	Gene Symbol	Gene Name	Relative Expression
Cell Migration	FLRT3	fibronectin leucine rich transmembrane protein 3	5.48
	TGFB2	transforming growth factor, beta 2	4.37
	GPNMB	glycoprotein (transmembrane) nmb	2.94
	DUSP1	dual specificity phosphatase 1	2.91
	PCLO	piccolo (presynaptic cytomatrix protein)	2.86
	ABCC5	ATP-binding cassette, sub-family C (CFTR/MRP), member 5	2.61
	CYR61	cysteine-rich, angiogenic inducer, 61	2.36
	ANXA1	annexin A1	2.30
	PAX6	paired box 6	-2.01
	ADAMTS15	ADAM metallopeptidase with thrombospondin type 1 motif, 15	-2.03
	RDX	radixin	-2.07
	SLC7A11	solute carrier family 7, (cationic amino acid transporter, y+ system) member 11	-2.09
	ANTXR1	anthrax toxin receptor 1	-3.24
	ELK3	ELK3, ETS-domain protein (SRF accessory protein 2)	-4.15
Cell Invasion	FLRT3	fibronectin leucine rich transmembrane protein 3	5.48
	TGFB2	transforming growth factor, beta 2	4.37
	FGF12	fibroblast growth factor 12	3.84
	GPNMB	glycoprotein (transmembrane) nmb	2.94

	DUSP1	dual specificity phosphatase 1	2.91
	ABCC5	ATP-binding cassette, sub-family C (CFTR/MRP), member 5	2.61
	ADAMTS15	ADAM metallopeptidase with thrombospondin type 1 motif, 15	-2.03
Cell Adhesion	FLRT3	fibronectin leucine rich transmembrane protein 3	5.48
	TGFB2	transforming growth factor, beta 2	4.37
	GPNMB	glycoprotein (transmembrane) nmb	2.94
	PCLO	piccolo (presynaptic cytomatrix protein)	2.86
	CYR61	cysteine-rich, angiogenic inducer, 61	2.36
	KRTAP3-1	keratin associated protein 3-1	2.01
	RDX	radixin	-2.07
	ANTXR1	anthrax toxin receptor 1	-3.24
Cell Proliferation	TGFB2	transforming growth factor, beta 2	4.37
	FGF12	fibroblast growth factor 12	3.84
	DUSP1	dual specificity phosphatase 1	2.91
	CDKN2B	cyclin-dependent kinase inhibitor 2B (p15, inhibits CDK4)	2.58
	CYR61	cysteine-rich, angiogenic inducer, 61	2.36
	ANXA1	annexin A1	2.30
	PAX6	paired box 6	-2.01
	DNAJC2	DnaJ (Hsp40) homolog, subfamily C, member 2	-2.02
	MDFIC	MyoD family inhibitor domain containing	-2.05
	MCM10	minichromosome maintenance complex component 10	-2.06
	HIPK1	homeodomain interacting protein kinase 1	-2.08
	BRCC3	BRCA1/BRCA2-containing complex, subunit 3	-2.20
	LAMP3	lysosomal-associated membrane protein 3	-2.28
	ASNS	asparagine synthetase (glutamine-hydrolyzing)	-2.31
	KIF23	kinesin family member 23	-2.40
	PRIM2	primase, DNA, polypeptide 2 (58kDa)	-2.62
	DDX18	DEAD (Asp-Glu-Ala-Asp) box polypeptide 18	-2.73
	PRKAR2B	protein kinase, cAMP-dependent, regulatory, type II, beta	-2.88
	PDZK1	PDZ domain containing 1	-3.00
	PSAT1	phosphoserine aminotransferase 1	-4.47
Cell apoptosis	TGFB2	transforming growth factor, beta 2	4.37
	FGF12	fibroblast growth factor 12	3.84
	DUSP1	dual specificity phosphatase 1	2.91
	ANXA1	annexin A1	2.30

	STRADB	STE20-related kinase adaptor beta	2.23
	DICER1	dicer 1, ribonuclease type III	2.01
	WT1	Wilms tumor 1	-2.07
	HIPK1	homeodomain interacting protein kinase 1	-2.08
	ASNS	asparagine synthetase (glutamine-hydrolyzing)	-2.31
	RNF130	ring finger protein 130	-2.37
	BRCC3	BRCA1/BRCA2-containing complex, subunit 3	-2.20
Angiogenesis	TGFB2	transforming growth factor, beta 2	4.37
	DUSP1	dual specificity phosphatase 1	2.91
	DICER1	dicer 1, ribonuclease type III	2.01
	HIPK1	homeodomain interacting protein kinase 1	-2.08
	ELK3	ELK3, ETS-domain protein (SRF accessory protein 2)	-4.15
Metabolic Process	SLC16A9	solute carrier family 16, member 9 (monocarboxylic acid transporter 9)	2.38
	OBFC2A	oligonucleotide/oligosaccharide-binding fold containing 2A	2.15
	GNG11	guanine nucleotide binding protein (G protein), gamma 11	-2.00
	RFK	riboflavin kinase	-2.02
	TMX3	thioredoxin-related transmembrane protein 3	-2.08
	EIF2S1	eukaryotic translation initiation factor 2, subunit 1 alpha, 35kDa	-2.11
	ALDH1L2	PDZ domain containing 1	-3.00
	PDZK1	PDZ domain containing 1	-3.00
Transcription Regulation	GTF2E2	general transcription factor IIE, polypeptide 2, beta 34kDa	-2.03
	EIF3J	eukaryotic translation initiation factor 3, subunit J	-2.08
	PHTF2	putative homeodomain transcription factor 2	-2.10
	MBNL1	muscleblind-like (Drosophila)	-2.12
	CBX3	chromobox homolog 3 (HP1 gamma homolog, Drosophila)	-2.35
	PRIM2	primase, DNA, polypeptide 2 (58kDa)	-2.62
	DPY30	dpy-30 homolog (C. elegans)	-3.86
Signal Transduction	STRADB	STE20-related kinase adaptor beta	2.23
	GNG11	guanine nucleotide binding protein (G protein), gamma 11	-2.00
	SLITRK4	SLIT and NTRK-like family, member 4	-2.03
	ODZ2	odz, odd Oz/ten-m homolog 2 (Drosophila)	-2.08
	RAB12	RAB12, member RAS oncogene family	-2.12

	CBS	cystathionine-beta-synthase	-2.20
	PRKAR2B	protein kinase, cAMP-dependent, regulatory, type II, beta	-2.88
Ion/Protein Transport	DNAJC24	DnaJ (Hsp40) homolog, subfamily C, member 24	-2.10
	C11orf54	chromosome 11 open reading frame 54	-2.19
	LARS	leucyl-tRNA synthetase	-2.22
	DNAJC21	DnaJ (Hsp40) homolog, subfamily C, member 21	-2.28
	NXT2	nuclear transport factor 2-like export factor 2	-2.34
	LMAN2	lectin, mannose-binding 2	-2.40

3.5 Downstream Molecules of *CHST3* Silencing

An extensive literature review was carried out to evaluate the potential functions of the genes from the microarray list. Among the genes, a few genes were found to be potentially involved in the observed phenotypic changes after regulation of *CHST3* in breast cancer cells. Two genes, that were up-regulated of their expression after *CHST3* was silenced in T47D breast cancer cells, were chosen to be examined further: glycoprotein transmembrane nbm (*GPNMB*) and fibronectin leucine-rich transmembrane (*FLRT3*).

GPNMB (or sometimes known as osteoactivin) is a type I transmembrane glycoprotein, localized on the cell surface and lysosomal membrane. It can also be secreted by cells (Tsui et al., 2012, Safadi et al., 2001). GPNMB has been studied in various carcinomas including melanoma, hepatocellular carcinoma, lung cancer, stomach cancer, as well as breast cancer (Loging et al., 2000, Nielsen et al., 2002, Haralanova-Ilieva et al., 2005, Borczuk et al., 2003, Rich et al., 2003). In skin malignancies, GPNMB expression level was significantly higher than that in normal and benign skin tissues. Also, GPNMB was positively immunostained in 87% of malignant melanoma cases and 80% of squamous cell carcinoma cases (Zhao et al., 2012).

GPNMB has been shown to have an oncogenic role in breast carcinoma; the over-expression of *GPNMB* in breast cancer cells caused increased cell invasion and metastasis (Rose et al., 2007). This result supports the phenotypic behavior changes observed in this study as cell invasion and cell migration were both reduced after down-regulating *GPNMB* in breast cancer cells. In another study (Rose et al., 2010), high expression of GPNMB can be observed in basal and triple negative types of breast cancer compared to normal breast tissues. Furthermore, high GPNMB level has been correlated to increased tumor recurrence risk, shorter time to tumor recurrence, and decreased overall patient survival (Rose et al., 2010). *GPNMB* was hence identified as a candidate gene that could be regulated by *CHST3* and is potentially involved in breast cancer metastasis, invasion, and growth.

As for *FLRT3*, no known expression profile and functional study of this cell surface protein have been carried out in human cells or tissues. In the developmental biology field, in Xenopus embryos, Flrt3 expression was observed at sites with higher occurrences of epithelial-mesenchymal (EMT) interactions, such as eyes, developing tooth buds, and hair follicles, hence indicating its importance in mediating cell migration (Gong et al., 2009). Apart from regulating cell migration, Flrt3 has been reported to inhibit C-cadherin-mediated cell adhesion after it is induced by Tgfβ signaling (Chen et al., 2009b). Additionally, Flrt3 co-expresses with Fgf8, interacts with Fgf receptors (Fgfr) to activate MAPK signaling cascade (Karaulanov et al., 2006). As *FLRT3* is not well-studied yet in cancer, it was chosen in order to examine its expression and functions in human breast cancer. Additionally, its association with *CHST3* would be examined.

In order to evaluate whether *CHST3* and *GPNMB* or *FLRT3* works together in regulating phenotypic behaviors of breast cancer cells, the functional assays were performed after double silencing *CHST3* together with either *GPNMB* or *FLRT3* in T47D cells. The hypothesis then would be that *GPNMB* and *FLRT3* are downstream molecules of *CHST3*, whereby *CHST3* regulates their expression levels and hence, brings rise to the observed phenotypic changes.

To elaborate more on the double silencing experiment design, four groups were performed namely (Group 1) double negative, (Group 2) *CHST3*-silenced, (Group 3) *GPNMB*- or *FLRT3*- silenced, and (Group 4) double silenced of either *CHST3* and *GPNMB* silenced or *CHST3* and *FLRT3* silenced. For Groups 1 to 3, additional scrambled siRNA was included to match the volume and concentration of siRNAs in Group 4.

3.5.1 CHST3 modulates GPNMB

3.5.1.1 Silencing Efficiency of CHST3 and GPNMB

GPNMB mRNA expression level was validated in *CHST3*-single-silenced T47D cells. As shown in Figure 3.23, *GPNMB* expression level increased by almost 2 folds after down-regulation of *CHST3*. Also, prior to carrying out the phenotypic assays, the expression levels of *CHST3* and *GPNMB* in double silenced groups were evaluated at mRNA (Figure 3.24 A and B) as well as protein level (Figure 3.24 (C to F). As observed from qPCR, *CHST3* was down-regulated by more than 80% in the *CHST3*-silenced group and *CHST3-GPNMB* silenced group. Its expression was not affected in the *GPNMB*-silenced group. As for *GPNMB* expression level, it was up-regulated by 41.1% in the *CHST3*-silenced group. *GPNMB* level was down-regulated by at least 65% in the *GPNMB*-silenced group and *CHST3-GPNMB* silenced group.

From the western blot results, a similar trend was observed. CHST3 was down-regulated by more than 45% in the *CHST3*-silenced group and *CHST3-GPNMB* silenced group. Its expression was not affected in the *GPNMB*-silenced group. Looking at GPNMB, it was up-regulated in both of its protein forms (80kDa and 115kDa) GPNMB expression was down-regulated in the *GPNMB*-silenced group and similar to double negative group in the *CHST3-GPNMB* silenced group.

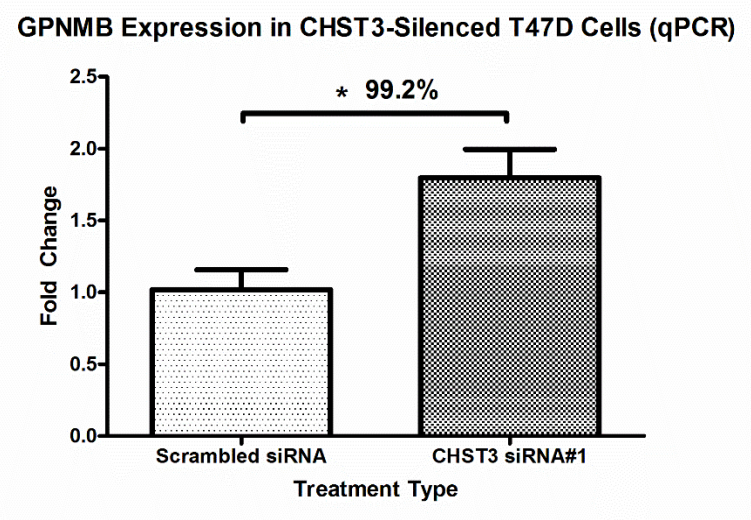

Figure 3.23: *GPNMB* expression in *CHST3* single-silenced T47D cells
The mRNA expression level of *GPNMB* was enhanced by almost 2 folds in T47D cells after single-silencing *CHST3*. *GAPDH* mRNA expression level was used as the house-keeping gene for normalization. Data shown was from one independent experiment performed with three biological replicates. * $P < 0.05$; ** $P < 0.01$; *** $P < 0.001$ compared with scrambled siRNA group.

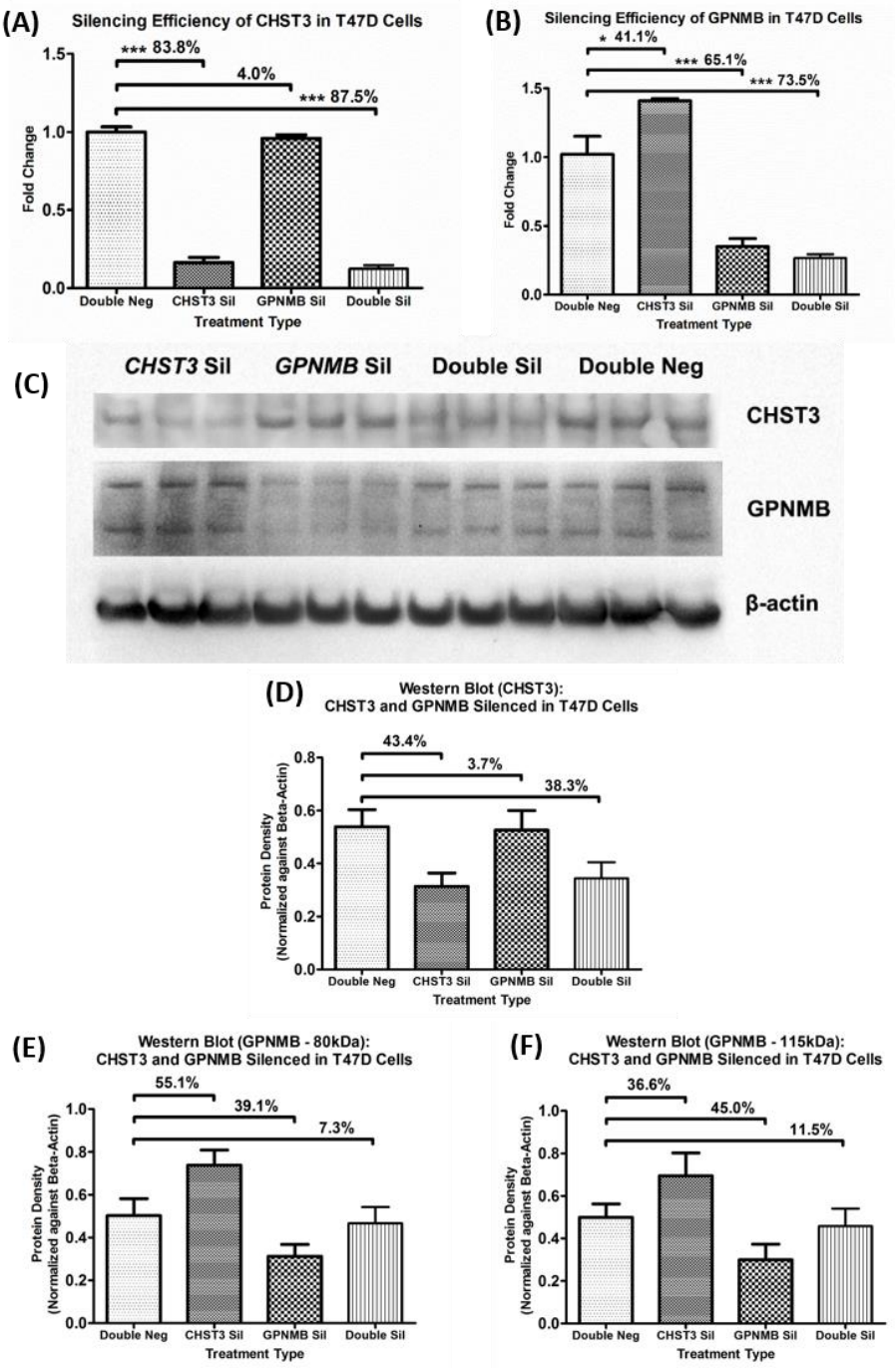

Figure 3.24: *CHST3* and *GPNMB* levels after different silencing treatments in T47D cells qPCR was carried out to evaluate the mRNA expression levels of (A) *CHST3* and (B) *GPNMB* in the various groups. *GAPDH* mRNA expression level was used as the house-keeping gene for normalization. From (C) western blot analyses, (D) CHST3 and (E and F) GPNMB protein levels were examined for the various silencing treatment groups. B-actin was used as the house-keeping protein for normalization. Data shown in (A) and (B) were from one independent experiment set performed with three biological replicates. Data shown in (D), (E), and (F) were from two independent experiment sets performed with three biological replicates each.* $P < 0.05$; ** $P < 0.01$; *** $P < 0.001$ compared with double negative group.

3.5.1.2 Regulation of Cellular Behaviors by CHST3 and GPNMB

3.5.1.2.1 Regulation of Cell Migration by CHST3 and GPNMB

Migration assay was carried out to examine the effect of double silencing *CHST3* and *GPNMB* on cell migration ability of T47D cells compared to the double negative, *CHST3*-silenced, and *GPNMB*-silenced groups. Post 48 hours transfection, the transfected cells were re-seeded into migration chambers and incubated for 24 hours. Silencing *CHST3* alone increased cell migration level. Silencing of *GPNMB* alone decreased cell migration. Rose et al had previously showed an increase in cell migration upon ectopic expression of *GPNMB* (Rose et al., 2007). As depicted in Figure 3.25, double silencing of *CHST3* and *GPNMB* abrogated these changes in cell migration level.

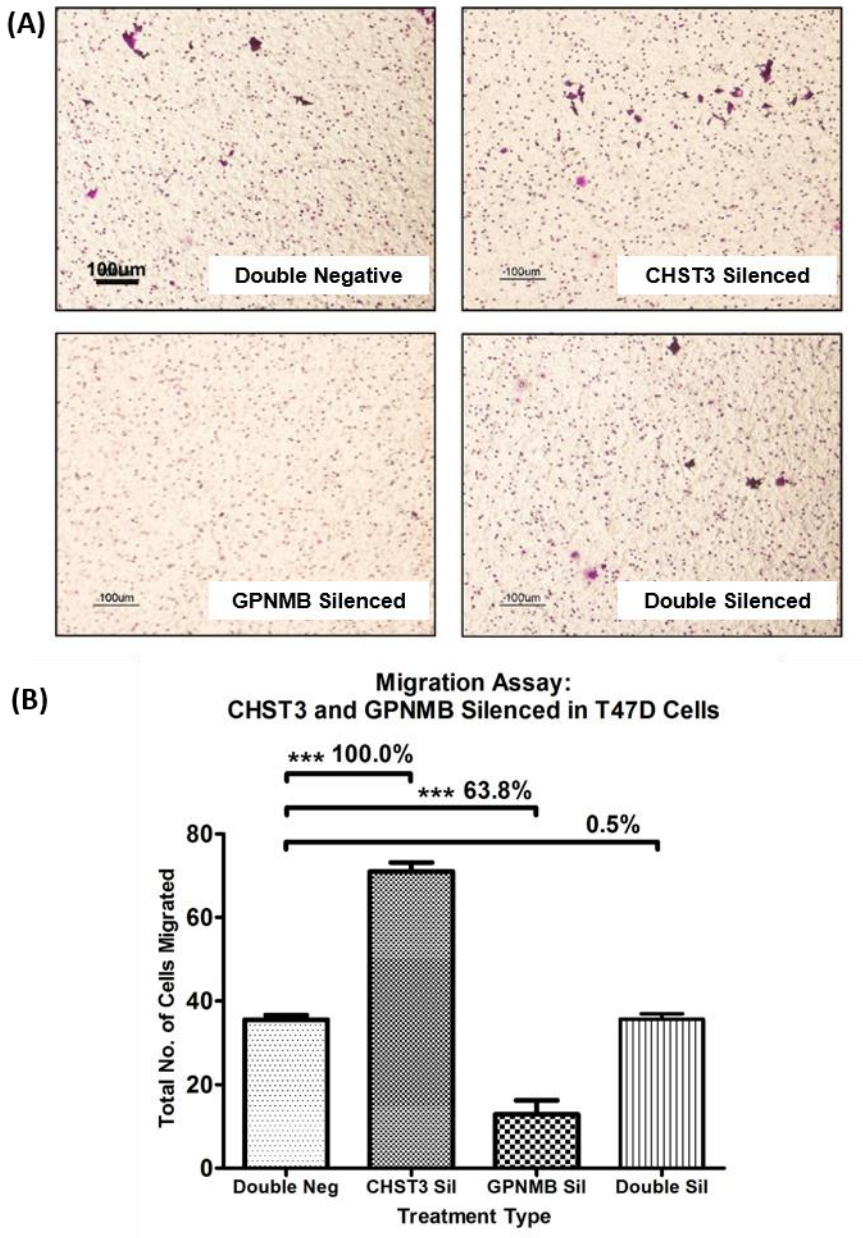

Figure 3.25: Effects of *CHST3* and *GPNMB* double silencing on cell migration
As shown in the (A) pictures and (B) graph, silencing of *CHST3* caused an increase in cell migration; while on the other hand, down-regulation of *GPNMB* caused a reduction in cell migration. Double silencing of *CHST3* and *GPNMB* abrogated these changes in cell migration level. Data shown were from two independent experiment sets performed with three biological replicates for each experiment set. * $P < 0.05$; ** $P < 0.01$; *** $P < 0.001$ compared with double negative group.

3.5.1.2.2 Regulation of Cell Invasion by CHST3 and GPNMB

Invasion assay, using Matrigel chambers, was carried out to evaluate the effect of double silencing *CHST3* and *GPNMB* on cell invasion ability of T47D cells compared to the double negative, *CHST3*-silenced, and *GPNMB*-silenced groups. After 48 hours transfection, the transfected cells were re-seeded into the invasion chambers and incubated for 24 hours. From the single-silenced experiment, it was observed that silencing of *CHST3* increased cell invasion level. Upon silencing of *GPNMB*, cell invasion decreased. From Figure 3.26, double silencing of *CHST3* and *GPNMB* abrogated these changes in cell invasion level.

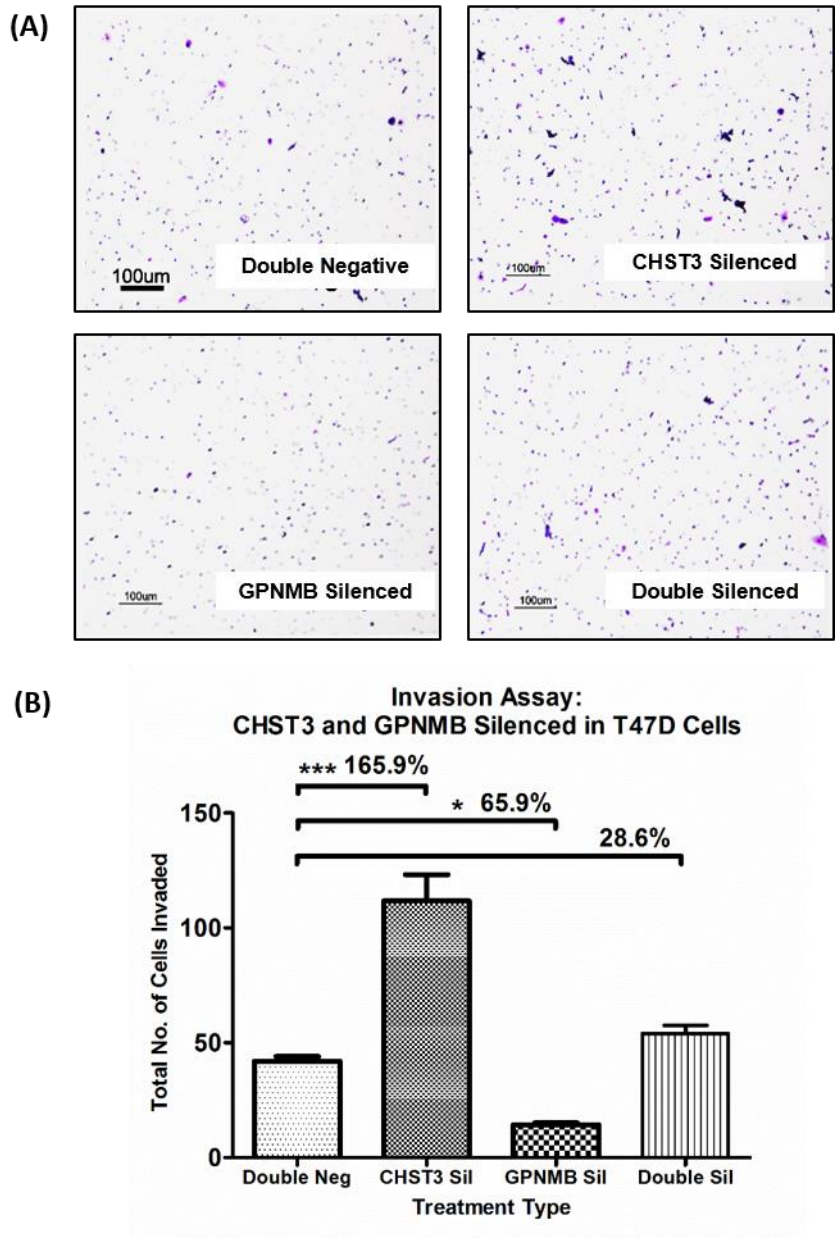

Figure 3.26: Effects of *CHST3* and *GPNMB* double silencing on cell invasion
As shown in the (A) pictures and (B) graph, silencing of *CHST3* caused an increase in cell invasion; while on the other hand, down-regulation of *GPNMB* caused a reduction in cell invasion. Double silencing of *CHST3* and *GPNMB* abrogated these changes in cell invasion level. Data shown was from one independent experiment set performed with three biological replicates. * $P < 0.05$; ** $P < 0.01$; *** $P < 0.001$ compared with double negative group.

3.5.1.2.3 Regulation of Cell Adhesion by CHST3 and GPNMB

Adhesion assay, using fibronectin- and collagen-coated plates, was performed to examine the effect of double silencing *CHST3* and *GPNMB* on regulating the adhesion capability of T47D cells on ECM components. Post 48 hours transfection, transfected cells were re-seeded into fibronectin- and collagen-coated plates. From the single-silenced experiment, it was observed that silencing of *CHST3* decreased cell adhesion level in the fibronectin-coated plate. Upon silencing of *GPNMB*, cell adhesion increased. Results in Figure 3.27A (using fibronectin-coated plate) suggest that double silencing of *CHST3* and *GPNMB* abrogated these changes in cell adhesion level. On the other hand, no significant changes were observed in the collagen-coated plate experiment.

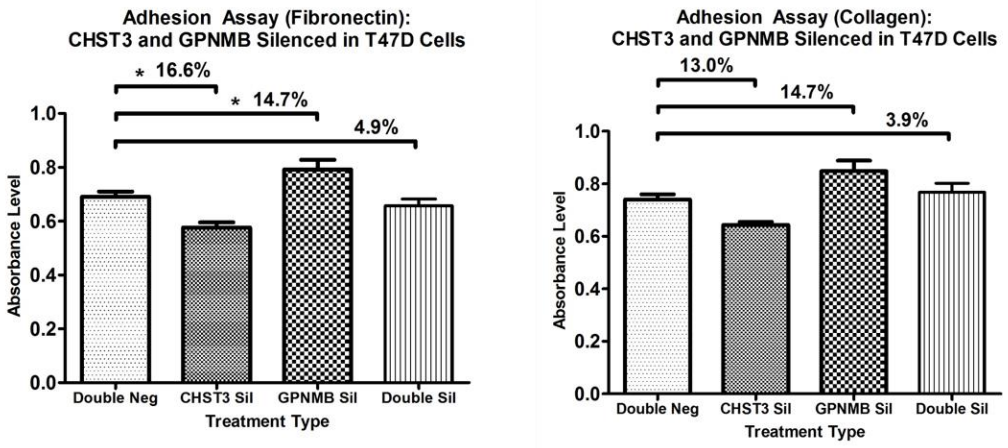

Figure 3.27: Effects of *CHST3* and *GPNMB* double silencing on cell adhesion
From the fibronectin-coated plate (A), silencing of *CHST3* caused a decrease in cell adhesion; while on the other hand, down-regulation of *GPNMB* caused an increase in cell adhesion. Double silencing of *CHST3* and *GPNMB* abrogated the changes in cell adhesion level. In contrast, no significant changes was observed in cell adhesion level in the collagen-coated plate. Data shown were from two independent experiment sets performed with three biological replicates each. * $P < 0.05$; ** $P < 0.01$; *** $P < 0.001$ compared with double negative group.

3.5.1.2.4 Regulation of Cell Proliferation by CHST3 and GPNMB

Proliferation assay, using MTS assay, was performed to evaluate the effect of double silencing *CHST3* and *GPNMB* on cell proliferation capability of T47D cells. Cell proliferation levels were assessed 48 hours after transfection. From the single-silenced experiment, it was observed that silencing of *CHST3* increased cell proliferation level. Upon silencing of *GPNMB*, cell proliferation decreased. From Figure 3.28, results suggest that double silencing of *CHST3* and *GPNMB* abrogated these changes in cell proliferation level.

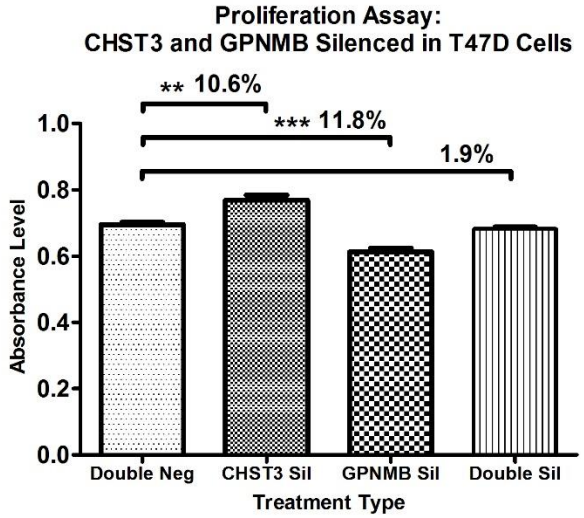

Figure 3.28: Effects of *CHST3* and *GPNMB* double silencing on cell proliferation
Silencing of *CHST3* caused an increase in cell proliferation; while on the other hand, down-regulation of *GPNMB* caused a decrease in cell proliferation. Double silencing of *CHST3* and *GPNMB* caused cell proliferation level to return to basal level (similar to double negative group). Data shown were from two independent experiment sets performed with three biological replicates each. * $P < 0.05$; ** $P < 0.01$; *** $P < 0.001$ compared with double negative group.

3.5.2 *FLRT3* in Breast Cancer Cells

Prior to carrying out double silencing experiments of *CHST3* and *FLRT3*, single silencing of *FLRT3* in T47D and MDA-MB-231 cells was performed. As no literature on *FLRT3* functional role in cancer is known thus far, it would be necessary to examine *FLRT3*'s role in the various cellular behaviors. Two breast cancer cell lines as well as two siRNA sequences specifically targeting *FLRT3* were used to validate the phenotypic changes observed.

3.5.2.1 Silencing Efficiency of FLRT3

The silencing efficiencies of FLRT3 at both mRNA and protein levels were firstly determined before carrying out of phenotypic assays. *FLRT3* was silenced through transient transfection in T47D and MDA-MB-231 cells using Silencer Select siRNA accompanied with delivery reagent, Oligofectamine. From the qPCR results, *FLRT3* mRNA was at least 72.3% and 74.3% silenced as compared to the scrambled siRNA groups in T47D cells (Figure 3.29B) and MDA-MB-231 cells (Figure 3.30B) respectively. From the immunofluorescence results, FLRT3 protein was at least 50.1% and 60.2% down-regulated in comparison to the scrambled siRNA groups in T47D cells (Figure 3.29A and C) and MDA-MB-231 cells (Figure 3.30A and C) respectively.

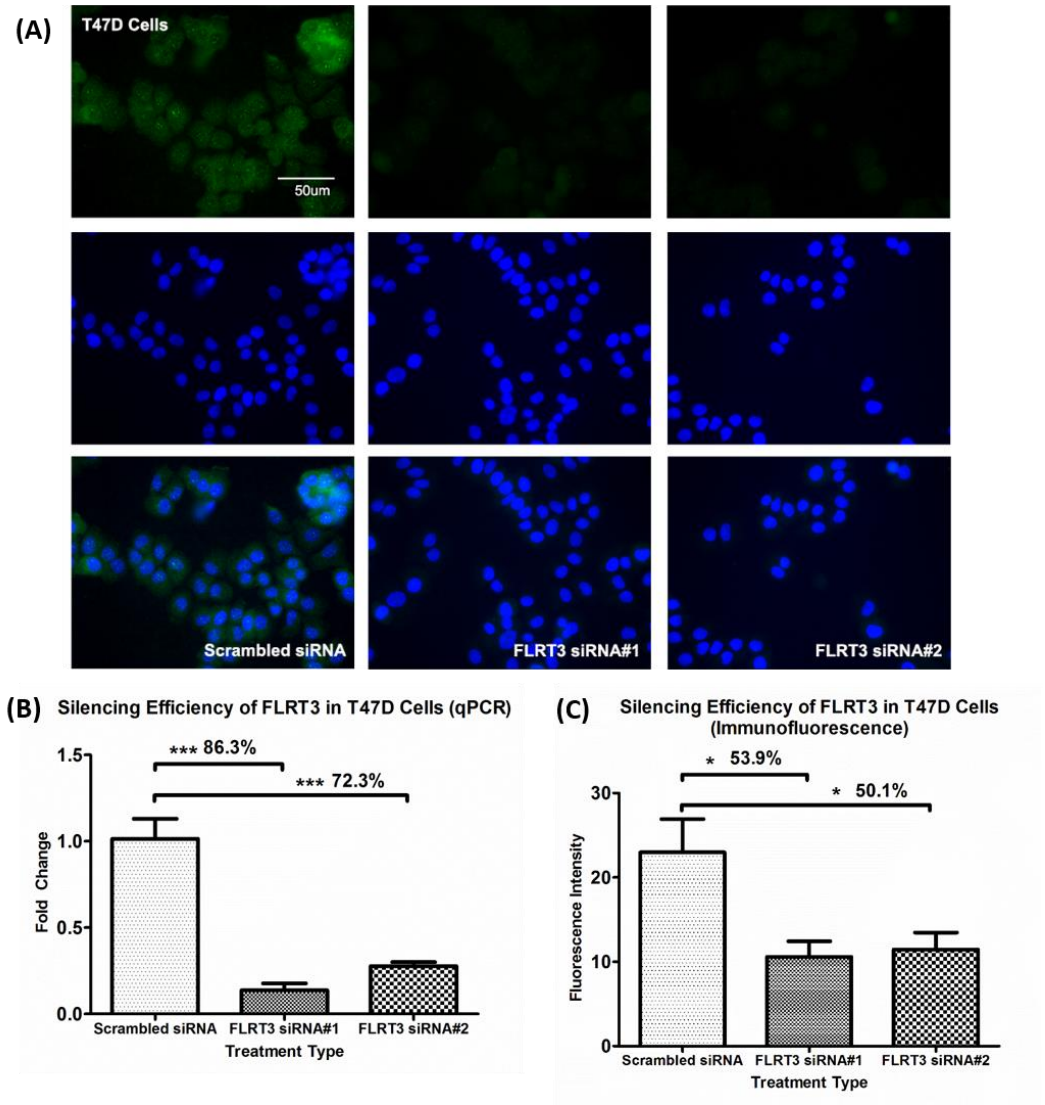

Figure 3.29: Silencing efficiencies of FLRT3 in T47D cells
Silencing efficiencies of FLRT3 mRNA and protein levels were obtained for both siRNA sequences specifically targeting *FLRT3*. In the qPCR analysis (B), the mRNA expression levels of *GAPDH* house-keeping genes were used for normalization. (A) Immunofluorescence staining depict the silencing efficiencies of FLRT3 protein expression level in T47D cells. Graph (C) shows the silencing efficiencies of FLRT3 protein observed in immunofluorescence. Data shown were each from one independent experiment performed with three biological replicates. * $P < 0.05$; ** $P < 0.01$; *** $P < 0.001$ compared with scrambled siRNA group.

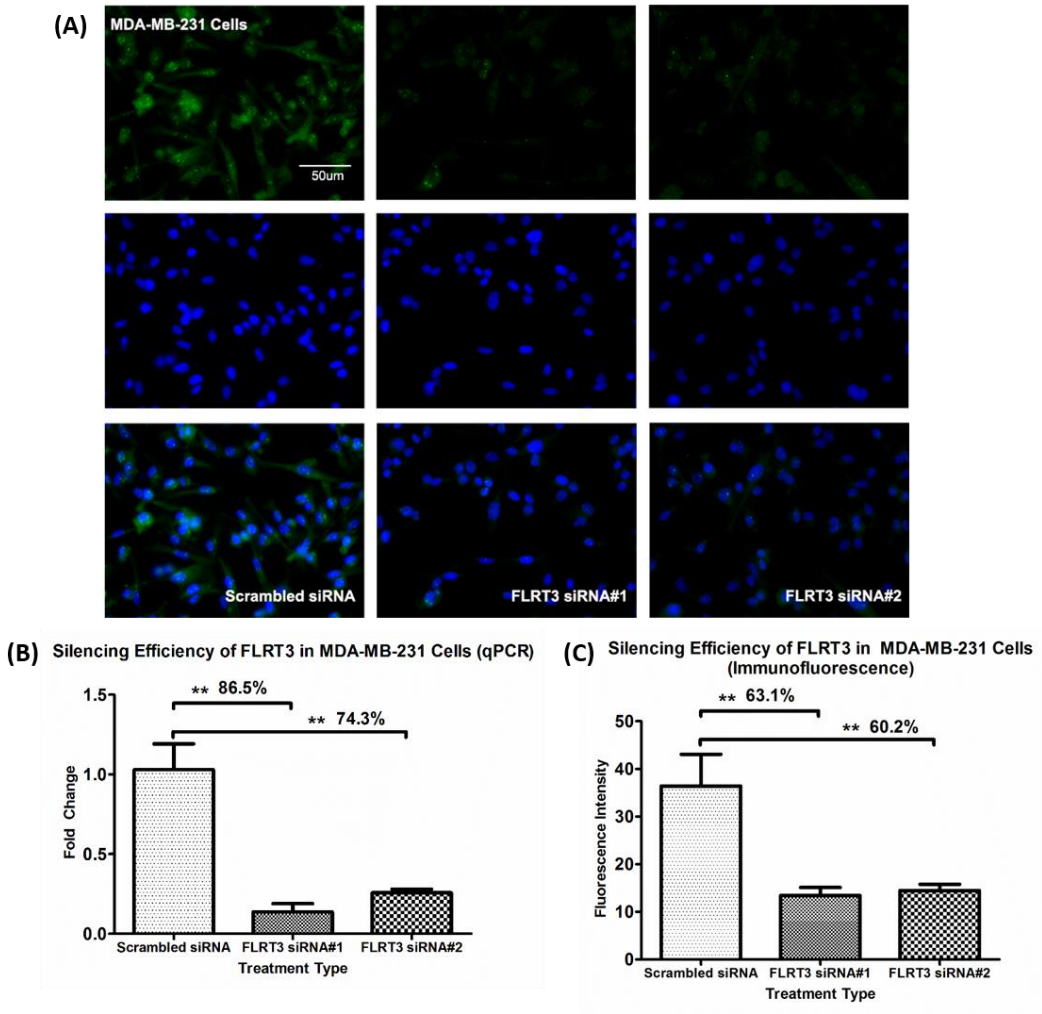

Figure 3.30: Silencing efficiencies of FLRT3 in MDA-MB-231 cells
Silencing efficiencies of FLRT3 mRNA and protein levels were obtained for both siRNA sequences specifically targeting *FLRT3*. In the qPCR analysis (B), the mRNA expression levels of *GAPDH* house-keeping genes were used for normalization. (A) Immunofluorescence staining depict the silencing efficiencies of FLRT3 protein expression level in MDA-MB-231 cells. Graph (C) shows the silencing efficiencies of FLRT3 protein observed in immunofluorescence. Data shown were each from one independent experiment performed with three biological replicates. * $P < 0.05$; ** $P < 0.01$; *** $P < 0.001$ compared with scrambled siRNA group.

3.5.2.2 FLRT3 affects Cell Migration in Breast Cancer Cells

The various phenotypic assays were performed to evaluate the role of *FLRT3* in breast cancer cells. Cell migration ability was assessed using the transwell migration chambers post 48 hours transfection in T47D and MDA-MB-231 cells. After silencing of *FLRT3* in T47D (Figure 3.31A and C) and MDA-MB-231 (Figure 3.31B and D) cells, migration level was observed to have decreased compared to the scrambled siRNA group.

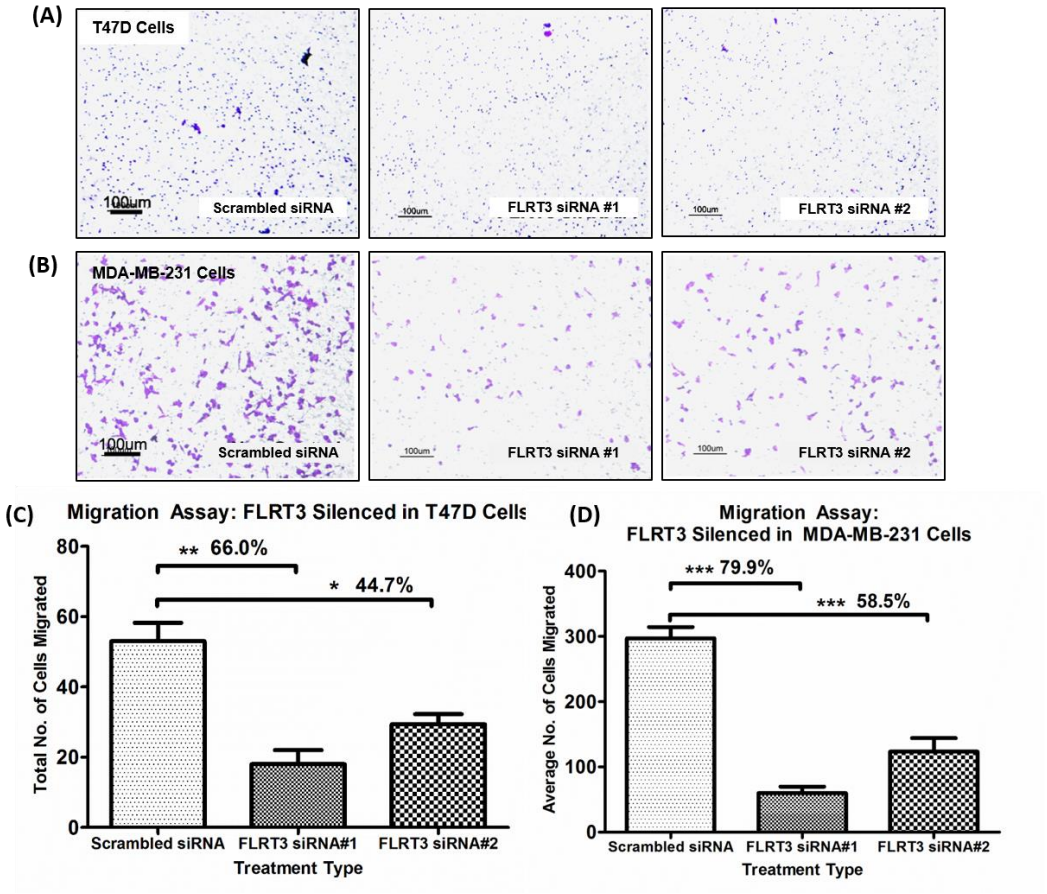

Figure 3.31: Cell migration level after silencing *FLRT3*
Decrease in cell migration was observed in the *FLRT3*-silenced groups compared to the scrambled siRNA group after down-regulation of *FLRT3* in (A and C) T47D and (B and D) MDA-MB-231 cells. Data shown were from one independent experiment performed with three biological replicates. * $P < 0.05$; ** $P < 0.01$; *** $P < 0.001$ compared with scrambled siRNA group.

3.5.2.3 FLRT3 affects Cell Invasion in Breast Cancer Cells

Cell invasion ability was also assessed using the matrigel-coated transwell chambers post 48 hours transfection. After silencing of *FLRT3* in T47D (Figure 3.32A and C) and MDA-MB-231 (Figure 3.32B and D) cells, invasion level was observed to have decreased compared to the scrambled siRNA group.

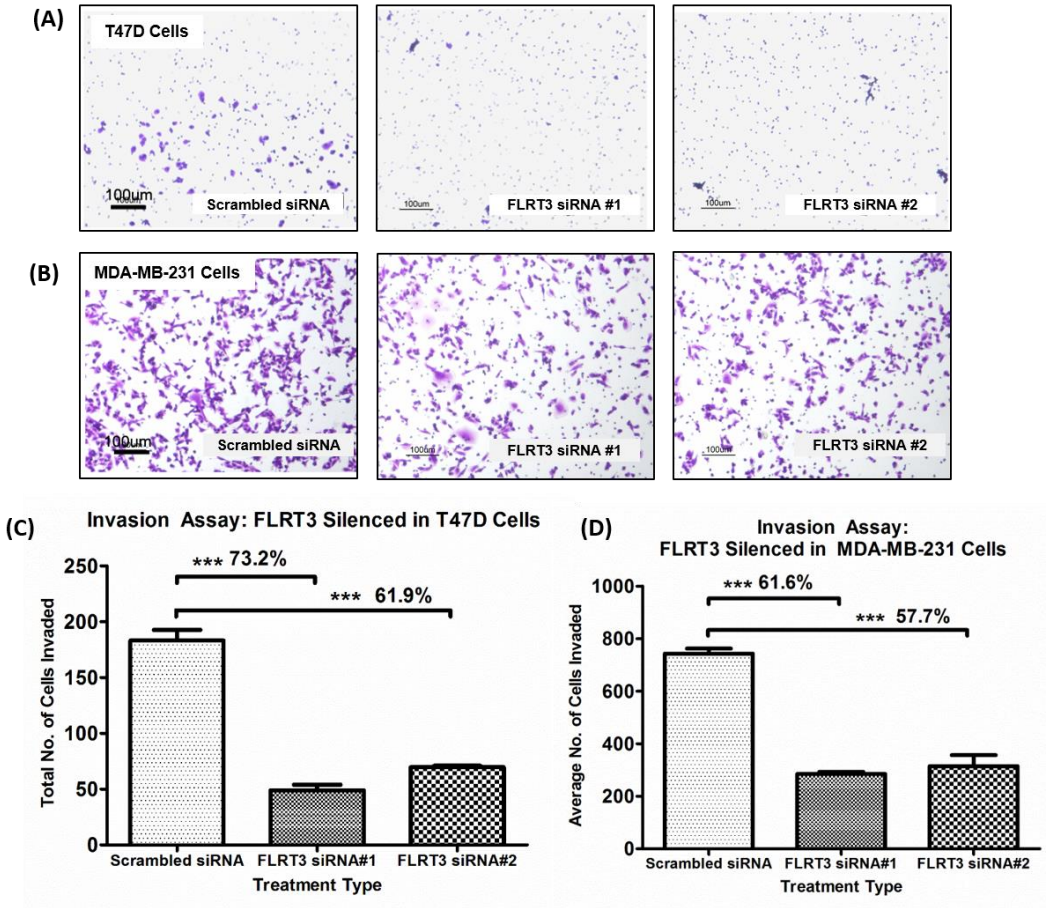

Figure 3.32: Cell invasion level after silencing *FLRT3*
Decrease in cell invasion was observed in the *FLRT3*-silenced groups compared to the scrambled siRNA group after down-regulation of *FLRT3* in (A and C) T47D and (B and D) MDA-MB-231 cells. Data shown were from one independent experiment performed with three biological replicates. * $P < 0.05$; ** $P < 0.01$; *** $P < 0.001$ compared with scrambled siRNA group.

3.5.2.4 FLRT3 affects Cell Adhesion in Breast Cancer Cells

Cell adhesion ability was next assessed using fibronectin- and collagen-coated plates, after a 48-hour transfection period. After silencing of *FLRT3* in T47D (Figure 3.33A and C) and MDA-MB-231 (Figure 3.33B and D) cells, adhesion level was observed to be enhanced compared to the scrambled siRNA group.

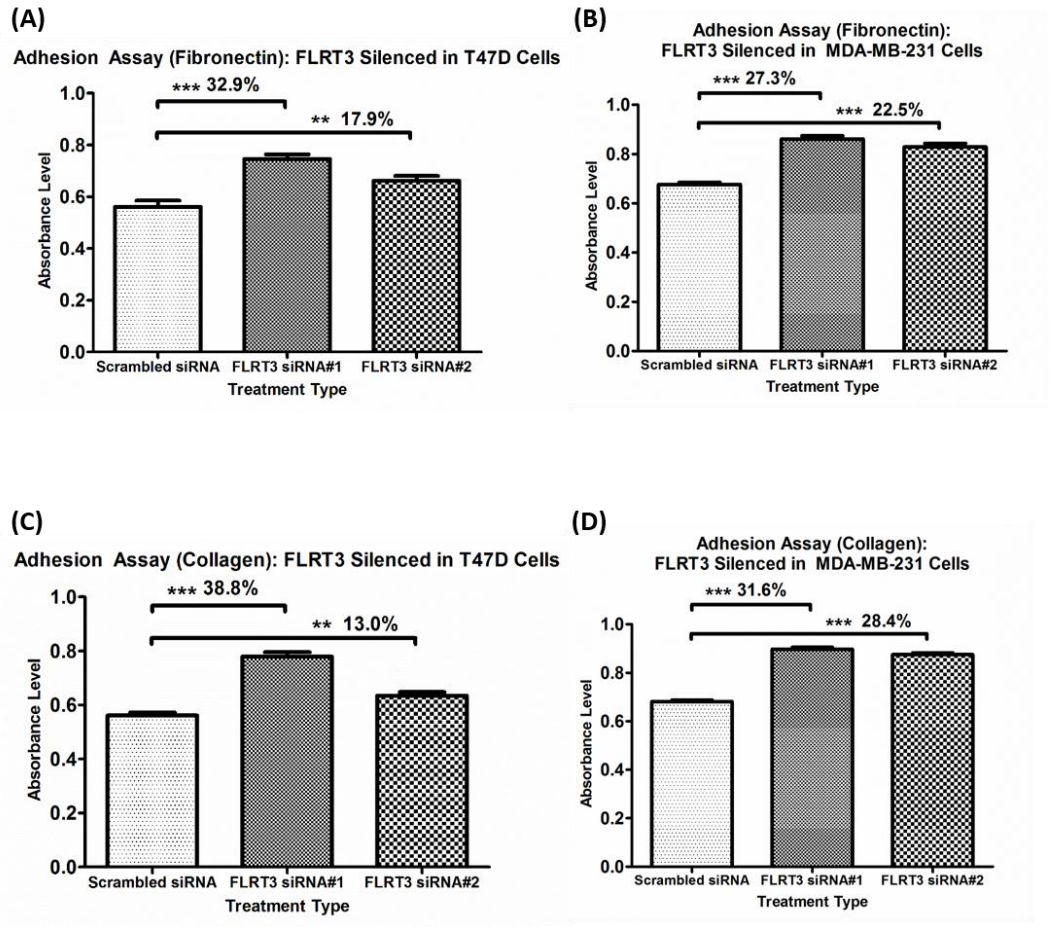

Figure 3.33: Cell adhesion level after silencing *FLRT3*
Increases in cell adhesion was observed in the *FLRT3*-silenced groups compared to the scrambled siRNA group after down-regulation of *FLRT3* in (A and C) T47D and (B and D) MDA-MB-231 cells, using fibronectin- and collagen-coated plates. Data shown were from one independent experiment performed with three biological replicates. * $P < 0.05$; ** $P < 0.01$; *** $P < 0.001$ compared with scrambled siRNA group.

3.5.2.5 FLRT3 affects Cell Proliferation in Breast Cancer Cells

Cell proliferation capability was examined using MTS assay after a 48-hour transfection period. After silencing of *FLRT3* in T47D (Figure 3.34A) and MDA-MB-231 (Figure 3.34B) cells, proliferation level was observed to be decreased compared to the scrambled siRNA group.

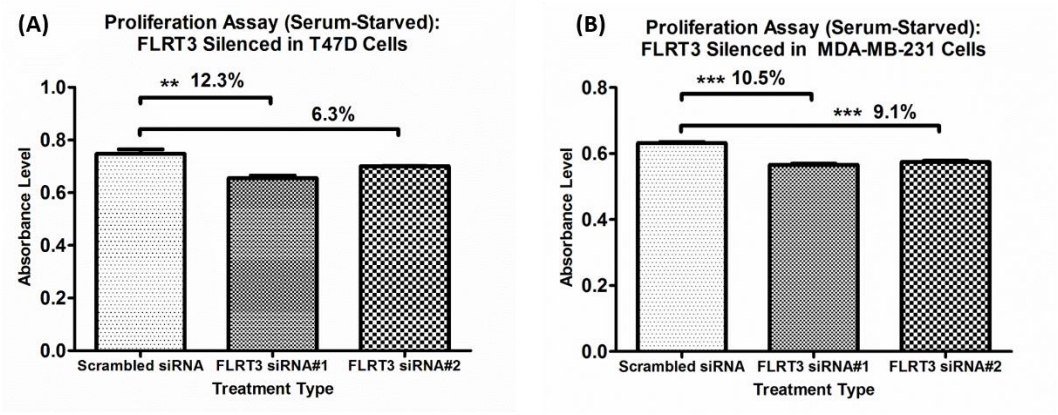

Figure 3.34: Cell proliferation level after silencing *FLRT3*
Small decreases in cell proliferation were observed in the *FLRT3*-silenced groups compared to the scrambled siRNA group after down-regulation of *FLRT3* in (A) T47D and (B) MDA-MB-231 cells. Data shown were from one independent experiment performed with three biological replicates. * $P < 0.05$; ** $P < 0.01$; *** $P < 0.001$ compared with scrambled siRNA group.

3.5.3 CHST3 modulates FLRT3

From the single-silenced experiments, the down-regulation of *FLRT3* showed decreases in metastatic capability and aggressiveness, suggesting *FLRT3* to be a tumor promoter gene. Double silencing experiments were next performed to evaluate whether *CHST3* acts through *FLRT3*, giving rise to the various phenotypic changes observed in the *CHST3*-silenced experiments.

3.5.3.1 Silencing Efficiency of CHST3 and GPNMB

FLRT3 mRNA expression level was firstly validated in *CHST3*-single-silenced T47D cells. As shown in Figure 3.35, *FLRT3* expression level increased by almost 2 folds after down-regulation of *CHST3*. Also, prior to carrying out the phenotypic assays, the expression levels of *CHST3* and *FLRT3* in double silenced groups were evaluated at mRNA (Figure 3.36A and B) as well as protein level (Figure 3.36C to

E). As observed from qPCR, *CHST3* was down-regulated by more than 67% in the *CHST3*-silenced group and *CHST3*-*FLRT3* silenced group. Its expression was not affected in the *FLRT3* -silenced group. As for *FLRT3* expression level, it was up-regulated by 94.5% in the *CHST3*-silenced group. *FLRT3* level was down-regulated by at least 61.7% in the *FLRT3*-silenced group and *CHST3*-*GPNMB* silenced group. *FLRT3* returned to basal level (similar to the double negative group) in the *CHST3*-*FLRT3* silenced group.

From the western blot results, the same trend was observed. CHST3 was down-regulated by more than 44.5% in the *CHST3*-silenced group and *CHST3*-*FLRT3* silenced group. Its expression was not affected in the *FLRT3*-silenced group. Looking at FLRT3, it was up-regulated of its expression level in the *CHST3*-silenced group. Also, FLRT3 expression was down-regulated by 38.2% in the *FLRT3*-silenced group and similar to the double negative group in the *CHST3*-*FLRT3* silenced group.

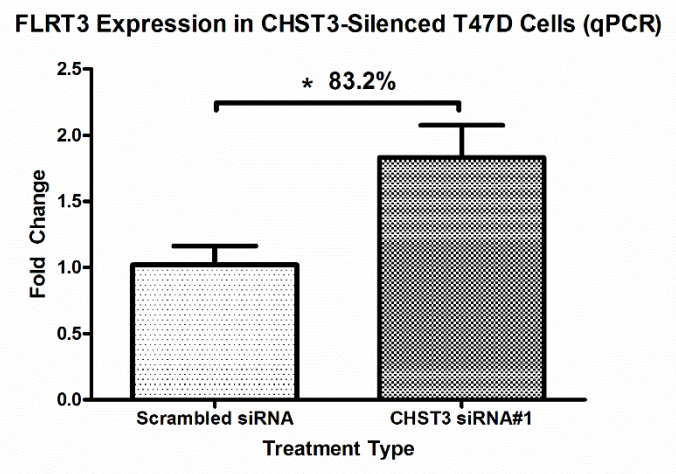

Figure 3.35: *FLRT3* expression in *CHST3* single-silenced T47D cells
The mRNA expression level of *FLRT3* was enhanced by almost 2 folds in T47D cells after single-silencing *CHST3*. *GAPDH* mRNA expression level was used as the house-keeping gene for normalization. Data shown was from one independent experiment performed with three biological replicates. * $P < 0.05$; ** $P < 0.01$; *** $P < 0.001$ compared with scrambled siRNA group.

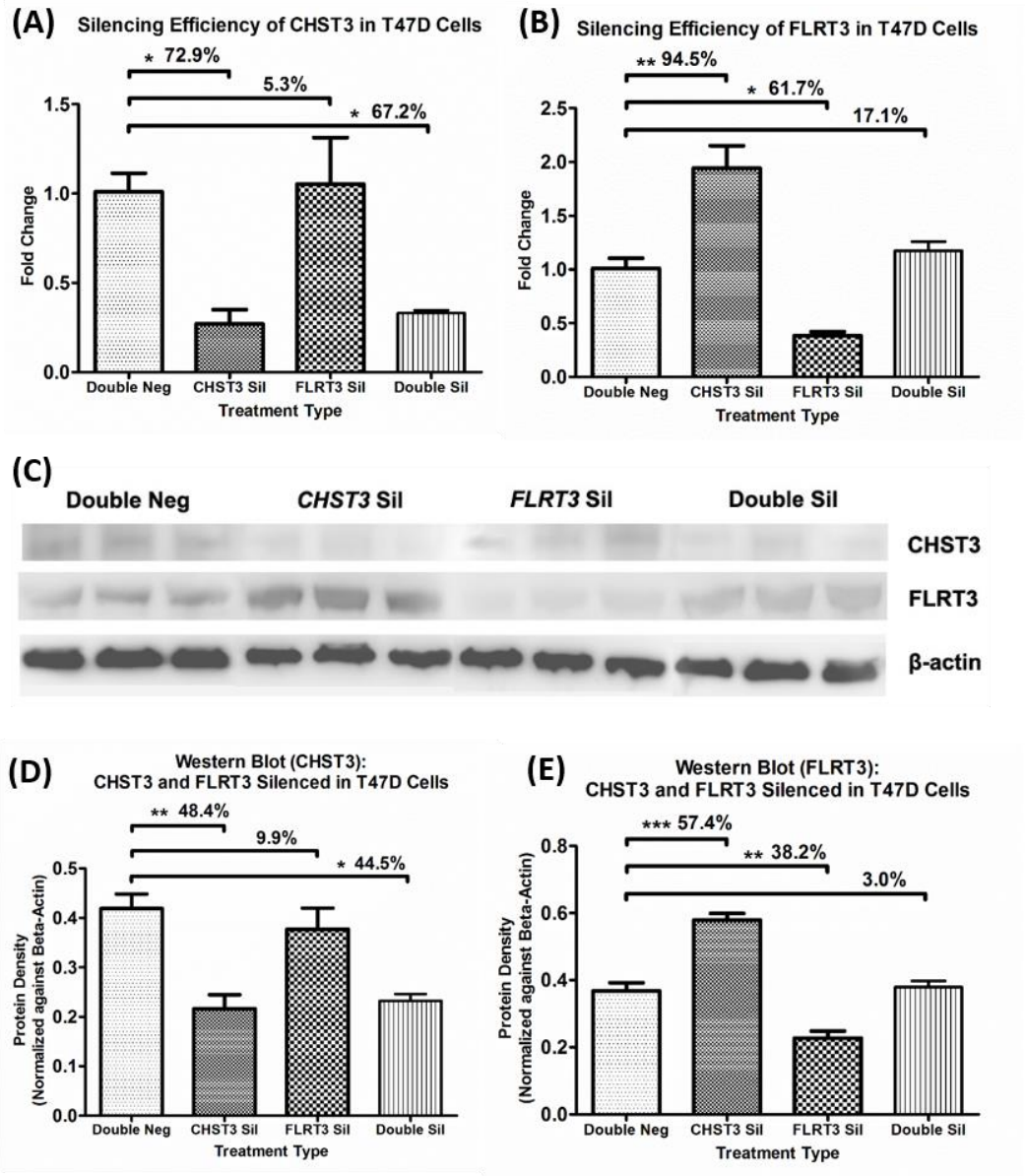

Figure 3.36: *CHST3* and *FLRT3* levels after different silencing treatments in T47D cells qPCR was carried out to evaluate the mRNA expression levels of (A) *CHST3* and (B) *FLRT3* in the various groups. *GAPDH* mRNA expression level was used as the house-keeping gene for normalization. From (C) western blot analyses, (D) CHST3 and (E and F) *FLRT3* protein levels were examined for the various silencing treatment groups. B-actin was used as the house-keeping protein for normalization. Data shown was from one independent experiment performed with three biological replicates. * $P < 0.05$; ** $P < 0.01$; *** $P < 0.001$ compared with double negative group.

3.5.3.2 Regulation of Cellular Behaviors by CHST3 and FLRT3

3.5.3.2.1 Regulation of Cell Migration by CHST3 and FLRT3

After obtaining the silencing efficiencies of *FLRT3*, phenotypic assays were performed. Cell migration ability was assessed with transwell migration chambers to examine the effect of double silencing *CHST3* and *FLRT3* against double negative, *CHST3*-silenced, and *FLRT3*-silenced groups. The transfected cells were re-seeded into the migration chambers after a 48-hour transfection period. From the single-silenced experiments, it was observed that silencing of *CHST3* increased cell migration level while silencing of *FLRT3* decreased cell migration level. From Figure 3.37, double silencing of *CHST3* and *FLRT3* abrogated these changes in cell migration level.

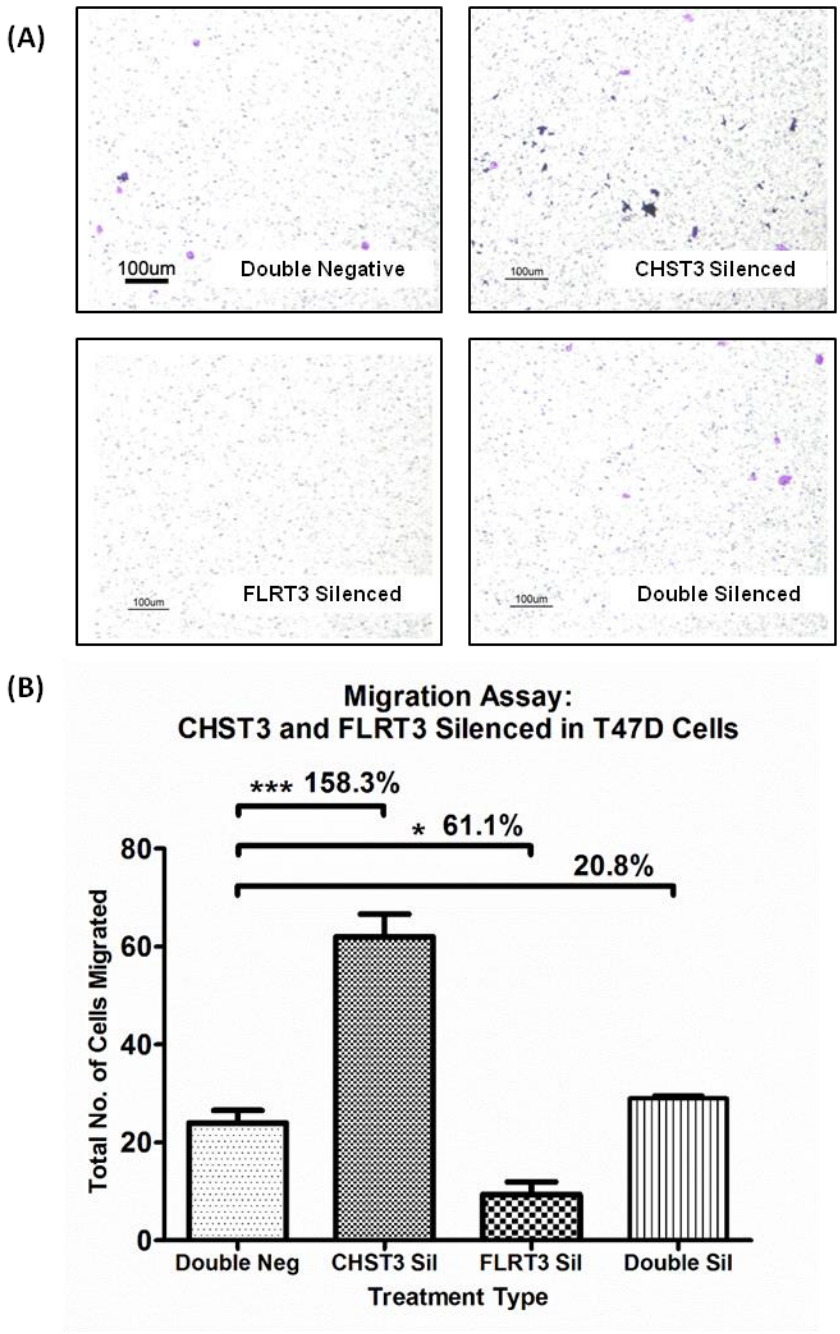

Figure 3.37: Effects of *CHST3* and *FLRT3* double silencing on cell migration
As shown in the (A) pictures and (B) graph, silencing of *CHST3* caused an increase in cell migration; while on the other hand, down-regulation of *FLRT3* caused a reduction in cell migration. Double silencing of *CHST3* and *FLRT3* caused cell migration level to return to basal level (similar to double negative group). Data shown was from one independent experiment performed with three biological replicates. * $P < 0.05$; ** $P < 0.01$; *** $P < 0.001$ compared with double negative group.

3.5.3.2.2 Regulation of Cell Invasion by CHST3 and FLRT3

Cell invasion ability was next evaluated to compare the effect of double silencing *CHST3* and *FLRT3* with the double negative and other silencing treatment groups. After 48 hours transfection, the transfected cells were re-seeded into matrigel invasion chambers and incubated for 24 hours. From the single-silenced experiments, it was observed that silencing of *CHST3* increased cell invasion level while silencing of *FLRT3* decreased cell invasion level. Figure 3.38 shows double silencing of *CHST3* and *FLRT3* abrogated these changes in cell invasion level.

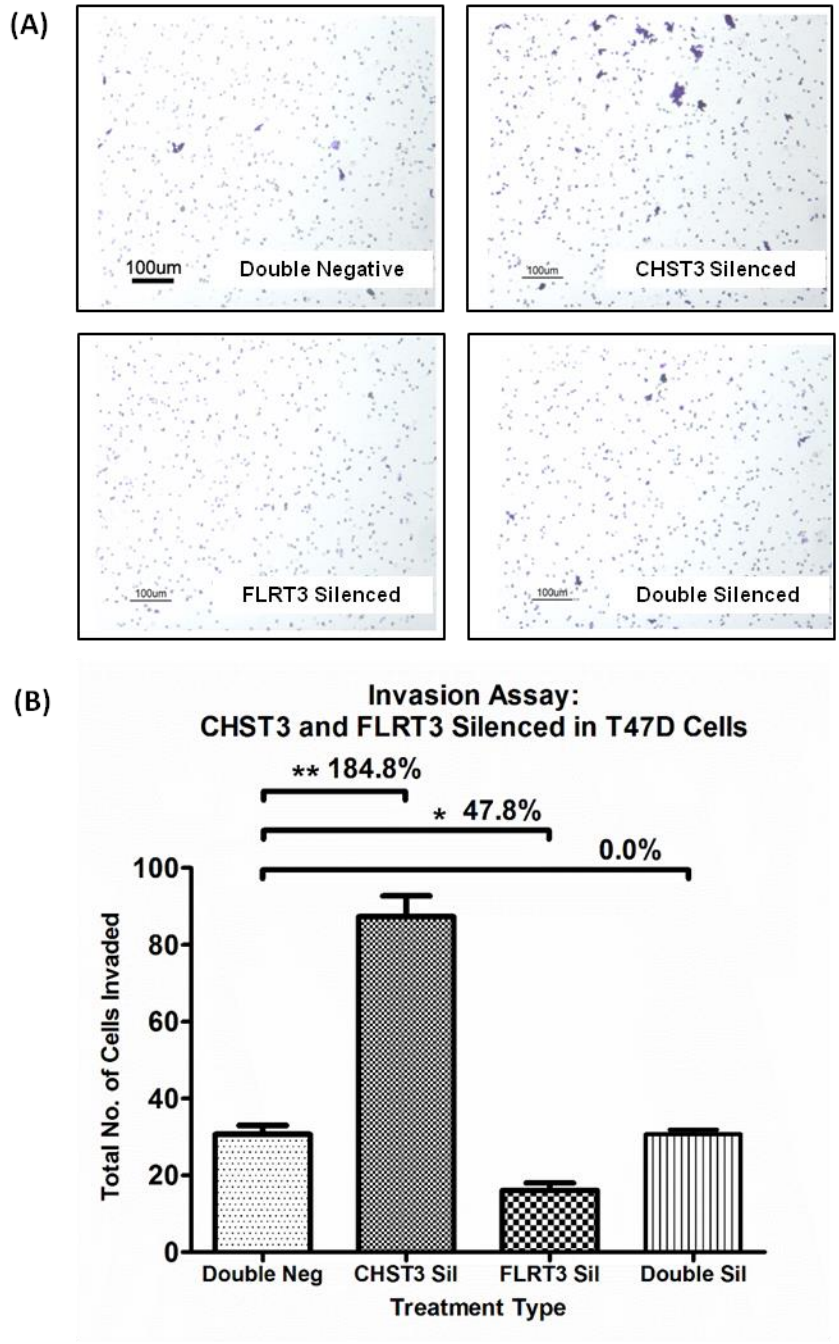

Figure 3.38: Effects of *CHST3* and *FLRT3* double silencing on cell invasion
As shown in the (A) pictures and (B) graph, silencing of *CHST3* caused an increase in cell invasion; while on the other hand, down-regulation of *FLRT3* caused a reduction in cell invasion. Double silencing of *CHST3* and *FLRT3* caused cell invasion level to return to basal level (similar to double negative group). Data shown was from one independent experiment performed with three biological replicates. * $P < 0.05$; ** $P < 0.01$; *** $P < 0.001$ compared with double negative group.

3.5.3.2.3 Regulation of Cell Adhesion by CHST3 and FLRT3

Cell adhesion capability to ECM-components, fibronectin and collagen, was examined for the effect of double silencing *CHST3* and *FLRT3* in T47D cells compared to double negative and other silencing treatment groups. After a 48-hour transfection period, transfected cells were re-seeded into fibronectin- and collagen-coated plates. From the single-silenced experiments, it was observed that silencing of *CHST3* decreased cell adhesion level while silencing of *FLRT3* increased cell adhesion level. Results in Figure 3.39 suggest that double silencing of *CHST3* and *FLRT3* abrogated these changes in cell adhesion level.

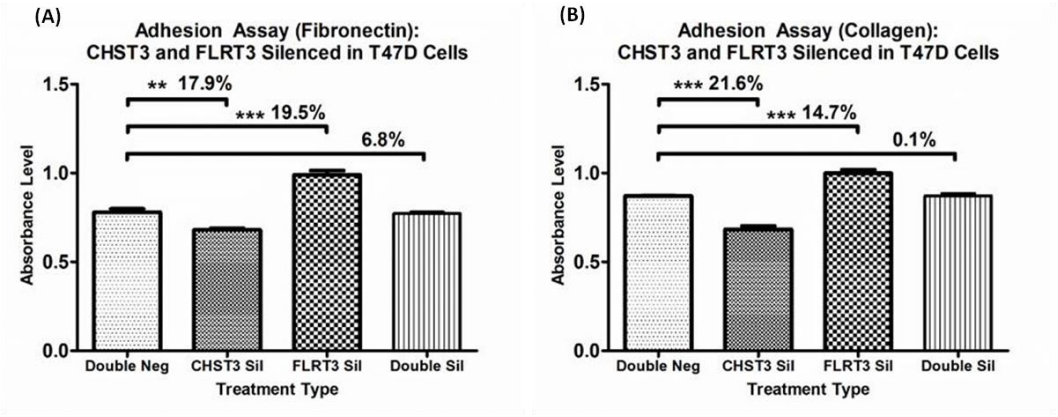

Figure 3.39: Effects of *CHST3* and *FLRT3* double silencing on cell adhesion
Silencing of *CHST3* caused a decrease in cell adhesion; while on the other hand, down-regulation of *FLRT3* caused an increase in cell adhesion for both fibronectin- and collagen-coated plates. From the (A) fibronectin- and (B) collagen-coated plate, double silencing of *CHST3* and *FLRT3* caused cell adhesion level to return to basal level (similar to double negative group). Data shown was from one independent experiment performed with three biological replicates. * $P < 0.05$; ** $P < 0.01$; *** $P < 0.001$ compared with double negative group.

3.5.3.2.4 Regulation of Cell Proliferation by CHST3 and FLRT3

Cell proliferation was also examined after double silencing *CHST3* and *FLRT3*. Evaluation was performed post 48 hours transfection using MTS assay. From the single-silenced experiments, it was observed that silencing of *CHST3* increased cell proliferation level while silencing of *FLRT3* decreased cell proliferation level. Results in Figure 3.40 depict double silencing of *CHST3* and *FLRT3* abrogated these changes in cell proliferation level.

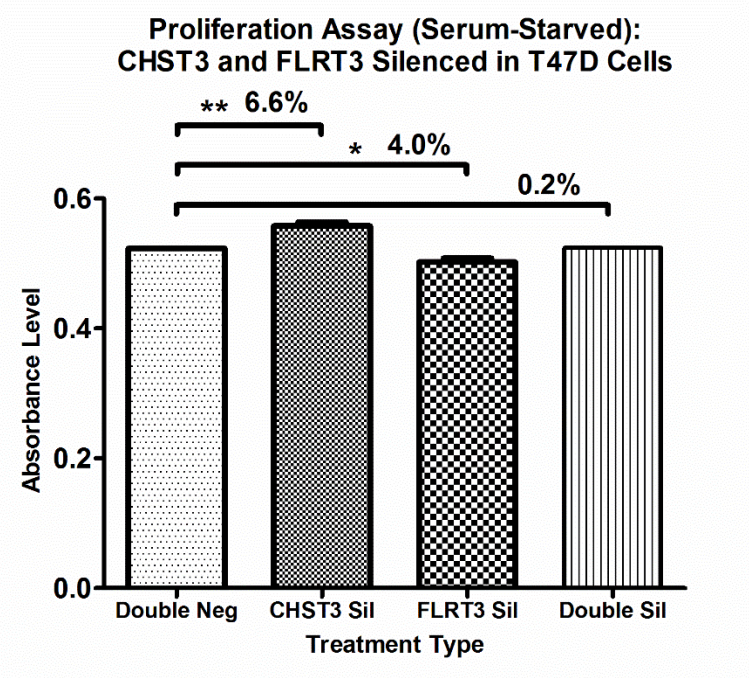

Figure 3.40: Effects of *CHST3* and *FLRT3* double silencing on cell proliferation
Silencing of *CHST3* caused a small increase in cell proliferation; while on the other hand, down-regulation of *FLRT3* caused a small decrease in cell proliferation. Double silencing of *CHST3* and *GPNMB* caused cell proliferation level to return to basal level (similar to double negative group). Data shown was from one independent experiment performed with three biological replicates. * $P < 0.05$; ** $P < 0.01$; *** $P < 0.001$ compared with double negative group.

3.5.4 Relationship of *GPNMB* and *FLRT3*

From the *in vitro* results, it is observed that both *GPNMNB* and *FLRT3* are tumor promoters. After down-regulation of the genes in breast cancer cells, cellular behavior became less proliferative and metastatic. The next step would be to evaluate whether *GPNMB* and *FLRT3* regulate one another in the cellular process. qPCR was performed whereby *GPNMB* expression was examined in *FLRT3*-silenced cells and *FLRT3* expression was evaluated in *GPNMB*-silenced cells. Results as shown in Figure 3.41 unveil that both *GPNMB* and *FLRT3* do not regulate one another as there were no significant changes observed from the qPCR results.

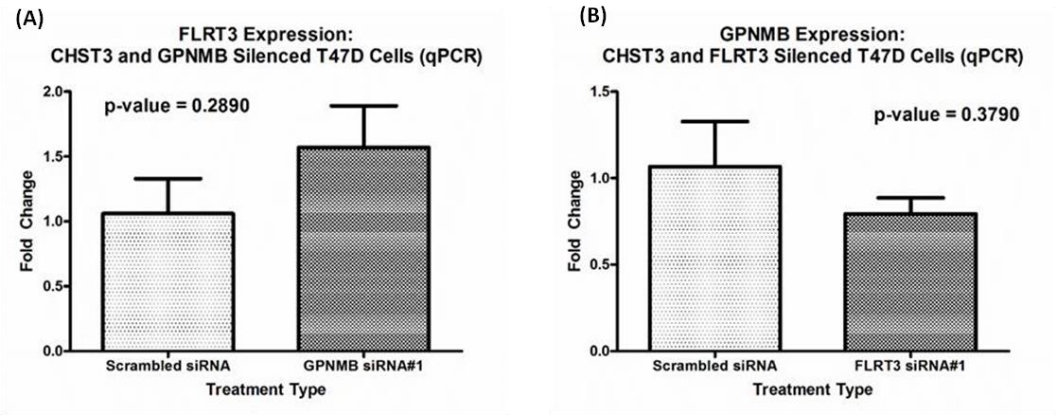

Figure 3.41: *GPNMB* and *FLRT3* correlation in T47D cells
(A) *FLRT3* expression in *GPNMB*-silenced T47D cells showed no significant difference between the scrambled siRNA and *GPNMB*-silenced groups. (B) *GPNMB* expression in *FLRT3*-silenced T47D cells showed no significant difference between scrambled siRNA and *FLRT3*-silenced groups. This indicates that *FLRT3* expression level is not affected or regulated by *GPNMB* change in expression, as well as vice versa. Data shown was from one independent experiment performed with three biological replicates. * $P < 0.05$; ** $P < 0.01$; *** $P < 0.001$ compared with double negative group.

3.6 Expression Analysis of CHST3 in Invasive Ductal Carcinoma Tissues

From the *in vitro* studies, it is observed that *CHST3* plays a tumor suppressor role in breast cancer tumorigenesis; the down-regulation of *CHST3* brings forth more aggressive and metastatic behaviors in breast cancer cells. Therefore, investigation was further extended to clinical patient samples. It was hypothesized that low expression of CHST3 in human breast cancer tissue is correlated with worse prognosis and clinical parameters.

3.6.1 Clinicopathological Parameters of IDC Patient Cases

A total of 255 human IDC cases and 77 normal non-malignant ductal tissue cases, in tissue microarray format, were used for immunohistochemical evaluation of CHST3 protein. The patients' age ranged from 23 to 89 years old, with a mean of 56.1 years and a median of 55.5 years. As a result of tissue loss during the immunohistochemistry process, the expression patterns of CHST3 were examined in 259 cases (218 IDC cases and 41 normal ductal cases). The clinicopathological features of the malignant cases and normal cases are summarized in Table 3.3 and 3.4 respectively.

Patient survival and tumor recurrence data were available for 213 (97.7%) of the 218 IDC cases studied. The follow-up period ranged from 0 to 175.5 months. There was death occurrence in 22.5% of patients, with the mean and median of OS period being 106.7 and 99.9 months respectively. All death cases arose from the cancer disease itself. Tumor recurrences were found in 30.7% of cases, and the mean and median DFS time were 100.2 months and 98.0 months. Among patients with tumor recurrence, 19.6% of them had died of the cancer at the end of the study period, with a mean SAR time of 6.5 months and median SAR time of 0 month.

Table 3.3 Clinicopathological features of 218 cases of IDC tissues

Clinicopathological features		**Clinicopathological features**	
Age (years)		Tumor size (mm)	
Mean	56.1	Mean	34.6
Median	55.5	Median	30.0
Minimum	23.0	Minimum	5.0
Maximum	89.0	Maximum	140.0
Clinicopathological features	**No. of cases**	**Clinicopathological features**	**No. of cases**
Age (years)		Lymphovascular invasion	
≤ 56	135	Absent	87
> 56	83	Present	70
		NA	61
Ethnicity		Lymphovascular invasion stage	
Chinese	154	1	
Malay	15	2	101
Indian	7	3	49
Others	9	NA	55
NA	33		13
Tumor size (mm)		Lymph node status	
≤ 30	117	1	105
> 30	99	2	51
NA	2	3	48
		NA	14
Histological tumor grade		Tubule Formation Stage	
1	13	1	7
2	80	2	42
3	120	3	103
NA	5	NA	66
Tumor stage		Estrogen receptor status	
1	17	Negative	104
2	81	Positive	93
3	12	NA	21
NA	108		
Mitotic Stage		Progesterone receptor status	
1	27	Negative	85
2	46	Positive	111
3	79	NA	22
NA	66		
Pleomorphism Stage		HER2 receptor status	
1	4	Negative	134
2	67	Positive	63
3	81	NA	192
NA	66		

NA = Not Available

Table 3.4 Clinicopathological features of 41 cases of normal ductal cases

Clinicopathological features	Value (years)	Clinicopathological features	Frequency distribution
Age (years)		Ethnicity	
Mean	65.8	Chinese	18
Median	71.0	Malay	1
Minimum	35.00	Indian	1
Maximum	89.00	Others	1
		NA	20

3.6.2 CHST3 Expression Pattern in Breast Tissues

CHST3 expression staining was positive in the epithelial compartment of both normal and malignant breast tissues as shown in Figure 3.42. Additionally, Figure 3.42 depicts the CHST3 staining intensities of 0, 1+, 2+, and 3+ in breast ductal tissues.

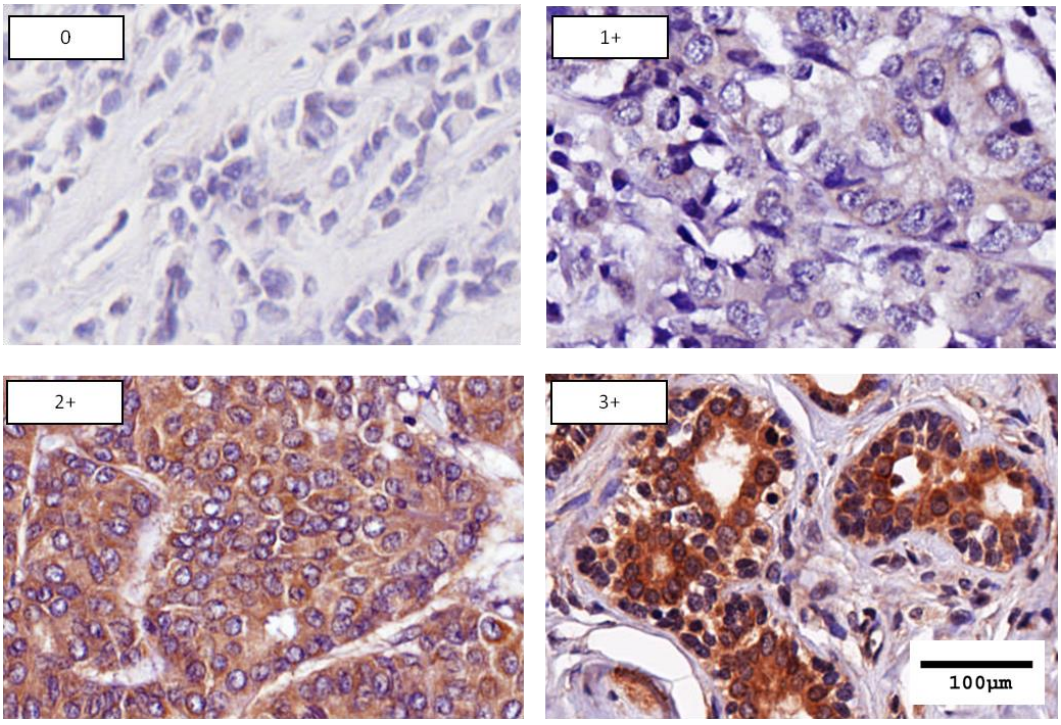

Figure 3.42: Staining pattern of CHST3 in breast tissues
CHST3 staining intensities of 0, 1+, 2+, and 3+ were observed in the epithelial compartment of breast tissues. Images indicating staining intensities of 0, 1+, and 2+ were taken from malignant tissue samples while the image indicating staining intensity 3+ was taken from a non-malignant sample.

3.6.3 CHST3 Selected Cut-off Point

To select a suitable cut-off point for CHST3, the distribution curve was first analysed. As a non-normal distribution curve (Figure 3.43A) was observed, the median was selected to be the cut-off point for CHST3 (Figure 3.43C). Also, an ROC curve analysis was performed to evaluate the sensitivity and specificity of the median cut-off point of CHST3 (Figure 3.43B). The median cut-off point shows a sensitivity score of 0.732 (Figure 3.43D), false positivity score between 0.413 and 0.482 (Figure 3.43D), and area under curve is 0.667 (Figure 3.43B), which is above 0.500.

(A)

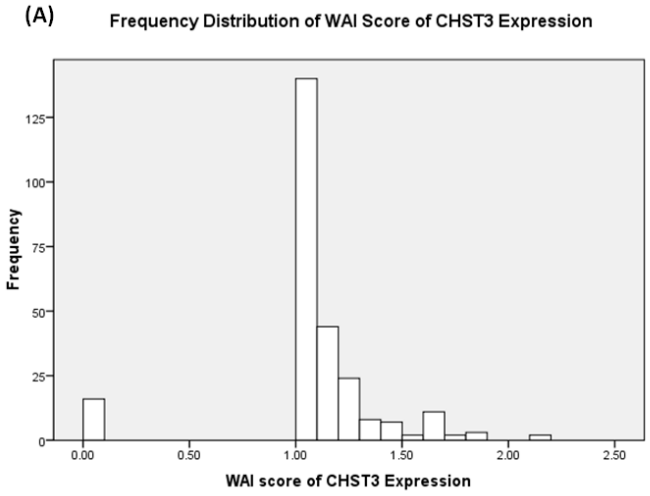

(B)

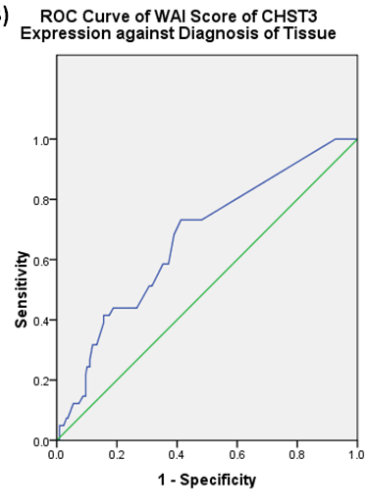

(C)

	Mean	Median	Mode	Min	Max	25th Percentile	50th Percentile	75th Percentile
WAI	1.07	1.06	1.00	0.00	2.16	1.00	1.06	1.17

(D)

WAI Score	Sensitivity	1-Specificity
0.50	1.000	0.927
1.03	0.732	0.482
1.07	0.732	0.413
1.09	0.683	0.390

Figure 3.43: Frequency distribution and ROC curve of CHST3 expression among normal and malignant tissues
(A) Histogram illustrates the frequency distribution of the WAI score of CHST3 expression across both normal and malignant tissues. (B) ROC curve depicts WAI score of CHST3 expression of normal and malignant tissues following their sensitivity and 1-specificity score. The area under curve is 0.667, which is above 0.500.

3.6.4 CHST3 Expression in Normal and Malignant Breast Tissues

Expression of CHST3 epitope was evaluated in the epithelial (cytoplasm) compartment of ductal specimens. Analysis of the tissue microarrays showed that normal ductal tissues had enhanced staining in comparison to malignant IDC tissues as shown in Figure 3.44 and Table 3.5 (p-value = 0.000). Further analysis was also performed on paired normal and malignant breast tissues, of which results showed higher CHST3 expression level in the normal tissues compared to its paired malignant counterpart tissue (Figure 3.45).

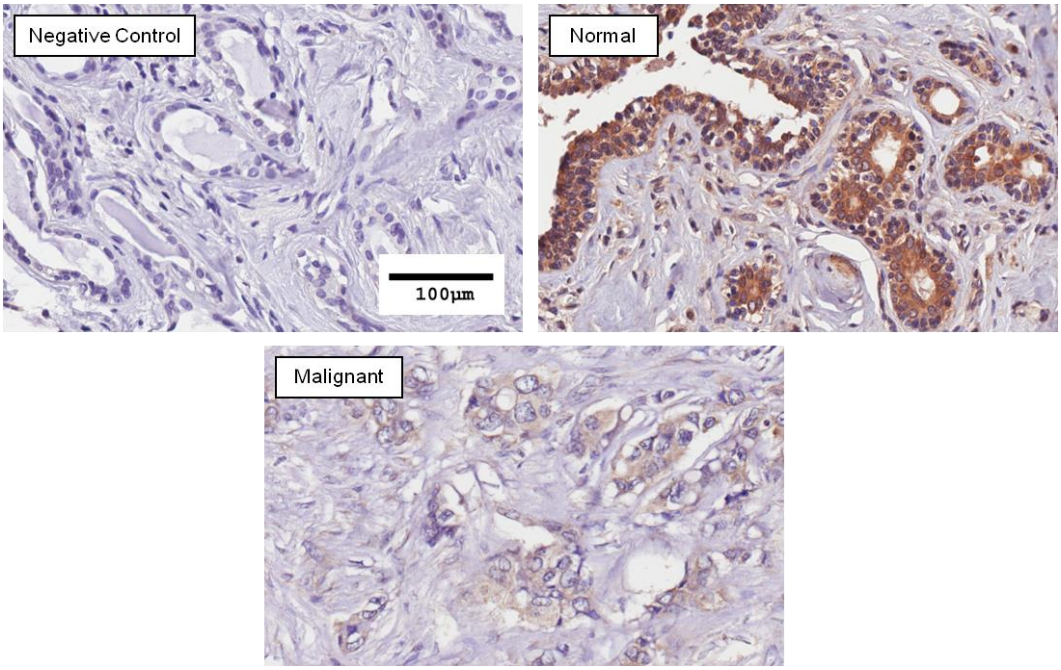

Figure 3.44: CHST3 immunostaining in normal and malignant breast tissues
Higher expression of CHST3 was observed in normal ductal tissues compared to malignant breast tissues. Staining intensities of 2+ and 3+ are shown in the above normal tissues whereas staining intensities of 0 and 1+ are depicted in the above malignant tissues.

Table 3.5: Analysis of CHST3 expression between normal and malignant breast tissues

CHST3 expression is significantly enhanced in normal ductal tissues in comparison to malignant tissues.

	Weighted Average Score (WAI)		
	≤ 1.06	**> 1.06**	**p-value**
Diagnosis			
Normal	11	30	0.000*
Malignant	128	90	

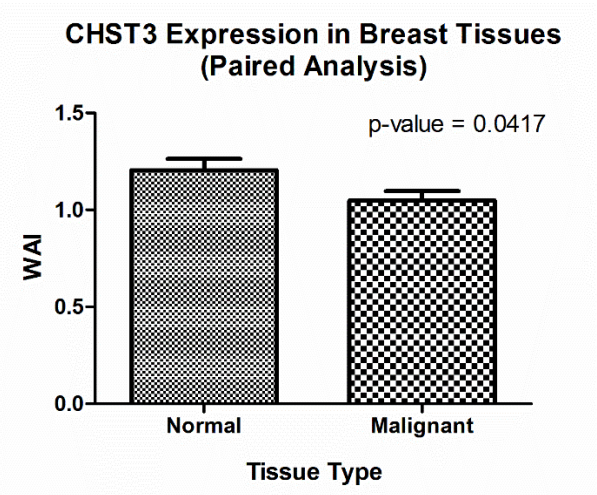

Figure 3.45: Paired analysis of CHST3 expression in 33 paired normal and malignant breast tissue samples.
Normal tissues shows enhanced expression level of CHST3 compared to malignant tissues.

3.6.5 CHST3 Correlations with Clinicopathological Parameters

Among the malignant tissues, higher CHST3 expression was significantly correlated with lower tumor stage (Figure 3.46 and Table 3.6) and borderline significantly associated with smaller tumor size (Table 3.6).

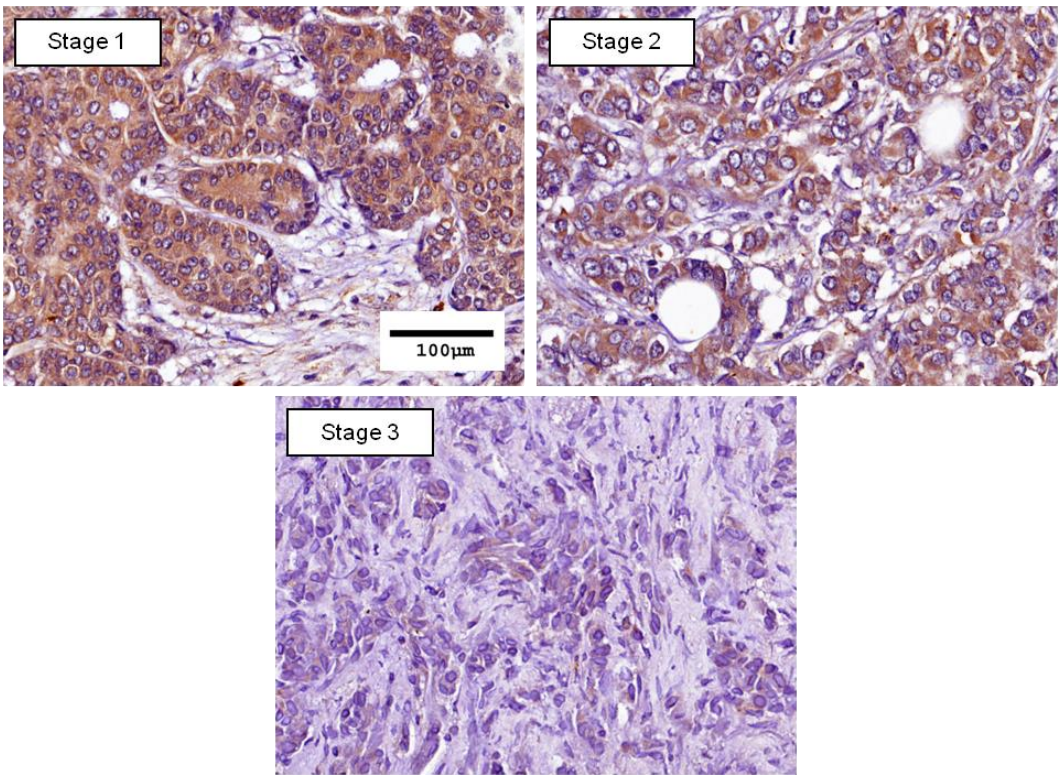

Figure 3.46: CHST3 immunostaining in breast tissues of different tumor stage
Higher expression of CHST3 was observed in IDC of lower tumor stage. Stage 1 shows staining intensity of 2+, stage 2 depicts intensities of 1+ and 2+, and stage 3 displays mostly 0 intensity and a small area with 1+ intensity.

Table 3.6: Correlations between CHST3 expression and clinicopathological features of IDC

	WAI				WAI		
	≤ 1.06	**> 1.06**	**p-value**		**≤ 1.06**	**> 1.06**	**p-value**
Age (years)				Lymphovascular invasion			
≤ 56	81	54	0.672	Absent	47	40	0.751
> 56	47	36		Present	36	34	
NA	0	0		NA	45	16	
Ethnicity				Lymphovascular invasion stage			
Chinese	89	65	0.561	1	57	44	0.691
Malay	7	8		2	28	21	
Indian	3	4		3	33	22	
Others	9	0		NA	10	3	
NA	20	13					
Tumor size (mm)				Lymph node status			
≤ 30	62	55	**0.052**	1	57	48	0.397
> 30	66	33		2	31	20	
NA	0	2		3	29	19	
				NA	11	3	
Histological tumor grade				Tubule Formation Stage			
1	8	5	0.634	1	5	2	0.657
2	44	36		2	23	19	
3	72	48		3	64	39	
NA	4	1		NA	36	30	
Tumor stage				ER status			
1	7	10	**0.004***	Negative	62	42	0.472
2	46	35		Positive	50	43	
3	12	0		NA	16	5	
NA	63	45					
Mitotic Stage				PR status			
1	15	12	0.309	Negative	54	31	0.110
2	26	20		Positive	57	54	
3	51	28		NA	17	5	
NA	36	30					
Pleomorphism Stage				HER2 receptor status			
				Negative	75	59	0.644
1	2	2	0.998	Positive	38	25	
2	41	26		NA	15	6	
3	49	32					
NA	36	20					

NA = Not Available

3.6.6 urvival Analysis of CHST3 Expression

3.6.6.1 Survival Analysis using Kaplan Meier

Survival analysis was first performed using Kaplan Meier curves to observe any general trends between CHST3 expression and tumor recurrence and mortality rate. No significant trends were observed for CHST3 expression with patients' tumor recurrence and mortality rate, as shown in Figure 3.47.

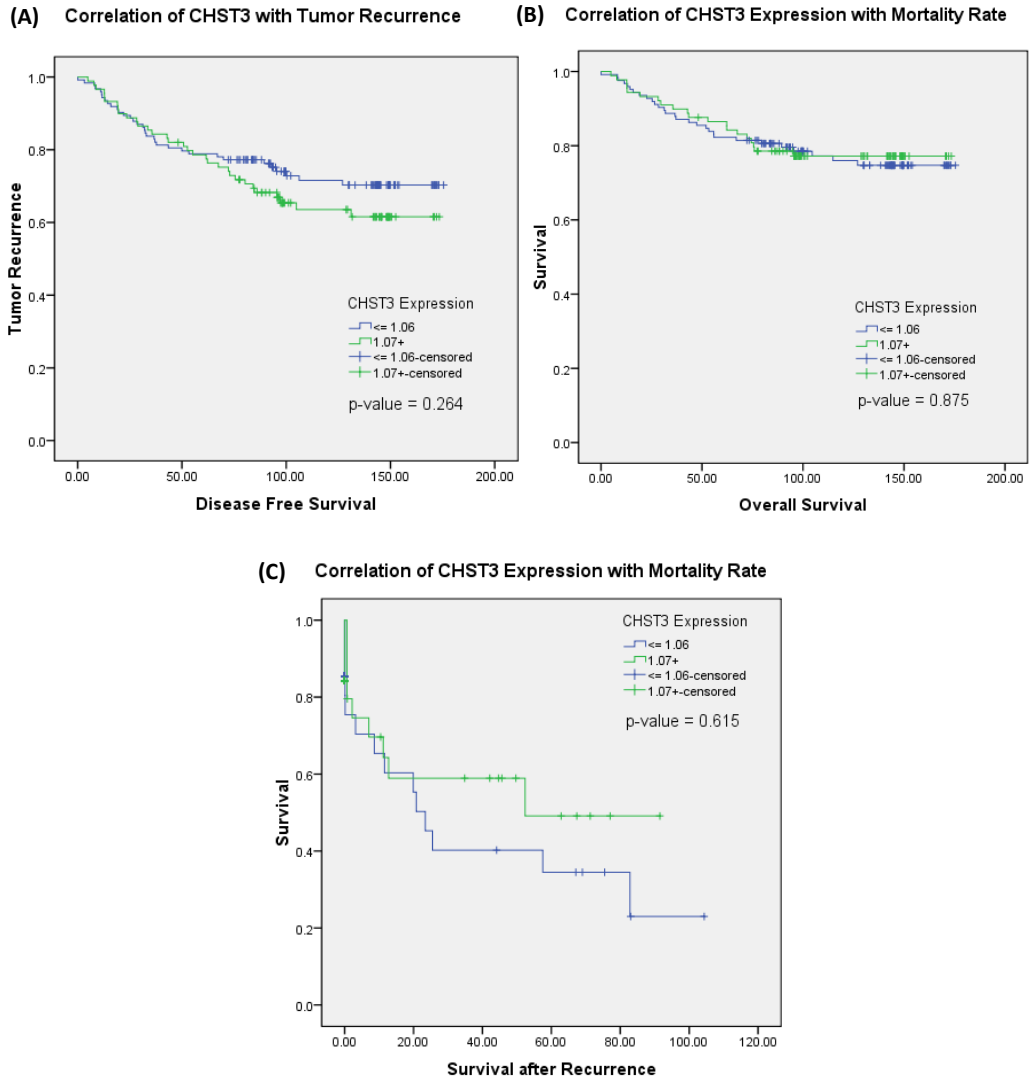

Figure 3.47: Kaplan Meier curves using CHST3
No significant trend was observed between CHST3 expression and (A) tumor recurrence, (B) overall survival, and (C) survival after recurrence.

3.6.6.2 Survival Analysis using Cox Regression Univariate

Cox regression analysis using univariate method was performed to determine the hazard ratio of CHST3 expression as well as for the clinicopathological parameters. Several significant hazard ratios were obtained for various clinical parameters. However, no significant hazard ratios were attained for CHST3 expression in disease-free survival (Table 3.7), overall survival (Table 3.8), as well as survival after recurrence (Table 3.9) time period.

Table 3.7: Univariate Cox regression analysis of CHST3 and clinicopathological parameters using DFS time period

	Disease Free Survival			
			95% CI	
	p-value	Hazard ratio	Lower	Upper
Increased CHST3 expression	.531	1.451	.452	4.673
Presence of lymph node invasion	.448	1.508	.522	4.360
PR+ status	.036	4.713	1.106	20.080
ER+ status	.327	.603	.219	1.659
HER2+ status	.328	.557	.173	1.798
Increased lymphovascular invasion stage	.898	.000	.000	3.426E52
Increased tumor stage	.496	1.570	.429	5.743
Race	.366	.745	.393	1.411
Increased histological grade	.802	1.266	.199	8.041
Increased tubule formation stage	.716	.792	.226	2.775
Increased pleomorphism stage	.313	2.010	.518	7.802
Increased mitotic index	.685	1.227	.457	3.299
Increased lymph node stage	.901	3778.146	.000	6.341E59
Larger tumor size	.382	.640	.236	1.738
Increased age	.060	3.286	.952	11.348

Table 3.8: Univariate Cox regression analysis of CHST3 and clinicopathological parameters using OS time period

	Overall Survival			
			95% CI	
	p-value	Hazard ratio	Lower	Upper
Increased CHST3 expression	.198	.362	.077	1.699
Presence of lymph node invasion	.302	1.955	.547	6.983
PR+ status	.036	6.572	1.134	38.084
ER+ status	.331	.541	.157	1.867
HER2+ status	.759	.818	.227	2.950
Increased lymphovascular invasion stage	.904	.000	.000	6.920E57
Increased tumor stage	.838	.833	.144	4.802
Race	.247	.619	.275	1.394
Increased histological grade	.634	1.784	.165	19.262
Increased tubule formation stage	.383	.501	.106	2.372
Increased pleomorphism stage	.305	2.434	.445	13.310
Increased mitotic index	.497	1.530	.449	5.212
Increased lymph node stage	.906	5364.575	.000	2.233E65
Larger tumor size	.513	.656	.185	2.323
Increased age	.026	6.558	1.247	34.477

Table 3.9: Univariate Cox regression analysis of CHST3 and clinicopathological parameters using SAR time period

	Survival after Recurrence			
			95% CI	
	p-value	Hazard ratio	Lower	Upper
Increased CHST3 expression	.480	.566	.117	2.742
Presence of lymph node invasion	.956	.967	.292	3.202
PR+ status	.285	2.372	.487	11.562
ER+ status	.352	.490	.109	2.199
HER2+ status	.457	1.712	.415	7.060
Increased lymphovascular invasion stage	.926	.000	.000	1.132E77
Increased tumor stage	.875	.863	.137	5.417
Race	.284	.546	.180	1.653
Increased histological grade	.974	.962	.092	10.099
Increased tubule formation stage	.646	.708	.162	3.086
Increased pleomorphism stage	.583	1.689	.260	10.973
Increased mitotic index	.791	1.179	.349	3.986
Increased lymph node stage	.925	7595.428	.000	6.112E84
Larger tumor size	.898	.919	.256	3.303
Increased age	.069	5.087	.879	29.458

3.6.6.3 Survival Analysis using Cox Regression Multivariate

Following this, Cox regression multivariate survival analysis (Table 3.10-3.12) using clinicopathological parameters were carried out for DFS, OS, and SAR time period respectively. This was performed to examine if CHST3 is a good prognostic marker after adjusting for various important clinical parameters. No significant hazard ratio was obtained for CHST3 expression level. However, tumor size was found to have significant hazard ratio after adjusting for confounding factors in all time periods.

Table 3.10: Multivariate Cox regression analysis of CHST3 expression using DFS.

		p-value	Hazard Ratio	95% Confidence Interval	
				Lower	Upper
Step 1	Increased CHST3 expression	.952	.973	.402	2.354
	Presence of lymph node invasion	.224	1.659	.734	3.752
	PR+ status	.225	1.848	.685	4.982
	ER+ status	.131	.510	.213	1.223
	HER2+ status	.204	.535	.204	1.405
	Increased tumor stage	.717	1.197	.452	3.168
	Race	.999	1.000	.575	1.738
	Larger tumor size	.023	2.969	1.161	7.594
	Increased age	.812	1.107	.479	2.557
Step 2	Increased CHST3 expression	.952	.973	.403	2.353
	Presence of lymph node invasion	.215	1.659	.745	3.694
	PR+ status	.225	1.848	.686	4.979
	ER+ status	.130	.510	.214	1.218
	HER2+ status	.197	.535	.207	1.384
	Increased tumor stage	.713	1.197	.459	3.121
	Larger tumor size	.022	2.969	1.168	7.550
	Increased age	.807	1.107	.489	2.504
Step 3	Increased CHST3 expression	.982	.990	.413	2.374
	Presence of lymph node invasion	.214	1.661	.746	3.697
	PR+ status	.195	1.898	.720	5.001
	ER+ status	.122	.505	.213	1.200
	HER2+ status	.197	.535	.207	1.383
	Increased tumor stage	.705	1.201	.464	3.110
	Larger tumor size	.021	2.991	1.179	7.587
Step 4	Increased CHST3 expression	.866	.933	.414	2.102
	Presence of lymph node invasion	.185	1.707	.774	3.764
	PR+ status	.179	1.939	.739	5.088
	ER+ status	.114	.497	.209	1.182
	HER2+ status	.167	.518	.204	1.315
	Larger tumor size	.008	3.201	1.346	7.611
Step 5	Increased CHST3 expression	.847	.924	.413	2.069
	PR+ status	.210	1.841	.709	4.778
	ER+ status	.131	.516	.219	1.219
	HER2+ status	.201	.549	.219	1.377
	Larger tumor size	.003	3.532	1.514	8.238
Step 6	Increased CHST3 expression	.967	1.017	.459	2.252
	ER+ status	.275	.636	.282	1.433
	HER2+ status	.142	.504	.202	1.257
	Larger tumor size	.003	3.593	1.540	8.382
Step 7	Increased CHST3 expression	.992	1.004	.452	2.229
	HER2+ status	.235	.588	.245	1.413
	Larger tumor size	.004	3.501	1.501	8.167
Step 8	Increased CHST3 expression	.931	.965	.437	2.135
	Larger tumor size	.006	3.237	1.402	7.476

Table 3.11: Multivariate Cox regression analysis of CHST3 expression using OS.

		p-value	Hazard Ratio	95% Confidence Interval	
				Lower	Upper
Step 1	Increased CHST3 expression	.340	.579	.189	1.779
	Presence of lymph node invasion	.373	1.558	.587	4.132
	PR+ status	.543	1.432	.450	4.553
	ER+ status	.199	.487	.162	1.459
	HER2+ status	.234	.502	.162	1.559
	Increased tumor stage	.709	.795	.239	2.646
	Race	.849	.938	.485	1.814
	Larger tumor size	.009	5.188	1.502	17.921
	Increased age	.886	1.077	.389	2.981
Step 2	Increased CHST3 expression	.347	.587	.193	1.780
	Presence of lymph node invasion	.376	1.552	.586	4.112
	PR+ status	.498	1.467	.484	4.447
	ER+ status	.186	.481	.162	1.424
	HER2+ status	.233	.502	.162	1.557
	Increased tumor stage	.717	.803	.244	2.639
	Race	.824	.929	.487	1.772
	Larger tumor size	.009	5.202	1.508	17.949
Step 3	Increased CHST3 expression	.354	.592	.195	1.795
	Presence of lymph node invasion	.344	1.586	.610	4.121
	PR+ status	.502	1.464	.481	4.453
	ER+ status	.180	.475	.160	1.409
	HER2+ status	.214	.492	.161	1.506
	Increased tumor stage	.669	.778	.245	2.467
	Larger tumor size	.010	5.158	1.492	17.829
Step 4	Increased CHST3 expression	.408	.640	.222	1.842
	Presence of lymph node invasion	.363	1.551	.602	3.993
	PR+ status	.537	1.411	.473	4.209
	ER+ status	.190	.491	.170	1.423
	HER2+ status	.236	.511	.168	1.552
	Larger tumor size	.008	4.659	1.487	14.603
Step 5	Increased CHST3 expression	.466	.678	.239	1.925
	Presence of lymph node invasion	.390	1.510	.590	3.867
	ER+ status	.249	.555	.204	1.511
	HER2+ status	.205	.490	.163	1.476
	Larger tumor size	.007	4.784	1.533	14.935
Step 6	Increased CHST3 expression	.440	.664	.235	1.877
	ER+ status	.255	.562	.209	1.516
	HER2+ status	.231	.515	.173	1.527
	Larger tumor size	.005	5.087	1.650	15.683
Step 7	Increased CHST3 expression	.426	.655	.231	1.856
	HER2+ status	.384	.629	.222	1.783
	Larger tumor size	.006	4.920	1.597	15.163
Step 8	Increased CHST3 expression	.374	.625	.222	1.762
	Larger tumor size	.007	4.633	1.517	14.147

Table 3.12: Multivariate Cox regression analysis of CHST3 expression using SAR.

		p-value	Hazard Ratio	95% Confidence Interval	
				Lower	Upper
Step 1	Increased CHST3 expression	.448	.640	.203	2.025
	Presence of lymph node invasion	.997	1.002	.355	2.832
	PR+ status	.874	1.102	.332	3.660
	ER+ status	.297	.529	.160	1.749
	HER2+ status	.541	.697	.218	2.223
	Increased tumor stage	.728	.787	.205	3.029
	Race	.654	.826	.359	1.903
	Larger tumor size	.028	4.120	1.167	14.542
	Increased age	.934	.960	.361	2.551
Step 2	Increased CHST3 expression	.448	.640	.203	2.024
	PR+ status	.873	1.102	.334	3.637
	ER+ status	.296	.529	.161	1.745
	HER2+ status	.533	.697	.224	2.168
	Increased tumor stage	.726	.787	.207	2.995
	Race	.634	.826	.375	1.817
	Larger tumor size	.025	4.122	1.191	14.261
	Increased age	.935	.960	.362	2.545
Step 3	Increased CHST3 expression	.439	.637	.203	1.995
	PR+ status	.882	1.094	.336	3.565
	ER+ status	.294	.534	.165	1.725
	HER2+ status	.536	.700	.226	2.168
	Increased tumor stage	.728	.788	.207	3.010
	Race	.638	.827	.376	1.821
	Larger tumor size	.023	4.079	1.211	13.734
Step 4	Increased CHST3 expression	.447	.648	.211	1.985
	ER+ status	.266	.557	.199	1.560
	HER2+ status	.540	.702	.227	2.173
	Increased tumor stage	.744	.802	.213	3.013
	Race	.644	.831	.379	1.823
	Larger tumor size	.023	4.059	1.209	13.625
Step 5	Increased CHST3 expression	.481	.674	.225	2.018
	ER+ status	.281	.571	.206	1.581
	HER2+ status	.559	.715	.232	2.204
	Race	.491	.780	.385	1.581
	Larger tumor size	.023	3.854	1.204	12.337
Step 6	Increased CHST3 expression	.384	.624	.216	1.805
	ER+ status	.338	.615	.228	1.662
	Race	.450	.761	.375	1.545
	Larger tumor size	.027	3.624	1.156	11.365
Step 7	Increased CHST3 expression	.466	.676	.237	1.934
	ER+ status	.432	.681	.262	1.774
	Larger tumor size	.037	3.337	1.074	10.370
Step 8	Increased CHST3 expression	.494	.693	.243	1.980
	Larger tumor size	.037	3.354	1.077	10.442

3.7 Expression Analysis of FLRT3 in Invasive Ductal Carcinoma Tissues

The evaluation of FLRT3 was also extended to clinical tissue work as no studies thus far have reported on FLRT3 expression in breast cancer. FLRT3 expression in IDC patient cases was evaluated using the same tissue microarray used for CHST3 expression analysis. From the *in vitro* studies, it can be concluded that *FLRT3* plays a tumor promoter role in breast cancer tumorigenesis; the down-regulation of *FLRT3* brings forth less aggressive and metastatic behaviors in breast cancer cells. Therefore, we would like to investigate if these observations can be extended to clinical patient samples. We would hypothesize that high expression of FLRT3 in human breast cancer tissue is correlated with worse prognosis and clinical parameters. As a result of tissue loss during the immunohistochemistry process, the expression patterns of CHST3 were examined in 258 cases (208 IDC cases and 50 normal ductal cases).

3.7.1 FLRT3 Expression Pattern in Breast Tissues

FLRT3 expression staining was positive in the epithelial compartment of both normal and malignant breast tissues as shown in Figure 3.48.

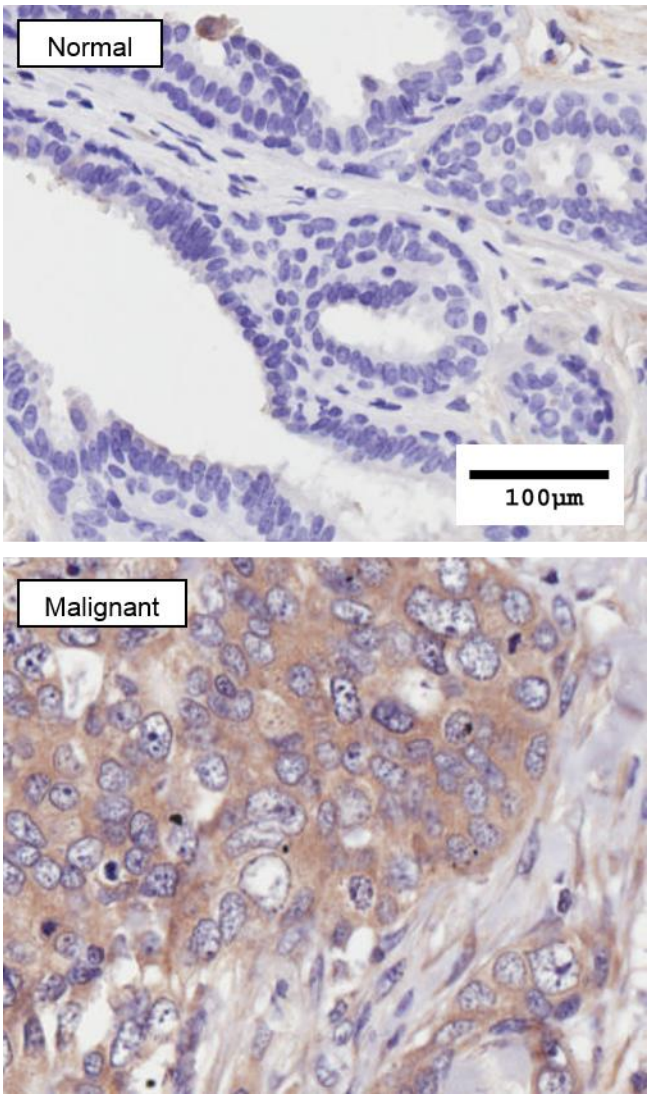

Figure 3.48: Staining pattern of FLRT3 in breast tissues.
FLRT3 expression was observed in the epithelial compartment of normal and malignant breast tissues, each showing staining intensity of 0 and 1+ respectively.

3.7.2 FLRT3 Selected Cut-off Point

Selecting a suitable cut-off point for FLRT3 was also carried out first analysing the distribution curve of the staining intensities gathered from the breast tissues. Though a non-normal distribution curve (Figure 3.49A) was observed, the mean was selected to be the cut-off point for FLRT3 (Figure 3.49C) as the mean compared to the median cut-off point has a better balance in terms of sensitivity and false positivity scores. The mean cut-off point shows a sensitivity score of 0.601 (Figure 3.49D), false positivity score between 0.000 and 0.180 (Figure 3.49D), and area under curve is 0.719 (Figure 3.49B), which is above 0.500.

(A)

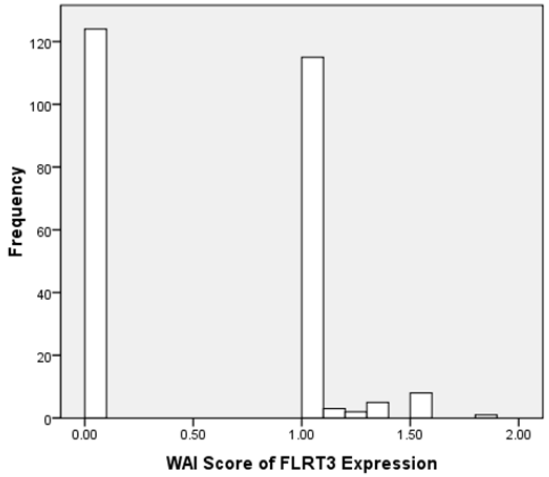

(B)

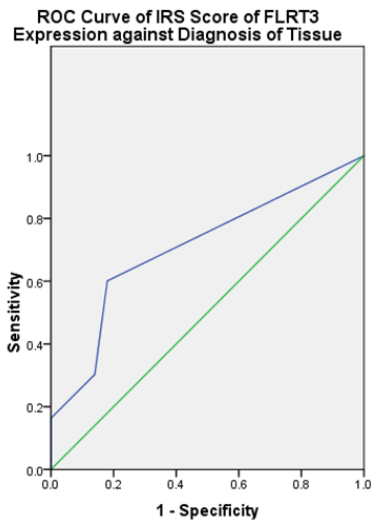

(C)

	Mean	Median	Mode	Min	Max	25th Percentile	50th Percentile	75th Percentile
WAI	0.55	1.00	0.00	0.00	1.89	0.00	1.00	1.00

(D)

WAI Score	Sensitivity	1-Specificity
0.50	0.601	0.180
1.09	0.091	0.000

Figure 3.49: Frequency distribution and ROC curve of FLRT3 expression among normal and malignant tissues
(A) Histogram illustrates the frequency distribution of the WAI score of FLRT3 expression across both normal and malignant tissues. (B) ROC curve depicts WAI score of FLRT3 expression of normal and malignant tissues following their sensitivity and 1-specificity score. The area under curve is 0.719, which is above 0.500.

3.7.3 FLRT3 Expression in Normal and Malignant Breast Tissues

Expression of FLRT3 epitope was evaluated in the epithelial (cytoplasm) compartment of ductal specimens. Analysis of the tissue microarrays showed that malignant IDC tissues had enhanced staining in comparison to normal ductal tissues as shown in Figure 3.50 and Table 3.13 (p-value = 0.000). Further analysis was also performed on paired normal and malignant breast tissues, of which results showed decreased FLRT3 expression level in the normal tissues compared to its paired malignant counterpart tissue (Figure 3.51).

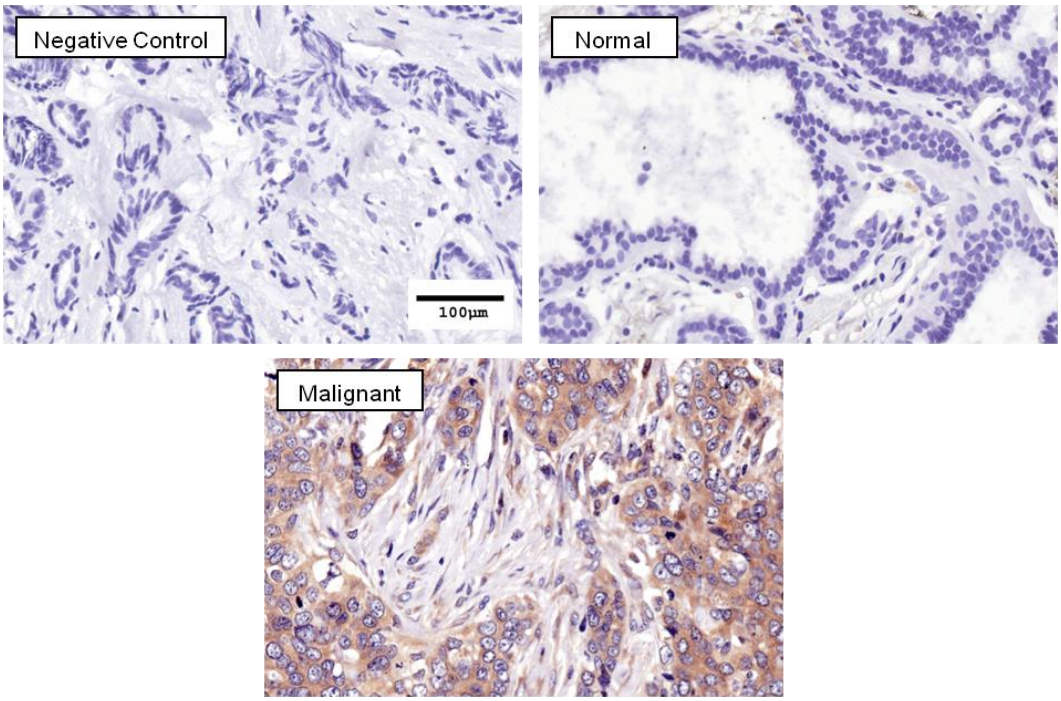

Figure 3.50: FLRT3 immunostaining in normal and malignant breast tissues
Higher expression of FLRT3 was observed in malignant breast tissues (with overall staining intensities of 1+ and 2+) compared to the normal breast tissues (with overall staining intensity of 0).

Table 3.13: Analysis of FLRT3 expression between normal and malignant breast tissues

FLRT3 expression is significantly enhanced in malignant breast tissues in comparison to normal breast tissues.

	Total Percentage Staining		
	≤ 0.55	**> 0.55**	**p-value**
Diagnosis			
Normal	41	9	**0.000***
Malignant	83	125	

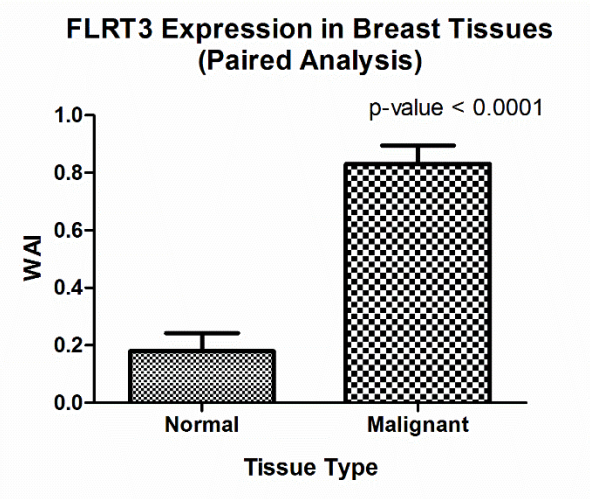

Figure 3.51: Paired analysis of FLRT3 expression in 26 paired normal and malignant breast tissue samples.
Normal tissues shows reduced expression level of FLRT3 compared to malignant tissues.

3.7.4 FLRT3 Correlations with Clinicopathological Parameters

Following expression analysis using WAI (cutoff at 0.55), FLRT3 expression level was analyzed against the various clinicopathological parameters (Table 3.14). Enhanced FLRT3 staining was observed in patients with enhanced lymphovascular invasion stage (p-value = 0.018) and patients of older age (p-value = 0.003).

Table 3.14 Correlations between FLRT3 expression and clinicopathological features of IDC

	WAI				**WAI**		
	≤ 0.55	**> 0.55**	**p-value**		**≤ 0.55**	**> 0.55**	**p-value**
Age (years)				Lymphovascular invasion			
≤ 56	62	68	**0.003***				
> 56	21	57		Absent	39	38	0.139
NA	0	0		Present	27	44	
				NA	17	43	
Ethnicity				Lymphovascular invasion stage			
Chinese	67	79	0.587				
Malay	6	5		1	47	50	**0.018***
Indian	1	3		2	17	30	
Others	6	4		3	14	35	
NA	3	34		NA	5	10	
Tumor size (mm)				Lymph node status			
≤ 30	51	62	0.096	1	46	57	0.157
> 30	31	61		2	19	28	
NA	1	2		3	13	29	
				NA	5	11	
Histological tumor grade				Tubule Formation Stage			
1	2	11	0.511	1	2	4	0.855
2	32	43		2	18	19	
3	46	67		3	43	55	
NA	3	4		NA	20	47	
Tumor stage				ER status			
1	12	7	0.204	Negative	40	62	0.767
2	30	39		Positive	33	57	
3	4	5		NA	10	6	
NA	37	74					
Mitotic Stage				PR status			
1	9	18	0.095	Negative	31	54	0.765
2	19	27		Positive	42	64	
3	35	33		NA	10	7	
NA	20	47					
Pleomorphism Stage				HER2 receptor status			
				Negative	52	80	1.000
1	0	4	0.686	Positive	23	36	
2	29	33		NA	8	9	
3	34	41					
NA	20	47					

NA = Not Available

3.7.5 Survival Analysis of FLRT3 Expression

3.7.5.1 Survival Analysis using Kaplan Meier

Survival analysis was performed using Kaplan Meier curves to observe any general trends between FLRT3 expression and tumor recurrence and mortality rate. No significant trends were observed for FLRT3 expression with patients' tumor recurrence and mortality rate, as shown in Figure 3.52.

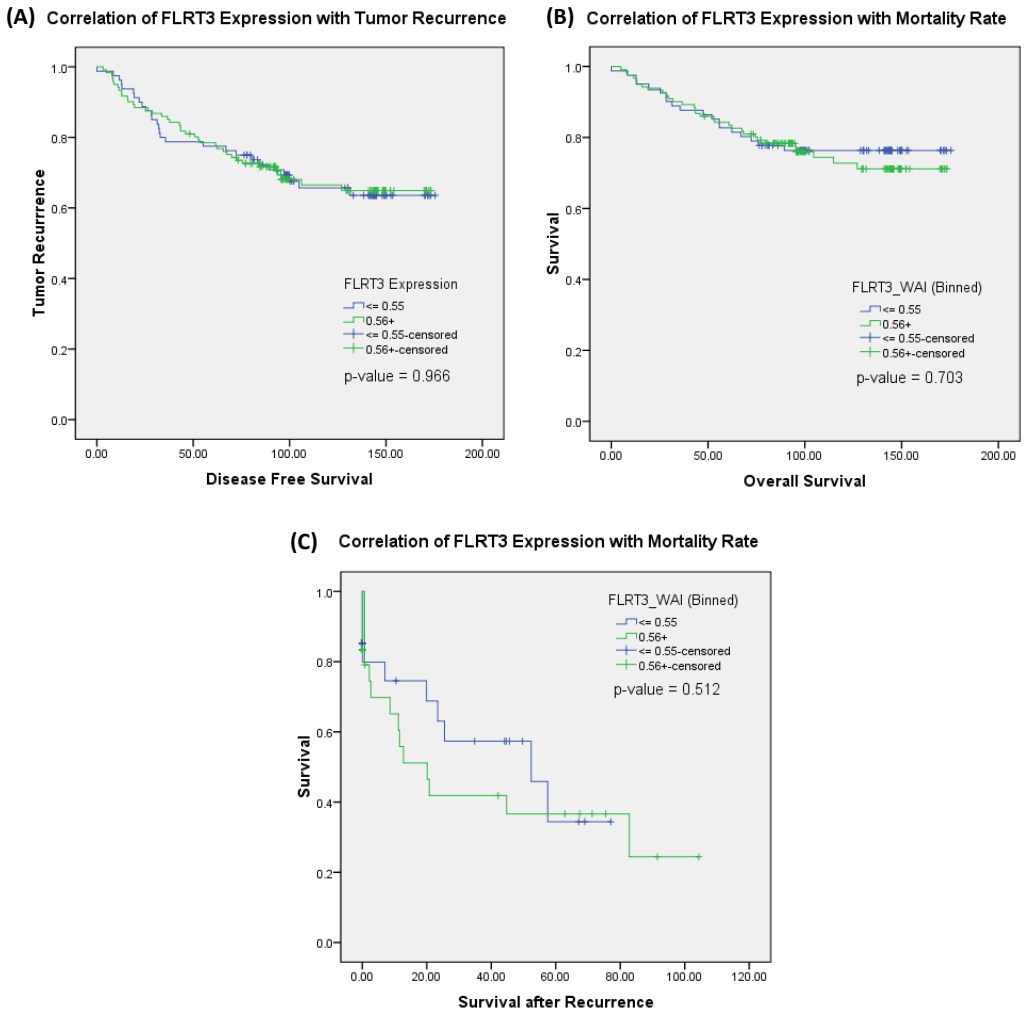

Figure 3.52: Kaplan Meier curves using FLRT3
No significant trend was observed between FLRT3 expression and (A) tumor recurrence, (B) overall survival, and (C) survival after recurrence.

3.7.5.2 Survival Analysis using Cox Regression Univariate

Cox regression analysis using univariate method was performed to determine the hazard ratio of FLRT3 expression as well as for the clinicopathological parameters. Several significant hazard ratios were obtained for various clinical parameters. However, no significant hazard ratios were attained for FLRT3 expression in disease-free survival (Table 3.15), overall survival (Table 3.16), as well as survival after recurrence (Table 3.17) time period.

Table 3.15: Univariate Cox regression analysis of FLRT3 and clinicopathological parameters using DFS time period

	Disease Free Survival			
			95% CI	
	p-value	Hazard ratio	Lower	Upper
Increased FLRT3 expression	.795	1.164	.371	3.663
Presence of lymph node invasion	.813	1.158	.345	3.889
PR+ status	.051	5.512	.993	30.600
ER+ status	.638	.763	.247	2.357
HER2+ status	.353	.487	.107	2.219
Increased lymphovascular invasion stage	.915	.000	.000	1.365E63
Increased tumor stage	.328	1.942	.514	7.338
Race	.152	.532	.224	1.263
Increased histological grade	.863	1.191	.164	8.646
Increased tubule formation stage	.788	.834	.222	3.133
Increased pleomorphism stage	.590	1.508	.338	6.721
Increased mitotic index	.299	1.764	.605	5.143
Increased lymph node stage	.918	3303.709	.000	1.893E70
Larger tumor size	.780	.854	.282	2.583
Increased age	.101	2.867	.813	10.104

Table 3.16: Univariate Cox regression analysis of FLRT3 and clinicopathological parameters using OS time period

	Overall Survival			
			95% CI	
	p-value	Hazard ratio	Lower	Upper
Increased FLRT3 expression	.291	2.445	.466	12.838
Presence of lymph node invasion	.463	1.837	.363	9.297
PR+ status	.054	12.006	.956	150.760
ER+ status	.358	.481	.101	2.290
HER2+ status	.775	1.305	.211	8.076
Increased lymphovascular invasion stage	.920	.000	.000	2.575E74
Increased tumor stage	.842	.826	.126	5.401
Race	.109	.256	.048	1.359
Increased histological grade	.540	2.533	.130	49.446
Increased tubule formation stage	.422	.416	.049	3.536
Increased pleomorphism stage	.688	1.503	.206	10.944
Increased mitotic index	.100	3.507	.786	15.641
Increased lymph node stage	.921	9873.267	.000	2.754E82
Larger tumor size	.883	.889	.186	4.253
Increased age	.025	8.297	1.300	52.949

Table 3.17: Univariate Cox regression analysis of FLRT3 and clinicopathological parameters using SAR time period

	Survival after Recurrence			
			95% CI	
	p-value	Hazard ratio	Lower	Upper
Increased FLRT3 expression	.073	5.272	.857	32.434
Presence of lymph node invasion	.711	1.352	.274	6.677
PR+ status	.160	7.163	.458	111.954
ER+ status	.182	.288	.046	1.794
HER2+ status	.647	1.600	.215	11.931
Increased lymphovascular invasion stage	.899	.000	.000	4.808E53
Increased tumor stage	.701	.666	.083	5.310
Race	.071	.118	.012	1.199
Increased histological grade	.970	.940	.039	22.774
Increased tubule formation stage	.770	.708	.070	7.160
Increased pleomorphism stage	.599	1.952	.162	23.565
Increased mitotic index	.093	4.030	.793	20.486
Increased lymph node stage	.901	4376.959	.000	1.113E61
Larger tumor size	.496	1.874	.307	11.451
Increased age	.035	7.519	1.158	48.838

3.7.5.3 Survival Analysis using Cox Regression Multivariate

As no significant hazard ratio was obtained through the univariate method, analysis using Cox regression multivariate survival analysis (Table 3.18-20) using clinicopathological parameters were performed. A borderline significant trend that high FLRT3 expression in IDC patients was associated with higher tumor recurrence with a hazard ratio of 2.445 (p-value = 0.054) when adjusted for the clinicopathological parameters. Tumor size was also found to have significant hazard ratios after adjusting for confounding factors in all time periods.

Table 3.18: Multivariate Cox regression analysis of FLRT3 expression using DFS.

		p-value	Hazard Ratio	95% Confidence Interval	
				Lower	Upper
Step 1	Increased FLRT3 expression	.088	2.247	.887	5.714
	Presence of lymph node invasion	.746	1.161	.471	2.864
	PR+ status	.212	2.038	.666	6.243
	ER+ status	.380	.656	.256	1.681
	HER2+ status	.121	.413	.135	1.262
	Increased tumor stage	.451	1.508	.519	4.383
	Race	.341	.689	.321	1.482
	Larger tumor size	.040	2.830	1.048	7.645
	Increased age	.369	1.502	.618	3.652
Step 2	Increased FLRT3 expression	.085	2.262	.893	5.714
	PR+ status	.219	2.014	.659	6.149
	ER+ status	.390	.663	.260	1.693
	HER2+ status	.128	.426	.142	1.277
	Increased tumor stage	.389	1.576	.560	4.439
	Race	.307	.674	.316	1.437
	Larger tumor size	.035	2.886	1.078	7.729
	Increased age	.349	1.524	.631	3.682
Step 3	Increased FLRT3 expression	.054	2.445	.983	6.061
	PR+ status	.340	1.659	.586	4.701
	HER2+ status	.165	.462	.155	1.373
	Increased tumor stage	.339	1.673	.582	4.804
	Race	.276	.655	.306	1.403
	Larger tumor size	.036	2.852	1.069	7.604
	Increased age	.350	1.529	.628	3.726
Step 4	Increased FLRT3 expression	.068	2.294	.942	5.587
	PR+ status	.248	1.828	.656	5.094
	HER2+ status	.212	.508	.176	1.471
	Increased tumor stage	.374	1.587	.573	4.392
	Race	.214	.618	.290	1.320
	Larger tumor size	.029	2.972	1.120	7.884
Step 5	Increased FLRT3 expression	.093	2.075	.885	4.854
	PR+ status	.263	1.788	.646	4.948
	HER2+ status	.179	.487	.171	1.390
	Race	.272	.667	.324	1.373
	Larger tumor size	.004	3.660	1.526	8.776
Step 6	Increased FLRT3 expression	.072	2.198	.932	5.181
	HER2+ status	.099	.420	.150	1.179
	Race	.270	.665	.323	1.372
	Larger tumor size	.003	3.734	1.550	8.996
Step 7	Increased FLRT3 expression	.100	2.041	.872	4.785
	HER2+ status	.098	.420	.150	1.174
	Larger tumor size	.005	3.500	1.458	8.398

Table 3.19: Multivariate Cox regression analysis of FLRT3 expression using OS.

		p-value	Hazard Ratio	95% Confidence Interval	
				Lower	Upper
Step 1	Increased FLRT3 expression	.345	1.733	.554	5.405
	Presence of lymph node invasion	.910	1.066	.351	3.239
	PR+ status	.584	1.454	.380	5.564
	ER+ status	.465	.636	.189	2.139
	HER2+ status	.141	.346	.084	1.421
	Increased tumor stage	.875	.890	.210	3.780
	Race	.331	.513	.133	1.974
	Larger tumor size	.014	5.279	1.392	20.017
	Increased age	.600	1.336	.452	3.948
Step 2	Increased FLRT3 expression	.337	1.742	.561	5.405
	PR+ status	.590	1.443	.380	5.477
	ER+ status	.469	.644	.195	2.124
	HER2+ status	.139	.352	.088	1.405
	Increased tumor stage	.893	.908	.223	3.698
	Race	.321	.507	.133	1.936
	Larger tumor size	.014	5.314	1.409	20.036
	Increased age	.592	1.343	.457	3.946
Step 3	Increased FLRT3 expression	.298	1.783	.600	5.291
	PR+ status	.595	1.433	.380	5.402
	ER+ status	.475	.650	.200	2.116
	HER2+ status	.141	.354	.089	1.412
	Race	.301	.498	.133	1.865
	Larger tumor size	.006	5.092	1.585	16.360
	Increased age	.592	1.343	.457	3.942
Step 4	Increased FLRT3 expression	.236	1.908	.656	5.555
	ER+ status	.604	.754	.260	2.190
	HER2+ status	.124	.338	.085	1.347
	Race	.312	.508	.137	1.887
	Larger tumor size	.006	5.162	1.606	16.592
	Increased age	.514	1.421	.495	4.082
Step 5	Increased FLRT3 expression	.215	1.957	.677	5.650
	HER2+ status	.148	.372	.098	1.419
	Race	.310	.509	.138	1.875
	Larger tumor size	.006	5.119	1.598	16.400
	Increased age	.541	1.388	.485	3.978
Step 6	Increased FLRT3 expression	.221	1.931	.842	5.524
	HER2+ status	.165	.393	.105	1.469
	Race	.280	.487	.132	1.797
	Larger tumor size	.005	5.273	1.650	16.849
Step 7	Increased FLRT3 expression	.413	1.529	.554	4.219
	Race	.274	.454	.111	1.867
	Larger tumor size	.008	4.699	1.491	14.814
Step 8	Increased FLRT3 expression	.468	1.458	.528	4.016
	Larger tumor size	.013	4.287	1.364	13.480

Table 3.20: Multivariate Cox regression analysis of FLRT3 expression using SAR.

		p-value	Hazard Ratio	95% Confidence Interval	
				Lower	Upper
Step 1	Increased FLRT3 expression	.919	1.062	.334	3.378
	Presence of lymph node invasion	.686	.782	.238	2.571
	PR+ status	.672	1.359	.329	5.619
	ER+ status	.374	.554	.150	2.039
	HER2+ status	.254	.437	.105	1.812
	Increased tumor stage	.790	.804	.161	4.012
	Race	.279	.416	.085	2.039
	Larger tumor size	.027	4.500	1.191	16.999
	Increased age	.582	1.364	.451	4.126
Step 2	Increased FLRT3 expression	.846	1.115	.371	3.356
	Presence of lymph node invasion	.623	.751	.239	2.358
	PR+ status	.697	1.318	.328	5.298
	ER+ status	.388	.574	.162	2.027
	HER2+ status	.264	.451	.111	1.825
	Race	.225	.388	.084	1.788
	Larger tumor size	.021	4.211	1.239	14.307
	Increased age	.576	1.371	.454	4.136
Step 3	Increased FLRT3 expression	.797	1.153	.387	3.436
	Presence of lymph node invasion	.600	.737	.235	2.308
	ER+ status	.447	.653	.218	1.956
	HER2+ status	.277	.464	.116	1.854
	Race	.238	.406	.091	1.813
	Larger tumor size	.022	4.186	1.232	14.216
	Increased age	.541	1.406	.471	4.198
Step 4	Increased FLRT3 expression	.854	1.106	.376	3.257
	ER+ status	.433	.643	.214	1.936
	HER2+ status	.241	.440	.111	1.737
	Race	.263	.431	.099	1.882
	Larger tumor size	.026	3.876	1.179	12.740
	Increased age	.586	1.348	.461	3.943
Step 5	Increased FLRT3 expression	.834	1.121	.385	3.268
	ER+ status	.442	.648	.215	1.958
	HER2+ status	.265	.459	.117	1.803
	Race	.266	.435	.100	1.888
	Larger tumor size	.017	4.137	1.283	13.337
Step 6	Increased FLRT3 expression	.806	1.144	.391	3.344
	HER2+ status	.356	.540	.146	1.998
	Race	.296	.467	.112	1.948
	Larger tumor size	.021	3.892	1.223	12.383
Step 7	Increased FLRT3 expression	.990	1.007	.351	2.890
	Race	.281	.440	.099	1.957
	Larger tumor size	.027	3.688	1.157	11.751
Step 8	Increased FLRT3 expression	.889	1.076	.384	3.012
	Larger tumor size	.043	3.296	1.040	10.444

3.8 Correlation of CHST3 and FLRT3 Expression in Invasive Ductal Carcinoma

Evaluation was also performed on whether the expression levels of CHST3 and FLRT3 are correlated in human tissue samples of IDC. No significant association was observed between the expression levels of CHST3 and FLRT3 in the evaluated set of IDC tissues (Table 3.21).

Table 3.21: Correlation of CHST3 with FLRT3 expression in IDC tissues

No significant association was obtained between CHST3 and FLRT3 expression levels in IDC breast tissues.

	FLRT3 expression		
	WAI ≤ 0.55	WAI > 0.55	p-value
CHST3 expression			
WAI ≤ 1.06	49	63	0.379
WAI > 1.06	31	53	
Not Available	3	19	

3.9 Summary of Results

This study first focused on the significance of *CHST3* in breast cancer phenotypic behaviors. The regulatory roles of *CHST3* were examined in T47D, MCF7 and MDA-MB-231 cell lines through various functional experiments including cell migration, invasion, adhesion, proliferation, cell cycle, and apoptosis assays. Also, several potential molecules were studied on their associations with *CHST3* pathway. This study would be the first evaluation performed to elucidate the functional roles as well as expression studies of *CHST3* and *FLRT3* in breast cancer. Table 3.22 and 3.23 summarize the results obtained.

Table 3.22: Summary table of *in vitro* studies

	Cell Migration	**Cell Invasion**	**Cell Adhesion**	**Cell Proliferation**	**Cell Apoptosis**
***CHST3* Silenced**	↑	↑	↓	↑	↓
***CHST3* Over-expressed**	↓	↓	↑	↓	
***FLRT3* Silenced**	↓	↓	↑	↓	
***CHST3* + *FLRT3* Silenced**	≈	≈	≈	≈	
***GPNMB* Silenced (from literature search)**	↓	↓	N.A.	≈	
***CHST3* + *GPNMB* Silenced**	≈	≈	≈	≈	
	E-cadherin	**β-catenin**	**pJAK2**	**pSTAT3**	**pBAD**
***CHST3* Silenced**	↓	↓	≈	≈	↑

Table 3.23: Summary table of clinical IDC studies

	Tissue Type	**Tumor stage**	**Tumor size**	**Age**	**Lymphovascular invasion stage**	**Tumor recurrence**	**Mortality rate**
Low CHST3	Malignant	↑	↑	ns	ns	ns	ns
High FLRT3	Malignant	ns	ns	↑	↑	ns	ns

3.9.1 *CHST3* Regulates Cell Migration

Cancer cells have the potential to reach metastatic potential, migrating from the primary tumor to a distant secondary site (organ) via the blood vessels and lymphatic vessels (Simpson et al., 2010, Moutasim et al., 2011). To evaluate the effect of *CHST3* on cell motility, migration assay using migration chambers was carried out after silencing as well as over-expression of *CHST3*. Significant increase in cell migration was observed upon silencing of *CHST3* whereas significant decrease was observed after over-expression of *CHST3* in the breast cancer cells.

3.9.2 *CHST3* Regulates Cell Invasion

Cell invasion of the tumor cell arise from the interaction of the cancer cells with surrounding cells as well as the extracellular matrix and stroma. Invasive tumors can metastasize to adjacent tissues as well as migrate to other organs in the body. In the case of breast cancer, the tumor cells usually metastasize to the lungs, liver, bone, and brain. The cancer cells will invade the basement membrane that lines the epithelial cells, hence invading to the surrounding environment. To replicate this event, invasion assay using matrigel invasion chambers was performed. Down-regulation of *CHST3* increased cell invasion whereas over-expression of *CHST3* decreased cell invasion.

3.9.3 *CHST3* Regulates Cell Adhesion

Cell adhesion also has a major role in cancer cell aggressive and metastatic behavior. Cancer cells will usually have weaker cell adhesion compared to normal cells, causing the cancer cells to metastasize more easily to surrounding tissues and other organs (Ruoslahti, 1984). Adhesion assay was performed using either collagen I or fibronectin coated plates. Upon silencing of *CHST3*, small decreases in cell adhesion in both coated plates were observed. The opposite observation was obtained for cells over-expressed with *CHST3*, which is an increase in cell adhesion.

These would suggest that *CHST3* modulates the expression level of adhesion molecule(s), which would in turn adhere to collagen and/or fibronectin, and regulates cell adhesion level.

3.9.4 *CHST3* Regulates Cell Proliferation

In the proliferation assay performed using MTS solution, silencing of *CHST3* resulted in a small increase in the number of viable T47D and MDA-MB-231 cells. On the other hand, over-expression of *CHST3* in MCF7 and MDA-MB-231 cells led to a small decrease in cell proliferation. It should be noted that the change in cell viability can not only be attributable to rate of cell proliferation but also rate of cell apoptosis or both events. Flow cytometry was also performed to further analyze cell proliferation and to observe whether cell death occurred after silencing of *CHST3*. Cell cycle analysis showed decreases in cell death at the sub-G1 phase for T47D and MDA-MB-231 cell lines. However, only T47D cell line showed a slight change (reduction) at the DNA replication phase (S phase). This may signify the changes in cell numbers could be due more to cell death.

3.9.5 *CHST3* Regulates Cell Apoptosis

To verify the sub-G1 observations, apoptosis assay was performed. Fluorescence measurement showed reductions in caspases 3 and 7 levels upon down-regulation of *CHST3*. This hence indicates the potential ability of *CHST3* in regulating cell viability through cell apoptosis.

3.9.6 *CHST3* Effects on Downstream Molecules

Moving on to the downstream molecular work, based on the microarray analysis, both *GPNMB* and *FLRT3* were found to be up-regulated after down-regulation of *CHST3*. Therefore, the downstream relationship of *GPNMB* or *FLRT3* and *CHST3* was validated through functional studies. Silencing of *CHST3* increased cell survival and cell motility whereas silencing of *GPNMB* or *FLRT3 showed*

otherwise, decreased cell survival and cell motility. Upon double silencing of *CHST3* and *GPNMB* or *FLRT3*, the levels of cell proliferation, cell adhesion, cell migration, and cell invasion were similar to that of the control group, indicating that phenotypic behavior changes observed during single silencing of either *CHST3* or *GPNMB* or *FLRT3* were diminished and returned to basal level. This suggests that *GPNMB* and *FLRT3* are downstream molecules of *CHST3* given that the cellular behaviors were similar to the double negative group after double silencing.

In addition to *GPNMB* and *FLRT3*, silencing of *CHST3* in T47D cells gave rise to reduced expression of E-cadherin and β-catenin as well as enhanced expression of pBAD/BAD, all of which have involvement in the various cellular behavior changes especially for the main alterations in cell migration and invasion. This will be further elaborated later in this chapter.

3.9.7 CHST3 and FLRT3 in Breast Tissues

From the immunohistochemistry analysis, CHST3 and FLRT3 expression levels were observed to be significantly higher and lower respectively in the epithelial compartment of normal ductal tissues as compared to that of the malignant tissues. Significant associations were also found between CHST3 expression and several clinicopathological parameters that are low CHST3 expression is significantly linked to higher tumor stage. Additionally, CHST3 expression is borderline significantly associated with larger tumor size. Significant correlations were also found between FLRT3 expression and clinicopathological parameters – higher FLRT3 expression was associated with patients with older age and greater stage of lymphovascular invasion. In terms of prognosis, from the multivariate survival analysis, no observable trend was observed for CHST3. For FLRT3, there was borderline significance in that higher tumor recurrence risk was observed for enhanced FLRT3 expression upon adjusting for confounding factors. Additionally, there was no significant association between CHST3 and FLRT3 expression levels in breast cancer.

CHAPTER 4:
DISCUSSION

4 DISCUSSION

4.1 Potential Role of CHST3 in Breast Cancer

With growing evidence that proteoglycans and their glycosaminoglycan chains play substantial roles in regulating cancer behavior, the roles of chondroitin- and heparan-related enzymes have also been investigated in recent years. A few of the more well studied enzymes in this field are heparanase (Ilan et al., 2006, Vlodavsky et al., 2007a, Vlodavsky et al., 2007b) and chondroitin sulfotransferase 11 or CHST11 (Cooney et al., 2011, Potapenko et al., 2010), both enzymes having been associated with tumorigenesis. CHST3, or otherwise known as chondroitin-6-sulfotransferase 1 (C6ST1), has been investigated in greater detail in the field of musculoskeletal disease; the de-regulation of CHST3 expression level is associated with the diagnosis of spondyloepiphyseal dysplasia which has a deficiency in the expression level of CHST3 (Tuysuz et al., 2009, van Roij et al., 2008). The interest to pursue evaluations of CHST3 built up when it is also found to be potentially regulating cancer cell behavior, such as those studied by Kalathas et al and Maupin et al (Kalathas et al., 2010, Maupin et al., 2010) in laryngeal and pancreatic cancer respectively. Being a relatively new enzyme, CHST3 is yet to be evaluated for its potential roles in breast cancer and its signaling pathways is yet to be uncovered.

This study has been carried out with a focus on evaluating the expression level as well as the functional roles of CHST3 in breast cancer and whether CHST3 is a potential marker for diagnosis, prognosis, or therapy in breast cancer. The *in vitro* experiments that were carried out included cell migration, invasion, adhesion, proliferation, and cell cycle assays, which were performed to investigate CHST3's potential role in regulating typical cancer cell behaviors or hallmarks. Taken together the observations obtained from this study, they potentially support the notion that CHST3 expression level in epithelial breast cancer cells affect metastatic phenotype. Upon silencing or overexpressing *CHST3* in the three different breast cancer cells (T47D, MCF7, and MDA-MB-231), CHST3 is

observed to regulate cell migration and cell invasion substantially and at greater extent compared to the other phenotypic assays carried out. Further evaluations of microarray-analyzed genes (GPNMB and FLRT3), EMT markers (E-cadherin and β-catenin), and other signaling pathways' molecules (JAK2, STAT3, and BAD) showed expression changes after modulation of *CHST3* expression level, pointing to the possibility of CHST3 having a substantial role in their signaling processes. In the IDC tissue expression study, it is observed that low CHST3 expression levels is correlated with malignant tissues as compared to normal ductal tissues. Additionally, lower levels of CHST3 expression is found to be associated with higher tumor grade in IDC tissue samples.

The next critical question then would be on how CHST3 potentially regulates the phenotypic behaviors observed. To have a certain understanding of how CHST3 functions or regulates, one may look into its substrate's functional roles, expression levels, and regulation in breast cancer instead. CHST3 is a sulfotransferase enzyme responsible for the carbon-6 sulfation pattern of galactosamine unit in chondroitin sulfate. The chondroitin sulfate itself or together with the proteoglycan portion, chondroitin sulfate proteoglycan, has been evaluated in breast cancer and has shown regulating capabilities towards cellular behavior in breast cancer. Also, the closest related gene or protein studied to date in breast carcinoma would be CHST11, which will be elaborated later on.

4.1.1 Potential Role of CHST3 through Chondroitin Sulfate

Past studies conducted have shown significant associations of CS expression with regards to breast cancer. Researchers studied CS expression in general, showing that changes in the cell surface CS expression level consequently alters ECM-degradative enzymes, such as matrix metalloproteinases, which in turn affects the breast cancer cells' invasiveness and cell-matrix interactions (Yip et al., 2006). From *in vitro* studies, breast cancer cells have been seen to have general increased expression of CS levels and are linked to augmented cell proliferation and

migration, making the cells more aggressive and metastatic (Kieber-Emmons et al., 2011, Alini and Losa, 1991, Olsen et al., 1988). At the tissue level, CS levels are observed to be significantly elevated in the stromal compartment of breast tumors (Ricciardelli et al., 2002, Suwiwat et al., 2004). Cooney et al evaluated the effect of specific chondroitin sulfate types in breast cancer. Carbon-4 sulfated CSA is shown to be expressed at increased levels in human breast cancer cells with high metastatic capacity (MDA-MB-231 and MDA-MET) compared to less aggressive cell line, MCF7 (Cooney et al., 2011)). CSE, another CS containing carbon-4 sulfation pattern, has also been considered a tumor promoter molecule, whereby functional studies *in vitro* showed over-expression of CSE promotes angiogenesis and anti-apoptotic cell behavior (Cooney et al., 2011, Grose and Dickson, 2005). Unlike their carbon-4 sulfated CS counterparts, carbon-6 sulfated CSC and CSD chains have been observed to be down-regulated in breast carcinomas (Potapenko et al., 2010), hence may be characterized as tumor suppressors. The differential roles of the various chondroitin sulfate types are also observed in other cases. In wound healing, Zou et al studied the effects of chondroitin-4-sulfate (CSA) and chondroitin-6-sulfate (CSC) on wound healing in which the group observed CSC to increase while CSA decreases cell adhesion levels in palatal fibroblasts (Zou et al., 2004).

At the sulfotransferase level, CHST11 is responsible for the transfer of a sulfate group to the carbon 4 of galactosamine unit to form CSA and CSE. The epithelial expression level of CHST11 is significantly up-regulated in more aggressive breast cancer cells (MDA-MB-231, MDA-MB-468, and MDA-MET) in comparison to their less aggressive metastatic cell line counterpart (MCF7). The same trend is also displayed at the tissue level, whereby CHST11 is over-expressed in malignant specimens against their adjacent non-malignant breast tissues (Cooney et al., 2011, Potapenko et al., 2010). One of CHST11 product, CSA, as mentioned has increased expression level in breast cancer cells of higher tumor grade. This would lead to further plausibility that CHST11 and its product, CSA are correlated to aggressive and metastatic capacities of breast cancer cells.

In view of these observations, the expression level of CHST3 as well as potentially its product, CSC, may then be suppressed when there are enhanced levels of CHST11 and its CS products, causing tumor suppressing effects to be reduced. From the observations in this study, CHST3 has shown the opposite trends compared to CHST11. Through the patient IDC tissue samples, it is observed that a significant proportion of IDC tissues samples display lower levels of CHST3 as compared to the normal ductal tissues. This observation is similar to that observed *in vitro* whereby the breast cancer cells have decreased levels of CHST3 in comparison to MCF12A normal breast cells. Both cell line work and tissue study show expression of CHST3 within the epithelial cells. In the tissue study, it is noted that CHST3 is not expressed in the stroma region of the ductal tissue for both malignant and normal types. Further examination of the expression levels of CHST3 in the malignant tissues showed significant association between low levels of CHST3 and greater tumor stage. Again, this can be observed from the *in vitro* studies of which Grade 1 breast cancer cell lines T47D and MCF7 have higher levels of CHST3 against Grade 3 MDA-MB-231 breast cancer cells. It is to be noted that tumor size has a borderline association with CHST3 expression level. Further evaluations would be necessary to investigate whether both CHST3 and CHST11 act from within the epithelial regions and affects the CS chains as well as CSPGs that are on the cell surface and stroma regions.

Another notion in this study was to investigate whether the regulation of CHST3 has different effects on different grades and hormonal status of breast cancer cells. The establishment of the hormonal type and grade of cancer the patient has determined the type of therapy strategy as well as most importantly, ascertain the survival rate of the patient. Molecular diagnosis using various established biomarkers such as *BRCA1*, *BRCA2*, ER, PR, and HER2 are performed for diagnostic examination in breast cancer (Huston, 2005). In recent years, CSPGs such as versican (VCAN or CSPG2) and CSPG4 have been evaluated of their diagnostic and prognostic capabilities as a biomarker in breast cancer. Both VCAN

and CSPG4 are up-regulated in malignant breast tissues compared to normal breast tissues (Yee et al., 2007, Wang et al., 2010b). Survival analysis indicated VCAN expression is a good predictor of relapse-free survival; enhanced expression of VCAN in the stromal is associated with higher risk and rate of relapse in breast cancer patients (Ricciardelli et al., 2002, Suwiwat et al., 2004). Additionally, it is evaluated that increased VCAN expression is associated with higher expression levels of ER and PR in malignant–appearing microcalcifications (MAMCs) (Skandalis et al., 2011). In the case of CSPG4, CSPG4-specific antibody has been shown to inhibit tumor growth and metastasis as well as reduce risk of tumor recurrence *in vivo* in a lung metastasis model (Wang et al., 2010a). No associations of CSPG4 with ER or PR status have since been reported.

Comparing the changes in phenotypic behavior in the three breast cancer cells examined in this study, the extent of changes are relatively similar with the exception of cell invasion. Compared against T47D and MCF7 Grade 1 (ER+/PR+) breast cancer cells, MDA-MB-231 Grade 3 (ER-/PR-) breast cancer cells showed lesser extent of changes in cell invasion for both silencing and overexpression studies. Moreover, there were no significant correlation between CHST3 expression levels with the various hormonal biomarker statuses in the IDC tissue expression study. The reason(s) to this limitation will need to be explored further; a difference in gene expression may potentially be the cause to the difference in extent of changes observed. One possible method will be to carry out microarray studies on *CHST3*-silenced and *CHST3*-overexpressed MDA-MB-231 cells. The gene list generated from the microarray studies can then be compared against those obtained from the microarray study carried out using T47D cells.

From past CS-related *in vitro* studies, there has been associations of CS levels and its effect on cellular behavior such as cell proliferation, apoptosis, migration, and invasion. From the various cell lines experimented on in this study, little impact has been observed for cell proliferation phenotype. There are also observations that differ between the observations from the *in vitro* studies and that in the expression

studies on human IDC tissues. While the *in vitro* work showed impact towards cellular migratory and invasive behaviors, the analysis carried out on the ductal tissues showed otherwise. As an example, there is no significant association between CHST3 expression level and lymphovascular invasion. Though CHST3 has some diagnostic value, no significant value is found in this population of patients' tissues in terms of it being a potential prognostic marker.

Looking further into detail from the results of the experiments, in the case of cell adhesion, apart from investigating whether cell adhesion would be affected upon regulation of *CHST3* expression, it was also to be evaluated whether the breast cancer cells' adhesive behavior would be similar or different towards various extracellular matrix components such as fibronectin and collagen. In the case of chondroitin sulfate cousin molecules - heparan sulfate - depending on the cell type, cell surface heparan sulfate can have different binding affinity towards different ECM components; in myeloma, heparan sulfate can attach to collagen but has no adhesiveness towards fibronectin (Stamatoglou and Keller, 1983). It is firstly observed, in the *in vitro* study, that the changes are to a small extent for the cell adhesion experiments performed, signifying that CHST3 may not have much biological importance in cell adhesion in breast cancer cells. Similar extent of changes are also observed when either collagen or fibronectin was used in the experiments for the three breast cancer cell lines. This may indicate that CHST3 effects are similar in the different breast cancer cells during the presence of collagen or fibronectin.

Cell proliferation changes are also not as substantial as cell migration and cell invasion in all the experiments carried out; the small extent of changes are consistent throughout the silencing and overexpressing experiments as well as for the various breast cancer cells used. Nevertheless, cell cycle assays were also carried out to validate the observations. The cell cycle assay showed that cell death may be at play and that the cell growth changes may potentially be affected by changes in the S phase (DNA replication) of cell cycle. Additionally, from the

microarray carried out for the *CHST3*-silenced T47D cells, a total of 20 genes having functional roles in cell proliferation are seen to have more than 2-fold changes. For cell migration, 14 genes having migratory roles are picked up after analysis. This may indicate that there are cancelation effects by the genes affected or that some of the genes that have been regulated do not serve any functional importance for cell proliferation.

Apart from understanding CHST3's regulatory effect on the functional roles observed in breast cancer from this main potential angle, there are other possibilities of how CHST3 regulates the various phenotypic behaviors in breast cancer.

4.1.2 CHST3 affects Downstream Molecules GPNMB and FLRT3

The CHST3 pathway was evaluated through a microarray study. *GPNMB* and *FLRT3* genes were selected from the microarray list for further evaluation on whether both molecules are involved in *CHST3* pathway that affected the phenotypic changes occurred. Results from the double silencing experiments have suggested that *GPNMB* and *FLRT3* are downstream of *CHST3* in regulating the phenotypic changes observed. As mentioned previously, it is important to note the small changes in cell proliferation observed in this study, as compared to the more substantial changes seen in cell migration and invasion. GPNMB has been previously studied by Rose et al (Rose et al., 2010) whereby it was observed that overexpression of ectopic GPNMB increases the invasive and migratory phenotypes in BT549 breast cancer cells by at least 50%. Their complementary experiments through silencing of GPNMB in SUM1315 cells brought forth reduction in cell invasion capability. The cell invasion assays carried out in this study validates the research group's findings whereby T47D cells' invasive capability decreased upon silencing of *GPNMB*. This effect is observed to be neutralized upon double silencing of *CHST3* and *GPNMB*, indicating *GPNMB* to be downstream of *CHST3*. Additionally, Rose et al observed that cell growth was unaffected after overexpressing GPNMB in BT549 cells. In this study, *GPNMB*-

silenced cells was observed to have non-substantial change in cell proliferation level. This possibly indicates that the effects of GPNMB in breast cancer cell migration and invasion is not, at a large extent, attributed to the enhancement in cell proliferation. Additionally, this may suggest that *CHST3* have a biologically non-important cell proliferation role in breast cancer.

Similar to CHST3, FLRT3 is also a relatively new gene of which its expression level and functional roles are yet to be unraveled in the cancer field. From the *in vitro* work carried out, it is observed that FLRT3 plays an oncogenic role as compared to tumor suppressor CHST3. Indeed, the pro-metastatic changes by FLRT3 are neutralized by CHST3 in the double silencing study of both genes. Additionally, to note, the effects of FLRT3 on cell proliferation and cell adhesion are similar to the effects shown from regulation of CHST3 or GPNMB, whereby smaller degree and non-substantial changes were observed in both of these phenotypic behaviors.

For FLRT3, the observations from the *in vitro* work are partly extended to the observations collected in the tissue expression study. FLRT3 expression is seen to display greater intensity in malignant ductal cells compared to its normal ductal cell counterpart. *In vitro*, it is only observed that FLRT3 expression is greater in Grade 3 breast cancer cells compared to Grade 1 breast cell lines. This observation or association is not significant when analysis was carried out between FLRT3 expression in the malignant ductal tissues and grades of the tissues. Nevertheless, from the FLRT3 tissue study, FLRT3 expression in the invasive ductal tissues is significantly correlated to lymphovascular invasion stage. Also, its expression level is analyzed to be not significantly correlated to tumor size. This potentially indicates that there are certain extensity of the observations from *in vitro* to human tissue samples. This is as, from the cell line work, silencing of *FLRT3* caused significant changes in cell migration and invasion but little changes in cell proliferation.

Due to the similar characteristics observed for GPNMB and FLRT3, it was hypothesized that GPNMB and FLRT3 may potentially be regulated by one another's cellular processes. The down-regulation of GPNMB or FLRT3 had a similar extent of changes in T47D cells' phenotypic behaviors; there are decreases in cell migration and cell invasion by about 50% and small changes in cell proliferation and adhesion in T47D breast cancer cells. However, from the qPCR experiment carried out, it is seen that GPNMB and FLRT3 do not regulate one another's expression level. This may possibly indicate that these two downstream molecules of CHST3 work independently of one another and may not have cumulative effects on the evaluated phenotypic behaviors.

In addition, as CHST3 and FLRT3 are observed to have associated functional roles in breast cancer cells, it is appropriate to test their association in human ductal tissues as well. As the same human patient samples were used in both CHST3 and FLRT3 expression studies, analysis was carried out to test both molecules' expression in terms of their correlation with one another. No significant correlation is found between the expression levels of CHST3 and FLRT3 in the breast tissues. An additional tissue expression study in a different Singapore cohort of breast cancer patients should be studied to validate the expression studies carried out. Moreover, an expression study of GPNMB in the Singapore patient cohort diagnosed with IDC should also be performed. This will allow evaluation of the associations of the three molecules (CHST3, FLRT3, and GPNMB) as well as analyses with associated clinicopathological factors. Overall, from the two tissue studies, CHST3 and FLRT3 preliminarily has potential as diagnostic markers when evaluating a patient's malignant ductal tissues and surrounding normal tissues in terms of the epithelial cells' expression levels of CHST3 and FLRT3. Low CHST3 expression is correlated with larger tumor size and higher tumor stage, while high FLRT3 expression is associated with patients with older age and enhanced stage of lymphovascular invasion. This could also potentially lead CHST3 and FLRT3 as diagnostic biomarkers to detect the possibility of the patients having metastasis. However, CHST3 and FLRT3 did not appear to be potential prognostic biomarkers

in breast cancer in this study. No significant association was observed between their expression levels and tumor recurrence or mortality risk. Nevertheless, it is observed that tumor size has prognostic prediction for both tumor recurrence and survival after adjusting for confounding factors.

One factor, however, to be noted from the expression studies in the ductal tissues is that both CHST3 and FLRT3 are not associated to the expression levels of the well-established biomarkers ER, PR, and HER2. Hence, there is the possibility of both CHST3 and FLRT3 being non-associated with particular breast cancer subtypes such as luminal breast cancer (mostly having ER/PR positive statuses) or basal breast cancer type (usually having ER/PR/HER2 negative statuses). This may somewhat explain why ER/PR positive breast cancer cell lines MCF7 and T47D as well as ER/PR negative MDA-MB-231 breast cancer cells display similar extensity of changes when CHST3 expression is affected.

One common signaling pathway that CHST3, GPNMB, and FLRT3 have is the MAPK signaling cascade. GPNMB has been shown to be enhanced of its expression level in breast cancer tissues (Rose et al., 2010, Rose et al., 2007), of which its up-regulated expression level and aggressive phenotype features have been associated with increasing tumor grade of the breast tissues and enhanced MAPK signaling (Vaklavas et al., 2013). In the case of regulation through *FLRT3*, its effect has been observed in regulating cell migration and adhesion in Xenopus tissues. Upon Tgfβ signaling induction, Flrt3 co-expresses with Fgf12 growth factor to activate Mapk signaling cascade (Karaulanov et al., 2006, Chen et al., 2009b). Hence, it is possible that CHST3 together with GPNMB and FLRT3 have a role to play in the MAPK signaling pathway. Further studies will be needed to investigate whether there are associations between CHST3, GPNMB, FLRT3 and MAPK-related molecules as well as whether the molecules are upstream or downstream of CHST3, GPNMB, and FLRT3.

4.1.3 Potential Regulatory Role of CHST3 through Other Pathways

EMT is an important event during embryogenesis and normal development (Thiery et al., 2009). However, EMT also takes place in tumor progression during late cancer stages, promoting metastases and treatment resistance (Polyak and Weinberg, 2009). It involves the detachment of tumor cells from the primary tumor site, whereby intercellular contacts are disrupted and cell motility is enhanced. The progression of the epithelial cell phenotype to mesenchymal phenotype would allow tumor cell invasion and migration allowing metastases and secondary tumor site formation (Guarino et al., 2007, Simic et al., 2013). Also, the transformed epithelial cells would adopt capabilities resisting cell apoptosis to allow increased survivability of the transformed tumor cells (Hanahan and Weinberg, 2000).

Nadanaka et al showed that either the exogenous treatment of CSE or regulation of CSE levels via modulating CHST11 expression has a downstream effect in reducing β-catenin expression levels (Nadanaka et al., 2011). In this study, through immunofluorescence observations, EMT markers (E-cadherin and β-catenin) were observed to be down-regulated after silencing of *CHST3* in T47D cells. These corroborate with the phenotypic behavior changes, promoting metastatic-like events and cell invasion in the breast cancer cells studied.

Transforming growth factor-β (TGFβ) that is up-regulated as observed from the microarray study and other growth factors (such as midkine (MK) and fibroblast growth factor 2 (FGF2)) are involved in initiating extensive crosstalk and feedback control of different gene expression levels (Lamouille and Derynck, 2007, Wang et al., 2010c). In breast cancer cells, FGF2 is observed to down-regulate E-cadherin via the activation of MAPK signaling pathway (Lau et al., 2013, Pece and Gutkind, 2000). In the example of MK, it decreases epithelial markers E-cadherin and β-catenin, through activation of downstream molecule neurogenic locus notch homolog protein 2 (NOTCH2) (Huang et al., 2008a, Huang et al., 2008b). Additionally, transcription factor Wilms' tumor suppressor gene (WT1), which is

down-regulated by 2.07 folds in the microarray study, regulates expression level of E-cadherin (Hosono et al., 2000, Brett et al., 2013, Morrison et al., 2008). Moreover, WT1 is regulated by MK via MK's binding site for WT1 (Adachi et al., 1996) of which the over-expression of MK down-regulates WT1 (Konishi et al., 1999). Hence, MK and other growth factors may potentially be upstream of *CHST3*, initiating various EMT markers (E-cadherin and β-catenin) and intermediary molecules (MAPK, NOTCH2, and WT1).

The EMT process also includes the survival capability of tumor cells which is vital for the cells to migrate, invade, and to grow a distant secondary tumor successfully. Cell proliferation, from this study's observations, may possibly be non-biogically important in terms of *CHST3* functional roles in breast cancer cells, due to the small changes observed after regulating *CHST3*. The change in cell death, while slightly more in extent compared to cell proliferation change, is still considerably small and may only be a minor functional role comparing with that in cell migration and invasion. Pro-apoptotic BAD was also observed to be slightly increased of its deactivated protein form after silencing of *CHST3*, indicating *CHST3* has some potentiality to regulate cell survival through BAD and thereafter caspase 3/7 pathway. Growth factors such as TGFβ and FGF2 (Dufour et al., 2008) are also key molecules in this case for EMT. The growth factors signal transducts mitogen activated protein kinase (MAPK) signaling pathways, of which the activated MAPK pathway will phosphorylate pro-apoptotic BAD protein, prohibiting mitochondrial death cascade, promoting cell survival and EMT event (Lahiry et al., 2010, Suman et al., 2012). These provide insight to possibilities in the CHST3 pathway. Further studies will be needed to evaluate the signaling order of CHST3 pathway, possibly starting from the signal transducting growth factors to intermediary molecules stated.

4.1.4 Potential Role of CHST3 through Non-Enzymatic Activity Role

To be noted, the phenotypic behavior observations in this study should be analyzed with caution of their source of regulation, which remains uncertain at this point in time. To elaborate, even after down-regulating *CHST3* in the breast cancer cells, it is uncertain whether the phenotypic changes were due to the active CHST3 molecule itself or changes in level/sulfation pattern of CHST3's known substrate, 6-O-sulfated CS. The phenotypic changes observed in this study could be due to the fact that *CHST3* had modulated the cellular behavior changes through sulfation at the carbon 6 of galactosamine of CS. In laryngeal cancer, an association was observed whereby both *CHST3* and C-6 sulfation of galactosamine were shown to decrease as tumor stage increases (Kalathas et al., 2010). Hence, the difference in levels of C6S molecules would affect cell signaling behavior through different binding of ligands such as growth factors, cytokines, and apoptotic factors. On the other hand, *CHST3* may have enzymatic activity-independent function that regulates breast cancer cell behaviors. To elaborate, *CHST3* may regulate cancer cell behaviors via upstream or downstream molecular targets such as *GPNMB* and *FLRT3*, without having to pass through the effect of C-6 sulfation level. Heparanase is of one example of a GAG-related enzyme that has enzymatic activity-independent function (Kessenbrock et al., 2010). It is has been known to be involved in degradation of heparan sulfate. Studies however showed that heparanase also exhibit non-enzymatic related activities that are independent of its involvement in the degradation of heparan sulfate (Levy-Adam et al., 2010). Amongst such activities include stimulating AKT signaling pathway, enhancing PI3K-dependent cell migration and up-regulating VEGF, all of which are involved in cancer metastasis and angiogenesis (Ilan et al., 2006, Vlodavsky et al., 2007a, Vlodavsky et al., 2007b). To address this, the effect of C-6 sulfation can be investigated by treating breast cancer cells with C6S, prior to carrying out the phenotypic assays. Changes observed and caused by C6S in the assays would be compared to the changes obtained from regulating *CHST3*. This would hence allow observations as of whether *CHST3* has indeed enzymatic activity-independent

functions in breast cancer. For now, one should look at the potential signaling pathways that CHST3 may be involved in such as the follows.

4.2 Regulation of CHST3 Expression

As downstream targets like GPNMB and FLRT3 of CHST3 pathway have been identified, it is also important to evaluate potential upstream molecules that may regulate *CHST3* expression, hence giving rise to the phenotypic behavioral changes observed. As the focus in this study tended towards the downstream molecules of CHST3 regulation, one may hypothesize on the possible upstream molecules that can regulate CHST3 expression and functions.

4.2.1 Regulation by Ligands

Studies have determined the interactions of growth factors and cytokines with CSPGs at the cell surface. One likely mechanism *CHST3* may regulate and may be regulated is through the interaction and effect of different ligands at the cell surface level, which in turn stimulate different signaling pathways, affecting its expression level. TGFβ, in this study, has shown up-regulated expression level of 4.37 folds after down-regulation of *CHST3*. TGFβ, in breast cancer, has been controversial. One analysis showed that high TGFβ expression in breast cancer patients is associated with better prognosis than those with low TGFβ expression level. However, some studies have depicted the opposite whereby the overexpression of TGFβ is correlated with worse prognosis and associated with metastatic events (Kubiczkova et al., 2012).

Nevertheless, in the case of CHST3, the variation in levels of ligands such as TGFβ can affect the composition of cell surface CS expression, which in turn can potentially lead to altered regulation of CHST3 expression and carbon-6 sulfation pattern. In human arterial cells, TGFβ was observed to stimulate the synthesis of C4S and C6S (Chen et al., 1991), and regulate CHST11 or chondroitin-4-

sulfotransferase 1 (Kluppel et al., 2012), suggesting higher possibility that TGFβ is upstream of CHST3. Additionally, TGFβ can regulate the expression levels of CSPGs such as neurocan and brevican, as seen *in vitro* in astrocytes that were treated with TGFβ. It has been suggested by the research group that TGFβ may regulate CSPG expression via the PI3K-AKT-mTOR pathway (Jahan and Hannila, 2015). Perhaps, similar to heparanase, CHST3 may exert part of its role through this pathway, bringing rise to regulation of cell migration Hence, TGFβ can affect both CS chains and CSPGs which in turn will have an effect on CHST3 and cellular behaviors.

Another example will be the association of CSPG (lumican) with TGFβ. In acute lung injury, reduced expression of lumican is associated with enhanced levels of TGFβ, affecting its downstream molecules E-cadherin and β-catenin by reducing their expression levels (Li et al., 2013). Syndecan 4 proteoglycan, in breast cancer, is able to bind to FGF2 at the cell surface and promote FGF signaling pathway (Mundhenke et al., 2002). Therefore, CHST3 expression may potentially be regulated by CS and CSPG pool at the cell surface level, which affects ligands such as MK, TGFβ, and FGF2 that subsequently affects their downstream molecules, one of which may be CHST3. Also, as CHST11 and lumican proteoglycan are both associated with TGFβ and (for the latter molecule) associated with effect on biomarkers E-cadherin and β-catenin, this raises the possibility of CHST3 as well as CHST11 and lumican to be involved in the metastatic events.

In the EMT signaling pathway, as mentioned, TGFβ is upstream of E-cadherin and β-catenin (both molecules' expression level decreased after silencing of *CHST3*), causing loss of E-cadherin-β-catenin complexes at the cell membrane and re-localization of β-catenin to the cytosol and nucleus (Ma et al., 2010, Onder et al., 2008, Prasad et al., 2009). This will in turn cause loss of cell-cell junctions (adhesion), re-organization of the actin cytoskeleton, leading to cells turning spindle-like mesenchymal in morphology (Huber et al., 2005), and hence promoting further EMT-inducing stimuli, cell invasion and migration (Guarino et

al., 2007). Cytokine midkine is also a potential upstream molecule of CHST3 considering downstream molecules of MK studied (E-cadherin, β-catenin, and WT1) are affected in its signaling pathway. Another cytokine that has potentiality to be upstream of CHST3 is interferon-gamma (IFNγ). IFNγ has been reported to have tumor suppressing effects such as inhibition of cell proliferation in breast cancer cells. In an IHC study, the expression level of IFNγ was observed to be higher in in situ carcinoma against benign and infiltrating tumors (Garcia-Tunon et al., 2007). In skin fibroblasts, enhanced levels of IFNγ were found to down-regulate 4-O-sulfation and up-regulate 6-O-sulfation of CS chains (Praillet et al., 1996). This suggests the possibility of IFNγ regulating the expression level of CHST3, which subsequently affects the sulfation pattern type of the CS chains and thereafter the cellular behaviors.

From another perspective, CS sulfation pattern may affect potential upstream molecule such as MK, to subsequently have an effect in regulating CHST3. MK has been evaluated to have strong affinity to CS proteoglycans such as versican, CSPG4, and syndecans (Nakanishi et al., 1997, Zou et al., 2000, Ichihara-Tanaka et al., 2006) via their CS chains particularly tumor promoting CSE units (Muramatsu, 2010). Removal of the CS chain from the proteoglycans reduces binding of the proteoglycans to MK, which may affect the subsequent signaling pathway and CHST3 pathway.

4.2.2 Regulation at Gene Expression Level

Gene expression can be modulated at various steps; one of which include epigenetic regulation (e.g. methylation and acetylation). The expression of a gene can be highly dependent on its epigenetic regulation (Bergmann 2012). Epigenetic mechanisms define mitotically heritable differences in gene expression potential without changing the DNA sequence. These epigenetic changes can occur due to random mutation or environmental factors. Some examples of epigenetic marks include DNA methylation and chromatin modifications through histone acetylation

(Inbar-Feigenberg 2013). In general, DNA methyltransferases (DNMT) catalyze the methylation of cytosine to 5-methylcytosine. DNA methylation is able to cause failure in binding of a protein such as a transcription factor to its cognate DNA sequence, resulting in repression of tumor suppressor genes and enhancement of tumor promoter genes (Bird 2002). 5-aza-2'-deoxycytidine (5-AZA) is a DNMT inhibitor, capable of reversing promoter hypermethylation in cancers (Palii 2008).

Histone acetylation, on the other hand, is regulated by the antagonistic actions of two families of enzymes, namely histone acetyltransferases (HATs) and histone deacetylases (HDACs) (Haberland 2009). Catalyzed by HATs, histone acetylation involves the transfer of an acetyl group to the ε-amino group of lysine residues in N-terminal histone tail. This neutralizes the positive charge of lysine residues, weakens the charge-dependent interactions between histones and DNA, and hence relaxes the chromatin structure for transcription initiation (Feigenberg 2013 and Bannister 2011). In an opposing manner, histone deacetylation can occur catalyzed by HDACs, condensing the chromatin structure and repressing gene expression (Haberland 2009). Trichostatin A (TSA) is an antifungal antibiotic, used to inhibit HDAC and thereby restoring gene transcription (Dokmanovic 2007).

Initial evaluation of *CHST3* expression from Gene Expression Omnibus (GEO) microarray databases has shown little changes in *CHST3* expression level after treatment of either 5-AZA or TSA on various breast cancer cell lines (T47D, MCF7, and MDA-MB-231) (Dedeurwaerder et al., 2011, Sun et al., 2009). Till further validation is carried out, this initial literature review currently suggest that *CHST3* expression level is not regulated through epigenetic regulation methylation or acetylation.

Apart from epigenetic regulation, gene expression can also be regulated at the transcription level by transcription factors, defined as regulatory proteins that activate, or at times, inhibit, DNA transcription through their binding to specific DNA sequences, hence promoting or inhibiting gene expression (Phillips, 2008).

The binding of transcription factors to the DNA is the fundamental step to regulating gene expression. A certain transcription factor bound at a site can regulate genes that are of close proximity and possibly those that are further away with the aid of enhancers. A number of transcription factor-related genes (as shown in Table 4.1) have been noted from the microarray in this study. Though the change in expression of the genes were affected after down-regulation of *CHST3,* further evaluation is necessary to determine if the affected genes regulate *CHST3* expression in the transcription as well as translation processes, and whether the genes are upstream or downstream of *CHST3*. Future experiments such as chromatin immunoprecipitation (ChIP) can be performed to evaluate the genes affected by particular transcription factor binding sites (Maienschein-Cline et al., 2012).

Table 4.1 Potential transcription factors regulating *CHST3*

Gene	Changes after Silencing of *CHST3*	Fold Change	Function
ELK3	Down-regulated	4.15	• Member of the ETS-domain transcription factor and ternary complex factor (TCF) • Activates transcription when Ras is present
DPY30	Down-regulated	3.86	• Member of the MLL1/MLL complex • Role in methylation of histone for transcriptional activation
PRIM2	Down-regulated	2.62	• Subunit of DNA primase • Role in DNA replication, specifically to aid in synthesizing small RNA primers to create Okazaki fragments
LARS	Down-regulated	2.62	• Member of the tRNA synthetase family • Role in catalysing ATP-dependent ligation of leucine to tRNA (Leucine)
EIF2S1	Down-regulated	2.27	• A translation initiation factor • Role in catalysing protein synthesis

			• Role in promoting binding of tRNA to 40S ribosomal subunits
MBNL	Down-regulated	2.12	• Role in pre-mRNA alternative splicing regulation
HIPK1	Down-regulated	2.08	• Member of the HIPK subfamily • Member of the Ser/Thr family of protein kinases • Role in phosphorylating homeodomain of transcription factors
EIF3J	Down-regulated	2.08	• Member of the eukaryotic initiation factor 3 complex • Role in translation initiation • Role in recruiting mRNA and protein components to 40S ribosome
WT1	Down-regulated	2.07	• Consists of a DNA-binding domain • Regulates other genes' expression and activity through binding to specific regions of the DNA
MCM10	Down-regulated	2.05	• Member of the mini-chromosome maintenance proteins (MCM) • Role in initiation of genome replication • Role in formation of replication forks
DICER1	Up-regulated	2.01	• Role in production of miRNA • miRNA regulates gene expression via inhibition of the protein production process

4.3 Proposed CHST3 Pathway

Putting everything together, the evaluations in this study are of importance in terms of diagnosis and treatment response in breast cancer. A CHST3 pathway (as shown in Figure 4.1) was hence proposed based on the regulated genes picked up from the microarray as well as from candidate proteins potentially involved in the phenotypic behavior changes observed after modulation of *CHST3* in breast cancer cells.

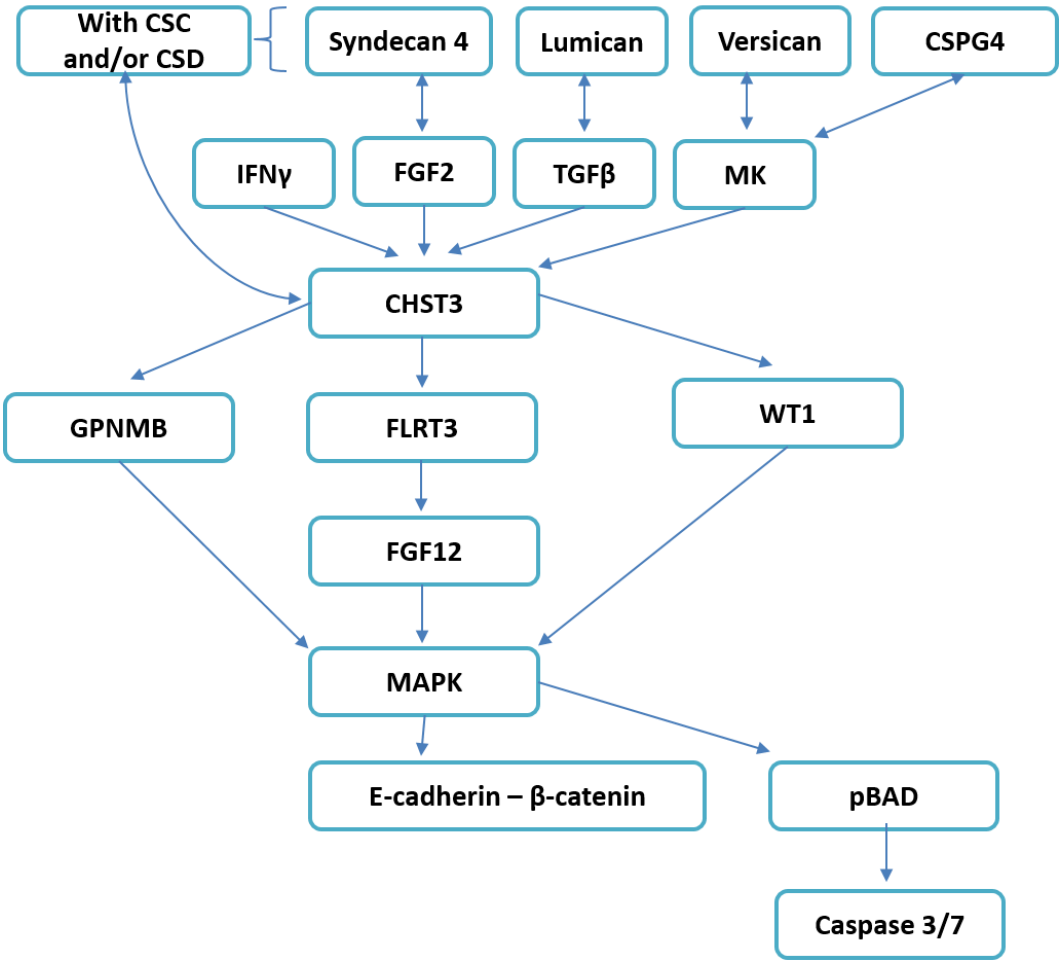

Figure 4.1: Proposed *CHST3* pathway in breast cancer.

4.4 Limitations in Study

4.4.1 Evaluation of CHST3 and CHST7 Functional Activities

It should be noted that CHST3 and CHST7 functional activities were not evaluated in this study. Hence, it remains unclear whether the down-regulation of *CHST3* led to a decrease in 6-O-sulfation of CS. High performance liquid chromatography (HPLC) to determine CS content should be carried out after silencing or over-expressing *CHST3*. Also, it is also uncertain whether CHST7 is functionally active and has compensated for the loss of CHST3 functional role. An enzyme activity assay needs to be performed to evaluate the functional activities of CHST3 and CHST7 after silencing or over-expressing *CHST3*.

4.4.2 Evaluation with Clinical Samples and Animal Models

In the tissue expression study, 218 cases were analyzed of the expression levels of CHST3 and FLRT3 with the various clinicopathological parameters. The preliminary analyses give a sense of the expression levels of both molecules in human ductal tissues and whether they are associated with any of the clinicopathological parameters. One should evaluate the associations using a larger patient sample size as well as a different cohort of patients diagnosed with IDC. Additionally, it is important to extend the investigation to animal models, such as to evaluate if an overexpression of *CHST3* in the cancer cells of the animal model will suppress cell migration or cell growth.

4.4.3 Evaluation using Different Assays

In experimental cell biology, phenotypic behaviors can be investigated via various methods depending on the objectives of the study. Through different methods, one is able to better understand the cellular behaviors of breast cancer cells upon regulation of *CHST3*. For cell migration in this study, the focus was on using a filter-assay method (transwell membrane chambers) to measure cell migration towards chemoattractant FBS. Other types of migration assays can also be carried

out such as (i) random walk assay which evaluates the rate of random motion of the cells that are sparsely distributed on a matrix-coated surface, (ii) wound healing assay that evaluates quantification and characterization of collective cell motility by measuring the wound geometry after a gentle wound scratch through a confluent cell monolayer, and (iii) cell-populated agarose drop which characterizes cell motility on various extracellular substrates by trapping cells within an agarose group, in which the cells will diffuse progressively out from the drop onto the surrounding extracellular substrate (Rosello et al., 2004).

Evaluation of cell proliferation was performed using MTS solution, a quantitative colorimetric assay that measures enzyme activity of mitochondrial dehydrogenase reflecting the metabolic status of a cell. Therefore, the absorbance change in color of the MTS solution is proportional to the number of metabolically active cells. Though simple and rapid, there must be precaution in concluding cell proliferation observations done using indirect measuring methods. MTS assay is sensitive towards cell size, hence there can be an increase in cell size without any cell division (Mosmann, 1983). More direct methods require measurements of DNA synthesis or cell division or cell number itself. Flow cytometry using propidium iodide and detergent-based method was also hence performed in this study to further evaluate cell growth and cell death based on the cellular DNA contents and cell cycle phases (Nunez, 2001). Other methods include 5-bromo-2'-deoxyuridine (BrdU) that specifically label DNA with a precursor molecule. BrdU can be detected through immunocytochemistry using an anti-BrdU antibody that labels the nuclei. Results will be generated based on the quantification of stained nuclei in different random fields (Gratzner, 1982, Waldman et al., 1991). Apart from BrdU, cells can also be immunostained with proliferation markers such as Ki-67 and proliferating cell nuclear antigen (PCNA) (Scholzen and Gerdes, 2000, Hughes and Mehmet, 2003). Cell proliferation can also be measured at its membrane integrity state through the usage of chemicals like trypan blue. A healthy viable cell with intact cell membrane will prevent trypan blue from entering the cell membrane. On the other hand, a dying or dead cells will allow trypan blue to enter their cell

membrane. The number of unstained viable cells hence can be counted manually or via an automated cell counter, making it less labor-intensive (Hughes and Mehmet, 2003).

As for cell adhesion, it is a complex cellular process involving various types of interactions, including cell-cell interactions, cell-matrix interactions, and cell receptor-ligand binding. In this study, adhesion assay (static cell-matrix attachment method) was used to evaluate the ability of the cancer cells to adhere to an adhesive substrate (collagen or fibronectin) (Kucik and Wu, 2005, Humphries, 2009). As the washing protocol is the most critical for cell-attachment method, the number of washing cycles had been optimized (Kueng et al., 1989). Also, to have an estimation for 100% cell attachment, unwashed wells containing cells attached to an adhesive substrate were measured by their absorbance level using MTS solution . It should also be noted that cell number was quantified using metabolic measuring MTS solution. In addition, as washing was carried out through manual pipetting, adhesion assay with hands-free agitation can be performed, that is placing the coated 96-well plate containing cell suspension on a shaker with mild rotation (100rpm) for 30 minutes (Mathieu and El-Battari, 2003)

CHAPTER 5
CONCLUSION AND FUTURE WORK

5 CONCLUSION AND FUTURE WORK

Biomarkers have been making their mark in cancer history in the last decades, having important roles in regulating signaling pathways involved in tumor progression. Some of the biomarkers have progressed to become diagnostic, prognostic, and/or therapeutic markers in breast cancer as well as other malignancies. This has led to improved early detection of breast cancer as well as better decision-making in administering the optimal personalized treatment. Today, more efforts are being made to achieve the "personalized medicine" vision. Developing biomarkers in breast cancer is one way to characterize a tumor's sensitivity towards a particular form of therapy and to improve diagnosis as well as prognosis estimation for the patients.

This study has unraveled the first insights of *CHST3* and its function as well as its clinical relevance in breast cancer. From the *in vitro* study, it was shown that CHST3 plays a tumor suppressor role, of which higher expression of CHST3 reduces cell migration, invasion, and proliferation as well as increases cell adhesion and cell apoptosis of breast cancer cells. In the immunohistochemical analysis, CHST3 was found to be down-regulated in invasive ductal tissues compared to normal ductal tissues. From this study, CHST3 shows potential to be diagnostic biomarker, but not a prognostic biomarker as no associations were obtained from the survival analyses. Genome wide microarray analysis revealed a list of genes altered after down-regulating *CHST3* in breast cancer cells. From the list of genes, two selected genes, *GPNMB* and *FLRT3* had significant importance in the *CHST3* pathway, whereby both genes are downstream molecules of *CHST3* in breast cancer. FLRT3 was also found to be a potential diagnostic biomarker as it is up-regulated of its expression in malignant ductal tissue compared to normal ductal tissue. Additionally, alteration in *CHST3* expression affected the E-cadherin/β-catenin, and apoptotic (BAD) pathways.

The findings from this study are of considerable significance as an interesting gene, *CHST3*, has been uncovered to regulate breast cancer cells' behaviors, specifically in the metastatic portion. Nevertheless, further studies should be carried out to fully

understand the functions and molecular pathways of *CHST3* before extending the study to *in vivo* studies as well as other cancers.

The potentiality of CHST3 and FLRT3 as diagnostic biomarkers should also be further evaluated. For example, both biomarkers could be examined in different cancers such as ovarian cancer as well as other breast cancer types such as lobular carcinoma and phyllodes tumor. Additionally, evaluation of the biomarkers should be carried out at the global level. The current study involves the Singaporean breast cancer patient cohort and hence, the two biomarkers should be further tested on other populations to investigate if the correlations observed in this study are consistent in other populations.

Additionally, as mentioned, the phenotypic changes observed in this study could be due to the fact that *CHST3* had modulated the cellular behavior changes through sulfation at the carbon 6 of galactosamine of CS or via its own enzymatic activity-independent role. Therefore, the effect of C-6 sulfation should be investigated by treating breast cancer cells with C6S, prior to carrying out the phenotypic assays. Cellular behavior changes observed and caused by C6S in the assays would then be compared to the alterations obtained from regulating *CHST3*. This would hence allow observations as of whether *CHST3* has indeed enzymatic activity-independent functions in breast cancer. Also, after treating the breast cancer cells with exogenous C6S, the expression levels of the downstream molecules inclusive of *GPNMB*, *FLRT3*, E-cadherin, β-catenin, pBAD as well as the speculated molecules involved in *CHST3* pathway should be evaluated.

6 REFERENCES

ABATI, A. & SIMSIR, A. 2005. Breast fine needle aspiration biopsy: prevailing recommendations and contemporary practices. *Clin Lab Med,* 25**,** 631-54, v.

ABERLE, H., SCHWARTZ, H. & KEMLER, R. 1996. Cadherin-catenin complex: protein interactions and their implications for cadherin function. *J Cell Biochem,* 61**,** 514-23.

ABRAHAMS, P. H., SPRATT, J. D., LOUKAS, M. & VAN SCHOOR, A. N. 2013. *McMinn and Abrahams' Clinical Atlas of Human Anatomy,* China, Elsevier Mosby.

ADACHI, Y., MATSUBARA, S., PEDRAZA, C., OZAWA, M., TSUTSUI, J., TAKAMATSU, H., NOGUCHI, H., AKIYAMA, T. & MURAMATSU, T. 1996. Midkine as a novel target gene for the Wilms' tumor suppressor gene (WT1). *Oncogene,* 13**,** 2197-203.

ALINI, M. & LOSA, G. A. 1991. Partial characterization of proteoglycans isolated from neoplastic and nonneoplastic human breast tissues. *Cancer Res,* 51**,** 1443-7.

AMERICAN CANCER SOCIETY 2011. Global Cancer Facts & Figures 2nd Edition. Atlanta: American Cancer Society.

AMERICAN CANCER SOCIETY 2012a. Breast Cancer Facts & Figures 2011-2012. Atlanta: American Cancer Society.

AMERICAN CANCER SOCIETY. 2012b. Cancer Facts & Figures 2012.

ANDERSON, B. O., YIP, C. H., SMITH, R. A., SHYYAN, R., SENER, S. F., ENIU, A., CARLSON, R. W., AZAVEDO, E. & HARFORD, J. 2008. Guideline implementation for breast healthcare in low-income and middle-income countries: overview of the Breast Health Global Initiative Global Summit 2007. *Cancer,* 113**,** 2221-43.

ANDERSON, W. F., CHU, K. C., CHATTERJEE, N., BRAWLEY, O. & BRINTON, L. A. 2001. Tumor variants by hormone receptor expression in white patients with node-negative breast cancer from the surveillance, epidemiology, and end results database. *J Clin Oncol,* 19**,** 18-27.

ANTONIOU, A., PHAROAH, P. D., NAROD, S., RISCH, H. A., EYFJORD, J. E., HOPPER, J. L., LOMAN, N., OLSSON, H., JOHANNSSON, O., BORG, A., PASINI, B., RADICE, P., MANOUKIAN, S., ECCLES, D. M., TANG, N., OLAH, E., ANTON-CULVER, H., WARNER, E., LUBINSKI, J., GRONWALD, J., GORSKI, B., TULINIUS, H., THORLACIUS, S., EEROLA, H., NEVANLINNA, H., SYRJAKOSKI, K., KALLIONIEMI, O. P., THOMPSON, D., EVANS, C., PETO, J., LALLOO, F., EVANS, D. G. & EASTON, D. F. 2003. Average risks of breast and ovarian cancer associated with BRCA1 or BRCA2 mutations detected in case Series unselected for family history: a combined analysis of 22 studies. *Am J Hum Genet,* 72**,** 1117-30.

ARBOUZOVA, N. I. & ZEIDLER, M. P. 2006. JAK/STAT signalling in Drosophila: insights into conserved regulatory and cellular functions. *Development,* 133**,** 2605-16.

ARNONE, P., ZURRIDA, S., VIALE, G., DELLAPASQUA, S., MONTAGNA, E., ARNABOLDI, P., INTRA, M. & VERONESI, U. 2010. The TNM classification of breast cancer: need for change. *Updates Surg,* 62**,** 75-81.

BAI, X., ZHOU, D., BROWN, J. R., CRAWFORD, B. E., HENNET, T. & ESKO, J. D. 2001. Biosynthesis of the linkage region of glycosaminoglycans: cloning and activity of galactosyltransferase II, the sixth member of the beta 1,3-galactosyltransferase family (beta 3GalT6). *J Biol Chem,* 276**,** 48189-95.

BALANIS, N., WENDT, M. K., SCHIEMANN, B. J., WANG, Z., SCHIEMANN, W. P. & CARLIN, C. R. 2013a. Epithelial-to-Mesenchymal Transition Promotes Breast Cancer Progression via a Fibronectin-Dependent Stat3 Signaling Pathway. *J Biol Chem,* 288**,** 17954-67.

BALI, J. P., COUSSE, H. & NEUZIL, E. 2001. Biochemical basis of the pharmacologic action of chondroitin sulfates on the osteoarticular system. *Semin Arthritis Rheum,* 31**,** 58-68.

BASELGA, J., NORTON, L., ALBANELL, J., KIM, Y. M. & MENDELSOHN, J. 1998. Recombinant humanized anti-HER2 antibody (Herceptin) enhances the antitumor activity of paclitaxel and doxorubicin against HER2/neu overexpressing human breast cancer xenografts. *Cancer Res,* 58**,** 2825-31.

BECK, A. H., ESPINOSA, I., GILKS, C. B., VAN DE RIJN, M. & WEST, R. B. 2008. The fibromatosis signature defines a robust stromal response in breast carcinoma. *Lab Invest,* 88**,** 591-601.

BEHERA, R., KUMAR, V., LOHITE, K., KARNIK, S. & KUNDU, G. C. 2010. Activation of JAK2/STAT3 signaling by osteopontin promotes tumor growth in human breast cancer cells. *Carcinogenesis,* 31**,** 192-200.

BERNDTSSON, M., KONISHI, Y., BONNI, A., HAGG, M., SHOSHAN, M., LINDER, S. & HAVELKA, A. M. 2005. Phosphorylation of BAD at Ser-128 during mitosis and paclitaxel-induced apoptosis. *FEBS Lett,* 579**,** 3090-4.

BERNFIELD, M., GOTTE, M., PARK, P. W., REIZES, O., FITZGERALD, M. L., LINCECUM, J. & ZAKO, M. 1999. Functions of cell surface heparan sulfate proteoglycans. *Annu Rev Biochem,* 68**,** 729-77.

BERTO, A. G., SAMPAIO, L. O., FRANCO, C. R., CESAR, R. M., JR. & MICHELACCI, Y. M. 2003. A comparative analysis of structure and spatial distribution of decorin in human leiomyoma and normal myometrium. *Biochim Biophys Acta,* 1619**,** 98-112.

BHARDWAJ, A., FRANKEL, W. L., PELLEGATA, N. S., WEN, P. & PRASAD, M. L. 2008. Intracellular versican expression in mesenchymal spindle cell tumors contrasts with extracellular expression in epithelial and other tumors--a tissue microarray-based study. *Appl Immunohistochem Mol Morphol,* 16**,** 263-6.

BORCZUK, A. C., GORENSTEIN, L., WALTER, K. L., ASSAAD, A. A., WANG, L. & POWELL, C. A. 2003. Non-small-cell lung cancer molecular signatures recapitulate lung developmental pathways. *Am J Pathol,* 163**,** 1949-60.

BOYLE, P. 2005. Breast cancer control: signs of progress, but more work required. *Breast,* 14**,** 429-38.

BRETT, A., PANDEY, S. & FRAIZER, G. 2013. The Wilms' tumor gene (WT1) regulates E-cadherin expression and migration of prostate cancer cells. *Mol Cancer,* 12**,** 3.

BRINTON, L. A., SCHAIRER, C., HOOVER, R. N. & FRAUMENI, J. F., JR. 1988. Menstrual factors and risk of breast cancer. *Cancer Invest,* 6**,** 245-54.

BROWN, L. F., GUIDI, A. J., SCHNITT, S. J., VAN DE WATER, L., IRUELA-ARISPE, M. L., YEO, T. K., TOGNAZZI, K. & DVORAK, H. F. 1999. Vascular stroma formation in carcinoma in situ, invasive carcinoma, and metastatic carcinoma of the breast. *Clin Cancer Res,* 5**,** 1041-56.

BURKE, W. M., JIN, X., LIN, H. J., HUANG, M., LIU, R., REYNOLDS, R. K. & LIN, J. 2001. Inhibition of constitutively active Stat3 suppresses growth of human ovarian and breast cancer cells. *Oncogene,* 20**,** 7925-34.

CAILLEAU, R., OLIVE, M. & CRUCIGER, Q. V. 1978. Long-term human breast carcinoma cell lines of metastatic origin: preliminary characterization. *In Vitro,* 14**,** 911-5.

CANNINGS, E., KIRKEGAARD, T., TOVEY, S. M., DUNNE, B., COOKE, T. G. & BARTLETT, J. M. 2007. Bad expression predicts outcome in patients treated with tamoxifen. *Breast Cancer Res Treat,* 102**,** 173-9.

CECCHI, F., PAJALUNGA, D., FOWLER, C. A., UREN, A., RABE, D. C., PERUZZI, B., MACDONALD, N. J., BLACKMAN, D. K., STAHL, S. J., BYRD, R. A. & BOTTARO, D. P. 2012. Targeted disruption of heparan sulfate interaction with hepatocyte and vascular endothelial growth factors blocks normal and oncogenic signaling. *Cancer Cell,* 22**,** 250-62.

CHAN, P. S., CARON, J. P. & ORTH, M. W. 2005. Effect of glucosamine and chondroitin sulfate on regulation of gene expression of proteolytic enzymes and their inhibitors in interleukin-1-challenged bovine articular cartilage explants. *Am J Vet Res,* 66**,** 1870-6.

CHEN, J. K., HOSHI, H. & MCKEEHAN, W. L. 1991. Stimulation of human arterial smooth muscle cell chondroitin sulfate proteoglycan synthesis by transforming growth factor-beta. *In Vitro Cell Dev Biol,* 27**,** 6-12.

CHEN, L. L., NOLAN, M. E., SILVERSTEIN, M. J., MIHM, M. C., JR., SOBER, A. J., TANABE, K. K., SMITH, B. L., YOUNGER, J. & MICHAELSON, J. S. 2009a. The impact of primary tumor size, lymph node status, and other prognostic factors on the risk of cancer death. *Cancer,* 115**,** 5071-83.

CHEN, X., KOH, E., YODER, M. & GUMBINER, B. M. 2009b. A protocadherin-cadherin-FLRT3 complex controls cell adhesion and morphogenesis. *PLoS One,* 4**,** e8411.

CHIANG, C. W., KANIES, C., KIM, K. W., FANG, W. B., PARKHURST, C., XIE, M., HENRY, T. & YANG, E. 2003. Protein phosphatase 2A dephosphorylation of phosphoserine 112 plays the gatekeeper role for BAD-mediated apoptosis. *Mol Cell Biol,* 23**,** 6350-62.

CHUMSRI, S., HOWES, T., BAO, T., SABNIS, G. & BRODIE, A. 2011. Aromatase, aromatase inhibitors, and breast cancer. *J Steroid Biochem Mol Biol,* 125**,** 13-22.

CLARKE, M., COLLINS, R., DARBY, S., DAVIES, C., ELPHINSTONE, P., EVANS, E., GODWIN, J., GRAY, R., HICKS, C., JAMES, S., MACKINNON, E., MCGALE, P., MCHUGH, T., PETO, R., TAYLOR, C. & WANG, Y. 2005. Effects of radiotherapy and of differences in the extent of surgery for early breast cancer on local recurrence and 15-year survival: an overview of the randomised trials. *Lancet,* 366**,** 2087-106.

COLDITZ, G. A., FESKANICH, D., CHEN, W. Y., HUNTER, D. J. & WILLETT, W. C. 2003. Physical activity and risk of breast cancer in premenopausal women. *Br J Cancer,* 89**,** 847-51.

COLLABORATIVE GROUP ON HORMONAL FACTORS IN BREAST CANCER 1996. Breast cancer and hormonal contraceptives: collaborative reanalysis of individual data on 53 297 women with breast cancer and 100 239 women without breast cancer from 54 epidemiological studies. Collaborative Group on Hormonal Factors in Breast Cancer. *Lancet,* 347**,** 1713-27.

COLLABORATIVE GROUP ON HORMONAL FACTORS IN BREAST CANCER 2001. Familial breast cancer: collaborative reanalysis of individual data from 52 epidemiological studies including 58,209 women with breast cancer and 101,986 women without the disease. *Lancet,* 358**,** 1389-99.

COLLABORATIVE GROUP ON HORMONAL FACTORS IN BREAST CANCER 2012. Menarche, menopause, and breast cancer risk: individual participant meta-analysis, including 118 964 women with breast cancer from 117 epidemiological studies. *Lancet Oncol,* 13**,** 1141-51.

COONEY, C. A., JOUSHEGHANY, F., YAO-BORENGASSER, A., PHANAVANH, B., GOMES, T., KIEBER-EMMONS, A. M., SIEGEL, E. R., SUVA, L. J., FERRONE, S., KIEBER-EMMONS, T. & MONZAVI-KARBASSI, B. 2011. Chondroitin sulfates play a major role in breast cancer metastasis: a role for CSPG4 and CHST11 gene expression in forming surface P-selectin ligands in aggressive breast cancer cells. *Breast Cancer Res,* 13**,** R58.

COWIN, P. & WYSOLMERSKI, J. 2010. Molecular mechanisms guiding embryonic mammary gland development. *Cold Spring Harb Perspect Biol,* 2**,** a003251.

CUNNINGHAM, R. E. 1994. Fluorescent labeling of DNA. *In:* JAVOIS, L. C. (ed.) *Immunocytochemical methods and protocols.* Totowa NJ: Humana Press.

DATTA, S. R., KATSOV, A., HU, L., PETROS, A., FESIK, S. W., YAFFE, M. B. & GREENBERG, M. E. 2000. 14-3-3 proteins and survival kinases cooperate to inactivate BAD by BH3 domain phosphorylation. *Mol Cell,* 6**,** 41-51.

DEDEURWAERDER, S., DESMEDT, C., CALONNE, E., SINGHAL, S. K., HAIBE-KAINS, B., DEFRANCE, M., MICHIELS, S., VOLKMAR, M., DEPLUS, R., LUCIANI, J., LALLEMAND, F., LARSIMONT, D., TOUSSAINT, J., HAUSSY, S., ROTHE, F., ROUAS, G., METZGER, O., MAJJAJ, S., SAINI, K., PUTMANS, P., HAMES, G., VAN BAREN, N., COULIE, P. G., PICCART, M., SOTIRIOU, C. & FUKS, F. 2011. DNA

methylation profiling reveals a predominant immune component in breast cancers. *EMBO Mol Med,* 3**,** 726-41.

DEEKEN, J. F., CORMIER, T., PRICE, D. K., SISSUNG, T. M., STEINBERG, S. M., TRAN, K., LIEWEHR, D. J., DAHUT, W. L., MIAO, X. & FIGG, W. D. 2010. A pharmacogenetic study of docetaxel and thalidomide in patients with castration-resistant prostate cancer using the DMET genotyping platform. *Pharmacogenomics J,* 10**,** 191-9.

DELEHEDDE, M., DEUDON, E., BOILLY, B. & HONDERMARCK, H. 1997. [Proteoglycans and breast cancer]. *Pathol Biol (Paris),* 45**,** 305-11.

DICKSON, R. B., BATES, S. E., MCMANAWAY, M. E. & LIPPMAN, M. E. 1986. Characterization of estrogen responsive transforming activity in human breast cancer cell lines. *Cancer Res,* 46**,** 1707-13.

DOUCET, S., SOUSSIGNAN, R., SAGOT, P. & SCHAAL, B. 2009. The secretion of areolar (Montgomery's) glands from lactating women elicits selective, unconditional responses in neonates. *PLoS One,* 4**,** e7579.

DUBOIS-MARSHALL, S., THOMAS, J. S., FARATIAN, D., HARRISON, D. J. & KATZ, E. 2011. Two possible mechanisms of epithelial to mesenchymal transition in invasive ductal breast cancer. *Clin Exp Metastasis,* 28**,** 811-8.

DUFFY, M. J. 2002. Urokinase plasminogen activator and its inhibitor, PAI-1, as prognostic markers in breast cancer: from pilot to level 1 evidence studies. *Clin Chem,* 48**,** 1194-7.

DUFFY, M. J. 2013. Tumor markers in clinical practice: a review focusing on common solid cancers. *Med Princ Pract,* 22**,** 4-11.

DUFOUR, C., HOLY, X. & MARIE, P. J. 2008. Transforming growth factor-beta prevents osteoblast apoptosis induced by skeletal unloading via PI3K/Akt, Bcl-2, and phospho-Bad signaling. *Am J Physiol Endocrinol Metab,* 294**,** E794-801.

DUMITRESCU, R. G. & COTARLA, I. 2005. Understanding breast cancer risk -- where do we stand in 2005? *J Cell Mol Med,* 9**,** 208-21.

EARLY BREAST CANCER TRIALISTS' COLLABORATIVE GROUP 2005. Effects of chemotherapy and hormonal therapy for early breast cancer on recurrence and 15-year survival: an overview of the randomised trials. *Lancet,* 365**,** 1687-717.

EKAS, L. A., CARDOZO, T. J., FLAHERTY, M. S., MCMILLAN, E. A., GONSALVES, F. C. & BACH, E. A. 2010. Characterization of a dominant-active STAT that promotes tumorigenesis in Drosophila. *Dev Biol,* 344**,** 621-36.

ELLOUMI, F., HU, Z., LI, Y., PARKER, J. S., GULLEY, M. L., AMOS, K. D. & TROESTER, M. A. 2011. Systematic bias in genomic classification due to contaminating non-neoplastic tissue in breast tumor samples. *BMC Med Genomics,* 4**,** 54.

ESCOBAR, P. F., PATRICK, R. J., RYBICKI, L. A., WENG, D. E. & CROWE, J. P. 2007. The 2003 revised TNM staging system for breast cancer: results of stage re-classification on survival and future comparisons among stage groups. *Ann Surg Oncol,* 14**,** 143-7.

ESPINOSA, E., GAMEZ-POZO, A., SANCHEZ-NAVARRO, I., PINTO, A., CASTANEDA, C. A., CIRUELOS, E., FELIU, J. & VARA, J. A. 2012. The present and future of gene profiling in breast cancer. *Cancer Metastasis Rev,* 31**,** 41-6.

FABIAN, C. J. 2007. The what, why and how of aromatase inhibitors: hormonal agents for treatment and prevention of breast cancer. *Int J Clin Pract,* 61**,** 2051-63.

FALO, C., MORENO, A., BENITO, E., LLOVERAS, B., VARELA, M., SERRA, J. M., PRIETO, L., AZPEITIA, D. & ESCOBEDO, A. 2005. Primary chemotherapy with cyclophosphamide, methotrexate, and 5-fluorouracil in operable breast carcinoma. *Cancer,* 103**,** 657-63.

FELDNER, P. C., JR., KATI, L. M., SARTORI, M. G., BARACAT, E. C., RODRIGUES DE LIMA, G., NADER, H. B., DIETRICH, C. P. & GIRAO, M. J. 2006. Sulfated glycosaminoglycans of the periurethral tissue in women with and without stress urinary incontinence, according to genital prolapse stage. *Eur J Obstet Gynecol Reprod Biol,* 126**,** 250-4.

FERLA, R., CALO, V., CASCIO, S., RINALDI, G., BADALAMENTI, G., CARRECA, I., SURMACZ, E., COLUCCI, G., BAZAN, V. & RUSSO, A. 2007. Founder mutations in BRCA1 and BRCA2 genes. *Ann Oncol,* 18 Suppl 6**,** vi93-8.

GABRIEL, C. A. & DOMCHEK, S. M. 2010. Breast cancer in young women. *Breast Cancer Res,* 12**,** 212.

GARCIA-TUNON, I., RICOTE, M., RUIZ, A. A., FRAILE, B., PANIAGUA, R. & ROYUELA, M. 2007. Influence of IFN-gamma and its receptors in human breast cancer. *BMC Cancer,* 7**,** 158.

GARTNER, L. P. & HIATT, J. L. 2007. Female reproductive system. *Color textbook of histology.* Saunders Elsevier.

GEBAUER, G., FEHM, T., LANG, N. & JAGER, W. 2002. Tumor size, axillary lymph node status and steroid receptor expression in breast cancer: prognostic relevance 5 years after surgery. *Breast Cancer Res Treat,* 75**,** 167-73.

GILBERT, M. M., WEAVER, B. K., GERGEN, J. P. & REICH, N. C. 2005. A novel functional activator of the Drosophila JAK/STAT pathway, unpaired2, is revealed by an in vivo reporter of pathway activation. *Mech Dev,* 122**,** 939-48.

GOKMEN-POLAR, Y. & BADVE, S. 2012. Molecular profiling assays in breast cancer: are we ready for prime time? *Oncology (Williston Park),* 26**,** 350-7, 361.

GONG, S. G., MAI, S., CHUNG, K. & WEI, K. 2009. Flrt2 and Flrt3 have overlapping and non-overlapping expression during craniofacial development. *Gene Expr Patterns,* 9**,** 497-502.

GOTTING, C., KUHN, J., ZAHN, R., BRINKMANN, T. & KLEESIEK, K. 2000. Molecular cloning and expression of human UDP-d-Xylose:proteoglycan core protein beta-d-xylosyltransferase and its first isoform XT-II. *J Mol Biol,* 304**,** 517-28.

GRANDE-ALLEN, K. J., OSMAN, N., BALLINGER, M. L., DADLANI, H., MARASCO, S. & LITTLE, P. J. 2007. Glycosaminoglycan synthesis and structure as targets for the prevention of calcific aortic valve disease. *Cardiovasc Res,* 76**,** 19-28.

GRATZNER, H. G. 1982. Monoclonal antibody to 5-bromo- and 5-iododeoxyuridine: A new reagent for detection of DNA replication. *Science,* 218**,** 474-5.

GREINER, M., PFEIFFER, D. & SMITH, R. D. 2000. Principles and practical application of the receiver-operating characteristic analysis for diagnostic tests. *Prev Vet Med,* 45**,** 23-41.

GROSE, R. & DICKSON, C. 2005. Fibroblast growth factor signaling in tumorigenesis. *Cytokine Growth Factor Rev,* 16**,** 179-86.

GUARINO, M., RUBINO, B. & BALLABIO, G. 2007. The role of epithelial-mesenchymal transition in cancer pathology. *Pathology,* 39**,** 305-18.

HAKIM, C. M., GANOTT, M. A., VOGIA, A. & J.H., S. 2012. Breast imaging modalities for pathologists. *In:* DABBS, D. J. (ed.) *Breast pathology.* Saunders Elsevier.

HAMAJIMA, N., HIROSE, K., TAJIMA, K., ROHAN, T., CALLE, E. E., HEATH, C. W., JR., COATES, R. J., LIFF, J. M., TALAMINI, R., CHANTARAKUL, N., KOETSAWANG, S., RACHAWAT, D., MORABIA, A., SCHUMAN, L., STEWART, W., SZKLO, M., BAIN, C., SCHOFIELD, F., SISKIND, V., BAND, P., COLDMAN, A. J., GALLAGHER, R. P., HISLOP, T. G., YANG, P., KOLONEL, L. M., NOMURA, A. M., HU, J., JOHNSON, K. C., MAO, Y., DE SANJOSE, S., LEE, N., MARCHBANKS, P., ORY, H. W., PETERSON, H. B., WILSON, H. G., WINGO, P. A., EBELING, K., KUNDE, D., NISHAN, P., HOPPER, J. L., COLDITZ, G., GAJALANSKI, V., MARTIN, N., PARDTHAISONG, T., SILPISORNKOSOL, S., THEETRANONT, C., BOOSIRI, B., CHUTIVONGSE, S., JIMAKORN, P., VIRUTAMASEN, P., WONGSRICHANALAI, C., EWERTZ, M., ADAMI, H. O., BERGKVIST, L., MAGNUSSON, C., PERSSON, I., CHANG-CLAUDE, J., PAUL, C., SKEGG, D. C., SPEARS, G. F., BOYLE, P., EVSTIFEEVA, T., DALING, J. R., HUTCHINSON, W. B., MALONE, K., NOONAN, E. A., STANFORD, J. L., THOMAS, D. B., WEISS, N. S., WHITE, E., ANDRIEU, N., BREMOND, A., CLAVEL, F., GAIRARD, B., LANSAC, J., PIANA, L., RENAUD, R., IZQUIERDO, A., VILADIU, P., CUEVAS, H. R., ONTIVEROS, P., PALET, A., SALAZAR, S. B., ARISTIZABEL, N., CUADROS, A., TRYGGVADOTTIR, L., TULINIUS, H., BACHELOT, A., LE, M. G., PETO, J., FRANCESCHI, S., LUBIN, F., MODAN, B., RON, E., WAX, Y., FRIEDMAN, G. D., HIATT, R. A., LEVI, F., BISHOP, T., KOSMELJ, K., et al. 2002. Alcohol, tobacco and breast cancer--collaborative reanalysis of individual data from 53 epidemiological studies, including 58,515 women with breast cancer and 95,067 women without the disease. *Br J Cancer,* 87**,** 1234-45.

HANAHAN, D. & WEINBERG, R. A. 2000. The hallmarks of cancer. *Cell,* 100**,** 57-70.

HARALANOVA-ILIEVA, B., RAMADORI, G. & ARMBRUST, T. 2005. Expression of osteoactivin in rat and human liver and isolated rat liver cells. *J Hepatol,* 42**,** 565-72.

HARPER-WYNNE, C., ROSS, G., SACKS, N., SALTER, J., NASIRI, N., IQBAL, J., A'HERN, R. & DOWSETT, M. 2002. Effects of the aromatase inhibitor letrozole on normal breast epithelial cell proliferation and metabolic indices in postmenopausal women: a pilot study for breast cancer prevention. *Cancer Epidemiol Biomarkers Prev,* 11**,** 614-21.

HARRIS, L., FRITSCHE, H., MENNEL, R., NORTON, L., RAVDIN, P., TAUBE, S., SOMERFIELD, M. R., HAYES, D. F. & BAST, R. C., JR. 2007. American Society of Clinical Oncology 2007 update of recommendations for the use of tumor markers in breast cancer. *J Clin Oncol,* 25**,** 5287-312.

HATSELL, S., HIREMATH, M., SHAMAMIAN, P. & COWIN, P. 2005. Molecular, cellular, and developmental biology of breast cancer. *In:* ROSES, D. F. (ed.) *Breast cancer*. Philadelphia: Elsevier.

HEISEY, R. E., CARROLL, J. C., WARNER, E., MCCREADY, D. R. & GOEL, V. 1999. Hereditary breast cancer. Identifying and managing BRCA1 and BRCA2 carriers. *Can Fam Physician,* 45**,** 114-24.

HIRAOKA, N., NAKAGAWA, H., ONG, E., AKAMA, T. O., FUKUDA, M. N. & FUKUDA, M. 2000. Molecular cloning and expression of two distinct human chondroitin 4-O-sulfotransferases that belong to the HNK-1 sulfotransferase gene family. *J Biol Chem,* 275**,** 20188-96.

HIROSE, J., KAWASHIMA, H., YOSHIE, O., TASHIRO, K. & MIYASAKA, M. 2001. Versican interacts with chemokines and modulates cellular responses. *J Biol Chem,* 276**,** 5228-34.

HODA, S. A. 2012. Normal breast and developmental disorders. *In:* DABBS, D. J. (ed.) *Breast pathology.* Elsevier Saunders.

HORTOBAGYI, G. N. 1998. Treatment of breast cancer. *N Engl J Med,* 339**,** 974-84.

HOSONO, S., GROSS, I., ENGLISH, M. A., HAJRA, K. M., FEARON, E. R. & LICHT, J. D. 2000. E-cadherin is a WT1 target gene. *J Biol Chem,* 275**,** 10943-53.

HOWARD, B. A. & GUSTERSON, B. A. 2000. Human breast development. *J Mammary Gland Biol Neoplasia,* 5**,** 119-37.

HOWELLS, C. C., BAUMANN, W. T., SAMUELS, D. C. & FINKIELSTEIN, C. V. 2010. The Bcl-2-associated death promoter (BAD) lowers the threshold at which the Bcl-2-interacting domain death agonist (BID) triggers mitochondria disintegration. *J Theor Biol*.

HUANG, D. 1974. Effect of extracellular chondroitin sulfate on cultured chondrocytes. *J Cell Biol,* 62**,** 881-6.

HUANG, N., ZHU, J., LIU, D., LI, Y. L., CHEN, B. J., HE, Y. Q., LIU, K., MO, X. M. & LI, W. M. 2012. Overexpression of Bcl-2-associated death inhibits A549 cell growth in vitro and in vivo. *Cancer Biother Radiopharm,* 27**,** 164-8.

HUANG, Y., HOQUE, M. O., WU, F., TRINK, B., SIDRANSKY, D. & RATOVITSKI, E. A. 2008a. Midkine induces epithelial-mesenchymal transition through Notch2/Jak2-Stat3 signaling in human keratinocytes. *Cell Cycle,* 7**,** 1613-22.

HUANG, Y., SOOK-KIM, M. & RATOVITSKI, E. 2008b. Midkine promotes tetraspanin-integrin interaction and induces FAK-Stat1alpha pathway contributing to migration/invasiveness of human head and neck squamous cell carcinoma cells. *Biochem Biophys Res Commun,* 377**,** 474-8.

HUBER, M. A., KRAUT, N. & BEUG, H. 2005. Molecular requirements for epithelial-mesenchymal transition during tumor progression. *Curr Opin Cell Biol,* 17**,** 548-58.

HUGHES, D. & MEHMET, H. 2003. *Cell proliferation and apoptosis,* Garland Science.

HULKA, B. S. & MOORMAN, P. G. 2008. Breast cancer: hormones and other risk factors. *Maturitas,* 61**,** 203-13; discussion 213.

HUMPHRIES, M. J. 2009. Cell adhesion assays. *Methods Mol Biol,* 522**,** 203-10.

HUSTON, T. L. 2005. Evaluating and staging the patient with breast cancer. *In:* ROSES, D. F. (ed.) *Breast cancer.* Philadelphia: Elsevier.

ICHIHARA-TANAKA, K., OOHIRA, A., RUMSBY, M. & MURAMATSU, T. 2006. Neuroglycan C is a novel midkine receptor involved in process elongation of oligodendroglial precursor-like cells. *J Biol Chem,* 281**,** 30857-64.

ILAN, N., ELKIN, M. & VLODAVSKY, I. 2006. Regulation, function and clinical significance of heparanase in cancer metastasis and angiogenesis. *Int J Biochem Cell Biol,* 38**,** 2018-39.

IRWIG, L., HOUSSAMI, N. & VAN VLIET, C. 2004. New technologies in screening for breast cancer: a systematic review of their accuracy. *Br J Cancer,* 90**,** 2118-22.

JAHAN, N. & HANNILA, S. S. 2015. Transforming growth factor beta-induced expression of chondroitin sulfate proteoglycans is mediated through non-Smad signaling pathways. *Exp Neurol,* 263**,** 372-84.

JANICKE, F., PRECHTL, A., THOMSSEN, C., HARBECK, N., MEISNER, C., UNTCH, M., SWEEP, C. G., SELBMANN, H. K., GRAEFF, H. & SCHMITT, M. 2001. Randomized adjuvant chemotherapy trial in high-risk, lymph node-negative breast cancer patients identified by urokinase-type plasminogen activator and plasminogen activator inhibitor type 1. *J Natl Cancer Inst,* 93**,** 913-20.

KALATHAS, D., TRIANTAPHYLLIDOU, I. E., MASTRONIKOLIS, N. S., GOUMAS, P. D., PAPADAS, T. A., TSIROPOULOS, G. & VYNIOS, D. H. 2010. The chondroitin/dermatan sulfate synthesizing and modifying enzymes in laryngeal cancer: expressional and epigenetic studies. *Head Neck Oncol,* 2**,** 27.

KARAULANOV, E. E., BOTTCHER, R. T. & NIEHRS, C. 2006. A role for fibronectin-leucine-rich transmembrane cell-surface proteins in homotypic cell adhesion. *EMBO Rep,* 7**,** 283-90.

KEMLER, R. 1993. From cadherins to catenins: cytoplasmic protein interactions and regulation of cell adhesion. *Trends Genet,* 9**,** 317-21.

KESSENBROCK, K., PLAKS, V. & WERB, Z. 2010. Matrix metalloproteinases: regulators of the tumor microenvironment. *Cell,* 141**,** 52-67.

KEYDAR, I., CHEN, L., KARBY, S., WEISS, F. R., DELAREA, J., RADU, M., CHAITCIK, S. & BRENNER, H. J. 1979. Establishment and characterization of a cell line of human breast carcinoma origin. *Eur J Cancer,* 15**,** 659-70.

KIEBER-EMMONS, A. M., JOUSHEGHANY, F. & MONZAVI-KARBASSI, B. 2011. On the role of cell surface chondroitin sulfates and their core proteins in breast cancer metastasis. *In:* GUNDUZ, M. & GUNDUZ, E. (eds.) *Breast cancer - focusing tumor microenvironment, stem cells and metastasis.* InTech.

KIERSZENBAUM, A. L. & TRES, L. L. 2011. *Histology and Cell Biology: An Introduction to Pathology*, Elsevier.

KITAGAWA, H., FUJITA, M., ITO, N. & SUGAHARA, K. 2000. Molecular cloning and expression of a novel chondroitin 6-O-sulfotransferase. *J Biol Chem,* 275**,** 21075-80.

KITAGAWA, H., TONE, Y., TAMURA, J., NEUMANN, K. W., OGAWA, T., OKA, S., KAWASAKI, T. & SUGAHARA, K. 1998. Molecular cloning and expression of glucuronyltransferase I involved in the biosynthesis of the glycosaminoglycan-protein linkage region of proteoglycans. *J Biol Chem,* 273**,** 6615-8.

KLUPPEL, M., SAMAVARCHI-TEHRANI, P., LIU, K., WRANA, J. L. & HINEK, A. 2012. C4ST-1/CHST11-controlled chondroitin sulfation interferes with oncogenic HRAS signaling in Costello syndrome. *Eur J Hum Genet,* 20**,** 870-7.

KNIGHT, C. H. & SORENSEN, A. 2001. Windows in early mammary development: critical or not? *Reproduction,* 122**,** 337-45.

KONISHI, N., NAKAMURA, M., NAKAOKA, S., HIASA, Y., CHO, M., UEMURA, H., HIRAO, Y., MURAMATSU, T. & KADOMATSU, K. 1999. Immunohistochemical analysis of midkine expression in human prostate carcinoma. *Oncology,* 57**,** 253-7.

KONTZOGLOU, K., PALLA, V., KARAOLANIS, G., KARAISKOS, I., ALEXIOU, I., PATERAS, I., KONSTANTOUDAKIS, K. & STAMATAKOS, M. 2013. Correlation between Ki67 and breast cancer prognosis. *Oncology,* 84**,** 219-25.

KOSSOFF, G., FRY, E. K. & JELLINS, J. 1973. Average velocity of ultrasound in the human female breast. *J Acoust Soc Am,* 53**,** 1730-6.

KUBICZKOVA, L., SEDLARIKOVA, L., HAJEK, R. & SEVCIKOVA, S. 2012. TGF-beta - an excellent servant but a bad master. *J Transl Med,* 10**,** 183.

KUCIK, D. F. & WU, C. 2005. Cell-adhesion assays. *Methods Mol Biol,* 294**,** 43-54.

KUENG, W., SILBER, E. & EPPENBERGER, U. 1989. Quantification of cells cultured on 96-well plates. *Anal Biochem,* 182**,** 16-9.

KUSCHE-GULLBERG, M. & KJELLEN, L. 2003. Sulfotransferases in glycosaminoglycan biosynthesis. *Curr Opin Struct Biol,* 13**,** 605-11.

LAHIRY, L., SAHA, B., CHAKRABORTY, J., ADHIKARY, A., MOHANTY, S., HOSSAIN, D. M., BANERJEE, S., DAS, K., SA, G. & DAS, T. 2010. Theaflavins target Fas/caspase-8 and Akt/pBad pathways to induce apoptosis in p53-mutated human breast cancer cells. *Carcinogenesis,* 31**,** 259-68.

LAMOUILLE, S. & DERYNCK, R. 2007. Cell size and invasion in TGF-beta-induced epithelial to mesenchymal transition is regulated by activation of the mTOR pathway. *J Cell Biol,* 178**,** 437-51.

LAU, M. T., SO, W. K. & LEUNG, P. C. 2013. Fibroblast growth factor 2 induces E-cadherin down-regulation via PI3K/Akt/mTOR and MAPK/ERK signaling in ovarian cancer cells. *PLoS One,* 8**,** e59083.

LESJAK, M. S. & GHOSH, P. 1984. Polypeptide proteinase inhibitor from human articular cartilage. *Biochim Biophys Acta,* 789**,** 266-77.

LEVY-ADAM, F., ILAN, N. & VLODAVSKY, I. 2010. Tumorigenic and adhesive properties of heparanase. *Semin Cancer Biol,* 20**,** 153-60.

LI, L. F., CHU, P. H., HUNG, C. Y., KAO, W. W., LIN, M. C., LIU, Y. Y. & YANG, C. T. 2013. Lumican regulates ventilation-induced epithelial-mesenchymal transition through extracelluar signal-regulated kinase pathway. *Chest,* 143**,** 1252-60.

LING, X., SPAETH, E., CHEN, Y., SHI, Y., ZHANG, W., SCHOBER, W., HAIL, N., JR., KONOPLEVA, M. & ANDREEFF, M. 2013. The CXCR4 antagonist AMD3465 regulates oncogenic signaling and invasiveness in vitro and prevents breast cancer growth and metastasis in vivo. *PLoS One,* 8**,** e58426.

LIVAK, K. J. & SCHMITTGEN, T. D. 2001. Analysis of relative gene expression data using real-time quantitative PCR and the 2(-Delta Delta C(T)) Method. *Methods,* 25**,** 402-8.

LO, S. L., THIKE, A. A., TAN, S. Y., LIM, T. K., TAN, I. B., CHOO, S. P., TAN, P. H., BAY, B. H. & YIP, G. W. 2011. Expression of heparan sulfate in gastric carcinoma and its correlation with clinicopathological features and patient survival. *J Clin Pathol,* 64**,** 153-8.

LOGING, W. T., LAL, A., SIU, I. M., LONEY, T. L., WIKSTRAND, C. J., MARRA, M. A., PRANGE, C., BIGNER, D. D., STRAUSBERG, R. L. & RIGGINS, G. J. 2000. Identifying potential tumor markers and antigens by database mining and rapid expression screening. *Genome Res,* 10**,** 1393-402.

LOOK, M., VAN PUTTEN, W., DUFFY, M., HARBECK, N., CHRISTENSEN, I. J., THOMSSEN, C., KATES, R., SPYRATOS, F., FERNO, M., EPPENBERGER-CASTORI, S., FRED SWEEP, C. G., ULM, K., PEYRAT, J. P., MARTIN, P. M., MAGDELENAT, H., BRUNNER, N., DUGGAN, C., LISBOA, B. W., BENDAHL, P. O., QUILLIEN, V., DAVER, A., RICOLLEAU, G., MEIJER-VAN GELDER, M., MANDERS, P., EDWARD FIETS, W., BLANKENSTEIN, M., BROET, P., ROMAIN, S., DAXENBICHLER, G., WINDBICHLER, G., CUFER, T., BORSTNAR, S., KUENG, W., BEEX, L., KLIJN, J.,

O'HIGGINS, N., EPPENBERGER, U., JANICKE, F., SCHMITT, M. & FOEKENS, J. 2003. Pooled analysis of prognostic impact of uPA and PAI-1 in breast cancer patients. *Thromb Haemost,* 90**,** 538-48.

LOVE, S. M. & BARSKY, S. H. 2004. Anatomy of the nipple and breast ducts revisited. *Cancer,* 101**,** 1947-57.

LU, L., ZHOU, D., JIANG, X., SONG, K., LI, K. & DING, W. 2012. Loss of E-cadherin in multidrug resistant breast cancer cell line MCF-7/Adr: possible implication in the enhanced invasive ability. *Eur Rev Med Pharmacol Sci,* 16**,** 1271-9.

LYNCH, P. J. & JAFFE, C. C. 2007. Breast anatomy normal scheme. Wikimedia Commons.

MA, L., YOUNG, J., PRABHALA, H., PAN, E., MESTDAGH, P., MUTH, D., TERUYA-FELDSTEIN, J., REINHARDT, F., ONDER, T. T., VALASTYAN, S., WESTERMANN, F., SPELEMAN, F., VANDESOMPELE, J. & WEINBERG, R. A. 2010. miR-9, a MYC/MYCN-activated microRNA, regulates E-cadherin and cancer metastasis. *Nat Cell Biol,* 12**,** 247-56.

MAIENSCHEIN-CLINE, M., ZHOU, J., WHITE, K. P., SCIAMMAS, R. & DINNER, A. R. 2012. Discovering transcription factor regulatory targets using gene expression and binding data. *Bioinformatics,* 28**,** 206-13.

MANJILI, M. H., NAJARIAN, K. & WANG, X. Y. 2012. Signatures of tumor-immune interactions as biomarkers for breast cancer prognosis. *Future Oncol,* 8**,** 703-11.

MASOOD, S. & DABBS, D. J. 2012. Patient safety in breast pathology. *In:* DABBS, D. J. (ed.) *Breast pathology.* Saunders Elsevier.

MATHIEU, S. & EL-BATTARI, A. 2003. Monitoring E-selectin-mediated adhesion using green and red fluorescent proteins. *J Immunol Methods,* 272**,** 81-92.

MAUPIN, K. A., SINHA, A., EUGSTER, E., MILLER, J., ROSS, J., PAULINO, V., KESHAMOUNI, V. G., TRAN, N., BERENS, M., WEBB, C. & HAAB, B. B. 2010. Glycogene expression alterations associated with pancreatic cancer epithelial-mesenchymal transition in complementary model systems. *PLoS One,* 5**,** e13002.

MCTIERNAN, A., RAJAN, K. B., TWOROGER, S. S., IRWIN, M., BERNSTEIN, L., BAUMGARTNER, R., GILLILAND, F., STANCZYK, F. Z., YASUI, Y. & BALLARD-BARBASH, R. 2003. Adiposity and sex hormones in postmenopausal breast cancer survivors. *J Clin Oncol,* 21**,** 1961-6.

MEYER, J. S., ALVAREZ, C., MILIKOWSKI, C., OLSON, N., RUSSO, I., RUSSO, J., GLASS, A., ZEHNBAUER, B. A., LISTER, K. & PARWARESCH, R. 2005. Breast carcinoma malignancy grading by Bloom-Richardson system vs proliferation index: reproducibility of grade and advantages of proliferation index. *Mod Pathol,* 18**,** 1067-78.

MEYER, K. & PALMER, J. W. 1934. The polysaccharide of the vitreous humor. *J Biol Chem,* 107**,** 629-634.

MIKAMI, T. & KITAGAWA, H. 2013. Biosynthesis and function of chondroitin sulfate. *Biochim Biophys Acta,* 1830**,** 4719-4733.

MIKKOLA, M. L. & MILLAR, S. E. 2006. The mammary bud as a skin appendage: unique and shared aspects of development. *J Mammary Gland Biol Neoplasia,* 11**,** 187-203.

MILLA-SANTOS, A., MILLA, L., PORTELLA, J., RALLO, L., PONS, M., RODES, E., CASANOVAS, J. & PUIG-GALI, M. 2003. Anastrozole versus tamoxifen as first-line therapy in postmenopausal patients with hormone-dependent advanced breast cancer: a prospective, randomized, phase III study. *Am J Clin Oncol,* 26**,** 317-22.

MOORE, K. L. & AGUR, A. M. R. 2007. Thorax: breasts. *Essential clinical anatomy.* Lippincott Williams & Wilkins.

MORRISON, D. J., KIM, M. K., BERKOFSKY-FESSLER, W. & LICHT, J. D. 2008. WT1 induction of mitogen-activated protein kinase phosphatase 3 represents a novel mechanism of growth suppression. *Mol Cancer Res,* 6**,** 1225-31.

MOSMANN, T. 1983. Rapid colorimetric assay for cellular growth and survival: application to proliferation and cytotoxicity assays. *J Immunol Methods,* 65**,** 55-63.

MOURIDSEN, H., GERSHANOVICH, M., SUN, Y., PEREZ-CARRION, R., BONI, C., MONNIER, A., APFFELSTAEDT, J., SMITH, R., SLEEBOOM, H. P., JAENICKE, F., PLUZANSKA, A., DANK, M., BECQUART, D., BAPSY, P. P., SALMINEN, E., SNYDER, R., CHAUDRI-ROSS, H., LANG, R., WYLD, P. & BHATNAGAR, A. 2003. Phase III study of letrozole versus tamoxifen as first-line therapy of advanced breast cancer in postmenopausal women: analysis of survival and update of efficacy from the International Letrozole Breast Cancer Group. *J Clin Oncol,* 21**,** 2101-9.

MOUTASIM, K. A., NYSTROM, M. L. & THOMAS, G. J. 2011. Cell migration and invasion assays. *Methods Mol Biol,* 731**,** 333-43.

MUNDHENKE, C., MEYER, K., DREW, S. & FRIEDL, A. 2002. Heparan sulfate proteoglycans as regulators of fibroblast growth factor-2 receptor binding in breast carcinomas. *Am J Pathol,* 160**,** 185-94.

MURAMATSU, T. 2010. Midkine, a heparin-binding cytokine with multiple roles in development, repair and diseases. *Proc Jpn Acad Ser B Phys Biol Sci,* 86**,** 410-25.

NACCARATO, A. G., VIACAVA, P., VIGNATI, S., FANELLI, G., BONADIO, A. G., MONTRUCCOLI, G. & BEVILACQUA, G. 2000. Bio-morphological events in the development of the human female mammary gland from fetal age to puberty. *Virchows Arch,* 436**,** 431-8.

NADANAKA, S., KINOUCHI, H., TANIGUCHI-MORITA, K., TAMURA, J. & KITAGAWA, H. 2011. Down-regulation of chondroitin 4-O-sulfotransferase-1 by Wnt signaling triggers diffusion of Wnt-3a. *J Biol Chem,* 286**,** 4199-208.

NAKANISHI, T., KADOMATSU, K., OKAMOTO, T., ICHIHARA-TANAKA, K., KOJIMA, T., SAITO, H., TOMODA, Y. & MURAMATSU, T. 1997. Expression of

syndecan-1 and -3 during embryogenesis of the central nervous system in relation to binding with midkine. *J Biochem,* 121**,** 197-205.

NAM, S., XIE, J., PERKINS, A., MA, Y., YANG, F., WU, J., WANG, Y., XU, R. Z., HUANG, W., HORNE, D. A. & JOVE, R. 2012. Novel synthetic derivatives of the natural product berbamine inhibit Jak2/Stat3 signaling and induce apoptosis of human melanoma cells. *Mol Oncol,* 6**,** 484-93.

NATIONAL REGISTRY OF DISEASES OFFICE 2012. Trends in Cancer Incidence in Singapore 2006-2010.

NAWAZ, S. 2011. The normal breast and benign diseases of the breast. *In:* JACOBS, L. & FINLAYSON, C. (eds.) *Early diagnosis and treatment of cancer series: breast cancer*. Elsevier.

NIELSEN, T. O., WEST, R. B., LINN, S. C., ALTER, O., KNOWLING, M. A., O'CONNELL, J. X., ZHU, S., FERO, M., SHERLOCK, G., POLLACK, J. R., BROWN, P. O., BOTSTEIN, D. & VAN DE RIJN, M. 2002. Molecular characterisation of soft tissue tumours: a gene expression study. *Lancet,* 359**,** 1301-7.

NUNEZ, R. 2001. DNA measurement and cell cycle analysis by flow cytometry. *Curr Issues Mol Biol,* 3**,** 67-70.

O'RAHILLY, R. & MULLER, F. 2004. *Basic human anatomy: a regional study of human structure*, WB Saunders.

OLSEN, E. B., TRIER, K., ELDOV, K. & AMMITZBOLL, T. 1988. Glycosaminoglycans in human breast cancer. *Acta Obstet Gynecol Scand,* 67**,** 539-42.

ONDER, T. T., GUPTA, P. B., MANI, S. A., YANG, J., LANDER, E. S. & WEINBERG, R. A. 2008. Loss of E-cadherin promotes metastasis via multiple downstream transcriptional pathways. *Cancer Res,* 68**,** 3645-54.

ONITILO, A. A., ENGEL, J. M., GREENLEE, R. T. & MUKESH, B. N. 2009. Breast cancer subtypes based on ER/PR and Her2 expression: comparison of clinicopathologic features and survival. *Clin Med Res,* 7**,** 4-13.

OSTEEN, R. 2001. *Breast Cancer,* Atlanta, American Cancer Society.

PAIK, S., TANG, G., SHAK, S., KIM, C., BAKER, J., KIM, W., CRONIN, M., BAEHNER, F. L., WATSON, D., BRYANT, J., COSTANTINO, J. P., GEYER, C. E., JR., WICKERHAM, D. L. & WOLMARK, N. 2006. Gene expression and benefit of chemotherapy in women with node-negative, estrogen receptor-positive breast cancer. *J Clin Oncol,* 24**,** 3726-34.

PAINE, T. M., SOULE, H. D., PAULEY, R. J. & DAWSON, P. J. 1992. Characterization of epithelial phenotypes in mortal and immortal human breast cells. *Int J Cancer,* 50**,** 463-73.

PARCELL, S. 2002. Sulfur in human nutrition and applications in medicine. *Altern Med Rev,* 7**,** 22-44.

PARK, D., KARESEN, R., AXCRONA, U., NOREN, T. & SAUER, T. 2007. Expression pattern of adhesion molecules (E-cadherin, alpha-, beta-, gamma-catenin and claudin-7), their influence on survival in primary breast carcinoma, and their corresponding axillary lymph node metastasis. *APMIS,* 115**,** 52-65.

PARSONS, R. 2005. The oncogenetic basis of breast cancer. *In:* ROSES, D. F. (ed.) *Breast cancer.* Philadelphia: Elsevier.

PECE, S. & GUTKIND, J. S. 2000. Signaling from E-cadherins to the MAPK pathway by the recruitment and activation of epidermal growth factor receptors upon cell-cell contact formation. *J Biol Chem,* 275**,** 41227-33.

PHILLIPS, T. 2008. Regulation of transcription and gene expression in eukaryotes. *Nature Education,* 1**,** 199.

PIRINEN, R., LEINONEN, T., BOHM, J., JOHANSSON, R., ROPPONEN, K., KUMPULAINEN, E. & KOSMA, V. M. 2005. Versican in nonsmall cell lung cancer: relation to hyaluronan, clinicopathologic factors, and prognosis. *Hum Pathol,* 36**,** 44-50.

POLYAK, K. & WEINBERG, R. A. 2009. Transitions between epithelial and mesenchymal states: acquisition of malignant and stem cell traits. *Nat Rev Cancer,* 9**,** 265-73.

POLZIEN, L., BALJULS, A., ALBRECHT, M., HEKMAN, M. & RAPP, U. R. 2011. BAD contributes to RAF-mediated proliferation and cooperates with B-RAF-V600E in cancer signaling. *J Biol Chem,* 286**,** 17934-44.

POTAPENKO, I. O., HAAKENSEN, V. D., LUDERS, T., HELLAND, A., BUKHOLM, I., SORLIE, T., KRISTENSEN, V. N., LINGJAERDE, O. C. & BORRESEN-DALE, A. L. 2010. Glycan gene expression signatures in normal and malignant breast tissue; possible role in diagnosis and progression. *Mol Oncol,* 4**,** 98-118.

PRAILLET, C., LORTAT-JACOB, H. & GRIMAUD, J. A. 1996. Interferon gamma differentially affects the synthesis of chondroitin/dermatan sulphate and heparan sulphate by human skin fibroblasts. *Biochem J,* 318 (Pt 3)**,** 863-70.

PRASAD, C. P., GUPTA, S. D., RATH, G. & RALHAN, R. 2007. Wnt signaling pathway in invasive ductal carcinoma of the breast: relationship between beta-catenin, dishevelled and cyclin D1 expression. *Oncology,* 73**,** 112-7.

PRASAD, C. P., RATH, G., MATHUR, S., BHATNAGAR, D., PARSHAD, R. & RALHAN, R. 2009. Expression analysis of E-cadherin, Slug and GSK3beta in invasive ductal carcinoma of breast. *BMC Cancer,* 9**,** 325.

PUKKILA, M., KOSUNEN, A., ROPPONEN, K., VIRTANIEMI, J., KELLOKOSKI, J., KUMPULAINEN, E., PIRINEN, R., NUUTINEN, J., JOHANSSON, R. & KOSMA, V. M. 2007. High stromal versican expression predicts unfavourable outcome in oral squamous cell carcinoma. *J Clin Pathol,* 60**,** 267-72.

QUAGGIN, S. E. & KAPUS, A. 2011. Scar wars: mapping the fate of epithelial-mesenchymal-myofibroblast transition. *Kidney Int,* 80**,** 41-50.

RAGAZ, J., JACKSON, S. M., LE, N., PLENDERLEITH, I. H., SPINELLI, J. J., BASCO, V. E., WILSON, K. S., KNOWLING, M. A., COPPIN, C. M., PARADIS, M., COLDMAN, A. J. & OLIVOTTO, I. A. 1997. Adjuvant radiotherapy and chemotherapy in node-positive premenopausal women with breast cancer. *N Engl J Med,* 337**,** 956-62.

RAMAN, R., SASISEKHARAN, V. & SASISEKHARAN, R. 2005. Structural insights into biological roles of protein-glycosaminoglycan interactions. *Chem Biol,* 12**,** 267-77.

RAMSAY, D. T., KENT, J. C., HARTMANN, R. A. & HARTMANN, P. E. 2005. Anatomy of the lactating human breast redefined with ultrasound imaging. *J Anat,* 206**,** 525-34.

RASTOGI, T., DEVESA, S., MANGTANI, P., MATHEW, A., COOPER, N., KAO, R. & SINHA, R. 2008. Cancer incidence rates among South Asians in four geographic regions: India, Singapore, UK and US. *Int J Epidemiol,* 37**,** 147-60.

REBBECK, T. R., COUCH, F. J., KANT, J., CALZONE, K., DESHANO, M., PENG, Y., CHEN, K., GARBER, J. E. & WEBER, B. L. 1996. Genetic heterogeneity in hereditary breast cancer: role of BRCA1 and BRCA2. *Am J Hum Genet,* 59**,** 547-53.

RICCIARDELLI, C., BROOKS, J. H., SUWIWAT, S., SAKKO, A. J., MAYNE, K., RAYMOND, W. A., SESHADRI, R., LEBARON, R. G. & HORSFALL, D. J. 2002. Regulation of stromal versican expression by breast cancer cells and importance to relapse-free survival in patients with node-negative primary breast cancer. *Clin Cancer Res,* 8**,** 1054-60.

RICH, J. N., SHI, Q., HJELMELAND, M., CUMMINGS, T. J., KUAN, C. T., BIGNER, D. D., COUNTER, C. M. & WANG, X. F. 2003. Bone-related genes expressed in advanced malignancies induce invasion and metastasis in a genetically defined human cancer model. *J Biol Chem,* 278**,** 15951-7.

ROSE, A. A., GROSSET, A. A., DONG, Z., RUSSO, C., MACDONALD, P. A., BERTOS, N. R., ST-PIERRE, Y., SIMANTOV, R., HALLETT, M., PARK, M., GABOURY, L. & SIEGEL, P. M. 2010. Glycoprotein nonmetastatic B is an independent prognostic indicator of recurrence and a novel therapeutic target in breast cancer. *Clin Cancer Res,* 16**,** 2147-56.

ROSE, A. A., PEPIN, F., RUSSO, C., ABOU KHALIL, J. E., HALLETT, M. & SIEGEL, P. M. 2007. Osteoactivin promotes breast cancer metastasis to bone. *Mol Cancer Res,* 5**,** 1001-14.

ROSELLO, C., BALLET, P., PLANUS, E. & TRACQUI, P. 2004. Model driven quantification of individual and collective cell migration. *Acta Biotheor,* 52**,** 343-63.

ROSEN, P. P. 2009. *Rosen's breast pathology,* Philadelphia, Pa. ; London, Wolters Kluwer/Lippincott Williams & Wilkins.

ROSS, J. S. & FLETCHER, J. A. 1998. The HER-2/neu Oncogene in Breast Cancer: Prognostic Factor, Predictive Factor, and Target for Therapy. *Oncologist,* 3**,** 237-252.

RUOSLAHTI, E. 1984. Fibronectin in cell adhesion and invasion. *Cancer Metastasis Rev,* 3**,** 43-51.

RUSSO, J., HU, Y. F., SILVA, I. D. & RUSSO, I. H. 2001. Cancer risk related to mammary gland structure and development. *Microsc Res Tech,* 52**,** 204-23.

SAFADI, F. F., XU, J., SMOCK, S. L., RICO, M. C., OWEN, T. A. & POPOFF, S. N. 2001. Cloning and characterization of osteoactivin, a novel cDNA expressed in osteoblasts. *J Cell Biochem,* 84**,** 12-26.

SANSONE, P. & BROMBERG, J. 2012. Targeting the interleukin-6/Jak/stat pathway in human malignancies. *J Clin Oncol,* 30**,** 1005-14.

SASLOW, D., BOETES, C., BURKE, W., HARMS, S., LEACH, M. O., LEHMAN, C. D., MORRIS, E., PISANO, E., SCHNALL, M., SENER, S., SMITH, R. A., WARNER, E., YAFFE, M., ANDREWS, K. S. & RUSSELL, C. A. 2007. American Cancer Society guidelines for breast screening with MRI as an adjunct to mammography. *CA Cancer J Clin,* 57**,** 75-89.

SATO, T., GOTOH, M., KIYOHARA, K., AKASHIMA, T., IWASAKI, H., KAMEYAMA, A., MOCHIZUKI, H., YADA, T., INABA, N., TOGAYACHI, A., KUDO, T., ASADA, M., WATANABE, H., IMAMURA, T., KIMATA, K. & NARIMATSU, H. 2003. Differential roles of two N-acetylgalactosaminyltransferases, CSGalNAcT-1, and a novel enzyme, CSGalNAcT-2. Initiation and elongation in synthesis of chondroitin sulfate. *J Biol Chem,* 278**,** 3063-71.

SAYYAH, J., GNANASAMBANDAN, K., KAMARAJUGADDA, S., TSUDA, S., CALDWELL-BUSBY, J. & SAYESKI, P. P. 2011. Phosphorylation of Y372 is critical for Jak2 tyrosine kinase activation. *Cell Signal,* 23**,** 1806-15.

SCHMALHOFER, O., BRABLETZ, S. & BRABLETZ, T. 2009. E-cadherin, beta-catenin, and ZEB1 in malignant progression of cancer. *Cancer Metastasis Rev,* 28**,** 151-66.

SCHOLZEN, T. & GERDES, J. 2000. The Ki-67 protein: from the known and the unknown. *J Cell Physiol,* 182**,** 311-22.

SCULLY, R. & PUGET, N. 2002. BRCA1 and BRCA2 in hereditary breast cancer. *Biochimie,* 84**,** 95-102.

SEOW, A., DUFFY, S. W., MCGEE, M. A., LEE, J. & LEE, H. P. 1996. Breast cancer in Singapore: trends in incidence 1968-1992. *Int J Epidemiol,* 25**,** 40-5.

SHIOZAKI, H., OKA, H., INOUE, M., TAMURA, S. & MONDEN, M. 1996. E-cadherin mediated adhesion system in cancer cells. *Cancer,* 77**,** 1605-13.

SIEGEL, R., NAISHADHAM, D. & JEMAL, A. 2013. Cancer statistics, 2013. *CA Cancer J Clin,* 63**,** 11-30.

SILBERT, J. E. & SUGUMARAN, G. 2002. Biosynthesis of chondroitin/dermatan sulfate. *IUBMB Life,* 54**,** 177-86.

SIMIC, P., WILLIAMS, E. O., BELL, E. L., GONG, J. J., BONKOWSKI, M. & GUARENTE, L. 2013. SIRT1 Suppresses the Epithelial-to-Mesenchymal Transition in Cancer Metastasis and Organ Fibrosis. *Cell Rep,* 3**,** 1175-86.

SIMPSON, M. J., TOWNE, C., MCELWAIN, D. L. & UPTON, Z. 2010. Migration of breast cancer cells: understanding the roles of volume exclusion and cell-to-cell adhesion. *Phys Rev E Stat Nonlin Soft Matter Phys,* 82**,** 041901.

SINGLETARY, K. W. & GAPSTUR, S. M. 2001. Alcohol and breast cancer: review of epidemiologic and experimental evidence and potential mechanisms. *JAMA,* 286**,** 2143-51.

SINGLETARY, S. E. 2003. Rating the risk factors for breast cancer. *Ann Surg,* 237**,** 474-82.

SKANDALIS, S. S., LABROPOULOU, V. T., RAVAZOULA, P., LIKAKI-KARATZA, E., DOBRA, K., KALOFONOS, H. P., KARAMANOS, N. K. & THEOCHARIS, A. D. 2011. Versican but not decorin accumulation is related to malignancy in mammographically detected high density and malignant-appearing microcalcifications in non-palpable breast carcinomas. *BMC Cancer,* 11**,** 314.

SLAMON, D. J., CLARK, G. M., WONG, S. G., LEVIN, W. J., ULLRICH, A. & MCGUIRE, W. L. 1987. Human breast cancer: correlation of relapse and survival with amplification of the HER-2/neu oncogene. *Science,* 235**,** 177-82.

SLAMON, D. J., LEYLAND-JONES, B., SHAK, S., FUCHS, H., PATON, V., BAJAMONDE, A., FLEMING, T., EIERMANN, W., WOLTER, J., PEGRAM, M., BASELGA, J. & NORTON, L. 2001. Use of chemotherapy plus a monoclonal antibody against HER2 for metastatic breast cancer that overexpresses HER2. *N Engl J Med,* 344**,** 783-92.

SMITH, R. A., DUFFY, S. W., GABE, R., TABAR, L., YEN, A. M. & CHEN, T. H. 2004. The randomized trials of breast cancer screening: what have we learned? *Radiol Clin North Am,* 42**,** 793-806, v.

SO, J. Y., SMOLAREK, A. K., SALERNO, D. M., MAEHR, H., USKOKOVIC, M., LIU, F. & SUH, N. 2013. Targeting CD44-STAT3 signaling by Gemini vitamin D analog leads to inhibition of invasion in basal-like breast cancer. *PLoS One,* 8**,** e54020.

SOBIN, L., GOSPODAROWICZ, M. K. & WITTEKIND, C. 2009. *TNM Classification of Malignant Tumors 7th Edition,* UICC.

SOUZA-FERNANDES, A. B., PELOSI, P. & ROCCO, P. R. 2006. Bench-to-bedside review: the role of glycosaminoglycans in respiratory disease. *Crit Care,* 10**,** 237.

SPANGENBURG, E. E. & BOOTH, F. W. 2002. Multiple signaling pathways mediate LIF-induced skeletal muscle satellite cell proliferation. *Am J Physiol Cell Physiol,* 283**,** C204-11.

STAMATOGLOU, S. C. & KELLER, J. M. 1983. Correlation between cell substrate attachment in vitro and cell surface heparan sulfate affinity for fibronectin and collagen. *J Cell Biol,* 96**,** 1820-3.

STANDRING, S. 2008. Chapter 54 Chest Wall and Breast. *In:* STANDRING, S. (ed.) *Gray's Anatomy: The Anatomical Basis of Clinical Practice*. Edinburgh: Churchill Livingstone.

STEPHENS, R. W., BRUNNER, N., JANICKE, F. & SCHMITT, M. 1998. The urokinase plasminogen activator system as a target for prognostic studies in breast cancer. *Breast Cancer Res Treat,* 52**,** 99-111.

STRAVER, M. E., GLAS, A. M., HANNEMANN, J., WESSELING, J., VAN DE VIJVER, M. J., RUTGERS, E. J., VRANCKEN PEETERS, M. J., VAN TINTEREN, H., VAN'T VEER, L. J. & RODENHUIS, S. 2010. The 70-gene signature as a response predictor for neoadjuvant chemotherapy in breast cancer. *Breast Cancer Res Treat,* 119**,** 551-8.

SUGAHARA, K., MIKAMI, T., UYAMA, T., MIZUGUCHI, S., NOMURA, K. & KITAGAWA, H. 2003. Recent advances in the structural biology of chondroitin sulfate and dermatan sulfate. *Curr Opin Struct Biol,* 13**,** 612-20.

SUMAN, S., JOHNSON, M. D., FORNACE, A. J., JR. & DATTA, K. 2012. Exposure to ionizing radiation causes long-term increase in serum estradiol and activation of PI3K-Akt signaling pathway in mouse mammary gland. *Int J Radiat Oncol Biol Phys,* 84**,** 500-7.

SUN, F., CHAN, E., WU, Z., YANG, X., MARQUEZ, V. E. & YU, Q. 2009. Combinatorial pharmacologic approaches target EZH2-mediated gene repression in breast cancer cells. *Mol Cancer Ther,* 8**,** 3191-202.

SUWAN, K., HATANO, S., KONGTAWELERT, P., POTHACHAROEN, P. & WATANABE, H. 2009. Alteration of chondroitin sulfate composition on proteoglycan produced by knock-in mouse embryonic fibroblasts whose versican lacks the A subdomain. *Ups J Med Sci,* 114**,** 73-81.

SUWIWAT, S., RICCIARDELLI, C., TAMMI, R., TAMMI, M., AUVINEN, P., KOSMA, V. M., LEBARON, R. G., RAYMOND, W. A., TILLEY, W. D. & HORSFALL, D. J. 2004. Expression of extracellular matrix components versican, chondroitin sulfate, tenascin, and hyaluronan, and their association with disease outcome in node-negative breast cancer. *Clin Cancer Res,* 10**,** 2491-8.

SVENSSON, K. J., CHRISTIANSON, H. C., KUCHARZEWSKA, P., FAGERSTROM, V., LUNDSTEDT, L., BORGQUIST, S., JIRSTROM, K. & BELTING, M. 2011. Chondroitin sulfate expression predicts poor outcome in breast cancer. *Int J Oncol,* 39**,** 1421-8.

TAKEICHI, M. 1991. Cadherin cell adhesion receptors as a morphogenetic regulator. *Science,* 251**,** 1451-5.

TAN, P. H., CHIANG, G. S., NG, E. H., LOW, S. C. & NG, F. C. 1999. Screen detected breast cancer in an Asian population: pathological findings of the Singapore breast screening project. *Breast,* 8**,** 120-5.

TEO, M. C. & SOO, K. C. 2013. Cancer trends and incidences in Singapore. *Jpn J Clin Oncol,* 43**,** 219-24.

TERRY, M. B., ZHANG, F. F., KABAT, G., BRITTON, J. A., TEITELBAUM, S. L., NEUGUT, A. I. & GAMMON, M. D. 2006. Lifetime alcohol intake and breast cancer risk. *Ann Epidemiol,* 16**,** 230-40.

THIERY, J. P., ACLOQUE, H., HUANG, R. Y. & NIETO, M. A. 2009. Epithelial-mesenchymal transitions in development and disease. *Cell,* 139**,** 871-90.

TITUS-ERNSTOFF, L., LONGNECKER, M. P., NEWCOMB, P. A., DAIN, B., GREENBERG, E. R., MITTENDORF, R., STAMPFER, M. & WILLETT, W. 1998. Menstrual factors in relation to breast cancer risk. *Cancer Epidemiol Biomarkers Prev,* 7**,** 783-9.

TOYONAGA, T., NAKANO, K., NAGANO, M., ZHAO, G., YAMAGUCHI, K., KUROKI, S., EGUCHI, T., CHIJIIWA, K., TSUNEYOSHI, M. & TANAKA, M. 2003. Blockade of constitutively activated Janus kinase/signal transducer and activator of transcription-3 pathway inhibits growth of human pancreatic cancer. *Cancer Lett,* 201**,** 107-16.

TSUI, K. H., CHANG, Y. L., FENG, T. H., CHANG, P. L. & JUANG, H. H. 2012. Glycoprotein transmembrane nmb: an androgen-downregulated gene attenuates cell invasion and tumorigenesis in prostate carcinoma cells. *Prostate,* 72**,** 1431-42.

TUYSUZ, B., MIZUMOTO, S., SUGAHARA, K., CELEBI, A., MUNDLOS, S. & TURKMEN, S. 2009. Omani-type spondyloepiphyseal dysplasia with cardiac involvement caused by a missense mutation in CHST3. *Clin Genet,* 75**,** 375-83.

UYAMA, T., KITAGAWA, H., TAMURA JI, J. & SUGAHARA, K. 2002. Molecular cloning and expression of human chondroitin N-acetylgalactosaminyltransferase: the key enzyme for chain initiation and elongation of chondroitin/dermatan sulfate on the protein linkage region tetrasaccharide shared by heparin/heparan sulfate. *J Biol Chem,* 277**,** 8841-6.

VAKLAVAS, C., LOBUGLIO, A., SALEH, M., YELIN, M. & FORERO, A. 2013. CDX-011 (Glembatumumab Vedotin, CF011-vcMMAE). *In:* PHILLIPS, G. (ed.) *Antibody-drug conjugates and immunotoxins: from pre-clinical development to therapeutic applications.* New York: Springer Science.

VAN 'T VEER, L. J., DAI, H., VAN DE VIJVER, M. J., HE, Y. D., HART, A. A., MAO, M., PETERSE, H. L., VAN DER KOOY, K., MARTON, M. J., WITTEVEEN, A. T., SCHREIBER, G. J., KERKHOVEN, R. M., ROBERTS, C., LINSLEY, P. S., BERNARDS, R. & FRIEND, S. H. 2002. Gene expression profiling predicts clinical outcome of breast cancer. *Nature,* 415**,** 530-6.

VAN BOGAERT, L. J. 1981. Recent progress in the histological typing of human breast tumours. *Diagn Histopathol,* 4**,** 349-53.

VAN DE VIJVER, M. J., HE, Y. D., VAN'T VEER, L. J., DAI, H., HART, A. A., VOSKUIL, D. W., SCHREIBER, G. J., PETERSE, J. L., ROBERTS, C., MARTON, M. J., PARRISH, M., ATSMA, D., WITTEVEEN, A., GLAS, A., DELAHAYE, L., VAN DER VELDE, T., BARTELINK, H., RODENHUIS, S., RUTGERS, E. T., FRIEND, S. H.

& BERNARDS, R. 2002. A gene-expression signature as a predictor of survival in breast cancer. *N Engl J Med,* 347**,** 1999-2009.

VAN ROIJ, M. H., MIZUMOTO, S., YAMADA, S., MORGAN, T., TAN-SINDHUNATA, M. B., MEIJERS-HEIJBOER, H., VERBEKE, J. I., MARKIE, D., SUGAHARA, K. & ROBERTSON, S. P. 2008. Spondyloepiphyseal dysplasia, Omani type: further definition of the phenotype. *Am J Med Genet A,* 146a**,** 2376-84.

VERKOOIJEN, H. M., YAP, K. P., BHALLA, V., CHOW, K. Y. & CHIA, K. S. 2009. Multiparity and the risk of premenopausal breast cancer: different effects across ethnic groups in Singapore. *Breast Cancer Res Treat,* 113**,** 553-8.

VIANI, G. A., AFONSO, S. L., STEFANO, E. J., DE FENDI, L. I. & SOARES, F. V. 2007. Adjuvant trastuzumab in the treatment of her-2-positive early breast cancer: a meta-analysis of published randomized trials. *BMC Cancer,* 7**,** 153.

VIJAYAGOPAL, P., FIGUEROA, J. E. & LEVINE, E. A. 1998. Altered composition and increased endothelial cell proliferative activity of proteoglycans isolated from breast carcinoma. *J Surg Oncol,* 68**,** 250-4.

VLODAVSKY, I., ILAN, N., NADIR, Y., BRENNER, B., KATZ, B. Z., NAGGI, A., TORRI, G., CASU, B. & SASISEKHARAN, R. 2007a. Heparanase, heparin and the coagulation system in cancer progression. *Thromb Res,* 120 Suppl 2**,** S112-20.

VLODAVSKY, I., ILAN, N., NAGGI, A. & CASU, B. 2007b. Heparanase: structure, biological functions, and inhibition by heparin-derived mimetics of heparan sulfate. *Curr Pharm Des,* 13**,** 2057-73.

VOGEL, V. G. 2012. Epidemiology of breast cancer. *In:* DABBS, D. J. (ed.) *Breast pathology*. Saunders Elsevier.

WADE, A., ROBINSON, A. E., ENGLER, J. R., PETRITSCH, C., JAMES, C. D. & PHILLIPS, J. J. 2013. Proteoglycans and their roles in brain cancer. *FEBS J,* 280**,** 2399-417.

WAGNER, K. U. & SCHMIDT, J. W. 2011. The two faces of Janus kinases and their respective STATs in mammary gland development and cancer. *J Carcinog,* 10**,** 32.

WAKAHARA, R., KUNIMOTO, H., TANINO, K., KOJIMA, H., INOUE, A., SHINTAKU, H. & NAKAJIMA, K. 2012. Phospho-Ser727 of STAT3 regulates STAT3 activity by enhancing dephosphorylation of phospho-Tyr705 largely through TC45. *Genes Cells,* 17**,** 132-45.

WALDMAN, F. M., CHEW, K., LJUNG, B. M., GOODSON, W., HOM, J., DUARTE, L. A., SMITH, H. S. & MAYALL, B. 1991. A comparison between bromodeoxyuridine and 3H thymidine labeling in human breast tumors. *Mod Pathol,* 4**,** 718-22.

WALKER, S. R., NELSON, E. A., ZOU, L., CHAUDHURY, M., SIGNORETTI, S., RICHARDSON, A. & FRANK, D. A. 2009. Reciprocal effects of STAT5 and STAT3 in breast cancer. *Mol Cancer Res,* 7**,** 966-76.

WANG, S. C. 2003. The Singapore National Breast Screening Programme: principles and implementation. *Ann Acad Med Singapore,* 32**,** 466-76.

WANG, X., OSADA, T., WANG, Y., YU, L., SAKAKURA, K., KATAYAMA, A., MCCARTHY, J. B., BRUFSKY, A., CHIVUKULA, M., KHOURY, T., HSU, D. S., BARRY, W. T., LYERLY, H. K., CLAY, T. M. & FERRONE, S. 2010a. CSPG4 protein as a new target for the antibody-based immunotherapy of triple-negative breast cancer. *J Natl Cancer Inst,* 102**,** 1496-512.

WANG, X., WANG, Y., YU, L., SAKAKURA, K., VISUS, C., SCHWAB, J. H., FERRONE, C. R., FAVOINO, E., KOYA, Y., CAMPOLI, M. R., MCCARTHY, J. B., DELEO, A. B. & FERRONE, S. 2010b. CSPG4 in cancer: multiple roles. *Curr Mol Med,* 10**,** 419-29.

WANG, Z., LI, Y., KONG, D. & SARKAR, F. H. 2010c. The role of Notch signaling pathway in epithelial-mesenchymal transition (EMT) during development and tumor aggressiveness. *Curr Drug Targets,* 11**,** 745-51.

WATSON, C. J. & KHALED, W. T. 2008. Mammary development in the embryo and adult: a journey of morphogenesis and commitment. *Development,* 135**,** 995-1003.

WEIGELT, B., PETERSE, J. L. & VAN 'T VEER, L. J. 2005. Breast cancer metastasis: markers and models. *Nat Rev Cancer,* 5**,** 591-602.

WU, Y. J., LA PIERRE, D. P., WU, J., YEE, A. J. & YANG, B. B. 2005. The interaction of versican with its binding partners. *Cell Res,* 15**,** 483-94.

YANG, J., PRICE, M. A., NEUDAUER, C. L., WILSON, C., FERRONE, S., XIA, H., IIDA, J., SIMPSON, M. A. & MCCARTHY, J. B. 2004. Melanoma chondroitin sulfate proteoglycan enhances FAK and ERK activation by distinct mechanisms. *J Cell Biol,* 165**,** 881-91.

YANG, Q., SHEN, S. S., ZHOU, S., NI, J., CHEN, D., WANG, G. & LI, Y. 2012. STAT3 activation and aberrant ligand-dependent sonic hedgehog signaling in human pulmonary adenocarcinoma. *Exp Mol Pathol,* 93**,** 227-36.

YEE, A. J., AKENS, M., YANG, B. L., FINKELSTEIN, J., ZHENG, P. S., DENG, Z. & YANG, B. 2007. The effect of versican G3 domain on local breast cancer invasiveness and bony metastasis. *Breast Cancer Res,* 9**,** R47.

YIN, L. 2005. Chondroitin synthase 1 is a key molecule in myeloma cell-osteoclast interactions. *J Biol Chem,* 280**,** 15666-72.

YIP, G. W., SMOLLICH, M. & GOTTE, M. 2006. Therapeutic value of glycosaminoglycans in cancer. *Mol Cancer Ther,* 5**,** 2139-48.

ZAPPULLI, V., DE CECCO, S., TREZ, D., CALIARI, D., ARESU, L. & CASTAGNARO, M. 2012. Immunohistochemical expression of E-cadherin and beta-catenin in feline mammary tumours. *J Comp Pathol,* 147**,** 161-70.

ZHANG, S. M., LEE, I. M., MANSON, J. E., COOK, N. R., WILLETT, W. C. & BURING, J. E. 2007. Alcohol consumption and breast cancer risk in the Women's Health Study. *Am J Epidemiol,* 165**,** 667-76.

ZHAO, Y., QIAO, Z. G., SHAN, S. J., SUN, Q. M. & ZHANG, J. Z. 2012. Expression of glycoprotein non-metastatic melanoma protein B in cutaneous malignant and benign lesions: a tissue microarray study. *Chin Med J (Engl),* 125**,** 3279-82.

ZIMMERMANN, D. R. 2000. Versican. *In:* IOZZO, R. V. (ed.) *Proteoglycans: structure, biology and molecular interactions.* New York: CRC Press.

ZOU, K., MURAMATSU, H., IKEMATSU, S., SAKUMA, S., SALAMA, R. H., SHINOMURA, T., KIMATA, K. & MURAMATSU, T. 2000. A heparin-binding growth factor, midkine, binds to a chondroitin sulfate proteoglycan, PG-M/versican. *Eur J Biochem,* 267**,** 4046-53.

ZOU, X. H., FOONG, W. C., CAO, T., BAY, B. H., OUYANG, H. W. & YIP, G. W. 2004. Chondroitin sulfate in palatal wound healing. *J Dent Res,* 83**,** 880-5.

ZWEIG, M. H. & CAMPBELL, G. 1993. Receiver-operating characteristic (ROC) plots: a fundamental evaluation tool in clinical medicine. *Clin Chem,* 39**,** 561-77.